UNCLASS

SECURITY CLASSIFICATION OF THIS PAGE (When Data Entered)

AD-A142 889

REPORT DOCUMENTATION PAGE

READ INSTRUCTIONS BEFORE COMPLETING FORM

1. REPORT NUMBER AFIT/CI/NR 84-34T	2. GOVT ACCESSION NO.	3. RECIPIENT'S CATALOG NUMBER
4. TITLE (and Subtitle) Adsorption Equilibria and Performance of a Pressure Swing Adsorption Air Separation Unit		5. TYPE OF REPORT & PERIOD COVERED THESIS/~~DISSERTATION~~
		6. PERFORMING ORG. REPORT NUMBER
7. AUTHOR(s) George Walter Miller		8. CONTRACT OR GRANT NUMBER(s)
9. PERFORMING ORGANIZATION NAME AND ADDRESS AFIT STUDENT AT: The Ohio State University		10. PROGRAM ELEMENT, PROJECT, TASK AREA & WORK UNIT NUMBERS
11. CONTROLLING OFFICE NAME AND ADDRESS AFIT/NR WPAFB OH 45433		12. REPORT DATE 1984
		13. NUMBER OF PAGES 297
14. MONITORING AGENCY NAME & ADDRESS(if different from Controlling Office)		15. SECURITY CLASS. (of this report) UNCLASS
		15a. DECLASSIFICATION/DOWNGRADING SCHEDULE

16. DISTRIBUTION STATEMENT (of this Report)

APPROVED FOR PUBLIC RELEASE; DISTRIBUTION UNLIMITED

17. DISTRIBUTION STATEMENT (of the abstract entered in Block 20, if different from Report)

18. SUPPLEMENTARY NOTES

APPROVED FOR PUBLIC RELEASE: IAW AFR 190-17

Lynn Wolaver 3 Jul 84

LYNN E. WOLAVER
Dean for Research and
Professional Development
AFIT, Wright-Patterson AFB OH

19. KEY WORDS (Continue on reverse side if necessary and identify by block number)

20. ABSTRACT (Continue on reverse side if necessary and identify by block number)

ATTACHED

DTIC
ELECTE
JUL 1 1 1984
S D
E

84 07 10 161

DTIC FILE COPY

DD FORM 1 JAN 73 1473 EDITION OF 1 NOV 65 IS OBSOLETE

UNCLASS

SECURITY CLASSIFICATION OF THIS PAGE (When Data Entered)

THESIS ABSTRACT

THE OHIO STATE UNIVERSITY
GRADUATE SCHOOL
(Please type.)

NAME: George Walter Miller **QUARTER/YEAR:** Summer/84

DEPARTMENT: Chemical Engineering **DEGREE:** M.S.

TITLE OF THESIS: Adsorption Equilibria and Performance of a Pressure Swing Adsorption Air Separation Unit

Summarize in the space below the purpose and principal conclusions of your thesis.

Current pressure swing adsorption (PSA) air separation units operating on short cycle times suffer a reduction in product oxygen concentration when subjected to lower ambient temperatures (i.e., less than -10°C). This work investigates this problem based on analysis of adsorption equilibria, column breakthrough studies, and actual PSA system data.

Pure and multicomponent data for nitrogen, oxygen, and air on molecular sieve 5A were collected at 24, -40, and -70°C up to pressures of 4.3 atmospheres absolute. Using a statistical thermodynamic model pure component data were adequately predicted over the entire temperature range (24 to -70°C). The multicomponent data were predicted at 24°C by a statistical thermodynamic model and ideal adsorbed solution theory. At the lower temperatures the gas mixture behaved nonideally.

Column breakthrough data taken at 24 and -40°C shows that the length mass transfer front during nitrogen breakthrough remains nearly constant. In contrast, the length of the mass transfer front for oxygen breakthrough increases significantly. This may indicate a difficulty in desorbing nitrogen at the low temperatures.

Actual PSA system experiments at 24 and -40°C indicate improved performance at -40°C could be obtained by lengthening the system cycle time. A six-step versus two-step per cycle comparison revealed the six-step system had slightly higher oxygen purity and recovery at 24°C and both systems had little difference in product purity and recovery at -40°C.

Kent S. Knaebel
Adviser's Signature

ADSORPTION EQUILIBRIA AND PERFORMANCE OF A PRESSURE SWING ADSORPTION AIR SEPARATION UNIT

A Thesis

Presented in Partial Fulfillment of the Requirements
for the Degree Master of Science

by

George Walter Miller, B.S.Ch.E.

The Ohio State University
1984

Approved by

Kent S. Knaebel

Adviser

Department of
Chemical Engineering

ACKNOWLEDGEMENTS

I would like to express my sincere appreciation to Dr. Kent S. Knaebel for his guidance and sincere interest in this work. In addition, the software he developed to control the pressure swing adsorption unit greatly improved the efficiency and accuracy of the data collection process.

Special thanks are extended to the U. S. Air Force School of Aerospace Medicine (USAFSAM), Brooks A.F.B., Texas, and the U. S. Air Force Institute of Technology, Wright-Patterson A.F.B., Ohio, who kindly supported this research work. Thanks are also due to Dr. Carter Alexander, Dr. Richard L. Miller, and Dr. Kenneth G. Ikels of USAFSAM/VN for providing facilities where this work could be conducted in an efficient manner.

I am grateful to Union Carbide Corporation, Molecular Sieve Division, for making available their isotherm data.

I would also like to express my deepest appreciation to my family, Maxine, Becky, and Steven, for their sacrifices on my behalf during this work.

TABLE OF CONTENTS

Page

TABLE OF FIGURES

TABLE OF TABLES

SUMMARY

The pure component isotherms of nitrogen and oxygen on zeolite molecular sieve 5A were determined through use of a volumetric technique at 24, -40, and -70°C up to absolute pressures of 4.3 atmospheres. Using parameters derived from the pure component data, i.e. Henry's Law constant and the effective molecular volume, a statistical thermodynamic model correctly predicted the pure component data of Union Carbide.

The pure equilibrium apparatus was modified and multicomponent equilibrium data were collected using air and molecular sieve 5A. The pure component parameters were used with the extended statistical thermodynamic model and the IAST theory to predict the adsorption of nitrogen and oxygen from an air mixture on molecular sieve 5A. The predictions at 24 °C were excellent but those at -40 and -70°C had significant deviations. Adjustment of the apparent effective molecular volumes for nitrogen and oxygen led to a good fit of the data at the lower temperatures.

Breakthrough studies using one column of the pressure swing adsorption system revealed that the nitrogen breakthrough curves at 24°C and -40°C have the same shape and length, although due to the increased adsorption capacity of the bed at -40°C its front emerges from the bed at a later time. In contrast, when comparing oxygen breakthrough curves at these temperatures the time required to reach one percent

concentration of nitrogen in the effluent is significantly longer at -40 °C. These results imply that a longer cycle time should improve performance of a pressure swing adsorption unit operating at reduced temperature, however, the significantly longer time necessary for nitrogen desorption indicates performance should be less than that attained at room temperature. Data taken from an actual pressure swing adsorption unit appear to agree with these predictions.

A bench-scale pressure swing adsorption system was constructed to determine the effect of operating at room temperature and -40°C on system performance. Present systems experience reduced oxygen concentration at preset flow rates and cycle times while operating at low temperatures. It was determined that lengthening the system cycle time improved performance but the percent oxygen concentrations were still less than at room temperature. Cycles of six-steps versus two steps at both room temperature and -40°C were tried, with the six step system showing slightly better oxygen purity and recovery at room temperature and both systems having little difference in oxygen purity and recovery at -40°C.

CHAPTER I

INTRODUCTION

Pressure swing adsorption (PSA) has emerged as a popular method for air separation due to economic and operational advantages. Where 95% or less oxygen concentration is required at small to moderate flow rates PSA systems can compete successfully with conventional techniques, i.e. cryogenic fractionation, due to reduced complexity and smaller energy requirements (1). The chemical industry has been aware of the advantages of PSA technology in such areas as gas purification, chemical oxidation processes, and water treatment (2,3,4,5,6,7). It has been suggested that flowrates in the range of 1 to 80 ton/day of enriched oxygen may be produced more economically by PSA (2). PSA systems have been employed by the medical profession for out-patient oxygen therapy and as a source of oxygen for field hospitals (6). In the future such systems may possibly reduce air pollutants in automobile emissions by improving the efficiency of the combustion process.

PSA systems separate air by cyclic variation of pressure in fixed beds of adsorbent which preferentially adsorb nitrogen from an entering air flow, thereby increasing the oxygen concentration in the gas phase. Following the adsorption step is a desorption step where regeneration of the beds is accomplished by pressure reduction and purging by recycling a portion of the product flow. Although the general concept of separation has been in existence for the last two decades (28), the present impetus for its use is an economic one. The recent introduction of PSA systems operating on short cycle times has allowed these units to process large amounts of air with smaller bed sizes. Additionally, with adsorbent beds operated at ambient temperature and with the process being essentially isothermal the only energy consumed is that required for pressurizing the feed and cycling the valves.

Recently, the aviation industry and the military have placed significant emphasis on the development of an airborne oxygen generating system capable of separating air ,and thus, provide an inexhaustable source of breathable oxygen for aircrew hypoxia protection (8,9,10). Presently, oxygen in either liquid or gaseous form is stored onboard the aircraft and depleted during each flight. These stored supplies are costly and place constraints on the aircraft's potential effectiveness. Obviously with conventional systems, any decision involving the basing of aircraft in a remote location must address the availibility of oxygen in both the proper quantity and quality. The development of a system capable of delivering high purity oxygen for extended periods of time would result in substantial economic savings, greater flexibility in aircraft basing, and eliminate hazards associated with handling supplies of pure oxygen. An onboard oxygen generating system utilizing the principle of pressure swing adsorption is considered the prime candidate for full scale production and installation aboard military tactical aircraft.

Terrestial and airborne versions of the system employ molecular sieve 5A as the adsorbent, a synthetic zeolite, and are potentially capable of producing a product flow with a maximum oxygen concentration of approximately 95.7% with the remainder as argon. The breathing of this gas mixture, as opposed to 100% oxygen, by aviators has been shown to present no deleterious effects (11,12).

Environmental testing of a prototype onboard oxygen generating system resulted in an interesting observation. When a system producing approximately 95% oxygen at room temperature was subjected to a reduction in ambient temperature the oxygen product concentration also dropped significantly with the most dramatic rate of degradation occurring at approximately -20 °C. At -40 °C the product oxygen concentration had fallen to 70% . Clearly this poses a problem because the ambient temperature within the operational envelope of some aircraft may be as low as -40 °C.

This finding immediately presents two practical questions. Firstly, what mechanism is responsible for this decline in system performance at lower ambient temperatures. Secondly, what approach should be taken to nullify or minimize this reduction in oxygen concentration so that the system might return to an acceptable level of performance. An obvious first approach would involve thermal protection of the adsorbent beds,e.g. by electrical heating, to maintain a temperature above -20°C, maybe +20°C as previously suggested (10). This would certainly solve the problem for a powered aircraft which is gradually subjected to the lower temperatures. In contrast, an unpowered aircraft with adsorbent beds initially at a low temperature would most certainly require additional preparation time before flight due to the added requirement of heating the adsorbent beds to an operational temperature. The length of time required for heating the beds may be substantial due to the insulating characteristics of the molecular sieve. In most cases this may not pose a significant problem, but for a previously unpowered aircraft desiring an immediate departure, this delay could prove to be an unacceptable constraint. Although this problem could be solved by applying ground electricial power on a continous basis, the burden of providing suitable facilities and maintaining continuous service would make this option undesirable.

Providing answers to those questions is the focus of this work. The goals are twofold: one is to take a step toward understanding the mechanism which causes this reduction in performance; the second is to broaden the base of existing knowledge about PSA systems operating at low temperature. The topics in this area include overall system analysis, and since this is a stepwise approach into the low temperature regime, basic research in equilibria and kinetics of the process. Ultimately, these two mechanisms will control the theoretical and practical limits of the PSA process. As will become readily apparent,this work will stress equilibrium data (instead of kinetics), and methods which will predict this data with a reasonable degree of accuracy.

This investigation was organized into three general areas: equilibria, breakthrough data, and dual column PSA system expriments. As was previously mentioned, this work will stress the equilibrium data because accurate determination or prediction of isotherms is of fundamental importance in the design and modeling of PSA systems. Additionally, multicomponent equilibrium data are limited, and therefore, reliable techniques for predicting the behavior of the multicomponent system from the pure component data are crucial from a practical and theoretical standpoint. The multicomponent data may also lead to a better overall understanding of the interactions between the gas and solid phase.

Pure component data of nitrogen and oxygen, and multicomponent equilibrium data of air were measured at temperatures of 24, -40, and -70°C up to pressures of 4.3 atmospheres absolute. Any profound changes in the equilibrium adsorption isotherms would certainly affect the performance of the separation. Air was selected as the multicomponent mixture because its isotherms should come closest to simulating the actual PSA process. The adsorbent used in this work was Union Carbide Corporation of Tarrytown,New York, molecular sieve 5A due to its superior characteristics for air separation. Data at -70 °C were included so that a more complete data set over a wider range of temperature would be available for analysis. It was thought if any unusual observations were noticed at -40 °C their presence would be confirmed by a more pronounced effect occurring at -70 °C. These experiments were necessary because, in general, this data was not available in the literature. Considerable effort was expended in investigating techniques which could be employed to predict the experimental data within a reasonable degree of accuracy. Since multicomponent data collection is, in general, time consuming and tedious, reliable predictive models based on pure component data are of great value.

The breakthrough experiments were conducted at 24 and -40 °C, various flowrates, and pressures comparable to the actual column operating pressures, provided breakthrough curves which described the mass transfer zone within the column. Changes in the shape of the breakthrough curves and the time required to reach breakthrough would reveal any kinetic differences between operating the column at 24°C, as opposed to -40°C. In these experiments, one of the two column of the PSA apparatus was used and breakthrough curves were determined by flowing air and oxygen. Air and oxygen were chosen because these gases would better approximate the actual conditions within each PSA column,i.e. during the feed and purge steps.

A dual column, bench scale PSA apparatus was designed for laboratory use. Although built on a small scale, it is believed this system possessed similar characteristics of the larger systems. That is, trends occurring in the laboratory model should also present themselves in the larger scale models. Throughout these experiments the inlet pressure and exhaust pressure were held constant at 25 psia and

14.4 psia, respectively. Parameters varied were temperature (24 and -40 °C), cycle time, product flow rate, and purge flow rate. The purge flowrate was controlled by installation of different diameter orifices. The dependent variable of primary interest was the steady state oxygen concentration in the high pressure product. Data was collected only after the oxygen concentration in the product had reached a steady state value. The experiment was configured for both two-step and six-step cyclic operation, so that these configurations might be compared and contrasted based on product oxygen concentration, cycle time, and oxygen recovery.

CHAPTER II

BACKGROUND

This section presents a brief history behind the development of synthetic zeolites and the pressure swing adsorption process. Although zeolites have been applied widely in areas such as, catalytic cracking, isomerization, hydrocracking,etc., the ensueing discussion stresses zeolite development as it relates to air separation (13). It should become apparent that without the development of techniques for the manufacture of high quality synthetic zeolites pressure swing adsorption technology would not have evolved as a commercial separation method.

Baron Cronstedt, a Swedish mineralogist, discovered crystalline zeolites in 1756 and was the first to observe that upon heating water is evolved (13). In 1840 Damour noticed that these zeolites could be reversibly hydrated and dehydrated with no apparent change in the crystal structure whatsoever. One hundred and fifty three years after their first discovery Grandjean reported in 1909 that zeolites were capable of adsorbing organic vapors such as iodine, mercury, and ammonia (14). Weigel and Steinhoff in 1925 were the first to observe the molecular sieving properties of zeolites when they reported that chabazite adsorbed methanol, ethanol, and formic acid but excluded acetone, ether, and benzene (15). McBain in 1926 analyzed the Weigel and Steinhoff observations and concluded that the adsorption or exclusion could be explained by a molecular size discrimination process. He proposed the name "molecular sieve" (13).

Although research on zeolites from 1926 to 1948 progressed at a slow pace, some important work was reported. In the 1930's the crytal structures of analcite and natrolite were identified by X-ray diffraction studies (16,17). Also during this period R.M. Barrer of England became intensely interested in zeolite research. His work was instrumental because it suggested future applications of zeolites. In 1938 his experiments with nitrogen and argon showed that nitrogen was more strongly adsorbed on the zeolite, chabazite (21). This he attributed to the polarity of the nitrogen caused by its quadrupole moment interacting with the ionic crystal structure of the zeolite. He is credited with proposing that zeolites could be applied to the separation of normal from isoparaffins and of polar molecules from nonpolar molecules (18,19,20). In 1956 Barrer and Sutherland (25) doncluded that the permanent gases nitrogen, oxygen, and argon are selectively adsorbed based on the magnitude of their quadrupole moments (N2>O2,Ar), and thus the separation of nitrogen and oxygen occurred not due to any molecular sieving action but of different sorption affinity.

Although interest in zeolites grew during this period, the major obstacle confronting their commercial usage was the limited availibility of zeolites. It was recognized by researchers at the time that the unique characteristics of zeolites could only be used to full advantage if the naturally occurring species could be synthesized on a large scale, but prior to 1948 attempts at synthesizing zeolites in the laboratory were unsuccessful.

While investigating new approaches to air separation R.M. Milton of the Union Carbide Corporation became interested in the natural zeolite, chabazite. His belief that a synthetic analogue to chabazite could be developed sparked a research program at Union Carbide which culminated in the development of many synthetic zeolites, some not found in nature. A technological breakthrough occurred when methods were devised to produce these synthetic varieties in large quantities (22,23). The fundamental difference between Milton's approach and earlier attempts was the use of lower crystallization temperatures. He performed his crystallizations at 25 to 150°C, in contrast, to other researchers who employed temperatures in the range of 200 to 400°C. By 1952 type A and type X zeolites had been successfully synthesized by researchers at Union Carbide. Today there are thirty-four known types of zeolitic minerals and about one hundred synthetic varieties (70).

These synthetic zeolites were formed by precipitation from a supersaturated aluminosilicate gel consisting of sodium hydroxide, sodium aluminate, and sodium silicate with excess caustic. The type of components, their concentration in the gel, and a low crystallization temperature are critical factors in the synthesis of high quality synthetic zeolite materials. If the proper conditions are maintained, crystallization will be complete in two hours. This feature made the process economically feasible. A typical synthesis may be represented by the following equations (24),

$$\mathrm{NaOH(aq)} + \mathrm{NaAl(OH)_4\,(aq)} + \mathrm{Na_2SiO_3\,(aq)} \xrightarrow{20^{o}C}$$

$$\underset{\text{(gel)}}{[\mathrm{Na_a(AlO_2)_b(SiO_2)_c}, \mathrm{NaOH}, \mathrm{H_2O}]} \xrightarrow{<150^{o}C}$$

$$\underset{\text{(zeolite crystals)}}{\mathrm{Na_x[(AlO_2)_x(SiO_2)_y]}} \,.\, w\,\mathrm{H_2O} + \text{solution}$$

where,

w = number of water molecules.
y/x = varies between 1 to 5.

After separation from the mother liquor and drying the final product of the above process is a white powder with a particle size of 1 to 5 microns. Before commercial use the powder is impregnated with 20% inert clay binder and formed into pellets to minimize attrition of the crystal structure.

First mention of an industrial process utilizing the concepts of PSA, although not for air separation, was in 1959 by C.W. Skarstrom of Esso Research and Engineering Company, Linden, New Jersey (26,27,28). The apparatus was called a heatless drier because it dried air from a moisture content of 3800 ppm to 1 ppm and exhibited nearly isothermal operation. The unit had two adsorbent beds containing either alumina or silica gel and operated in a cyclic manner by alternating the flow of wet feed air to the two beds (See Fig 2-1). While bed A received a flow of wet air and delivered a product of dry air, bed B was regenerated by venting to atmospheric pressure and purging with some product flow from bed A. The desorbed water vapor was exhausted to the atmosphere, thereby, preparing the bed for the next cycle of operation. The cycles were controlled by an electric timer. Skarstrom noted that the actual volume of the low pressure purge gas had to exceed the actual volume of the high pressure input gas if the system was to produce extremely dry air. The beds remained essentially isothermal because heat liberated during the adsorption step was reclaimed during the desorption or regeneration step.

Surprisely, a similiar system configuration with a different adsorbent finds use today in the area of air separation (See Fig 2-2). Although PSA systems for air separation have become more sophisticated as designers strive for optimization, all systems operate on the same principles as the Skarstrom's heatless drier. An excellent review of the most important patents up to 1973 has been prepared by Lee and Stahl

(1).

Theoretical modeling of PSA systems has progressed in recent years but agreement between the predictions of theoretical models and experimental data rarely occurs unless some degree of empiricism has been incorporated into the model (35,36,37,38,39,40).

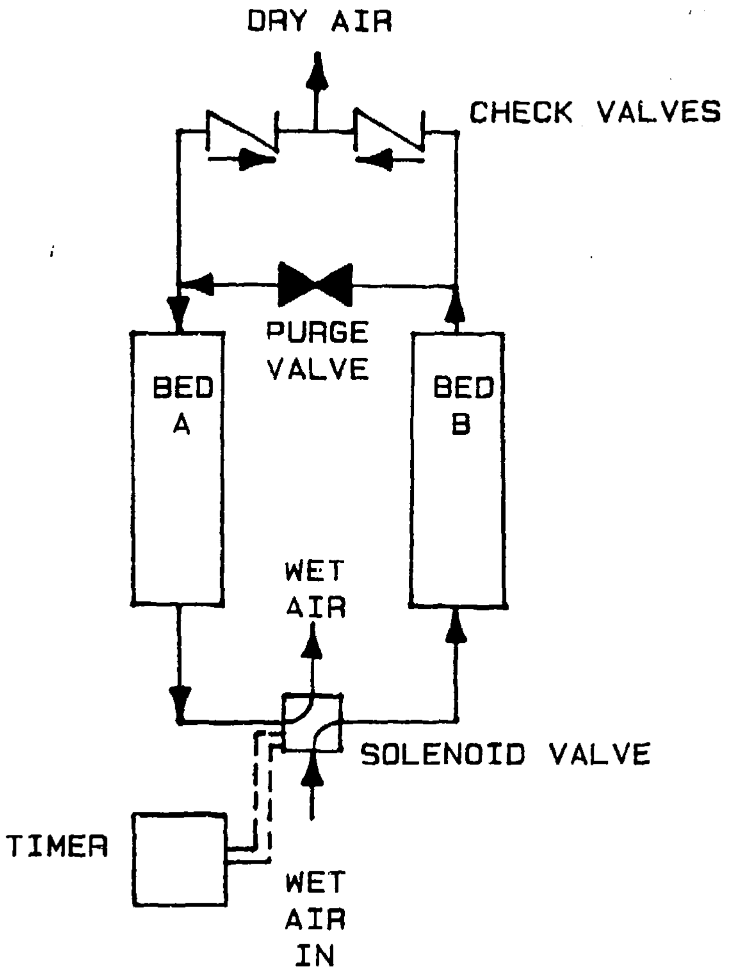

FIG 2-1. SKARSTROM'S HEATLESS ADSORPTION DRYER (27).

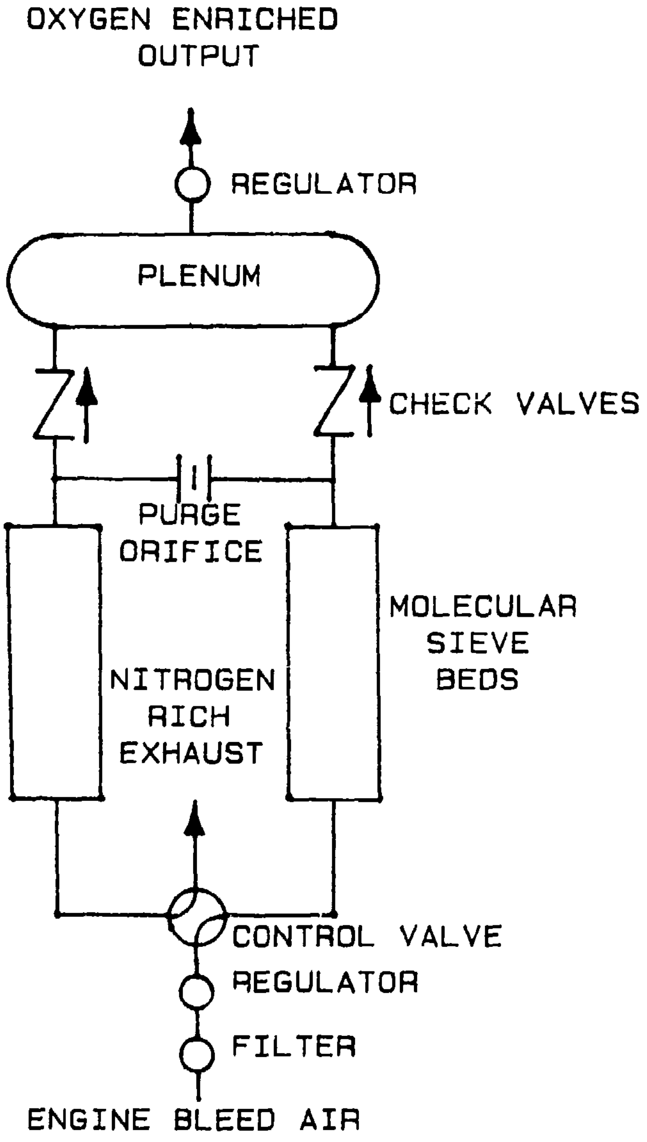

FIG 2-2. SCHEMATIC FLOW DIAGRAM FOR A TWO-MAN MOLECULAR SIEVE OXYGEN GENERATOR (10).

CHAPTER III

LITERATURE AND THEORY

Zeolite Structure

Smith defines a zeolite as " an aluminosilicate with a framework structure enclosing cavities occupied by large ions and water molecules, both of which have considerable freedom of movement, permitting ion exchange and reversible dehydration (29). The hydrated crystallographic unit cell of the type A zeolite is,

$$Me_{12/n}\,[(AlO_2)_{12}\,(SiO_2)_{12}]\,.\,27\,H_2O$$

where, n is the valence of the metal cation Me.

Upon dehydration the zeolite crystal structure will maintain its well defined shape and extremely uniform pore dimensions. The effective pore diameter of zeolites vary from 3 to 10 Angstroms depending on the type of zeolite and the cation present in the structure. The one univalent cation per $(AlO_2)^-$ tetrahedral unit is necessary to maintain electrical neutrality within the structure. These cations are easily exchanged if a different pore size is desired, for instance the Na^+ cations of molecular sieve 4A may be exchanged with Ca^{++} ions to form zeolite 5A.

The unit cell forms a cubo-octahedron building block which is constructed from twelve (AlO_2) tetrahedral units, twelve (SiO_2) tetrahedral units, and the required number of cations. These cubo-octahedrons are positioned at the corners of a 12.32 Å cubic lattice (See Fig 3-1). Entry into the spherical space, alpha or super cage (diameter = 11.3 Å, volume = 776 cubic Angstroms), within the cube is gained by passage through six eight-membered rings of oxygen atoms. In the case of zeolite 5A the effective pore diameter is 4.3 Å but molecules with critical diameters up to 5.5 Å may enter because of the constant vibration of these oxygen molecules. The cubo-octahedron units at the corners also have an internal cavity, beta cage (diameter = 6.6 Å), which can only be entered by the smallest molecules. The eight six-membered oxygen rings permitting access to the beta cage have an effective diameter of 2.2 Å. Only molecules such as water, helium, and ammonia are capable of entering this volume. Adsorption of nitrogen and oxygen only occurs in the alpha cage. The cubo-octahedron units are connected by cubes of oxygen atoms which attach to six four-membered rings. For complete descriptions of zeolite structure see Breck (7).

If an adsorbate molecule's effective diameter is larger than the zeolite pore diameter the molecule will be excluded from the intracrystalline volume, although it may be possible for the molecule to adsorb to the outer surface of the zeolite crystals. This outer surface only represents 1% of the inner surface area therefore, any adsorption here would be extremely small. The internal surface area has been estimated in the region of 800 to 1000 sq. meters/gm (70). Separations based on the exclusion of one or more species are refered to as molecular sieving.

Zeolites interact vigorously with molecules possessing dipole or quadrupole moments due to the ionic nature of the crystal structure. Molecules such as water, carbon dioxide, and nitrogen energetically interact with the potential fields within the zeolite. The strong interaction between the quadrupole moment of the nitrogen molecule and zeolite 5A makes air separation possible.

Sorption in zeolites

Upon dehydration zeolites become active adsorbents. Zeolite adsorption data is usually presented as quantity adsorbed versus pressure of the adsorbate in the gas phase at constant temperature which is referred to as an "isotherm". Adsorption and desorption isotherms for zeolites are usually identical due to the uniform structure of the crystal framework, although hysteresis may occur for some complex molecules.

Since sorption in zeolites is a pore filling process internal volume is the critical parameter and surface area has little meaning. Use of the conventional B.E.T. method for surface area determination is not applicable to zeolites. The pore filling process occurs rapidly sorption occurs nearly instantaneously (diffusional resistance may lengthen this process) and is easily reversed returning the adsorbate molecule and the surface of the zeolite to its original state, as discussed by Young and Crowell (32), Brunauer (81), Breck (7), and Oscik (30) in detailed treatments of physical adsorption.

Physical adsorption is always exothermic as will be shown by the following thermodynamic relationship,

$$\Delta G = \Delta H - T\Delta S$$

The more ordered state of the adsorbate molecule as opposed to its gas phase counterpart requires that the change in entropy decrease. Since adsorption occurs spontaneously, the change in the Gibbs free energy must be negative and furthermore the change in enthalpy must be negative.

The magnitude of the interaction between a diffusing adsorbate molecule and the zeolite framework is directly related to the heat of adsorption. At absolute zero (-273.15°C) (7),

$$\Delta Ha = I_D + I_R + I_P + I_{E-D} + I_{E-Q}$$

where,

I_D = energy contribution due to dispersion.
I_R = " " " " repulsion.
I_P = " " " " polarization.

I_{E-D} = energy contribution due to electrostatic-dipole interaction.

I_{E-Q} = energy contribution due to electrostatic-quadrupole interaction.

$$I_D = -A / r^6$$

$$I_R = B / r^{12}$$

$$I_P = -\omega \tau^2 / 2 r^4$$

$$I_{E-D} = -\tau \kappa / r^2$$

$$I_{E-Q} = \tau Q [3 (\cos \phi)^2 - 1] / 4 r^3$$

where,

τ = charge

ω = polarizability

κ = dipole moment

ϕ = angle between the axis of the quadrupole and the line between the centers of the two molecules.

The dispersion and repulsion energies are present whenever a sorbate molecule enters the zeolite framework. However, due to their small value these energies are only noticeable when the sorbate is a nonpolar molecular, such as argon or oxygen. Furthermore, as the concentration of a nonpolar adsorbate increases, the heat of adsorption also increases slightly reflecting the rise in dispersion/repulsion interactions (34).

The electrostatic interactions between specific adsorbate molecules and the zeolite may be substantial. The largest interaction energies (20-30 kcal/gmol) occur when molecules with permanent dipole moments (i.e. water,ammonia,etc.) enter the zeolite structure. The electrostatic-quadrupole interaction for nitrogen has been estimated at 1.5 to 2.5 kcal/mol (7). The initial heat of adsorption for molecules with dipole or quadrupole moments is generally large due to the availability of energetically active sites at low coverage and decreases monotonically with increasing sorbate concentration as the less energetic sites become occupied.

The strong positive charge of the exchangeable cation can induce dipoles on unsaturated molecules. The resulting polarized molecule is then strongly adsorbed. Attempts to predict equilibrium adsorption isotherms by modeling these interactions have not been successful (41).

The isosteric heat of adsorption, Ha, may be evaluated by applying the Clausius-Clapeyron equation to the two-phase system of gas and adsorbate.

$$\left[\frac{dP}{dT}\right]_c = \Delta Ha \; / \; T(Vg - Va)$$

Since Vg>>Va we can neglect Va with negligible loss of accuracy. Applying the ideal gas law gives,

$$\Delta Ha = R \left[\frac{d\ln P}{dT}\right]_c$$

If equilibrium isotherm data at various temperatures are available, the heat of adsorption may be evaluated. Reported values for oxygen and nitrogen adsorption on molecular sieve 5A are 3.3 and 5.0 Kcal/mole, respectively (46).

Isotherm Models

A. General

In general, the classical isotherm models,i.e. Langmuir, Freudlich, and Temkin (See Table 1), do not adequately represent sorption in zeolites (31,43,44,45,46,47,48). The Polanyi potential theory (61) has been extended for application to zeolitic adsorbents, although its primary value is the correlation of equilibrium data (31). Although these models may be of limited value in arriving at an empirical fit of zeolite data, the basic assumptions simply are not valid for zeolitic sorption.

Table 1. Common adsorption equations (73).

Name	Equation
Langmuir	$\theta = \dfrac{C\,P}{1 + C\,P}$
Freundlich	$\theta = C\,P^{k}$
Temkin	$P = k \exp(\theta)$
Volmer	$P = \dfrac{k\,\theta}{1 - \theta} \exp[\theta(1 - \theta)]$
B.E.T.	$\theta = \dfrac{c\,x}{(1 - x)\,[1 + (C - 1)x]}$
Sips	$\theta = \dfrac{(C\,P)^{k}}{1 + (C\,P)^{k}}$

Where: k = f(T), C and c = constants.

Although the Langmuir model has limited value in empirically fitting zeolite isotherm data for non-polar molecules, the basic postulates of this model render it useless in predicting zeolite adsorption isotherms. The assumption of a energetically uniform surface with distinct adsorption sites with no sorbate-sorbate interaction cannot explain the energetic heterogeneity of the zeolite toward molecules with dipole or quadrupole moments, nor can it account for the pore filling nature of zeolites.

The equation suggested by Sips (49) which combines the Freundlich and the Langmuir isotherms is successful as an empirical equation but the constants in this equation have little physical meaning. Additionally, the Sips model, Freundlich model, and Temkin model will not reduce to Henry's Law at very low pressures which Hill (50) has shown to be an important limit for adsorption equations.

B. Statistical Thermodynamic Approach

Ruthven (52) suggested an adsorption isotherm model based on statistical thermodynamics and applicable to zeolitic adsorption. He reasoned that zeolites are well defined, uniform structures and, therefore, it should be possible to analyze the adsorption process using statistical thermodynamics and arrive at a predictive model.

A number of studies which revealed the volume filling characteristics of zeolites led to the development of the statistical thermodynamic model. Barrer (21) observed that the apparent saturation values decrease linearly with temperature (See Table 2). He speculated that the volume of the sorbed molecules increase linearly with temperature. Barrer and Sutherland (53) concluded that at high temperatures the amount sorbed was determined by the affinity of the sorbate for the zeolite but at low temperatures and pressures the amount sorbed depended on the molecular volume of the sorbate molecule and its packing density. It appeared that the intracrystalline fluid had some of the properties of the bulk liquid (25,51). Another has speculated that adsorption in zeolites might be viewed as filling the intracrystalline volume with liquid sorbate (31). By linear interpolation between the saturated liquid molecular volume at the normal boiling point and the van der Waals molecular volume b at the critical temperature, the effective molecular volume could be estimated (31,56,57) and the saturation capacity of the zeolite could be predicted with reasonable accuracy by dividing the cavity volume V by the effective molecular volume B (55). This concept of volume filling forms the basis of the statistical thermodynamic model.

Table 2. The apparent saturation of sorption at different temperatures (21).

Zeolite	Gas	Temp. (K)	Apparent Saturation (cc NTP/gm)
chabazite	N2	89.2	164.0
		194.5	75.2
	+ N2	83.0	170.0
		193.0	90.0
analcite	N2	79.5	30.3
		194.5	15.1
	H2	62.2	33.0
		78.5	27.7
		90.0	23.7

+ Data of Rabinowitsch and Wood (54).

The derivation of the pure component isotherm equation based on the statistical thermodynamic model is presented below. More detail is given by Hill (50) and Ruthven (52).

Each zeolite cavity is assumed to be a totally independent site for adsorption, i.e. interaction with neighboring cavities are neglected. Consider a macroscopic system of M equivalent, independent, distinguishable cavities which contain s sorbate molecules where the number of sorbate molecules/cavity range from zero to m. Let the partition function below represent the cavity with s sorbate molecules adsorbed.

$$q(s) = \sum_j \exp(- \epsilon_j(s) / kT)$$

Let N be the total number of sorbate molecules in the system and a_s be the number of cavities with s molecules, then the canonical ensemble partition function for the system is,

$$C(N,M,T) = \sum_{\underline{a}} \frac{M!\, q(0)^{a_0}\, q(1)^{a_1} \ldots q(m)^{a_m}}{a_0!\, a_1! \ldots a_m!}$$

where, $\underline{a} = a_0, a_1, \ldots, a_m$ satisfying the restrictions:

$$\sum_{s=0}^{m} a_s = M \quad \text{and} \quad \sum_{s=0}^{m} s a_s = N$$

The grand partition function G is:

$$G = \sum_{N=0}^{mM} C(N,M,T)\,\lambda^{N}$$

$$G = \sum_{\underline{a}} \frac{M!\, q(0)^{a_0}\,[q(1)\,\lambda]^{a_1}\,[q(2)\,\lambda^{2}]^{a_2} \ldots [q(m)\,\lambda^{m}]^{a_m}}{a_0! \ldots a_m!}$$

Where the grand partition function may be represented as a product of a subsystem of grand partition functions,

$$G(\lambda,M,T) = Q(\lambda,T)^{M}$$

where,

$$Q = q(0) + q(1)\lambda + \ldots + q(m)\,\lambda^{m}$$

$$'' = \sum_{s=0}^{m} q(s)\,\lambda^{s} \quad \text{or,}$$

$$G(\lambda,M,T) = [\sum_{s=0}^{m} q(s)\,\lambda^{s}]^{M} = Q^{M}$$

Finding the average number of molecules in the macroscopic system,

$$n = \overline{N} = \lambda[\partial \ln G/\partial\lambda]_{M,T} = M\lambda[\partial \ln Q/\partial\lambda]_{T}$$

Then the average number of molecules/cavity c is:

$$c = \frac{n}{M} = \lambda[\partial \ln Q/\partial\lambda]_T = \frac{\sum_{s=0}^{m} sq(s)\,\lambda^s}{\sum_{s=0}^{m} q(s)\,\lambda^s}$$

Since $Z(s)\,a^s = q(s)\,\lambda^s$ where,

Z(s) is the configuration integral then,

$$c = \frac{n}{M} = \sum_{s=0}^{m} \frac{sZ(s)a^s}{Z(s)a^s} = \frac{Z_1 a + 2Z_2 a^2 + \ldots + mZ_m a^m}{1 + Z_1 a + Z_2 a^2 + \ldots + Z_m a^m}$$

where the configuration integral Z_s is:

$$Z_s = \frac{1}{s!}\int_V \exp[-U_s(r_1 \ldots r_s)/kT]\,dr_1 \ldots dr_s$$

and r_i = position vector, V = volume of the cavity, k = Boltzmann's constant, T = absolute temperature, U_s = potential energy for the subsystem, a = activity of the sorbate = p/kT for an ideal gas.

To evaluate the configuration integrals in terms of measurable quantities is very difficult therefore, the adsorbed molecules are treated as a van der Waals gas (52), and the following assumptions are applied:

(1) The form of the potential field within the cavity is independent of the number of molecules in the cavity.

(2) When two or more molecules are in the cavity, they move randomly and independently, and the molecular interaction is simply expressed as a reduction in free volume.

(3) The energy of interaction between sorbate molecules may be represented by the Sutherland potential as in the derivation of the van der Waals equation (50) :

$$U(r) = \infty\ ,\ r < \sigma\ ;\ U(r) = -\ \xi\,(\sigma / r)^{6}\ ,\quad r \geq \sigma$$

This potential assumes rigid spheres of diameter σ which attract each other according to an inverse power law. This model is simple and fairly accurate (74). These approximations give the following configuration integral,

$$Z_{s} = \frac{Z_{1}^{s}}{s!}\,(1 - sB/V)^{s}\,\exp(sB\,\xi / V\kappa T)$$

$$2 \leq s < V/B$$

where,

ξ and σ are molecular constants from the Sutherland potential function (in the absence of available Sutherland constants Lennard-Jones constants are generally used). The resulting equation for the adsorption of a pure component gas has been shown by Ruthven (52) to be:

$$c = \frac{Kp + (Kp)^2 (1-2B/V)^2 \exp(2B\xi/VkT) + \ldots + \frac{(Kp)^m}{(m-1)!} (1-mB/V)^m \exp(mB\xi/VkT)}{1 + Kp + \frac{1}{2!}(Kp)^2 (1-2B/V)^2 \exp(2B\xi/VkT) + \ldots + \frac{(Kp)^m}{m!} (1-mB/V)^m \exp(mB\xi/VkT)}$$

Where K is the Henry's Law constant and,

$$Kp = Z_1 a = Z_1 p/kT$$

$$m \leq V/B$$

c has units of molecules/cavity.

Based on estimates of available force constants it has been shown that the $\exp(mB \xi / VkT)$ term in the configuration integral which accounts for the intermolecular attraction of the sorbate molecules is generally small (46). Therefore, the configuration integral may be simplified to give,

$$Z_s = \frac{Z_1^s}{s!} (1 - sB/V)^s$$

The resulting isotherm equation then is,

$$c = \frac{Kp + (Kp)^2 (1 - 2B/V)^2 + \ldots + \frac{(Kp)^m}{(m-1)!} (1 - mB/V)^m}{1 + Kp + \frac{1}{2!} (Kp)^2 (1 - 2B/V)^2 + \ldots + \frac{(Kp)^m}{m!} (1 - mB/V)^m}$$

The (1 - mB/V) term corrects for the reduction in cavity volume which implies the integer $m \leq V/B$ since the correcting term must not be negative. Restricting m to integer values is a weakness in the model since experimental data generally do not conform to this assumption. In the model the Henry's Law constant K accounts for the sorbent-sorbate interaction and , B, the effective molecular volume, accounts for the sorbate-sorbate interactions. At low pressures this equation reduces to the familiar Henry's Law equation. Although K may be calculated theoretically for simple systems (52), generally its value is determined from experimental isotherm data at low pressures. A problem arises in selecting a value for B, the effective volume of the molecule, since the molar volume of the sorbate varies with temperature. The use of b, the van der Waals covolume, suggested in earlier work (52) has limited value. The value for B may be estimated by linear interpolation between van der Waals b at the critical temperature and the molecular volume of the saturated liquid at the boiling point (56,45). More recently Ruthven (46) suggested superimposing a plot of the theoretical isotherm curves with vary values of V/B over the actual isotherm data plotted on the same coordinates. K values may be predicted over a range of temperature from a vant Hoff plot where the K values derived from the data have been fit to a straight line and represented by the equation,

$$K = Ko \exp (qo / RT)$$

Although the assumptions may seem crude, this model has been widely and successfully applied for zeolite adsorption (31,45,46,52,58,75). The model is not without limitations, however. For systems approaching saturation ($\theta > 0.9$) this model may give unsatisfactory results (46). The model may also be inappropriate for adsorption of monotomic molecules and small polar molecules which tend to collect at the localized sites (31).

The statistical thermodynamic model can be extended to predict multicomponent mixture equilibria. Presented below is the derivation of the model equations for a binary mixture. For greater detail refer to Hill (50) and Ruthven (45). Proceeding with the same assumptions given for the pure component model, the grand partition function for the two component (A+B) mixture may be given as,

$$G_{AB} = \left[\sum_{j} \sum_{i} q(i,j) \lambda_A^{i} \lambda_B^{j} \right]^{M} = Q_{AB}^{M}$$

where $q(i,j)$ is the partition function for a cavity containing i molecules of A and j molecules of B. This summation must include all values of i and j which satisfy,

$$i B_A + j B_B \leq V$$

Since $q(i,j)\,\lambda_A^i\,\lambda_B^j = Z(i,j)\,a_A^i\,a_B^j$ then,

$$c_A = \frac{n_A}{M} = \lambda_A\left[\partial \ln Q_{AB}/\partial \lambda_A\right]_{\lambda_B,T} = \frac{\sum_j \sum_i i\,Z(i,j)\,a_A^i\,a_B^j}{\sum_j \sum_i Z(i,j)\,a_A^i\,a_B^j}$$

and,

$$c_B = \frac{n_B}{M} = \lambda_B\left[\partial \ln Q_{AB}/\partial \lambda_B\right]_{\lambda_A,T} = \frac{\sum_j \sum_i j\,Z(i,j)a_A^i\,a_B^j}{\sum_j \sum_i Z(i,j)a_A^i\,a_B^j}$$

The expressions for the configuration integrals are,

$$Z(0,0) = Z(0) = 1$$

$$Z(1,0)\,p_A/kT = Z(1,0)\,a_A = K_A p_A$$

$$Z(0,1)\,p_B/kT = Z(0,1)\,a_B = K_B p_B$$

$$Z(i,j) = \frac{Z(1,0)^i\;Z(0,1)^j}{i!\;j!}\,(1 - iB_A/V - jB_B/V)^{i+j}$$

Neglecting the sorbate-sorbate interaction term the final equations are,

$$c_A = \frac{K_A p_A + \sum_j \sum_i \dfrac{i(K_A p_A)^i\,(K_B p_B)^j\,(1 - iB_A/V - jB_B/V)^{i+j}}{i!\;j!}}{1 + K_A p_A + K_B p_B + \sum_j \sum_i \dfrac{(K_A p_A)^i\,(K_B p_B)^j\,(1 - iB_A/V - jB_B/V)^{i+j}}{i!\;j!}}$$

$$c_B = \frac{K_B p_B + \sum_j \sum_i \dfrac{j(K_A p_A)^i (K_B p_B)^j (1 - iB_A/V - jB_B/V)^{i+j}}{i!\, j!}}{1 + K_A p_A + K_B p_B + \sum_j \sum_i \dfrac{(K_A p_A)^i (K_B p_B)^j (1 - iB_A/V - jB_B/V)^{i+j}}{i!\, j!}}$$

where the summations are carried out over all values i and j satisfying both restrictions:

$$i + j \geq 2 \quad \text{and} \quad iB_A + jB_B \leq V$$

K_A, K_B, B_A, B_B are determined from the pure component isotherm data Since all parameters are known c_A and c_B may be calculated explicitly to give the mixed gas equilibria from the pure component data. This binary model has been applied successfully to a number of systems (45,46). Recently, the binary model gave an excellent representation of the oxygen-nitrogen equilibrium data of Sorial, Granville, and Daly (71) over the temperature range 278.15°K to 303.15°K and at total pressures of 1.7 and 4.4 bar. Furthermore, this method has been used to analyze the equilibrium data gathered in this work, as discussed in Chapter V.

C. The Ideal Adsorbed Solution Theory

The ideal adsorbed solution theory (IAST) of Myers and Prausnitz (60) represents zeolitic adsorption in certain systems (59). Ideal behavior implies that the components in a multicomponent mixture adsorb as if they were present as pure components at their partial pressure in the mixture. Ruthven (45) has shown that when $B_A \approx B_B$ and either,

$$\xi_A \approx \xi_B \quad \text{or} \quad B_A \xi_A / VkT, B_B \xi_B / VkT << 1$$

the statistical thermodynamic model predicts that ideal behavior should be observed even at high sorbate concentrations. In addition, ideal behavior will also occur if the sorbate concentration is less than about one molecule/cavity, even if the effective molecular volumes differ widely. Conversely, when these characteristics do not occur the system will tend toward nonideality.

IAST proposes that Raoult's Law, which has been used extensively for vapor-liquid equilibria of ideal mixtures, may be adapted for use in predicting mixed gas adsorption. Both equations are shown below for comparison,

T = constant

$$P y_i = P(T)_i^{sat} x_i \quad \text{(vapor-liquid equilibria)}$$

$$P y_i = P_i^o(\Pi) x_i \quad \text{(mixed gas adsorption)}$$

where,

Π = spreading pressure

$P(T)_i^{sat}$ = vapor pressure of component i at temperature T.

$P_i^o(\Pi)$= pressure that would be exerted by pure i at the spreading pressure of the system.

The adsorbates are assumed to have equal spreading pressures.

The thermodynamic equations which describe the mixed gas adsorption system require the following assumptions (60):

(1) The adsorbent is assumed to be thermodynamically inert. This implies that the change in thermodynamic properties, such as enthalpy, internal energy,etc., are small compared to the changes of these same properties for the adsorbing gas.

(2) The ideal gas law applies.

(3) The adsorbent has a temperature invariant area for adsorption which is the same for all adsorbates.

(4) Gibbs definition for adsorption applies (72), that is, ne, the surface excess amount of sorbed gas, is the excess number of moles of i present in the system above that number present in a reference system where no adsorption occurs at the same equilibrium pressure (30). The volumetric technique gives the experimental isotherms in terms of the surface excess (60).

The development of the IAST equations shown below may be found in Myers and Prausnitz (60). In writing the thermodynamic equations for the adsorbed phase, we substitute the spreading pressure, Π, for pressure, P, and substitute area, A, for the volume, V.

$$dU = TdS - \Pi\, dA + \sum \mu_i\, dn_i$$

$$dG = - SdT + A\, d\Pi + \sum \mu_i\, dn_i$$

Hence, the work term is ($-\Pi dA$), and since Π is positive for physical adsorption, the adsorbed phase does work on the adsorbent.

The Gibbs adsorption isotherm (72) is,

$$- A\, d\Pi + \sum n_i\, d\mu_i = 0 \quad \text{(constant T)}$$

which upon integration gives,

$$\Pi(P_i^o) = \frac{RT}{A} \int_{t=0}^{P_i^o} n_i^o(t)\, d\ln(t)$$

where t is a dummy variable. This integral is evaluated graphically by plotting n_i^o / P_i^o versus P_i^o and finding the area under the curve. The evaluation of this integral requires the pure component isotherm data at the proper temperature, i.e. $n_i^o = F(P_i^o)$. This step results with,

$$\Pi_1^o = F(P_1^o)$$

$$\Pi_2^o = F(P_2^o)$$

We may then write:

$$P y_1 = P_1^o x_1$$

$$P y_2 = P_2^o x_2$$

Assuming constant Π ,

$$\Pi_1^o = \Pi_2^o$$

$$1 = x_1 + x_2$$

$$1 = y_1 + y_2$$

There are nine unknowns and seven equations, so that, we must define two variables in order to analytically determine the remaining seven. The total adsorbed is subsequently found by,

$$n_t = \frac{1}{\frac{x_1}{n_1^o} + \frac{x_2}{n_2^o}}$$

where n_1^o and n_2^o are the amounts of pure component 1 and component 2 adsorbed at Π and T.

The advantages of the IAST are its elimination of a specific isotherm model and its simple computational method but this theory does have some drawbacks. Pure component data must be available at the desired temperature over a wide pressure range. Without a model, use of the theory outside the range of the available data is questionable. Assumption of equal areas of adsorption for all adsorbates may not be valid for zeolites where the area will depend on the effective molecular volume of the sorbate (60). The assumption that the adsorbent is thermodynamically inert may not be completely valid for zeolites. These drawbacks are not drastic, however, for permanent gases in zeolite 5A. Results of data analysis by this method are given in Chapter V.

Diffusion

A. Background

Important factors which influence the rate of diffusion in zeolite systems are: temperature, the rate at which diffusing molecules can reach the surface of the crystals (here we assume a system of zeolite pellets), the size of the molecules with respect to the size of the zeolite pores, the strength of the interactions between zeolite and the molecules, and adsorbate concentration. The resistances to zeolitic diffusion can be categorized as: external fluid film, macropore or intercrystalline, and micropore or intracrystalline (31). The macropore and micropore resistances are generally considered the most important.

The external fluid film resistance which occurs at the boundary of the zeolite pellet has been well studied. This resistance is generally of little importance in zeolite systems because the bulk fluid velocity is usually sufficient to minimize this effect (31). On the other hand, the macropore resistance, which involves the passage of the molecules through the elaborate pore system of the clay binder, may occur by the mechanism of Knudsen or by molecular diffusion, and has been shown (at least in some systems) to influence the overall rate of diffusion. Variation of the pellet size will reveal whether macropore resistance is significant. In many systems the rate of crystal surface diffusion is rapid, therefore, the assumption of local equilibrium at the crystal surface is valid (31). The relative magnitudes of external or bulk diffusion, macropore diffusion, and micropore diffusion are 10^{-1}, 10^{-3}, 10^{-11} cm^2/sec, respectively (7).

Intracrystalline diffusion in most cases is the rate limiting step in the diffusion process due to the combined effects of the molecular dimensioned channels and the strong potential fields emanating from the crystal framework. Investigations of activation energies and diffusion coefficients for the adsorption of gases suggest the diffusing molecule encounters periodic potential fields within the zeolite (7). As a result, attempts at predicting equilibrium isotherms, heats of adsorption, and diffusivities through the use of idealized models of the potential fields have been unsuccessful (41).

A number of investigations have attempted to determine whether the diffusion rate controlling step in zeolites occurs in the macropore or the micropores. Kondis and Dranoff (63) studied the diffusion of ethane in synthetic type A zeolite. Both pelleted and powdered zeolite gave identical diffusion rates and equilibrium data. Since the powdered form had no binder (hence no macropore system) it was concluded that intracrystalline diffusion was the controlling mechanism. In another experiment using erionite, a natural zeolite, both 1/8" pellet and 20X35 mesh granules gave rates of diffusion of the same order of magnitude, therefore, intracrystalline diffusion was reported as the controlling mechanism (76). In a third study, the rate of diffusion was compared using synthetic zeolite NaA pellets with an inert binder and pure crystals. The equilibrium data were corrected due to the presence of the binder. The results of the work indicated both had identical rates of diffusion and equilibrium data,i.e. the binder did not affect the rate of diffusion (77). In a fourth experiment, the rates of diffusion through pellets of NaA and CaA were measured using ethane. The calculated micropore and macropore diffusivities revealed that for NaA micropore diffusion was the limiting rate mechanism, but for CaA both macropore and micropore diffusion appeared to be important (7). Obviously, intracrystalline diffusion plays a significant role in most zeolite systems.

Zeolite diffusivities display a dramatic exponential sensitivity toward temperature indicative of an activated rate process (31). At very low temperature CO2, N2, and Ar adsorption on zeolite 4A is hindered because these molecules do not possess sufficient activation energy to pass through the narrow openings. Breck (7) reports that the rate of adsorption of argon and nitrogen on zeolite A powder decreases rapidly with temperature. Nitrogen will require a large activation energy for diffusion because of its strong quadrupole interaction with the zeolite (78).

Ruthven's (31) study of the diffusion of monotomic and diatomic gases in type A zeolite shows an interesting concentration dependence. In zeolite 5A the diffusivity dramatically drops in the Henry's Law region from an initially high value to a minimum value at about one third of the saturation concentration, and as concentration increases the diffusivity dramatically rises (31). This behavior is indicative of a collisional diffusion mechanism where the mean free path of the diffusing molecule is determined by the intermolecular collisions. This suggests that, when the molecules are sufficiently small relative to the windows, they pass freely from cavity to cavity and the collisional mechanism controls diffusion.

It has been pointed out that the true driving force for diffusion in zeolites is the gradient of the chemical potential rather than the concentration gradient (31). Therefore, since most early studies were based on the concentration gradient their results, particularly at high concentrations of adsorbate are questionable. The proper equation for the Fickian diffusivity D is,

$$D = D_o \, (d \ln p \, / \, d \ln c)$$

where,

$$D_o = D'_o \, / \, c$$

$$D'_o = D'_* \exp(- E \, / \, RT)$$

D_o is the diffusivity at zero concentration.

The term (dlnp/dlnc) would be equal to one at low concentration and at high concentrations becomes significant. For diffusion data of oxygen, nitrogen, and argon on zeolite 5A (See Table 3).

Table 3. Diffusion data for O2, N2, and Ar on zeolite 5A (62).

System	(A)	E (Kcal)	$D^{*'} \times 10^{7}$ (molecules cm^2 / cavity sec)
Ar-5A	3.4	<<1.0	0.01
O2-5A	3.5	1.0	0.026
N2-5A	3.7	1.5	0.052

In studies concerning the diffusion of water in zeolites the size of the water molecules (2.8 Å) eliminates any consideration that molecular size affects the diffusion process. Instead, the strong dipole moment of the water molecule interacts with the zeolite cations such that the molecules will actually cluster at the sites (7).

B. Experimental Methods

A number of techniques are available for the experimental measurement of diffusivities such as volumetric, gravimetric, and chromatographic (31). The simplest method is to measure transient adsorption/desorption curves. For a system of spherical particles subjected to a step change in concentration,

$$\frac{m_t}{m_\infty} = \frac{2A}{\upsilon}\left(\frac{D\ t}{\pi}\right)^{0.5} \qquad (m_t \ / \ m_\infty < 0.25)$$

$$'' = 1 - \frac{6}{\pi^2}\sum_{n=1}^{\infty}\frac{1}{n^2}\exp[-n^2 \pi^2 D\ t/ r^2]$$

and $A/\upsilon = 3/r$.

Listed below are some of the problem areas associated with obtaining reliable diffusivity data.

(1) Intraparticle diffusion must be the rate limiting process.

(2) Pressure (during step changes of concentration) must remain nearly constant.

(3) Isothermal conditions must be maintained.

(4) Differential measurements should be taken due to possible temperature effects over large intervals.

(5) Zeolite must be activated thoroughly before use because water in the bed will greatly affect the results.

(6) Crystals should not possess structural defects.

Rate experiments performed using breakthrough studies [illegible] packed column filled with adsorbent should give, in principle, the same zeolitic diffusivities as those obtained from the gravimetric method, but this method is generally not reliable (64). Breakthrough curves obtained from this technique are simply concentration profiles representing the mass transfer front at the effluent end of the column when a step change in concentration is applied to the bed inlet. The shape and time required for breakthrough of the front provides valuable information about the mass transfer resistance and operational parameters of the column. The length of the front will vary depending on the inlet flowrate, temperature, precsure, particle size, and the effects of coadsorbables. Under isothermal conditions the shape of the front is partially dependent on the adsorption rate. If the adsorption process is rapid, the front would appear almost vertical for a favorable isotherm in the absence of dispersion effects.

Separation Factor

The binary mixture separation factor is defined as,

$$\alpha_{(x,y,z)} = \frac{X_A Y_G}{X_G Y_A}$$

where,

X_A = mole fraction of component X in the adsorbed phase.

X_G = mole fraction of component X in the gaseous phase.

Y_A = " " " " Y " " adsorbed " .

Y_G = " " " " " " " gaseous " .

x = more strongly adsorbed component.

y = less " " " .

z = adsorbent.

For a binary mixture is a measure of the adsorption selectivity of the adsorbent toward adsorbates X and Y. If the value of $\alpha >> 1$, the adsorbent preferentially adsorbs component X, thus separation of components X and Y is possible. If $\alpha \sim 1$ the separation of components X and Y will be difficult or impossible.

Since the value of α is based on equilibrium data an $\alpha > 1$ is a necessary but not a sufficient criteria in determining the feasibility of a separation process. An extremely slow rate may render the separation infeasible. Predictions of α from pure component data have been unsuccessful. Therefore, α should be ascertained experimentally.

Sorial, Granville, and Daly (71) report α(N2,O2,5A) is relatively insensitive to temperature and pressure changes. Ruthven (46) has drawn some general conclusions about the relationship of the effective molecular volumes of the sorbates, separation factor, and system operating parameters. Where the component with the smaller effective molecular volume is adsorbed more strongly increases with increasing pressure, and conversely, where the component with the larger effective molecular volume is more strongly adsorbed (as in the case of the N2-O2 system) decreases with increasing pressure.

Domine and Hay report the following separation factors for the nitrogen-oxygen binary mixture at $20^{o}C$ (See Table 16).

Table 16. Separation factors reported by Domine and Hay (67).

	5A	13X
(N2,O2)	2.75	2.36
(O2,Ar)	1.08	1.10

Description of a PSA Process

Pressure swing adsorption (or as a two column version of the process is sometimes called, heatless adsorption) is capable of separating gas mixtures due to preferential adsorption of one or more of the components in the gas mixture. The process is operated on short cycles, whereby the high pressure feed is introduced to the columns of adsorbent in an alternating fashion, consequently, the less strongly adsorbed component or components concentrate in the product flow and the more strongly adsorbed components are collected in the exhaust/waste stream. For a nitrogen- oxygen separation regeneration of the beds is accomplished by pressure reduction, and a combination of displacement and purge stripping with the low pressure oxygen enriched purge flow. Critical parameters in the operation of the system are cycle time and purge/feed ratio.

We restrict our discussion to a two column system capable of operation at two- or six-steps per cycle (See Fig 3-2 and 3-3). The six-step system will be discussed first because the two-step system is a simplification of this system. Nitrogen-oxygen separation is considered with an adsorbent of molecular sieve 5A. The exhaust pressure P_L is assumed to be atmospheric pressure. Argon is neglected in the discussion, although in an actual air separation process it usually emerges in the product or enriched oxygen flow. A simplified schematic diagram of the flows associated with a 6-step and a 2-step system is shown (See Fig 3-4).

6-Step Cycle:

(1) Feed air at high pressure P_H enters column A through valve 3 while product oxygen-enriched flow exits through valve 5. Column B depressurizes from P_H to P_L by exhausting waste gas (slightly nitrogen-enriched air) through valve 1.

(2) Feed air and product flows continue as in step 1 ,valve 7 opens diverting a portion of the product flow through an orifice and countercurrently down column B finally exhausting through valve 1. Henceforth, this product flow which passes

through the columns countercurrently will be referred to as low pressure purge flow. The orifice may have a fixed diameter or in more sophisticated systems will be replaced by a variable flow control valve.

(3) Feed air and product flows continue as in step 1 but valve 1 closes and column B begins repressurization with a portion of the product flow from column A.

Column A and B reverse roles:

(4) Feed air at high pressure enters column B through valve 2 while product leaves through valve 6. Column A depressurizes through valve 4.

(5) Feed air and product flows continue as in step 4 and valve 7 opens to begin purging column A.

(6) Feed air and product flow continue as in step 4 but valve 4 closes as column A begins to repressurize with a portion of the low pressure purge flow from column B. This completes one cycle of operation.

2-Step Cycle.

(1) Feed air at high pressure repressurizes column A, product flow exits column A, and purge flow from column A passes through column B discharging at valve 1. Column B depressurizes to P_L and is countercurrently purged by flow from column A.

(2) Feed air at high pressure repressurizes column B, product

flow leaves column B, and purge flow from column B passes countercurrently through column A leaving through valve 4. Column A depressurizes to P_L and is purged by flow from column B. This completes one cycle of operation.

Brief Review of the Equilibrium Theory for Modeling PSA Processes

Shendalman and Mitchell (35) modeled a heatless adsorption process for separating a trace contaminant (1.09% CO2) which is preferentially adsorbed from a nonadsorbable carrier stream of helium. This specific feed gas was chosen to minimize the effect of coadsorbables and to ensure the concentration of CO2 at the feed pressure had nearly linear isotherms. The theoretical approach was based on the theory of parametric pumping developed by Pigford et.al. (79).

The model was applied to a four-step/cycle process (See Fig 3-5). During step 1 feed passes through column A producing a product flow and simultaneously a portion of this product flow is passed countercurrently through column B for purging accumulated adsorbate. In step 2 column A is depressurized and column B is repressurized to the inlet feed pressure. In step 3 and 4 the columns reverse roles. In step 3 high pressure feed enters column B and a product flow leaves while a portion of the product flow is diverted to column A for purging. In step 4 column A is repressurized to the feed pressure and column B enters blowdown or depressurization. It should be noted that during steps 2 and 4 the product flow from the columns ceases.

Two major assumptions were incorporated into the model equations. Firstly, equilibrium is always assumed to exist between the adsorbate and adsorbent. Secondly, a linear isotherm is assumed for the adsorption of CO_2 at its concentration and pressure in the feed gas. Other assumptions believed to be of less importance were:

(a) A non-adsorbing carrier gas, present in large excess.

(b) Isothermal process.

(c) One dimensional flow with no axial dispersion.

(d) Negligible pressure drop through the bed. This implies a linear velocity gradient in the bed.

(e) Ideal gas law applies.

A one dimensional component mass balance gives,

$$\varepsilon[\ (\partial c/\partial t) + \partial(vc)/\partial z)\ ] + (1 - \varepsilon)\ \partial n/\partial t = 0$$

ε = void fraction.

c = molar density in the gas phase.

n = molar density in the adsorbed phase.

t = time.

z = position.

v = interstial velocity.

y = mole fraction of adsorbate in gas the gas phase.

P = total pressure.

k = partition coefficient.

For an ideal isothermal compressible flow the equation of continuity is,

$$\partial P / \partial t + \partial vP / \partial z = 0$$

Let n = kc and combine,

$$P[\,\varepsilon + (1-\varepsilon)k]\,\partial y/\partial t + \varepsilon pv\,\partial y/\partial z + (1-\varepsilon)\,ky\,\partial P/\partial t = 0$$

This hyberbolic partial differential equation is solved by the method of Lagrange-Charpit or method of characteristics to yield a pair of ordinary differential equations,

$$dt/P[\,\varepsilon + k(1-\varepsilon)] = dz/\,\varepsilon Pv = -dy/(1-\varepsilon)\,ky\,(\,\partial P / \partial t)$$

The equations will then reveal the concentrations within the process with respect to time and position and afford an opportunity to investigate the effects of the individual parameters.

It was shown that only if the purge/feed ratio, $R = L_L/L_H > \{(P_H/\ P_L)\ \varepsilon/[\varepsilon + k(1-\varepsilon)]\}$ and no breakthrough of feed into the product occurs then the process will give perfect cleanup of the feed.

L_L = hypothetical penetration distance of a concentration front in a low pressure bed.

L_H = hypothetical penetration distance of a concentration front in a high pressure bed.

If $R \leq (P_H/P_L)\varepsilon/[\varepsilon + k(1-\varepsilon)]$ the process has inadequate purge flow and is not capable of perfect cleanup. The experimental data indicated an Rcrit (i.e. the minimum value of R which gives low concentrations of CO2 in the product) existed and was approximately equal to 1.2. The theory suggests that the CO2 level in the product is independent of R once the Rcrit is reached.

The experimental data and the predictions from the model gave poor agreement. Possible reasons for the discrepancies were non-linear isotherm, rate processes, and dispersion. The model did give qualitative agreement and led to improved understanding of the process.

In a later study Mitchell and Shendalman (36) extended their mathematical model for a trace contaminent which is preferentially adsorbed in an non-adsorbable carrier to include a mass transfer resistance. In these experiments the configuration of the process remained unchanged. The previous assumptions of equilibrium between the adsorbate and the adsorbent was replaced by a single mass transfer coefficient. The controlling step was assumed to be in the pores of the adsorbent pellet. The final mass balance equation was,

$$\varepsilon P v/RT\ \partial v/\partial z + \varepsilon p/RT\ \partial y/\partial t = -(1-\varepsilon)\ k_p A_p\ (K\ Py/RT - n)$$

$$\partial n/\partial t = k_p A_p\ (Kpy/RT - n)$$

k_p = mass transfer coefficient.

A_p = mass transfer area.

The following characteristic trajectories were obtained using the method of characteristics,

$$dy/dz = \frac{-(1-\varepsilon)k_p A_p (KPy/RT - n)}{\varepsilon Pv/RT} \qquad \text{(gas phase)}$$

$$dz/dt = v \qquad \text{(gas phase)}$$

$$dn/dt = k_p A_p (Kpy/RT - n) \qquad \text{(adsorbate)}$$

$$dz/dt = 0 \qquad \text{(adsorbate)}$$

Two approaches are undertaken in the analysis to identify the bounds of the process. In the first we assume equilibrium between the gas and sorbate occurs during steps 1 and 3 of the process. In the second we assume the pressure changes are so rapid that no mass transfer occurs between the gas and the solid. The values for K and $k_p A_p$ were determined by a breakthrough curve run at 4 atm. pressure. The mass transfer coefficient was assumed to be constant throughout the process. Comparison with experimental data was poor since the observed data fell between the two approaches taken but closer to the equilibrium approach. Qualitative agreement was achieved since the approaches did bracket the data.

Chan, Hill, and Wong (80) extended the equilibrium model to include separations of two components both adsorbable but one is a preferentially adsorbed trace contaminent. The assumptions were:

(1) Equilibrium exists between the gas and solid at all times.

(2) Isothermal operation.

(3) Pressure drop through each bed is small.

(4) Negligible dispersion axially and radially.

(5) Linear isotherms assumed.

(6) Ideal gas law applies.

After a brief examination of the performance characteristics of the process they concluded that gas mixtures with large separation factors required less purge flow for complete removal of the trace contaminant than did mixtures with small separation factors. Additionally, when the gas mixture to be separated has a large separation factor the system performance may be improved by increasing the pressure ratio, P_H / P_L. Increasing the pressure ratio in a system with small separation factor will not improve performance. Experimental results were not presented to support their theoretical conclusions.

Knaebel and Hill (82) further extended the equilibrium theory to include separation of a binary feed of arbitary composition. The assumptions of their work were:

(1) Linear, uncoupled isotherms

(2) Isothermal operation

(3) Ideal gas law assumed

(4) Diffusional resistance and dispersion neglected.

It was concluded that when β is small (i.e. small concentration of the heavy component in the feed) the purge requirement is minimal, perfect cleanup occurs over all pressure ratios, recoveries increase with increasing pressure ratio, and pressurization with product gives higher recoveries than pressurization with feed.

$$\beta = \beta_A / \beta_B$$

$$\beta_i = \frac{\varepsilon}{\varepsilon + (1 - \varepsilon)\, k_i}$$

k_i is the equilibrium distribution coefficient for species i.

Conversely, when β is large (i.e. large concentration of the heavy component in the feed) higher pressure ratios are required and recoveries are small.

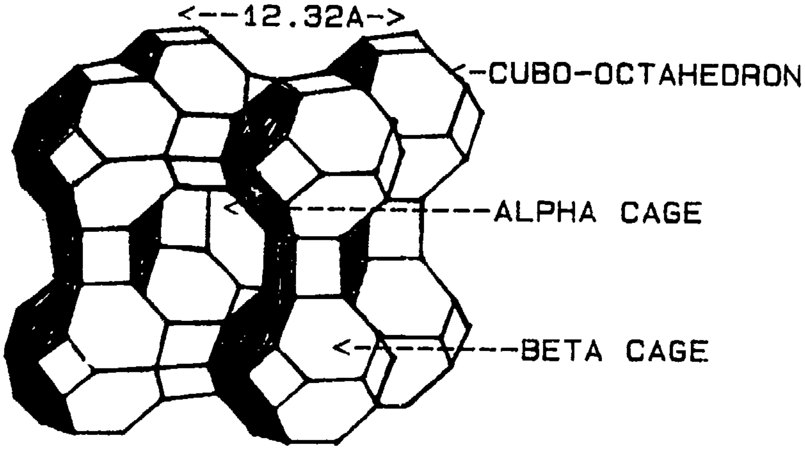

FIG 3-1. STRUCTURAL MODEL OF MOLECULAR SIEVE 5A.

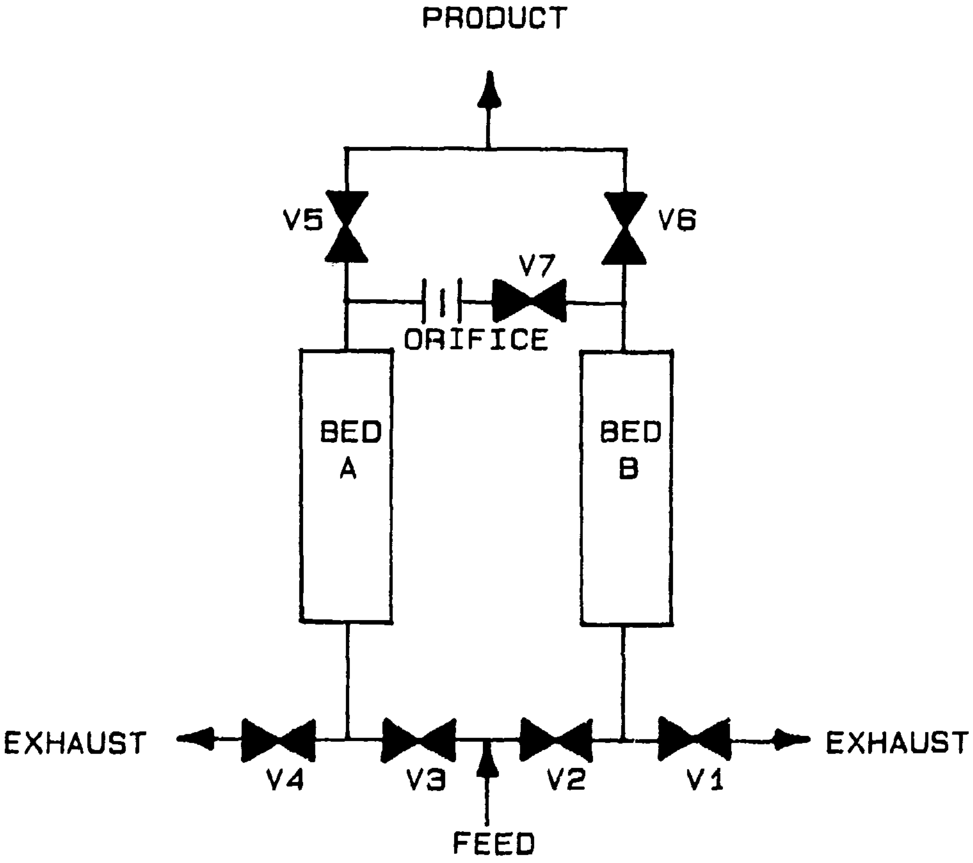

FIG 3-2. SIMPLIFIED SCHEMATIC DIAGRAM OF A DUAL COLUMN PSA AIR SEPARATION UNIT.

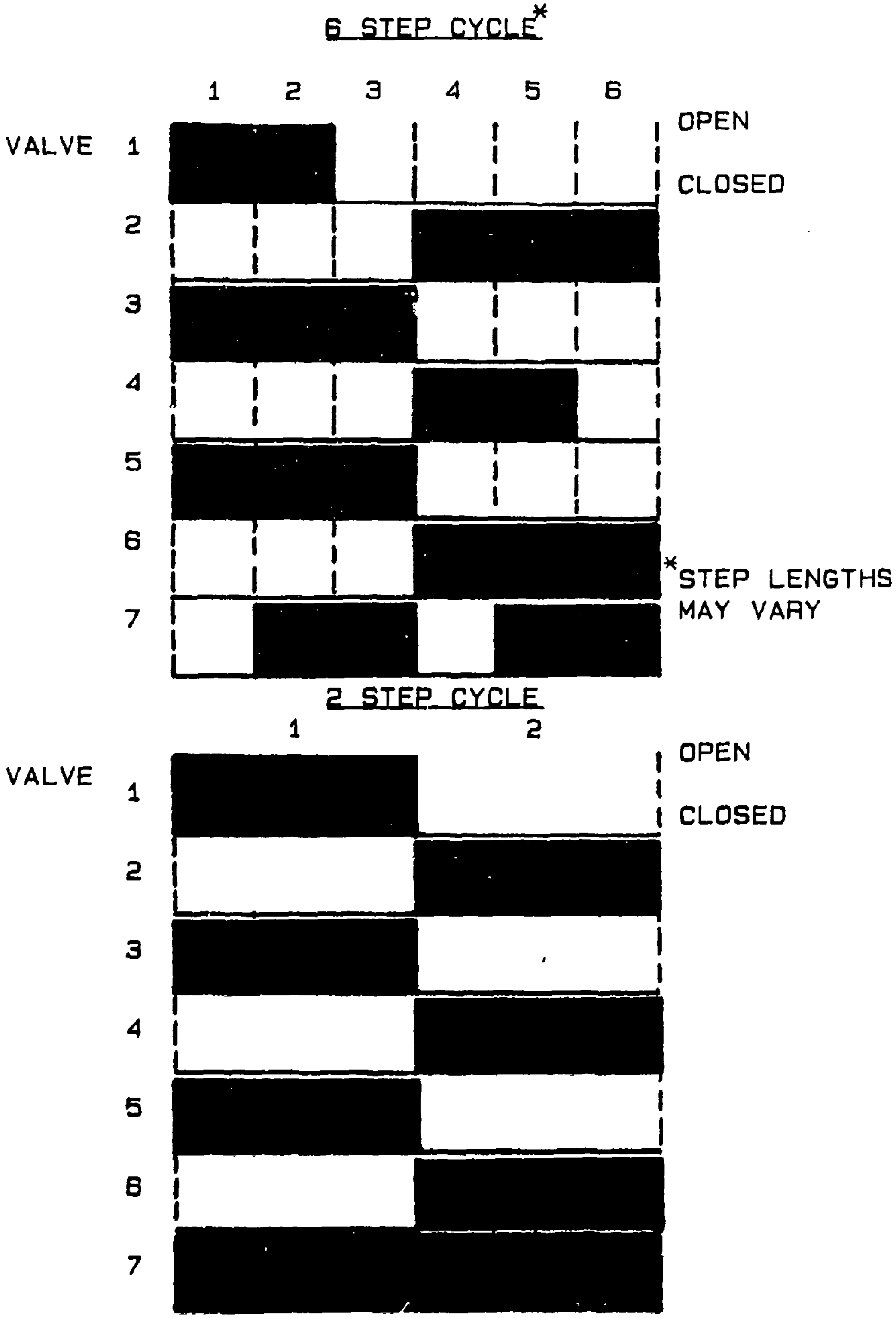

FIG 3-3. VALVE POSITIONS DURING ONE CYCLE FOR THE SYSTEM SHOWN IN FIG 3-2.

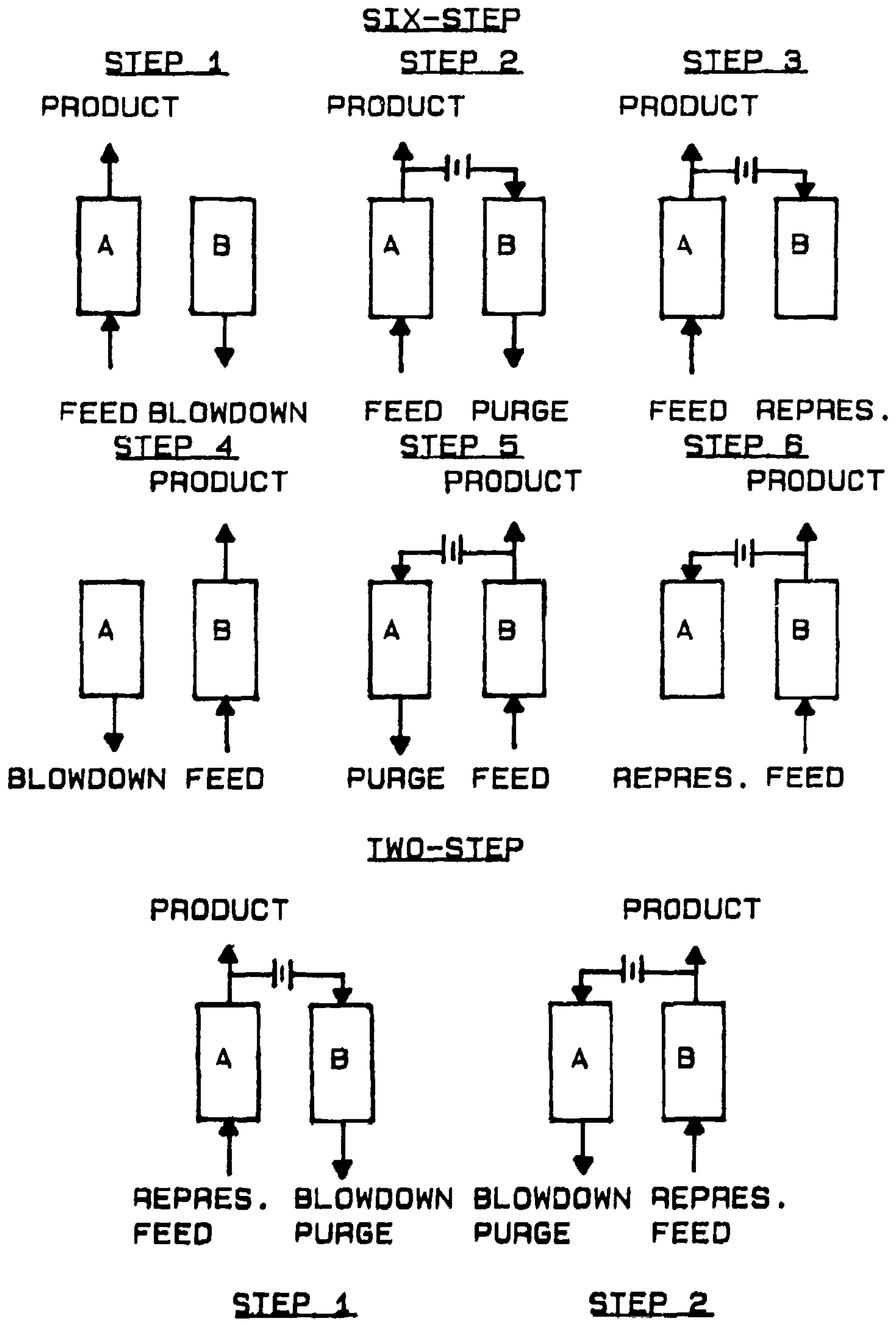

FIG 3-4. COMPARISON OF SIX-STEP AND TWO-STEP CYCLE.

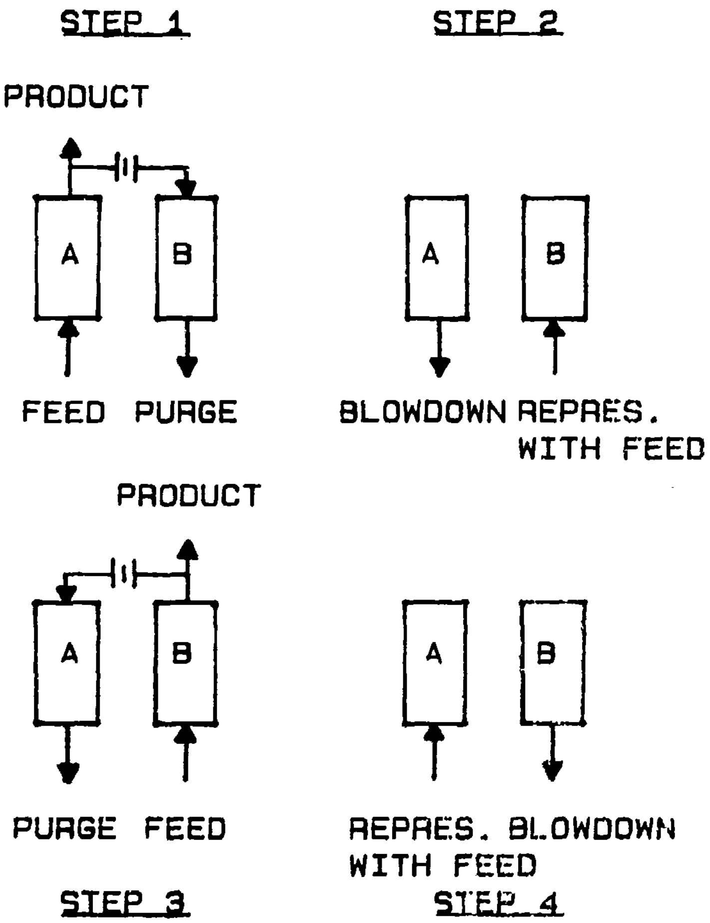

FIG 3-5. SHENDALMAN AND MITCHELL FOUR-STEP CYCLE.

CHAPTER IV

EXPERIMENTAL

A. Materials

The adsorbent employed in this work was Union Carbide Corp., 20X40 mesh (~0.0102" to ~0.0201" diameter), medical grade, molecular sieve 5A (Lot No. 9427800171) (See Fig 4-1 to 4-5). This sieve is reported by the manufacturer to be 80% anhydrous crystals and 20% inert clay binder. The chemical formula for the anhydrous crystal is,

$$Ca_{4.5}\,Na_{3}\,[\,(AlO_2)_{12}\,(SiO_2)_{12}\,]$$

Theoretically, the sieve is 75% exchanged with Ca^{++}.

The gases used in this work are listed in Table 4.

Table 4. Specifications of gases used in the equilibrium studies.

Gas	Purity	Supplier	Comment
Nitrogen	99.998%	Burdett Gas Products Co.	Water pump
Oxygen	99.99%	Matheson Gas Products	Ultra-high purity
Air[+]	20.9% O_2	Liquid Air Corp.	Compressed Air
	78.0% N_2	Lot. No.16787682C	Breathing quality
	0.96% Ar		(oil free)
	<30ppm H_2O		

[+] Air purity determined using a Perkin-Elmer MGA-1100 medical gas analyzer and a dew point meter.

B. Pure Component Equilibrium Apparatus

A volumetric type pure component equilibrium apparatus was constructed for measuring the isotherms of nitrogen and oxygen at 24, -40, and -70°C and up to pressures of approximately 4.3 atmospheres absolute (See Fig. 4-6 and 4-7). The unit was designed to satisfy five primary goals: accurate data collection; simple, reliable operation; economical construction; easy conversion to a multicomponent equilibrium apparatus; and convenient installation into the temperature controlled chamber. All the stated goals were attained. The apparatus had a length of approximately three feet, a width of one foot, a depth of 6", and weighed about 10 pounds.

The range of pressures and temperatures of operation prompted use of stainless steel construction. The sample chambers (C1 and C2) and their associated piping were mated through the use of stainless steel compression fittings with a design range which encompassed the range of operation. The sample chamber volumes (C1 and C2) were nominally 150 ml each and the outside diameter of the stainless steel tubing was largely 1/4" except for a short section of 3/8" tubing located at the inlet to the sample chamber (C1). The valves (V1-4) had stainless steel bodies and Kel-F seats for leakproof operation at both positive and negative pressures, and were manually operated.

System pressure measurements were accomplished through the use of Statham model PA208TC-50-350 stainless steel diaphragm pressure transducers (P1 and P2). The units outputted a low voltage DC signal which was sent to the electronics box (E) for signal conditioning, conversion to units of Torr or psia, and readout display. A high level conditioned DC signal was, simultaneously, sent to the strip chart recorder (S). The charge chamber temperature and sample temperature measurements were sensed by copper-constantan thermocouples and were displayed on readouts (R1 and R2) in units of °C.

Other units of the system were the rotary vacuum pump (V), temperature controlled chamber (T), variable transformer (X), and an electric tape heater (H).

The pressure transducers (P1 and P2) and the electronics box (E) were calibrated as a system over the range 0-75 psia with a calibrated high accuracy Wallace-Tiernan pressure gauges (Model FA129 and 61A-1A-0150). The transducer signals were linear from 0 to 75 psia and nonlinear above 75 psia.

The determination of the volume of the sample and charge chamber and their associated piping was accomplished by a water displacement method and these results were checked using several gas expansions. The volume to be measured was evacuated to ~1 Torr and then distilled water at room temperature was permitted to fill the volume. The weight of the water was determined by the difference method and its volume was calculated based on the reported densities of water (65) (See Table 5 and 6).

Table 5. Sample chamber volume determination using water displacement.

Test No.	Dry Weight (gm)	Wet Weight (gm)	Water Weight (gm)	Water Temp. (°C)	Water Density (gm/ml)	Calc. Chamber Volume (ml)
1	1396.0	1565.4	169.4	28	0.996264	170.0
2	1395.7	1565.2	169.5	26	0.996814	170.0
3	1395.8	1564.9	169.1	27	0.996544	169.7
4	1395.9	1565.4	169.5	26	0.996814	170.0
5	1396.0	1565.3	169.3	26	0.996814	169.8

Sample chamber volume = 170.0 ml

Table 6. Charge chamber volume determination using water displacement.

Test No.	Dry Weight (gm)	Wet Weight (gm)	Water Weight (gm)	Water Temp. (°C)	Water Density (gm/ml)	Calc. Chamber Volume (ml)
1	1206.8	1364.8	158.0	26	0.996814	158.5
2	1206.8	1364.6	157.8	"	"	158.3
3	1206.9	1364.7	157.8	"	"	158.3
4	1207.3	1365.4	158.1	"	"	158.6
5	1207.5	1365.6	158.1	"	"	158.6

Charge chamber volume = 158.6 ml

Several gas expansions were performed as a check of the results obtained using the water displacement method. The gas expansions were from the charge chamber (C2) into the sample chamber (C1) via valve (V3). The charge chamber volume was assumed to be 156.8 ml as previously determined from the water displacement experiment. The results of these experiments are shown below (See Table 7).

Table 7. Results from nitrogen and helium expansions into the sample chamber.

Run No.	Gas	Initial Charge Chamber Pressure (atm)	Initial Sample Chamber Pressure (atm)	Initial Volume of Gas (ml)	Temp. (°C)	Final Pressure (atm)	Calc. Volume of Sample Chamber (ml)
1	N2	2.041	~0	158.6	25	0.986	169.5
2	He	2.041	"	"	"	0.980	171.8
3	"	1.000	"	"	"	0.482	170.7

These results are in good agreement with the previous water displacement experiments, therefore, we conclude:

Volume of the Sample Chamber = 170.0 ml

" " " Charge " = 158.6 "

The anhydrous weight of the molecular sieve sample was determined by regenerating the sample at <1 Torr pressure and 350°C for a minimum of 12 hours. This regeneration procedure became standard practice and was accomplished before each equilibrium run. It was noted that when the heating tape temperature reached approximately 300 °C the sample began "boiling" violently, apparently releasing the residual water of hydration. The results of the initial regeneration are shown below,

Gross volume of sample = 50 ml

Weight of sample before regeneration = 33.7 gm

Weight of sample after regeneration = 32.8 gm
" lost during regeneration = 0.9 gm or

$$\frac{0.027 \text{ gm}}{\text{gm anhydrous wt.}}$$

This residual weight (mostly water) is close to the specification of ~ 2% residual water stated by the manufacturer. The anhydrous weight of the molecular sieve sample will be taken as 32.8 gm. It should be noted that this same sample was employed in all the equilibrium experiments.

To calculate the amount adsorbed the true dead space of the sample chamber must be ascertained. We define the true dead space as the volume of the sample chamber minus the volume of the solid crystal.

This dead space volume was obtained by a helium displacement technique. It is assumed that helium will fill the entire void volume of the zeolite but adsorb in negligible quantities at room temperature. The advantage of this technique is that the pressure of the pressure of the helium can be related directly to the true dead volume. The experimental approach taken was to expand helium into the sample chamber a sufficient number of times, so that, through application of statistical analysis we might arrive at a reasonable value for the true dead space volume. The data from twenty expansions are presented (See Table 8). Helium is assumed to be an ideal gas over the range of pressure in which the experiment was conducted (66).

Table 8. Determination of the true dead space of the sample chamber.

Run No.	Initial Pressure (Torr)	Final Pressure (Torr) (ml)	Calc. Sample Volume (ml)	Calc. True Dead Space Volume
1	1500	750	11.4	158.6
2	2000	1008	13.92	156.08
3	2500	1246	10.38	159.62
4	3000	1495	10.34	159.66
5	3500	1743	10.13	159.87
6	1500	750	11.40	158.6
7	2000	998	10.76	159.24
8	2500	1241	9.10	160.90
9	3000	1495	10.34	159.66
10	3500	1748	11.04	158.96
11	1500	750	11.40	158.60
12	2000	998	10.76	159.24
13	2500	1246	10.38	159.62
14	3000	1499	11.19	158.81
15	3500	1748	11.04	158.96
16	1500	752	12.24	157.76
17	2000	1003	12.35	157.65
18	2500	1246	10.38	159.62
19	3000	1500	11.40	158.60
20	3500	1748	11.04	158.96

Results:
Mean Sample Volume = 11.05 ml
Standard Deviation = 1.0004 ml
Solid volume based on a 95% confidence interval= 11.05 ± 0.047 ml
Solid density = 2.97 gm/ml

From these results we conclude:

Solid Volume of the Sample = 11.05 ml

True Dead Volume in the Sample Chamber = 158.9 ml

The confidence interval assumes normally distributed error in the individual obsevations about the true mean. Since the true standard deviation is not known, a two-tailed t distribution with 2.5%

probability in each tail and nineteen degrees of freedom was employed in the calculation of the confidence interval.

The procedure for operating this apparatus is straightforward and presented in Appendix B. Before each data run the molecular sieve sample is regenerated by heating the sample to 350 °C and applying a vacuum (< 1 Torr) for a minimum of twelve hours. After regeneration the temperature of the sample is stabilized at the desired experimental temperature. Injection of the gaseous phase adsorbate from the charge chamber to the sample chamber is accomplished by opening valve (V3). The quantity of adsorbate in the sample chamber is increased in a stepwise fashion and data are collected after equilibrium is reached in the sample chamber. Equilibrium was assumed to exist when the pressure in the sample chamber remained constant for at least a period of one hour. In general, an equilibrium state was reached after a period of six to eight hours. The amount adsorbed may then be determined by performing a mass balance (See Appendix C).

C. Multicomponent Equilibrium Apparatus

Modification of the pure component equilibrium apparatus to enable it to gather multicomponent data was accomplished by the addition of a gas sampling and analysis section (See Fig. 4-8, 4-9, and 4-10). This gas sampling section was comprised of a Perkin- Elmer MGA-1100 medical gas analyzer (MGA), a dual channel strip chart recorder (SC), MGA gas sampling probe (PR), two three way valves (V5 and V6), a MGA sampling volume (SV), and a rotary vacuum pump (V). Since the multicomponent system (N2-O2-Ar-5A) has four degrees of freedom the gas phase concentrations of at least two components are required (plus the temperature and total pressure) to fully define the system. It should be clear that air is to be injected into the sample chamber in all experiments, therefore, the molar ratios of N2:O2:Ar remain constant in the sample chamber. The advantage of this approach is that it should more closely simulate the actual gas concentrations in a PSA column.

Measurement of the gas phase concentrations poses a challenge. Direct measurement of the gas phase concentrations with the medical gas analyzer (MGA) would not allow accurate determination of the total mass removed from the sample chamber. This difficulty was overcome by allowing a small portion of the gas mixture to fill the previously evacuated MGA sampling volume (SV) so that a determination of the exact amount of mass of each component removed from the sample chamber (C1) could be made. The isolated gas mixture in the sampling volume (SV) is then permitted to flow through the gas sampling probe, and subsequently, to the MGA for concentration analysis.

The experimental technique adopted here represents somewhat of a departure from tradition methods. A traditional approach, considering only the binary system of nitrogen-oxygen, would dictate injecting the proper amounts of the pure gases so as to maintain the total pressure constant but vary the gas phase mole fractions from 0 to 1.0 . A second traditional approach would involve maintaining the gas phase concentrations constant and varying the pressure. Both traditional techniques require the injection of pure gases which could create areas of severe concentration heterogeniety. This difficulty is usually avoided through use of a circulation pump.

The approach of this work involves the injection of a homogeneneous mixture, therefore, the sample chamber is much less likely to possess the severe localized concentration gradients as the traditioal system would experience without the circulation pump. Our approach minimizes the complexity of the experiment without compromising the validity of the experimental results provided a sufficient period for gaseous diffusion is allowed. Also, as previously mentioned, the data obtained in this manner should approximate the concentrations in a PSA column. Comparison of the results of this work with other work will validate this technique.

The first step in the modification of the pure component apparatus was to determine the MGA sampling volume which would minimize the gas sampling time ,i.e. the volume of gas to be extracted, but allow ample time for the MGA to reach a steady state condition and thus provide stable signals at the strip chart recorder. The calibrated gas sampling probes used with the MGA covered four pressure ranges (See Table 9).

Table 9. Pressure range of the MGA gas sampling probes.

Probe No.	Pressure Range (Torr)
1	140 to 214
2	214 to 326
3	326 to 497
4	497 to 760

This selection of probes permitted gas analysis from 140 Torr to the high pressure constraint of the apparatus, 75 psia. Gas analysis above atmospheric pressure was possible by venting the sample to the atmosphere, while simultaneously, withdrawing a small portion. Tests were conducted at various pressures above and below atmospheric pressure with pure gases and with air to ensure the technique would provide accurate readings. These tests showed the probes would give accurate reading of their calibrated range. During these tests the minimum sampling time was determined to be approximately three seconds when using probe number one. An additional constraint on the system requires that during the sampling process the pressure in the sample volume must remain within the calibrated range of the probe. The MGA draws approximately 1 ml/sec of sampling gas and has a response time of 100 milliseconds. Assuming the ideal gas law applies, solution of two simultaneous equations based on the conditions of minimized sample volume and minimum allowable sample pressure gave the following result,

Theoretical MGA sample volume = 12 ml

The apparatus was modified and the actual MGA sampling volume was calculated, instead of measured by a displacement technique, since the volume consisted almost entirely of 1/4" OD tubing. The calculated volume was,

Actual MGA sampling volume = 12.9484 ml

The strip chart recorder and MGA were calibrated as a system using nitrogen, oxygen, and air. Air allowed the calibration of the argon signal.

The operational procedure of this apparatus is similar to that of the pure component equilibrium apparatus and is presented in detail in Appendix B. The basic difference involves the removal of a small gas sample for gas concentration analysis. The frequent MGA gas sampling probe changes required to ensure an accurate signal from the MGA increased the complexity of this experiment. The final results were obtained by a mass balance (See Appendix C).

D. Dual Column PSA Apparatus

A bench-scale, dual column PSA air separation apparatus was constructed (See Fig. 4-11 and 4-12). The unit was comprised of two identical columns (CL1 and CL2), seven solenoid valves (V1-7), three mass flowmeters (F1-3), a purge orifice (O), four pressure transducers (P1-4), a plenum chamber (P), a manual needle valve (V8), an inlet pressure gauge (PG), and a medical gas analyzer (MS) for monitoring the product concentration. The unit was operated at 24°C and then at -40 °C to evaluate the effects of low temperature on system performance. The apparatus was entirely computer controlled and constructed of stainless steel tubing and valves. The unit was mounted horizontally to a wooden framework for convenient access.

The three flowmeters monitored the mass flow in the inlet,exhaust, and product flows. At 24°C the flowmeter was configured to monitor the exhaust flow from one column, and at -40°C the flowmeter was configured to monitor the flow from both columns. These units were calibrated with a Singer DTM-200 volumetric flowmeter used as a standard. All units gave linear and reproducible outputs.

The columns of molecular sieve were contained within 1" O.D. thin wall stainless steel tubing approximately 8.5" in length and 0.965" I.D. The sieve was secured by stainless steel screens on each end of the column supported by heavy metal springs, such that, movement of the molecular sieve bed during the pressure fluctuations of each cycle was highly unlikely.

The molecular sieve pellets were loaded into the columns by a method known as "snowpacking". This technique involves passing the pellets through a funnel in which screens of various sizes have been placed perpendicular to the flow. The method is simple and proved to give the greatest packing density. The columns were packed with the following amounts of molecular sieve,

Table 10. Weight of molecular sieve in dual column PSA apparatus.

	24C	-40C
Bed A	82.07 gm	78.0 gm
Bed B	80.35 gm	84.7 gm

Data acquistion and valve control were accomplished through use of a PDP11/03 computer which precisely controlled the valve sequencing and collected ten channels of data. The data signals consisted of three flowmeter signals, four pressure transducer signals, and three gas concentration signals representing the composition of the product flow. Information required for control of each experimental run, such as cycle time, step times, etc., was stored in an input file which was read by the main control program prior to each run.

Several parameters of the system could be varied to investigate their effect on the oxygen concentration in the product flow. The configuration (6-step or 2-step) and cycle time were easily varied by changes to the computer program input file. The bed temperature was controlled by adjustment of the temperature setting on the enviromental chamber. The PSA system was operated at two temperatures: 24°C and -40 °C. The product flowrate was controlled by valve (V8) and monitored by flowmeter (F3). The purge flow was varied by installation of one of three different diameter orifices (0.010", 0.020", and 0.029"). The inlet pressure was held constant at 25 psia throughout this work.

Since this experiment was computer controlled the operating procedure was quite simple and is described in Appendix B. Desired operating parameters were entered into an input data file (XBASE.DAT) which was read by the main control program (TT.FOR). This program is shown in Appendix C. Once the control program is initiated the PSA unit operates based entirely upon commands originated at the PDP11/03 computer which are further processed by electronics interface boxes. As the PSA unit is operating the data channels are displayed on the screen of a VT-54 terminal in engineering units. For this work data was collected once the oxygen concentration in the product reached a steady state value which was usually after about thirty minutes of operation, although this time lengthened somewhat when operating at $-40^{o}C$. For actual data collection to commence the simply depresses the line feed key at the VT-54 terminal. The data for each run was stored on floppy diskettes initially and then transfered to the main facility computer for analysis.

Operation at $-40^{o}C$ posed some special problems due to traces of water in the feed air. These traces caused significant degradation of the sieve requiring them to be repacked. This problem was eliminated by switching to bottled air and placing a molecular sieve 13X trap before the inlet.

Breakthrough experiments were conducted by using one column of the PSA apparatus. The bed temperature for the breakthrough runs were 24°C and -40°C, and the bed pressures were ~14.7 psia and 25 psia. The gases used were air and oxygen so as to simulate as closely as possible the actual conditions of the PSA process.

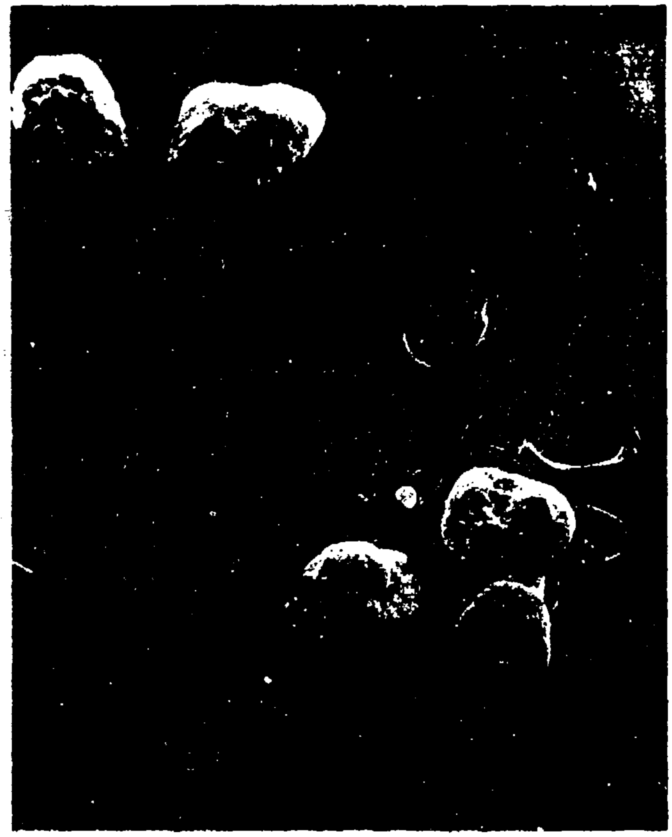

FIG 4-1. ELECTRON MICROGRAPH OF MOLECULAR SIEVE 5A (20X40) MESH PELLET (20X MAGNIFICATION).

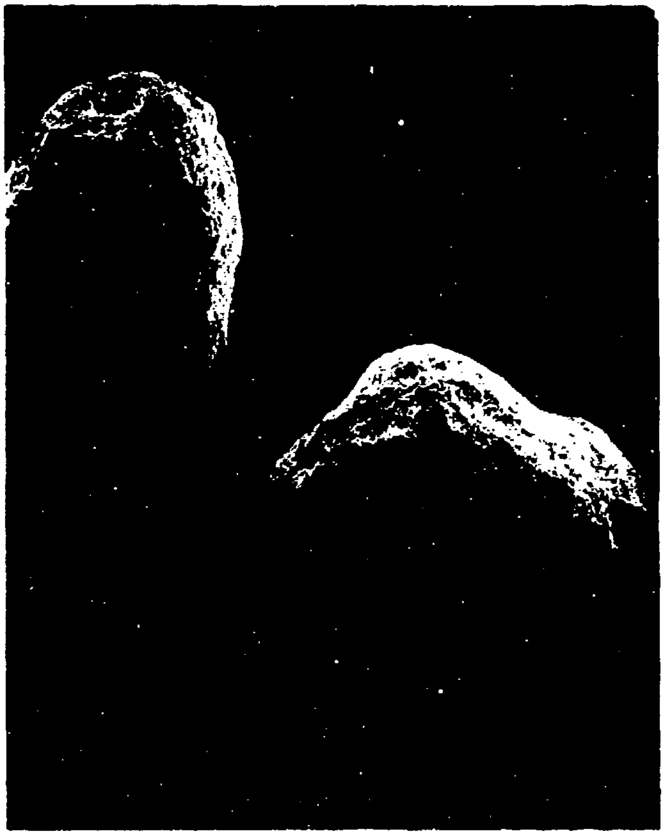

FIG 4-2. ELECTRON MICROGRAPH OF MOLECULAR SIEVE 5A (20X40) MESH PELLET (50X MAGNIFICATION).

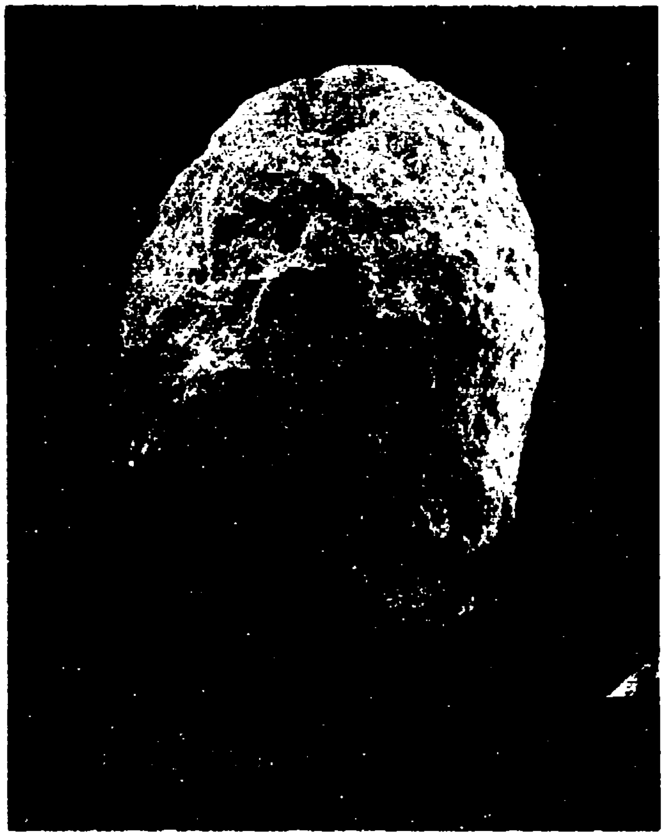

FIG 4-3. ELECTRON MICROGRAPH OF MOLECULAR SIEVE 5A (20X40) MESH PELLET (90X MAGNIFICATION).

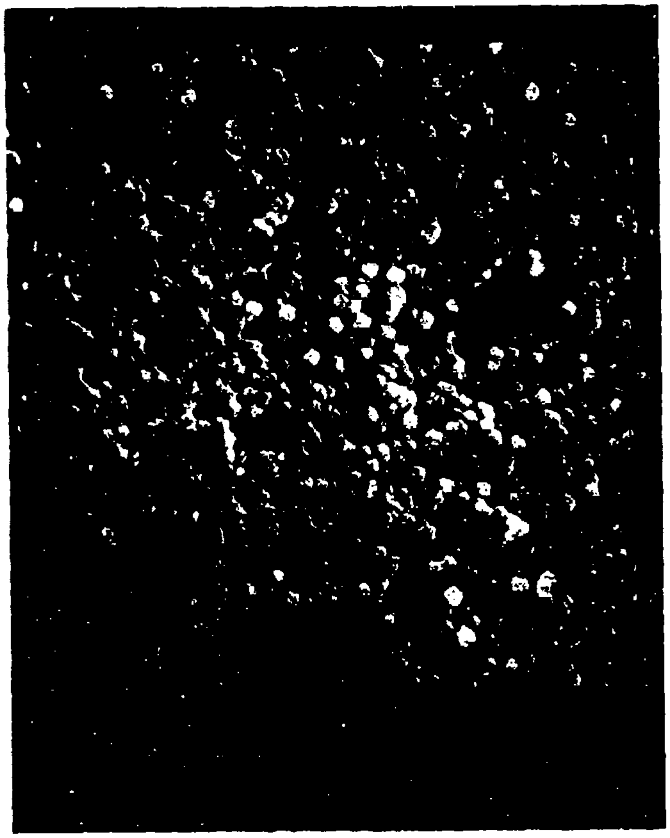

FIG 4-4. ELECTRON MICROGRAPH OF MOLECULAR SIEVE 5A (20X40) MESH CRUSHED PELLET (800X MAGNIFICATION).

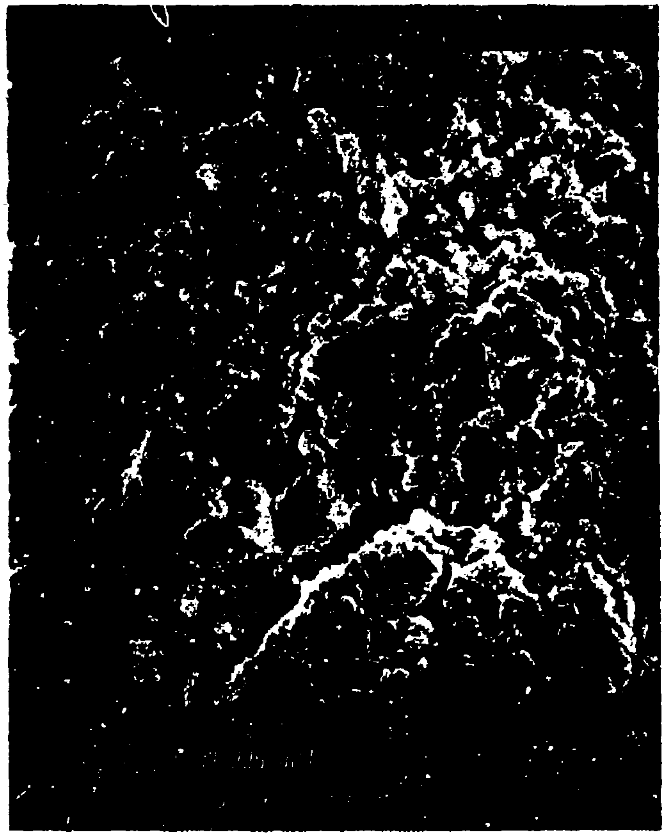

FIG 4-5. ELECTRON MICROGRAPH OF MOLECULAR SIEVE 5A (20X40) MESH CRUSHED PELLET (1000X MAGNIFICATION).

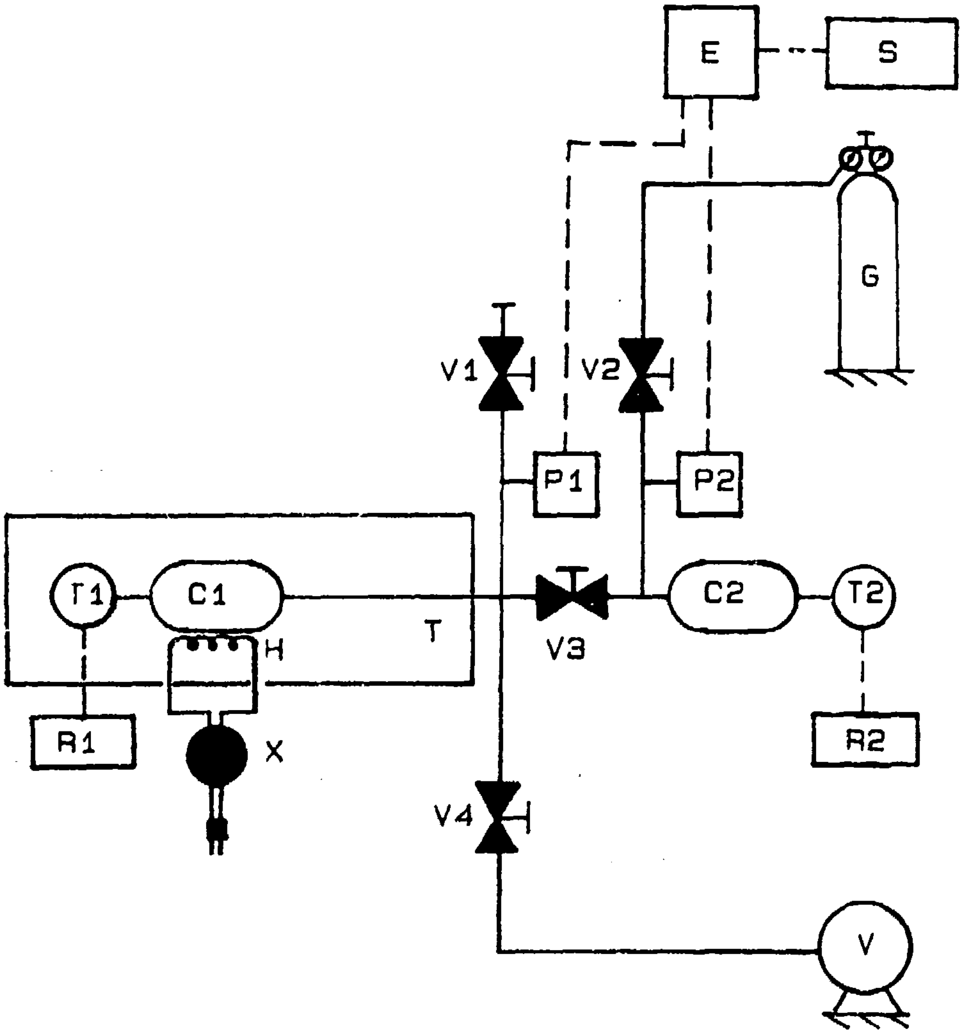

FIG 4-6. PURE COMPONENT EQUILIBRIUM APPARATUS. C1. SAMPLE CHAMBER, C2. CHARGE CHAMBER, E. PRESSURE TRANSDUCER ELECTRONICS BOX, G. BOTTLED GAS, H. HEATER, P1 AND P2. PRESSURE TRANSDUCERS, R1 AND R2. DIGITAL READOUTS, S. STRIP CHART RECORDER, T. ENVIRONMENTAL TEST CHAMBER, T1 AND T2. THERMOCOUPLES, V. VACUUM PUMP, V1-4. MANUAL VALVES, AND X. VARIAC.

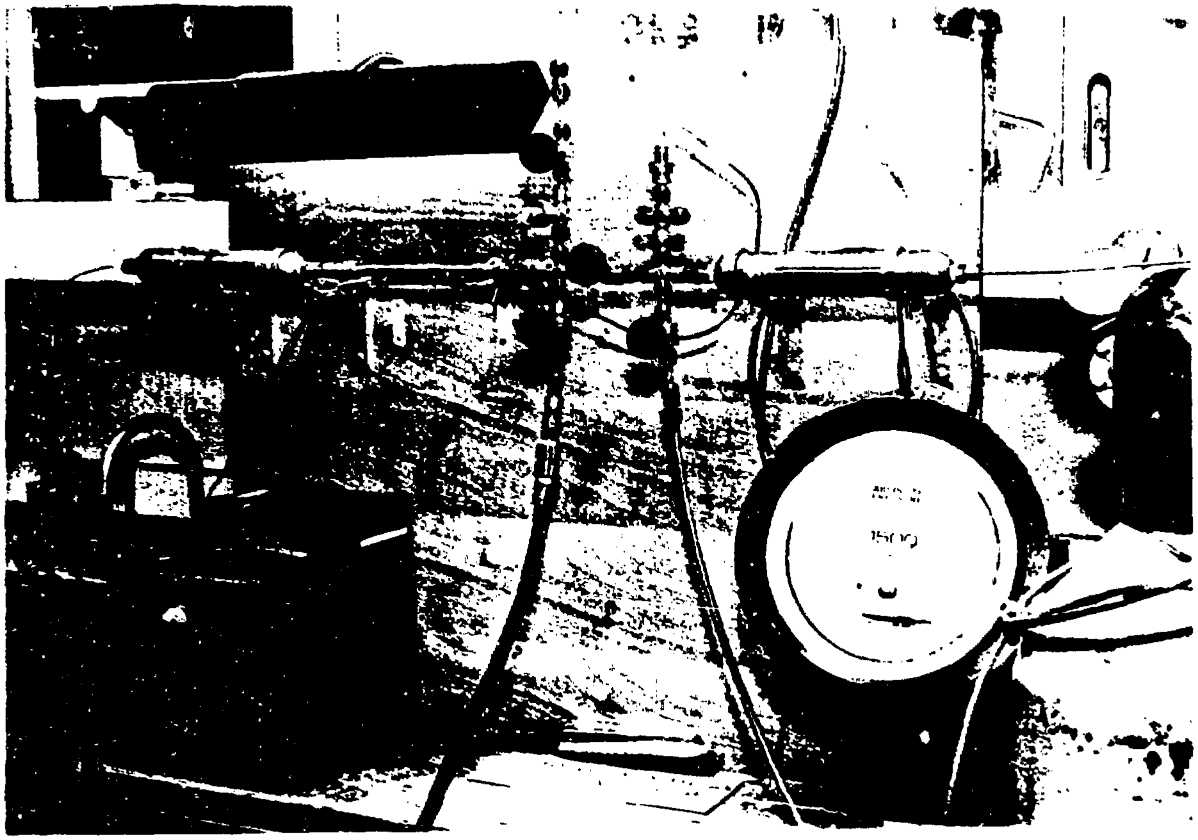

FIG 4-7. PHOTOGRAPH OF THE PURE COMPONENT EQUILIBRIUM APPARATUS.

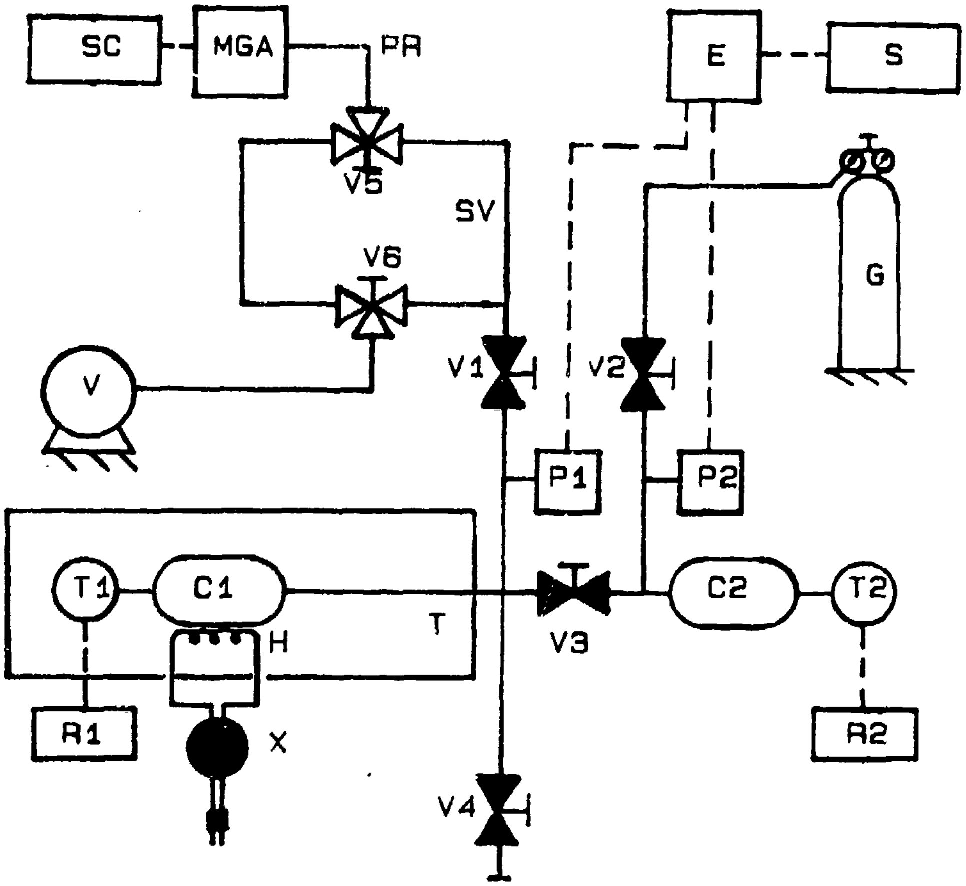

FIG 4-8. MULTICOMPONENT EQUILIBRIUM APPARATUS. C1. SAMPLE CHAMBER, C2. CHARGE CHAMBER, E. PRESSURE TRANSDUCER ELECTRONICS BOX, G. BOTTLED GAS, H. HEATER, P1 AND P2. PRESSURE TRANSDUCERS, R1 AND R2. DIGITAL READOUTS, S. STRIP CHART RECORDER, T. ENVIRONMENTAL TEST CHAMBER, T1 AND T2 THERMOCOUPLES, V. VACUUM PUMP, V1-4. MANUAL VALVES, X. VARIAC, MGA. MEDICAL GAS ANALYZER, SC. MGA STRIP CHART RECORDER, PR. MGA GAS SAMPLING PROBE, SV. MGA SAMPLING VOLUME, AND V5-6. THREE-WAY VALVES.

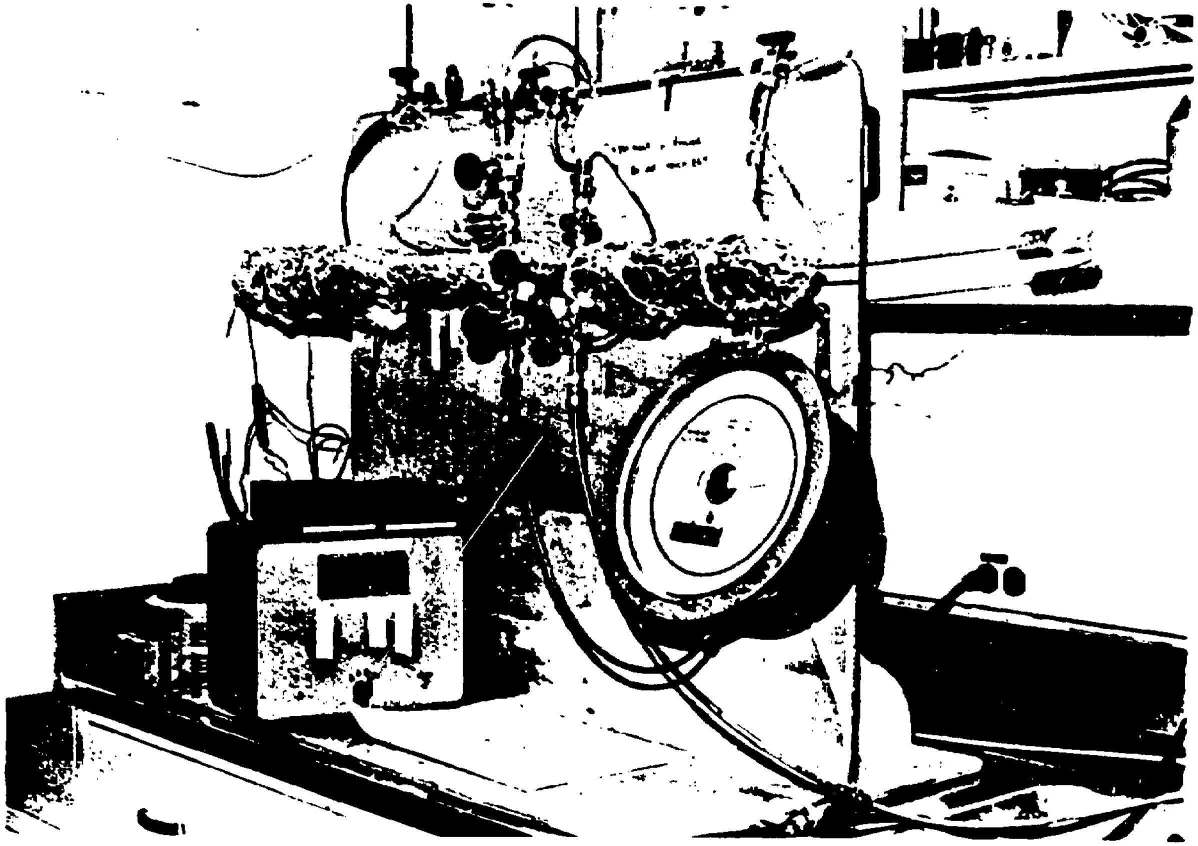

FIG 4-9. PHOTOGRAPH OF THE MULTICOMPONENT EQUILIBRIUM APPARATUS.

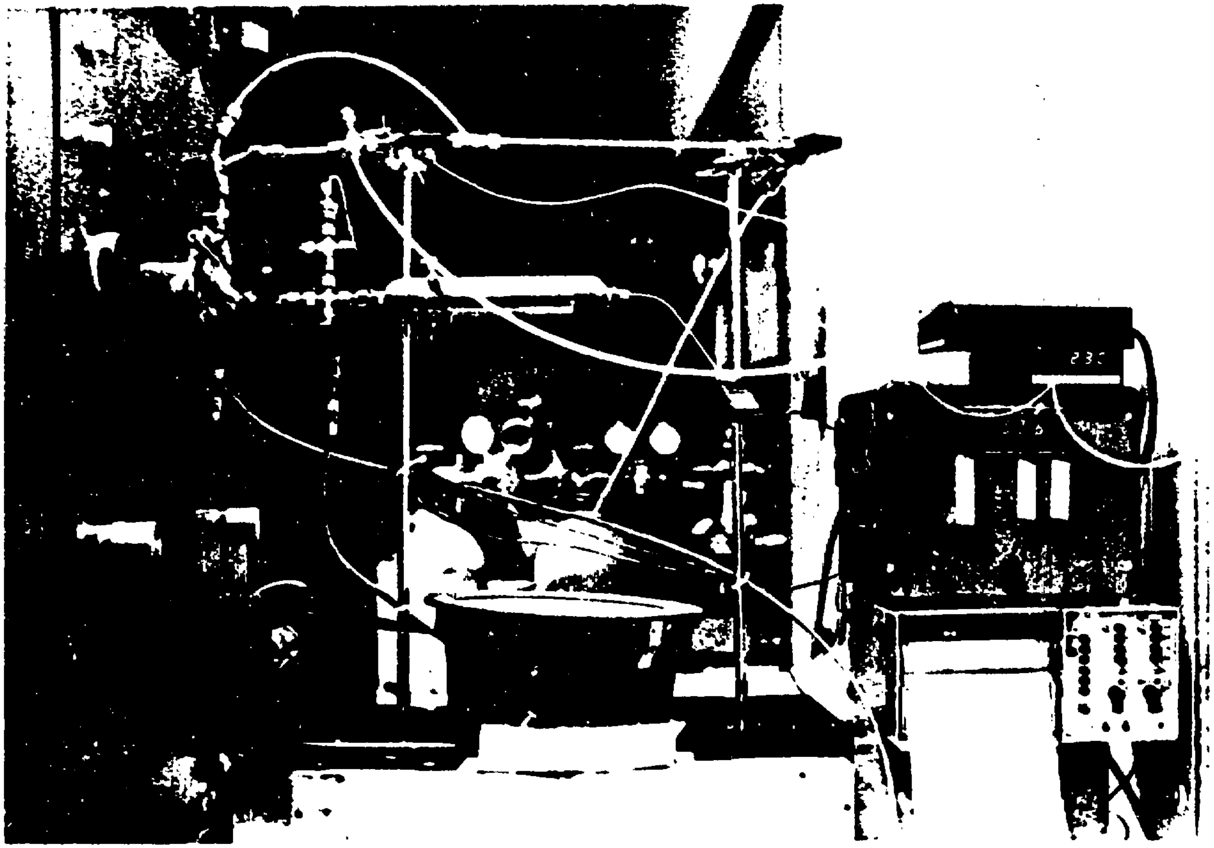

FIG 4-10. PHOTOGRAPH OF THE MULTICOMPONENT EQUILIBRIUM APPARATUS WITH SAMPLE CHAMBER INSERTED INTO THE ENVIRONMENTAL TEST CHAMBER.

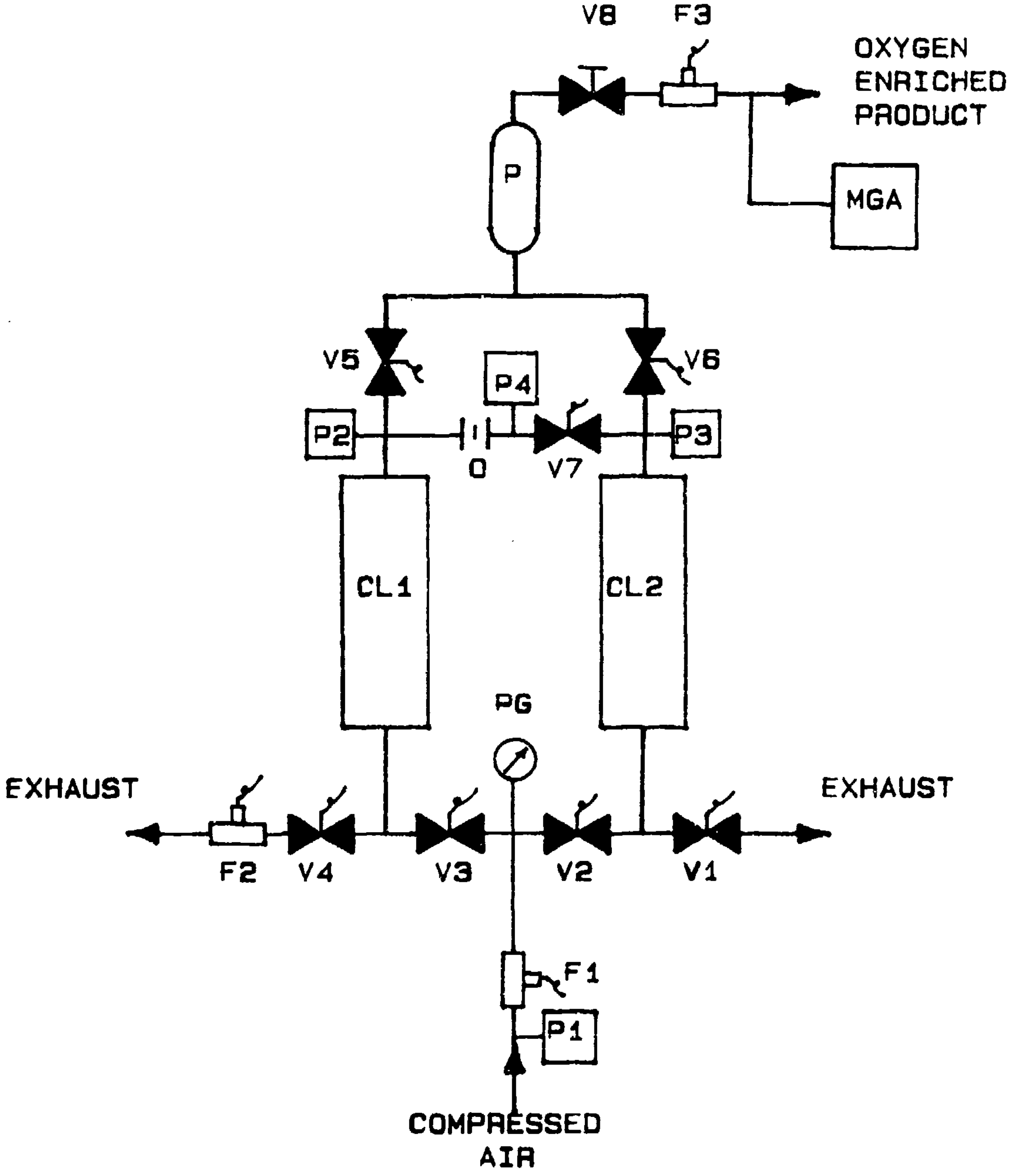

FIG 4-11. PSA AIR SEPARATION UNIT. F1-3. MASS FLOWMETERS, V1-7. SOLENOID VALVES, V8. MANUAL VALVE, P. PLENUM, MGA. MEDICAL GAS ANALYZER, P1-4. PRESSURE TRANSDUCERS, O. ORIFICE, CL1-2. COLUMNS OF MOLECULAR SIEVE, AND PG. PRESSURE GAUGE.

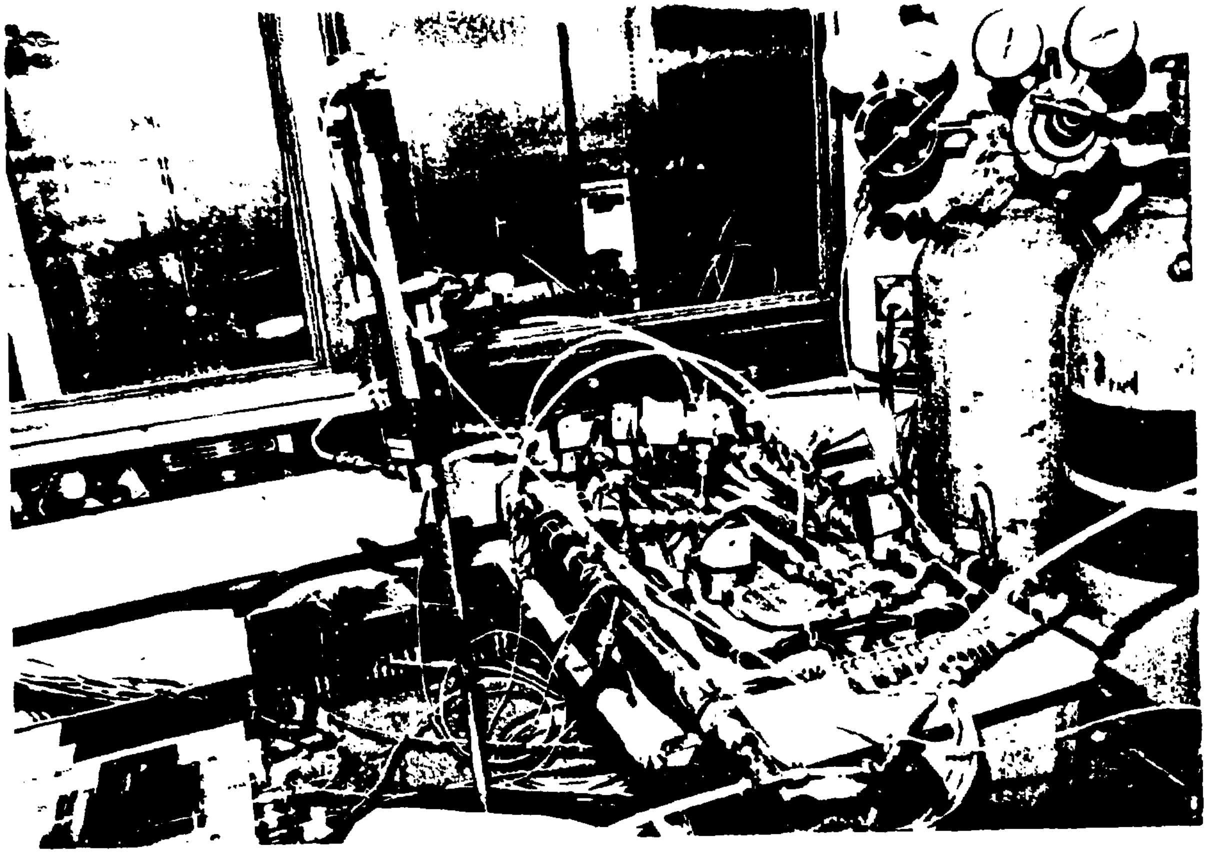

FIG 4-12. PHOTOGRAPH OF THE PSA AIR SEPARATION UNIT.

CHAPTER V

DATA AND RESULTS

A. Pure Component Isotherms

The pure component isotherms of nitrogen and oxygen on Union Carbide molecular sieve 5A (20X40 mesh) at temperatures of 24, -40, and -70 °C and up to pressures of approximately 3300 Torr were obtained by a volumetric technique with the pure component equilibrium apparatus described in Chapter IV (See Fig. 5-1 through 5-6). Calculation of the amount adsorbed was determined by performing a mass balance. The data presented show excellent reproducibility. At the temperatures of this work nitrogen adsorption is greater than oxygen adsorption, although as the temperature is lowered oxygen adsorption increases dramatically (See Fig. 5-7 through 5-9). The nitrogen and oxygen isotherms have been grouped together in Fig. 5-10 and 5-11 to show their temperature dependence.

As a validation of the measurement technique and the apparatus employed, the data of this work has been presented with other reported data (67,68,69) (See Fig. 5-12 through 5-15). The data correlates well with the Union Carbide Corporation oxygen and nitrogen data at 0 and 30 °C (69). Peterson (68) used Union Carbide molecular sieve 5A which he analyzed to be 70% exchanged with Ca^{++}. Correlation with Peterson's nitrogen data at 25°C is excellent.

The best fitting equations for the oxygen and nitrogen data were the Langmuir and Sips equations, respectively. The results are shown below,

$$q_{O2} = \frac{P1\, p_{O2}}{1 + P2\, p_{O2}}, \qquad q_{N2} = \frac{P1\, p_{N2}^{P3}}{1 + P2\, p_{N2}^{P3}}$$

where,

q has units of ml STP/gm.
p " " " Torr.

Table 11. Best fit parameters for the pure component data.

Gas	Temp. (C)	Run	$P1 \times 10^2$	$P2 \times 10^4$	P3	Minimum Residual
Oxygen	24	1	0.4730	0.4832	1.0	0.0695
"	"	2	0.4617	0.4477	"	0.1200
"	"	All	0.4669	0.4629	"	0.3050
"	-40	1	2.311	2.247	"	1.03
"	"	All	2.340	2.318	"	2.01
"	-70	1	6.638	5.629	"	1.48
"	"	2	6.273	5.345	"	0.396
"	"	All	6.501	5.513	"	19.9
Nitrogen	24	1	4.696	4.947	0.8264	0.765
"	"	2	5.020	5.612	0.8210	0.134
"	"	All	4.755	5.164	0.8263	1.09
"	-40	1	84.20	83.78	0.6573	2.23
"	"	2	73.60	75.77	0.6775	0.133
"	"	All	83.95	82.22	0.6545	3.17
"	-70	1	345.6	277.8	0.5509	1.32
"	"	2	349.1	280.2	0.5496	0.29
"	"	All	348.0	279.8	0.5500	1.75

Note: Points of desorption have been included in the analysis where "All" appears.

The actual fit of these equations to the data may be observed by viewing Fig. 5-16 through 5-21. In subsequent calculations these equations are employed to represent the data.

B. Heat of Adsorption

The heat of adsorption for pure nitrogen and oxygen on molecular sieve 5A was determined through use of the Clausius-Clapeyron equation,

$$\left[dP / dT\right]_c = \Delta Ha \; / \; T(Vg - Va)$$

The ideal gas law is assumed to apply and the volume of the adsorbed layer is assumed to be negligible (compared to the gas volume). The final equation is,

$$\Delta Ha = R \left[\frac{d\ln P}{d(\frac{1}{T})} \right]_c$$

The values for [dlnp / d(1/T)]c were determined from the slopes of the isosteric loading lines when lnp is plotted versus 1/T (See Fig. 5-22 and 5-23). The isosteric heat of adsorption for pure oxygen and nitrogen is plotted versus quantity adsorbed (See Fig. 5-24). The Ha for oxygen is nearly independent of the quantity adsorbed suggesting adsorption which occurs on an energetically homogeneous surface. The gradual rise in Ha as the loading increases has been observed for nonpolar molecules and was attributed to intermolecular interactions between the sorbate molecules (34). The initial heat of sorption for oxygen extrapolated to the y-axis is 3.37 kcal/mol which is in agreement with reported values of 3.30 kcal/mol (31,40).

For nitrogen the high values of Ha at low loading is explained by the strong quadrupole-cation interactions with the active sites. These interactions diminish as the active sites become filled. For oxygen at high loading, i.e. > 55 ml STP/gm, a gradual increase in Ha is observed, probably due to intermolecular interactions. The general trends shown in Fig. 5-24, that is, decreasing Ha for a molecule with a strong quadrupole moment and increasing Ha for a nonpolar molecule are expected results (31). The difference between the value of Ha and the heat of vaporization represents the energy of the combined interactions between the zeolite framework and the molecule, i.e. dispersion, repulsion, electrostatic-quadrupole interaction, etc.

C. Correlation and Prediction of Pure Component Isotherms

By application of the statistical thermodynamic model the pure component data were correlated and the data of Union Carbide (69) were predicted with a reasonable degree of accuracy. The pure component equation based on the statistical thermodynamic theory is,

$$c = \frac{Kp + (Kp)^2 (1-2B/V)^2 + \dots + \frac{(Kp)^m}{(m-1)!} (1-mB/V)^m}{1+Kp+ \frac{1}{2!}(Kp)^2 (1-2B/V)^2 + \dots + \frac{(Kp)^m}{m!} (1-mB/V)^m}$$

where $m \leq V/B$ (m is an integer).

The exponential factor shown in the equation in Chapter III has been omitted because its effect has been shown to be small (46). The two parameters which must be determined before this equation can be applied are K, Henry's Law constant, and B the effective molecular volume.

The values of K are found by analysis of the slope of the pure component isotherm in the region in which Henry's Law applies,i.e. the slope of the isotherm at low concentration. For oxygen, derivatives of the Langmuir equation were taken and p was set equal to zero to find K. For nitrogen the value of K was assumed to be the slope of the line from the origin to the first data point. This may have introduced some error in the analysis since the nitrogen isotherm rises steeply in the low pressure region. The values of K obtained by this method are shown in Figure 5-25 with other reported values in the literature (46). The K values obtained from data of this work agree with other literature values.

In the prediction of pure component isotherms of nitrogen and oxygen K values will be needed over a wide range of temperatures. Therefore, the K values previously obtained were fitted to the linearized form of the vant Hoff equation,

$$K = Ko \exp (qo \ / RT)$$

by a linear least squares technique. The resulting values for K and q are presented below (See Table 12).

Table 12. Values of Ko and qo giving the temperature dependence of K.

ystem	Ko (molecules/cavity Torr)	qo (kcal/mol)
N2-5A	9.0209×10^{-7}	4.52
O2-5A	1.4050×10^{-6}	3.37

The only other parameter required is B. This value is found by a method suggested by Ruthven (46) in which the isotherms are superimposed on a family of theoretical isotherm curves (See Fig. 5-26). The isotherm data must be plotted on the same coordinate system as the theoretical curves. The values for B and K are tabulated (See Table 13).

Table 13. Henry's Law constants and effective molecular volumes calculated from the pure component isotherms.

System	T(K)	K(molecules/cavity Torr)	V/B	B(cu.Angstroms)
N2-5A	203.15	0.06585	11	67
	233.15	0.01557	10	76
	297.15	0.001902	8	97
O2-5A	203.15	0.005952	20	38.8
	233.15	0.002031	20	38.8
	297.15	0.0004234	20	38.8

With these parameters identified the pure component isotherm data were correlated with reasonable results (See Fig. 5-27 through 5-32). To be able to predict isotherms of nitrogen and oxygen at other temperatures B was curve fit to a quadratic equation as a function of 1/T (See Fig. 5-33):

$$R = (1/T)\,(10^{3}) \qquad (T \text{ in degrees}\,^{\circ}K)$$

$$B = 5.465\,R^{2} - 64.56\,R + 252.4$$

With B and K defined for any temperature within the range of the original data we may predict other pure component isotherms.

The isotherms of Union Carbide (69) were predicted by the method above (See Fig. 5-34 through 5-38). The prediction for the oxygen isotherms at 273.15°K and 238.15°K are in excellent agreement, even the extrapolated prediction at 303.15°K is in good agreement. In the case of nitrogen the prediction gives good agreement at low pressures but at higher pressures the predicted curve deviates slightly from the actual data.

D. Prediction of the Multicomponent Data

The multicomponent equilibrium apparatus described in Chapter IV was employed in the collection of adsorption data for air on molecular sieve 5A at 24, -40, and -70°C (See Fig. 5-39 through 5-41). The data at all temperatures show excellent reproducibility. The isotherm for oxygen in the mixture appears to tend toward a saturation value at the lower temperatures. The argon loading is negligible at all temperatures when compared to the loading of the other components. The nitrogen mixture isotherm at the lower temperatures does not exhibit the marked curvature of the pure component isotherm at these temperatures.

In Figure 5-42 through 5-47 each component of the multicomponent mixture is plotted as quantity adsorbed versus its partial pressure in the mixture. The data plotted in this fashion display excellent reproducibility. This is evidenced by the argon data at very low partial pressures (See Fig. 5-47). Figures 5-48 through 5-50 show the partial pressures of nitrogen and oxygen in the multicomponent mixture plotted with the pure component isotherms. From these plots the departure from ideality of the mixture is evident at the lower temperatures. At 24°C both oxygen and nitrogen appear not to interact significantly since the mixture isotherms and the pure component isotherms are in most cases identical. For oxygen at higher pressure some interaction is occurring (See Fig. 5-48). We may conclude that at 24°C the lower concentration of molecules within the cavities of the zeolite permit each species to act independently. At the lower temperatures it is clear that significant intermolecular interactions are occurring.

The separation factors for this data are presented in Figure 5-51. At lower temperatures the separation factor exhibits a definite temperature dependence ,i.e. the separation factor is higher for the lower temperatures. We may conclude that the separation factor is inversely proportional to temperature at low pressures (<1 atm.) and at higher pressures (>1 atm.) the separation factor is nearly independent of temperature. The results shown on the plot agree with the published separation factor from the work of Domine and Hay (67).

In Figures 5-52 through 5-54 the multicomponent data were predicted by use of the binary statistical thermodynamic model where K and B are derived from the pure component data. At 24 °C the prediction gives excellent results, but at the lower temperatures deviation from the prediction is obvious. It should be noted that the model gives a reasonable prediction in the low pressure regime,i.e. where ideal behavior would be expected. Argon has been neglected in this prediction to minimize the complexity of the model. The assumption of a binary mixture should produce valid results since argon sorption is negligible.

In Figures 5-55 and 5-56 the value of B, the effective molecular volume, for oxygen and nitrogen was adjusted slightly and improved results were obtained. In Figure 5-57 the apparent effective molecular volumes for nitrogen and oxygen as a pure component and as a components in a binary mixture are plotted versus 1/T. This plot indicates that the apparent effective molecular volume of the nitrogen molecules is greater in a mixture with oxygen than for the pure component at the same temperature. The trend of decreasing molecular volume with temperature for the nitrogen molecule still exists. The oxygen molecules in the binary mixture are apparently packed more tightly than might otherwise be expected due to the reduction in the apparent effective molecular volume at the lower temperatures.

For prediction of binary data at other temperatures but the same total molar ratio, it may be of value to use curve fitted values for B:

$$R = (1/T)\ (10^{3})\ (K^{-1})$$

$$BN2 = 1.454\ R^{2} - 26.835\ R + 170.8$$

$$BO2 = 4.463\ R^{2} - 45.858\ R + 142.5$$

where,

BN2 = effective molecular volume for nitrogen in a binary mixture with the composition of air.

BO2 = effective molecular volume for oxygen in a binary mixture with the composition of air.

An attempt to predict the multicomponent data based on IAST theory lead to results similar to those obtained from the statistical thermodynamic model. The spreading pressure was calculated through use of the pure component isotherm fitting equations. The results of the predictions were obtained by an analytical method and are shown on Fig. 5-58 through 5-60. The prediction at 24°C is in excellent agreement with the observed data but at the lower temperatures the difference between the prediction and the data are of approximately the same magnitude as those encountered when using the statistical thermodynamic model. The nonideality of the mixture at low temperature is quite evident. A prediction of the N2-02 adsorption at 24 °C based on a statistical thermodynamic model is shown in Fig 5-112.

E. Breakthrough Experiments

Typical breakthrough data runs are shown on Fig. 5-61 through 5-68 for for a flowrate of 25 SLPM. The runs were made using two column pressures: 25 psia and atmospheric pressure. The gases used were air and oxygen so that the actual conditions of the PSA process could be approximated. Figure 5-69 shows a typical velocity/distance lag time plot which accounts for the time the gases are flowing through the associated piping. This lag time correction must be applied to the raw data to arrive at the true breakthrough time. This measurement is approached in the same manner as the column breakthrough experiments except the column of molecular sieve is absent. The spikes in the medical gas analyzer signal at about the one second mark in Figure 5-69 are due to this unit's pressure sensitivity upon switching of the gas flows. The final breakthrough results are shown below (See Fig. 5-70 through 5-73) :

Table 14. Breakthrough (B.T.) experiment results at 24°C.

Flowrate (SLPM)	N2 B.T. (sec)	O2 B.T. (sec)	1% N2 (sec)
High Pressure (25 psia)			
1.0	49.81	30.81	144.91
2.5	31.97	17.77	87.27
6.2	13.32	7.62	42.12
13.0	4.97	2.2	14.23
25.0	2.55	0.68	6.8
Low Pressure (14.4 psia)			
1.0	45.0	15.2	77.7
6.2	13.02	4.06	23.4
13.0	4.79	1.59	9.8
25.0	2.59	0.86	5.87

Table 15. Breakthrough (B.T.) experiment results at -40°C.

Flowrate (SLPM)	N2 B.T. (sec)	O2 B.T. (sec)	1% N2 (sec)
High Pressure (25 psia)			
1.0	137.3	60.55	———
6.2	38.89	14.66	244.96
13.0	12.81	4.49	95.26
25.0	6.71	2.07	50.02
Low Pressure (14.4 psia)			
1.0	127.9	39.0	586.5
6.2	37.7	13.8	167.0
13.0	11.8	4.3	87.7
25.0	6.05	1.0	42.4

Our rationale will be to analyze the data based on one of the flowrates and examine the data for any differences due to the pressure or temperature of the experiment. We will assume a hypothetical case of high pressure feed flow at 25 SLPM and a low pressure purge flow of 25 SLPM and analyze the effect of reduced temperature, i.e. 24°C to -40°C.

Reading from the above tables for 25 SLPM breakthrough runs at 24°C the time for high pressure nitrogen breakthrough, oxygen breakthrough, and 1% nitrogen concentration in the effluent are 2.55, 0.68, and 6.8 seconds, respectively. In comparison at 25 SLPM and -40°C these times at high pressure nitrogen breakthrough, oxygen breakthrough, and 1% nitrogen concentration in the effluent are 6.71, 1.0, and 42.4 seconds, respectively. It appears the lowered temperature has caused the nitrogen breakthrough period to lengthen by a factor of 2.6 and the period to reach 1% nitrogen in the effluent by a factor of 6.2.

The nitrogen breakthrough experiment relates to the high pressure feed step in the actual PSA process, and the oxygen breakthrough and attainment of 1% nitrogen in the effluent relates to the purge step in the actual PSA process. Inspection of the curves in Figures 5-74 and 5-75 shows that the lower temperature has increased the overall time for nitrogen breakthrough to occur but the length of the mass transfer front remains about the same at both temperatures. On the other hand, the mass transfer front at -40°C in the oxygen breakthrough experiment has lengthened considerably. This dramatic effect may possibly explain the reason for the observed reduction in system performance at -40°C. The increased length of the front may be due to a significant decrease in intracrystalline diffusion rate for nitrogen.

F. Dual Column PSA Experiments (2-Step and 6-Step Cycle)

Figures 5-76 through 5-87 show some typical data sets from the miniature PSA system configured for 2-step operation. A system optimized at 24°C was operated at -40°C to determine the effects of temperature. The data are presented in an alternating fashion, in that, the effect of reducing the operating temperature may be seen conveniently on each following page. Observing Figures 5-76 and 5-77, it can be seen that the inlet flowrate for the system at -40 °C is slightly greater due to the volume change at low temperature as we attempt to maintain the inlet pressure constant. The exhaust flowmeter (F2) was configured in the run at 24°C to monitor one of the column exhaust flows and at -40°C the flowmeter was setup to monitor exhaust flows from both columns. Since the flowmeter was outside its temperature range of operation at -40 °C its absolute readings are questionable. The actual exhaust flow was determined by a mass balance over one cycle based on the readings of the inlet flowmeter (F1) and the product flowmeter (F3). From Figures 5-80, 5-81, 5-84, and 5-85 it is observed that the product oxygen concentration is stable even though the the product flowrate is fluctuating.

With optimum system parameters for operation at 24 °C the ambient temperature was varied and the reduced performance reported by Miller et al. was observed (See Fig. 5-88). The significant decline in oxygen product concentration begins at approximately -10 °C as the ambient temperature is decreased. A limited number of runs were conducted at temperatures above ambient temperature up to 50°C with only a slight reduction in system performance observed.

Variation of purge flow, cycle time, and temperature was accomplished to determine their effect on the system performance (See Fig.5-89 through 5-91). The purge flow with the 0.020" orifice installed gave the best performance overall. The 2-step system configuration giving the highest purity of oxygen (94.2%) at 24°C had a 0.020" diameter purge orifice and operated on a six second cycle time. An improvement in performance at -40°C by lenthening the cycle time is worth noting, although attainment of 95% oxygen concentration was not observed (See Figure 5-90). This improvement was predicted by the breakthrough curves. The effect of product flowrate and temperature on the above 2-step system configuration giving highest purity is shown in Figures 5-92 through 5-95. The reduction in oxygen concentration with increased product flow occurs in all runs (See Figures 5-92 through 5-95).

A typical data set for a 6-step experiment is shown on Figures 5-96 through 5-107. With this system configuration all flows are much more stable. In Figures 5-96 and 5-97 the The 6-step system appears dependent on the purge flowrate but not as dependent on cycle time. The effect of cycle time and temperature on the 6-step/cycle system is shown in Figure 5-108. Oxygen recovery at 24°C is higher for the six-step system when compared to the 2-step but at -40°C they appear to be about the same (See Fig. 5-109 through 5-111). The data may not be conclusive because breakthrough data were unavailable for guidance on getting the step times.

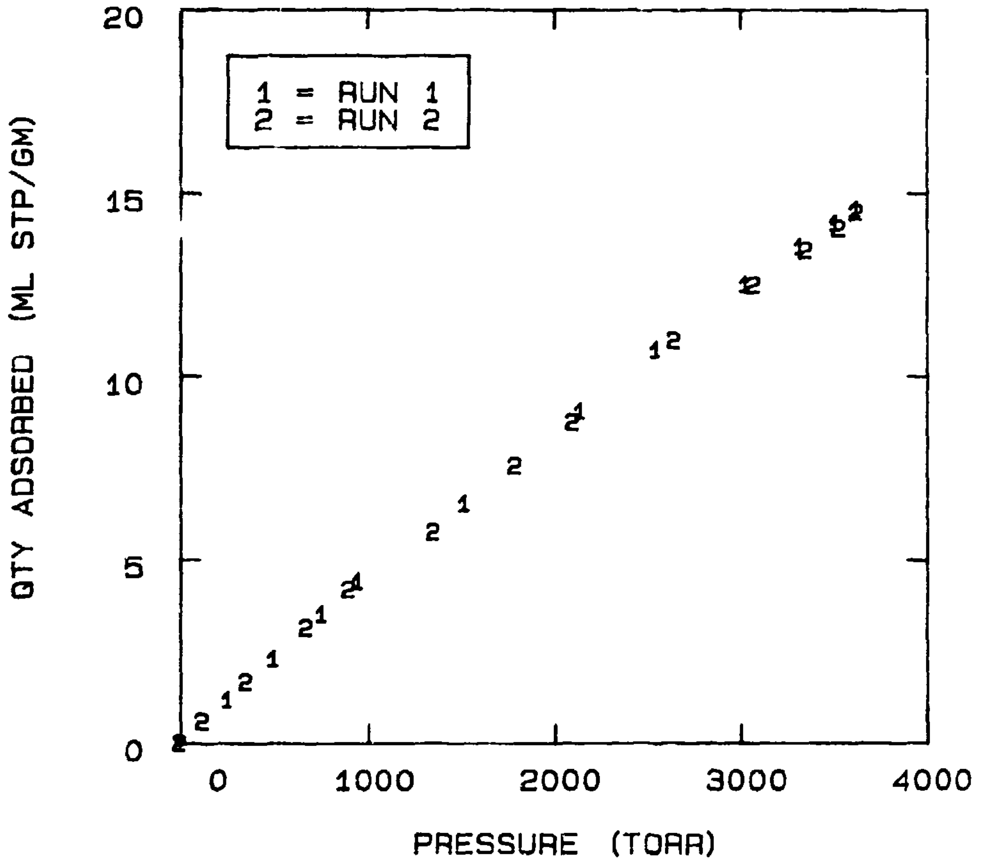

FIG 5-1. OXYGEN ON MOLECULAR SIEVE 5A AT 24°C

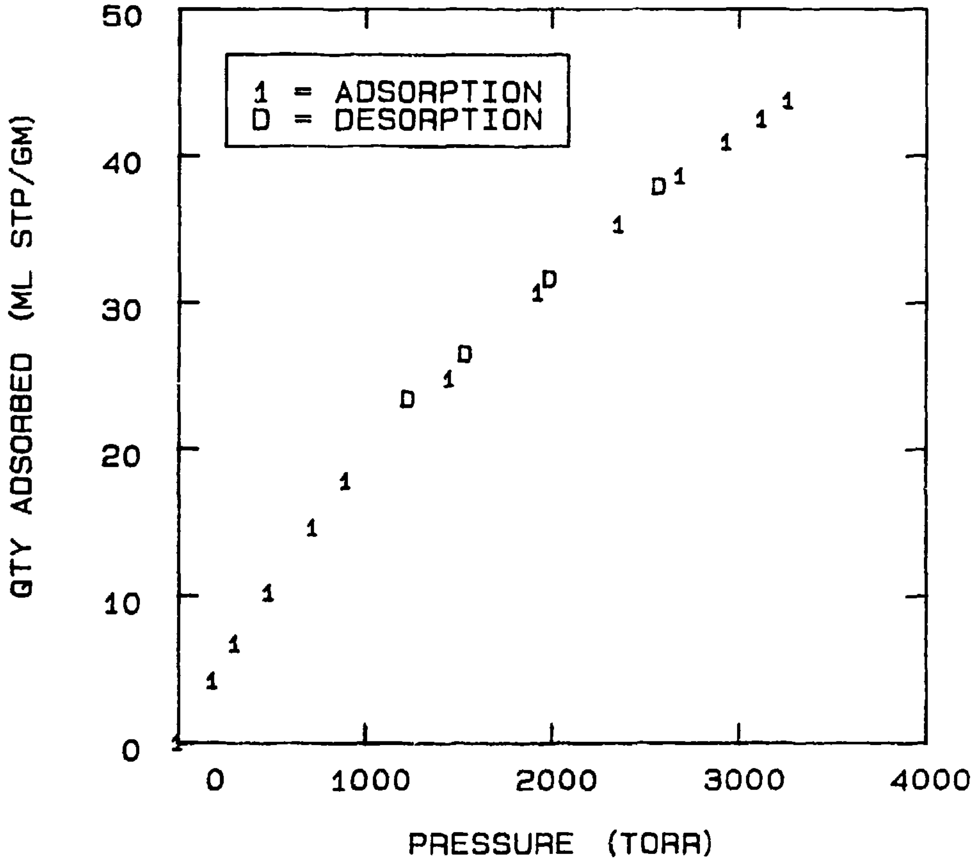

FIG 5-2. OXYGEN ON MOLECULAR SIEVE 5A AT -40°C

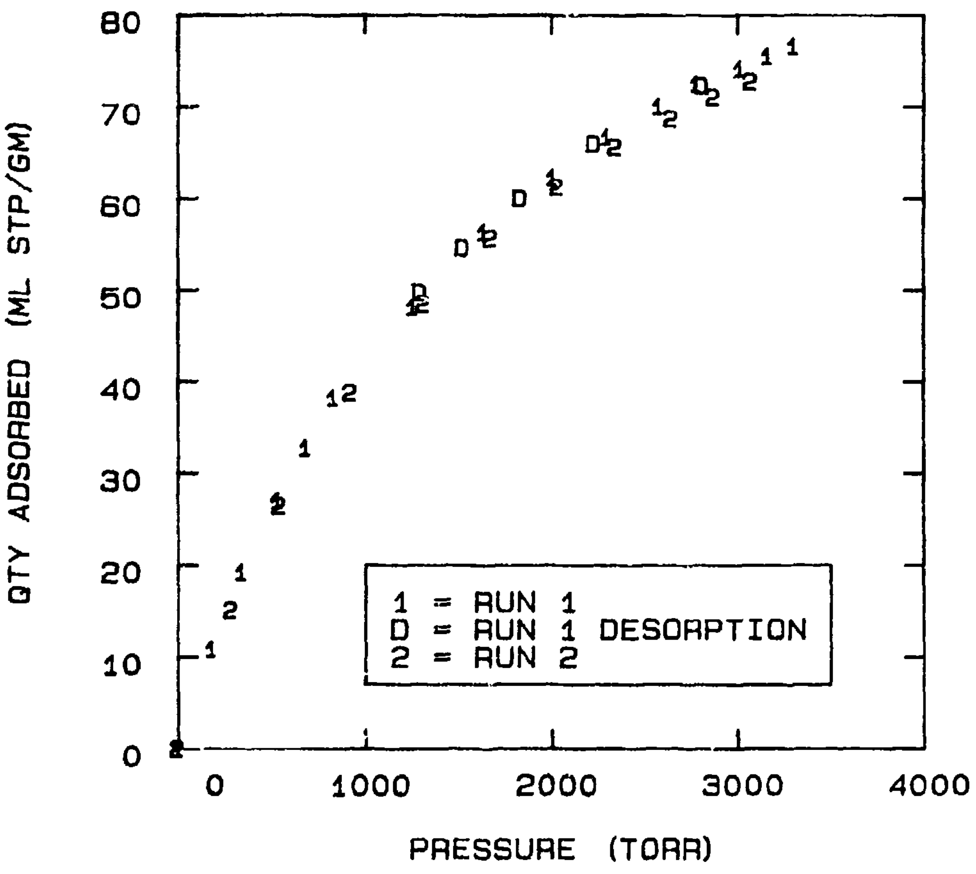

FIG 5-3. OXYGEN ON MOLECULAR SIEVE 5A AT -70°C

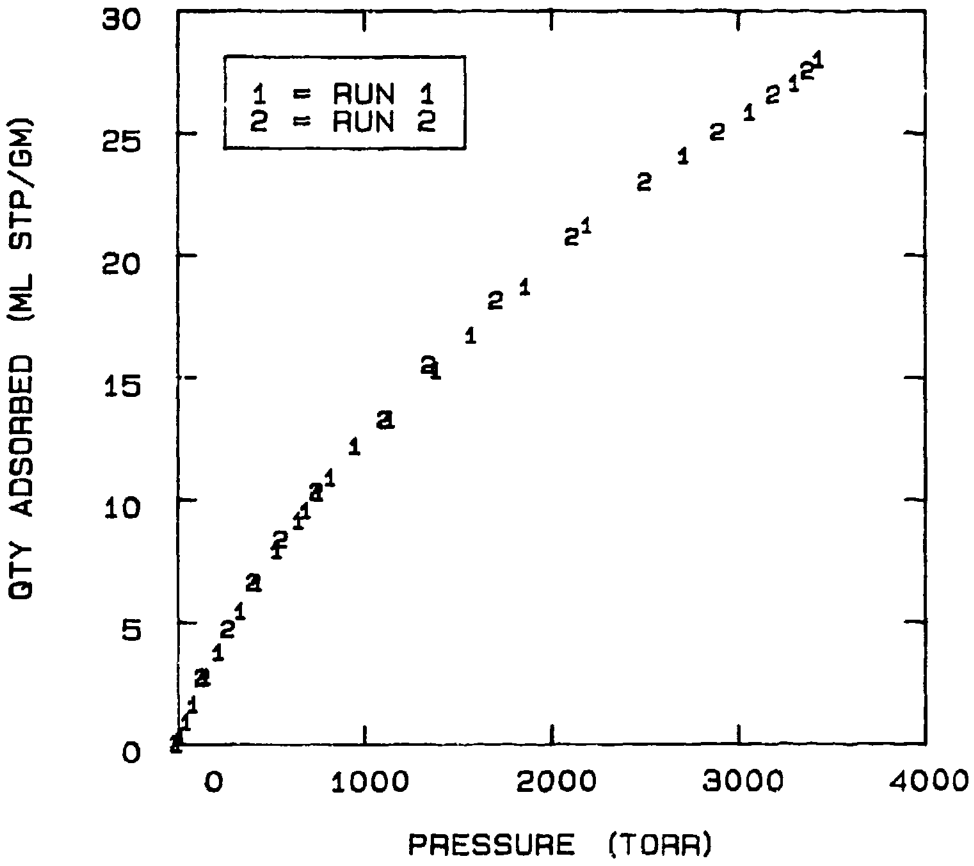

FIG 5-4. NITROGEN ON MOLECULAR SIEVE 5A AT 24°C

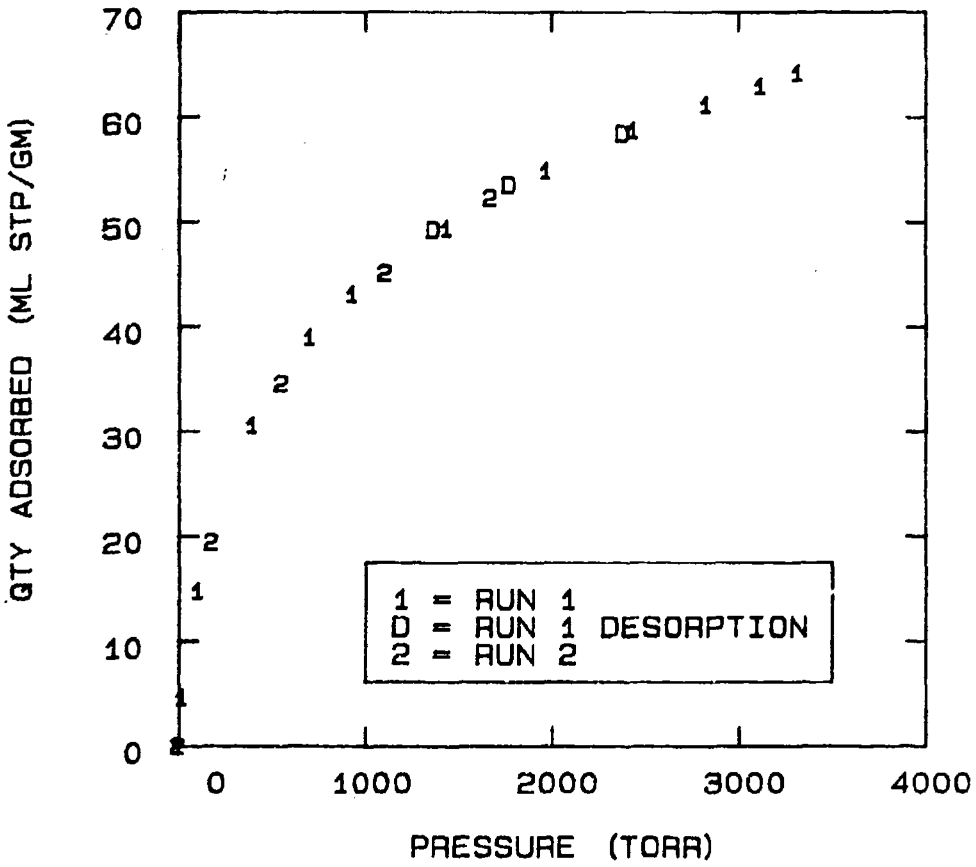

FIG 5-5. NITROGEN ON MOLECULAR SIEVE 5A AT -40°C

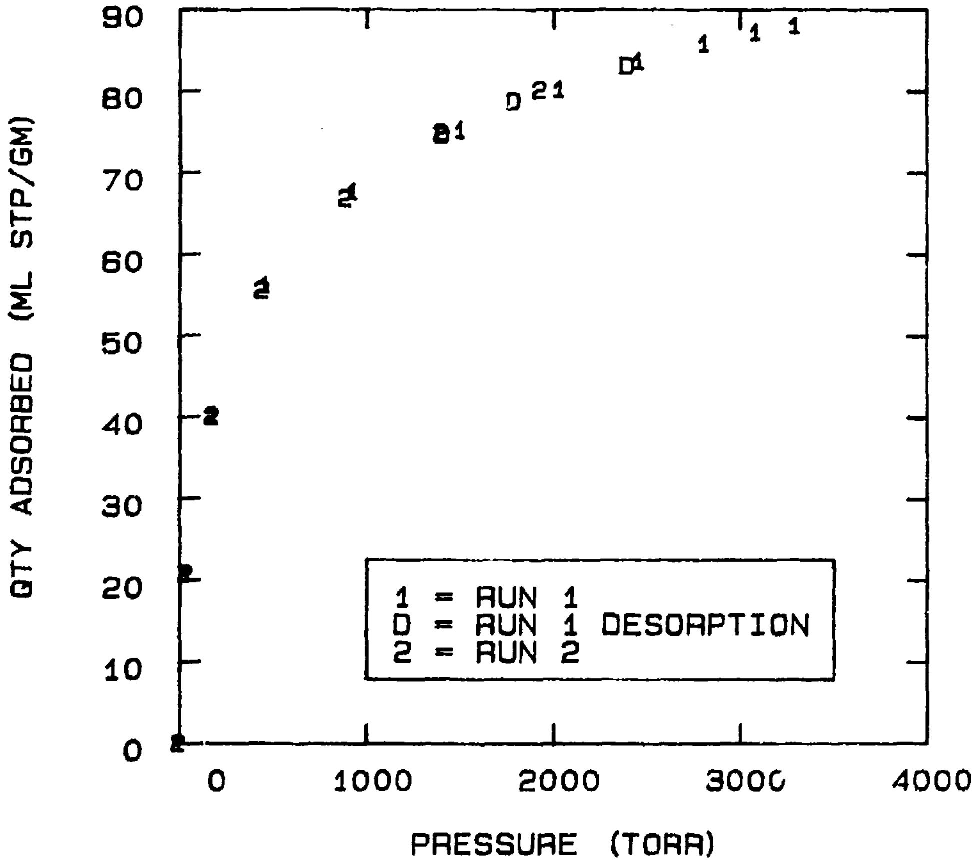

FIG 5-6. NITROGEN ON MOLECULAR SIEVE 5A AT -70°C

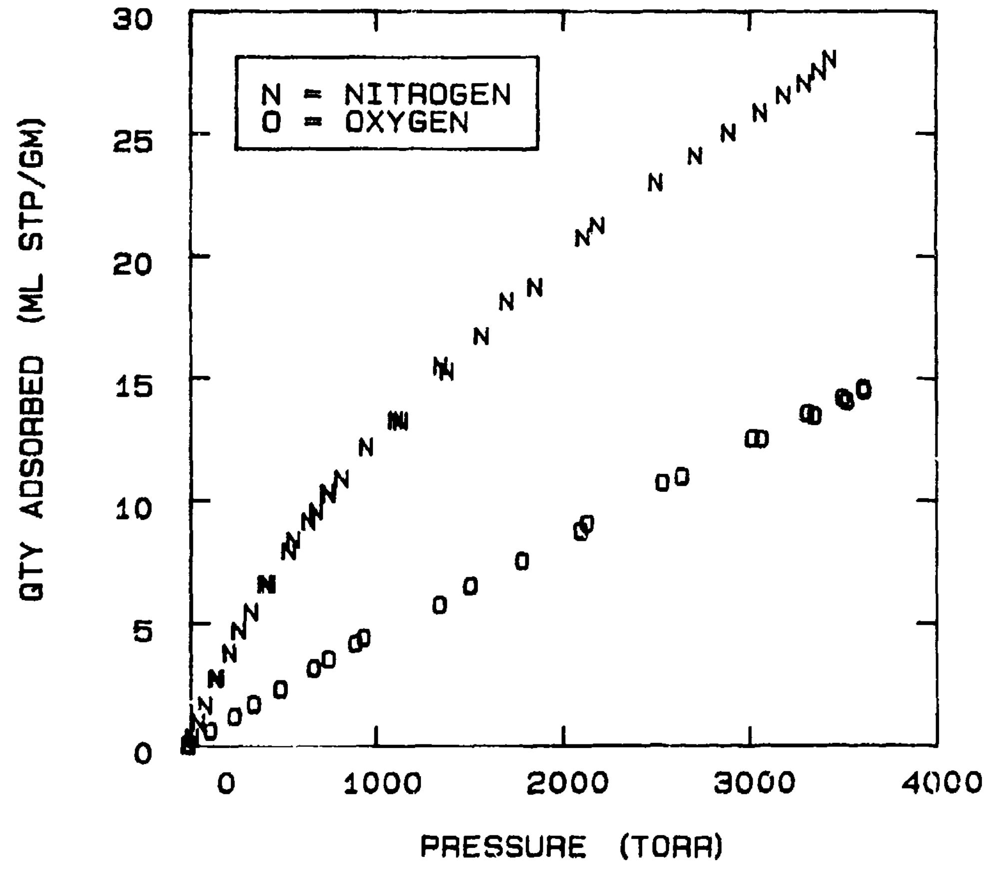

FIG 5-7. PURE NITROGEN AND OXYGEN ON MOLECULAR SIEVE 5A AT 24°C.

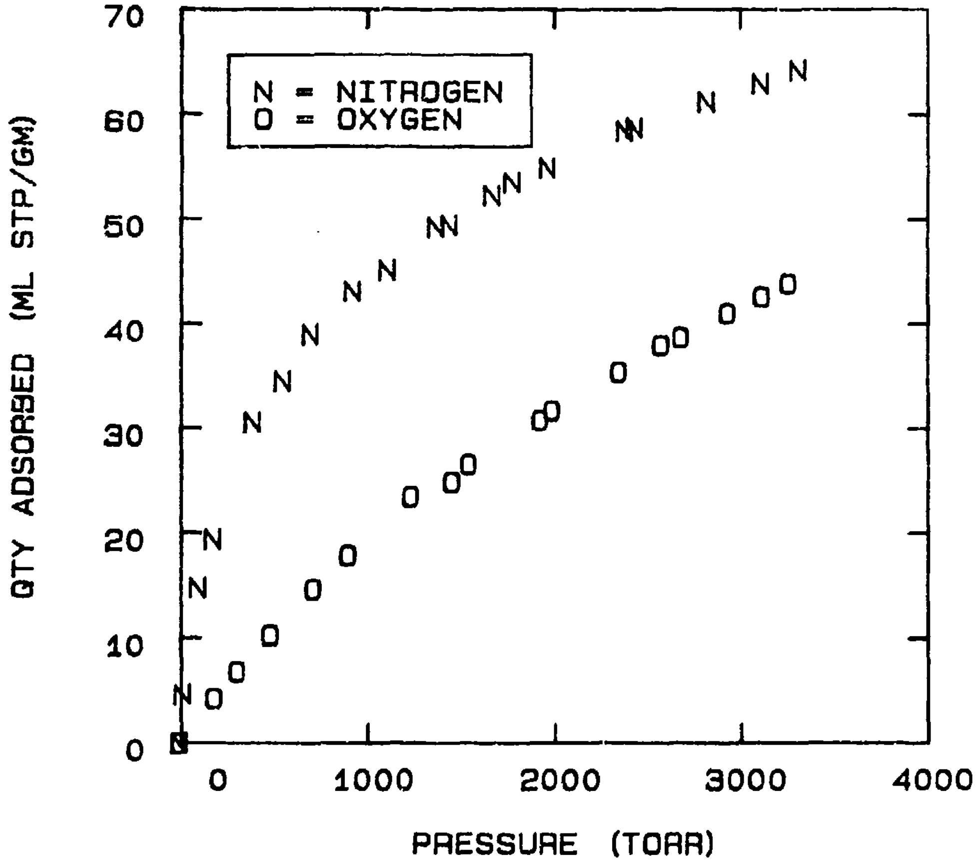

FIG 5-8. PURE NITROGEN AND OXYGEN ON MOLECULAR SIEVE 5A AT -40°C.

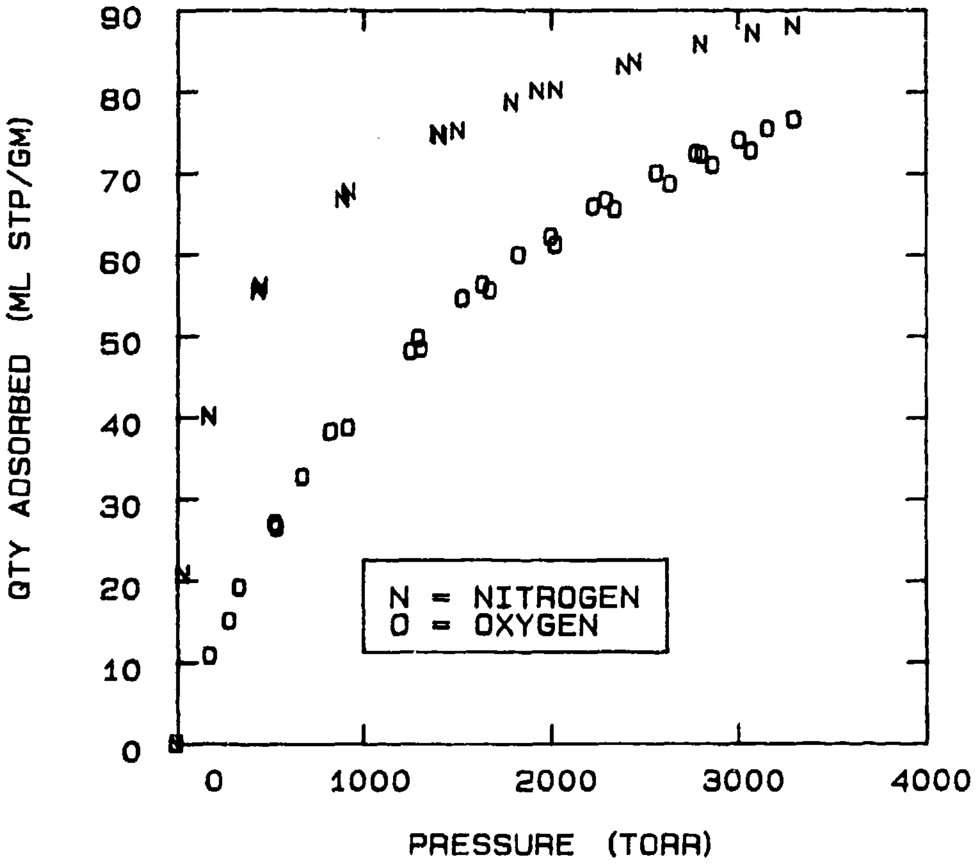

FIG 5-9. PURE NITROGEN AND OXYGEN ON MOLECULAR SIEVE 5A AT -70°C.

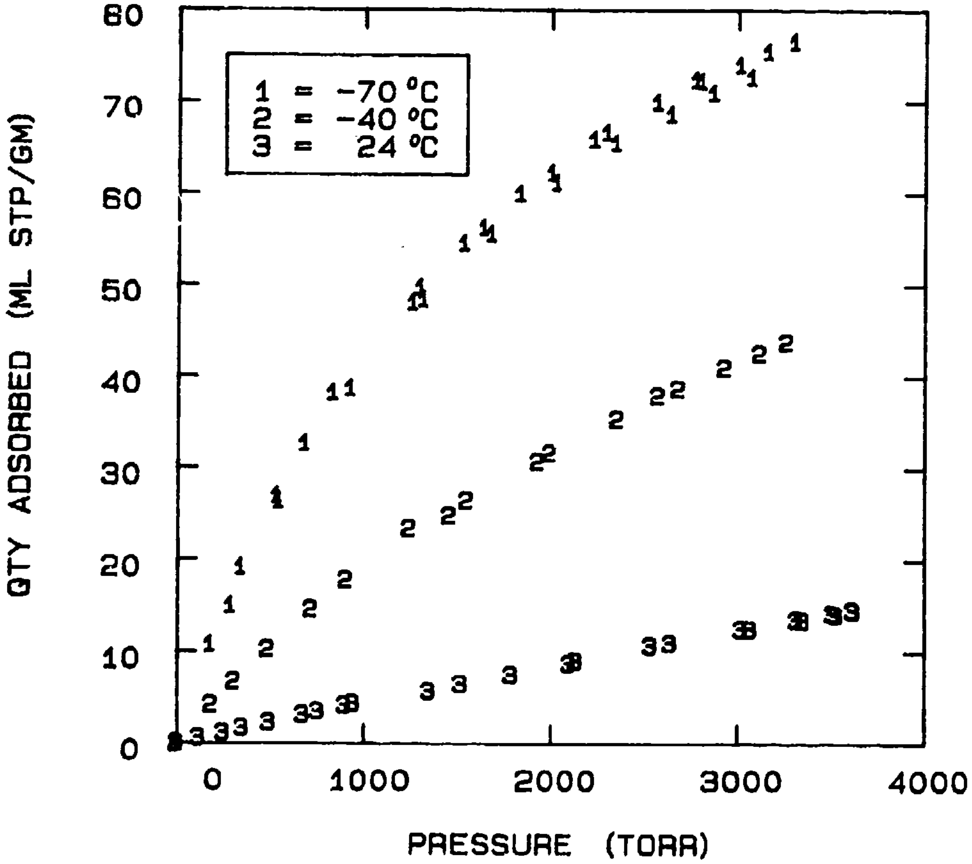

FIG 5-10. OXYGEN ISOTHERMS ON MOLECULAR SIEVE 5A.

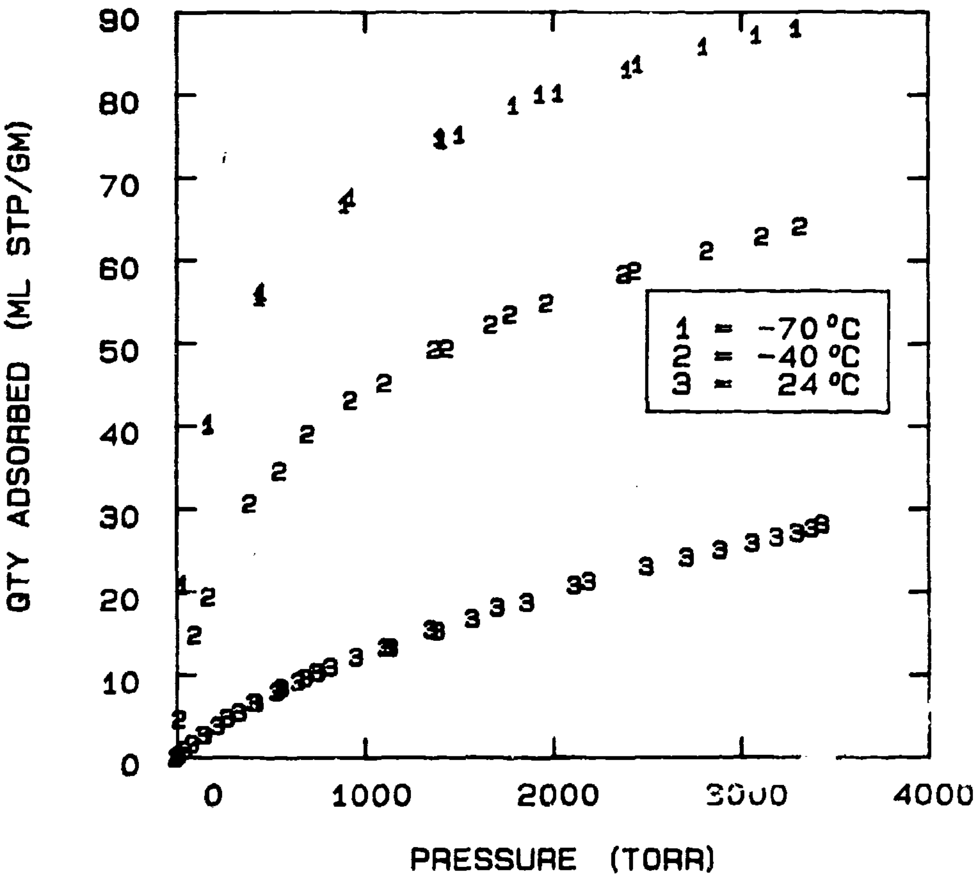

FIG 5-11. NITROGEN ISOTHERMS ON MOLECULAR SIEVE 5A.

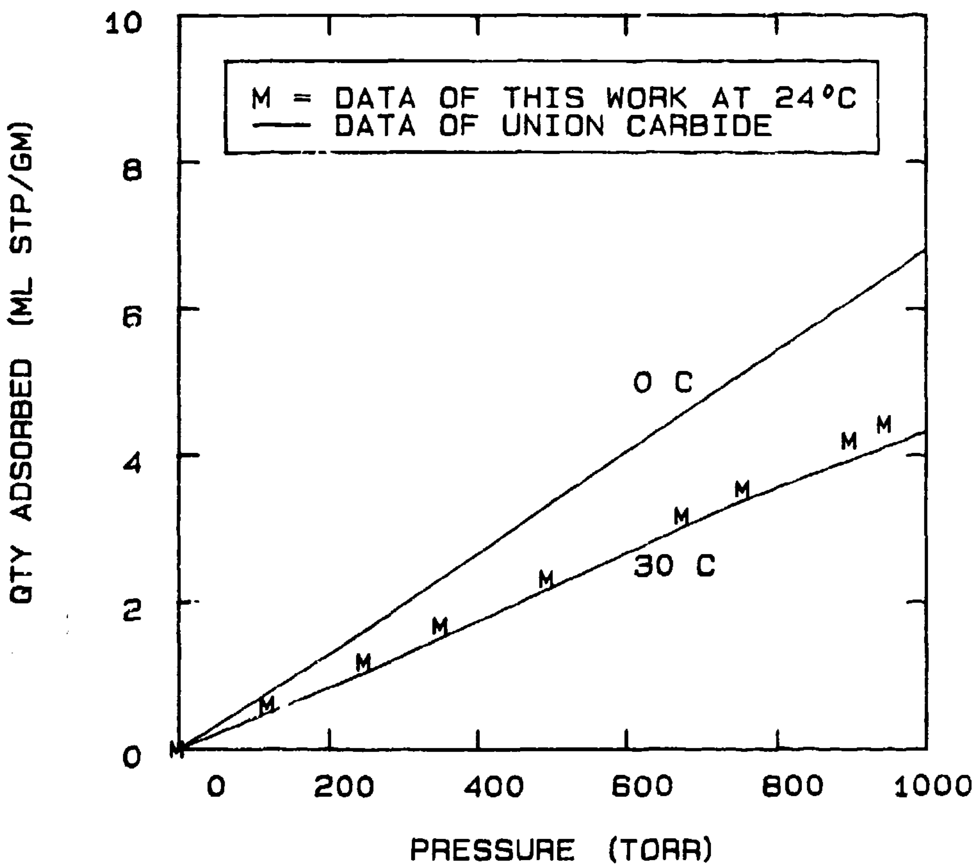

FIG 5-12. OXYGEN ISOTHERM ON MOLECULAR SIEVE 5A AT 24°C SHOWN WITH THE DATA OF UNION CARBIDE AT LOW PRESSURE.

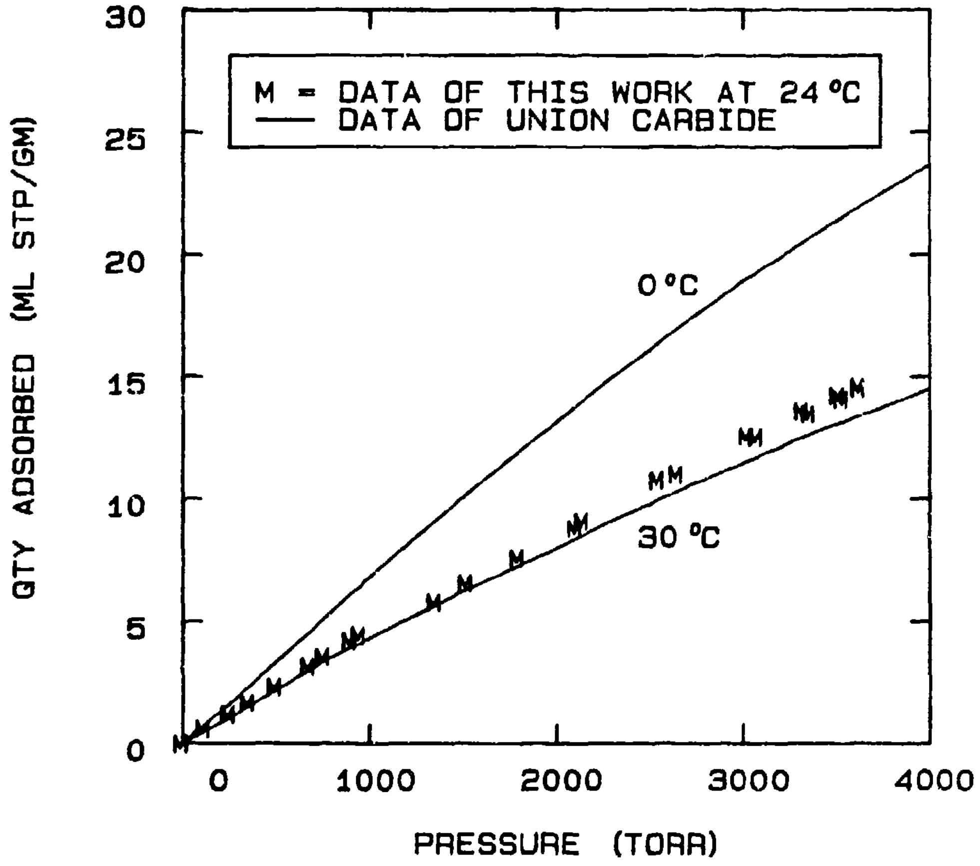

FIG 5-13. OXYGEN ISOTHERM ON MOLECULAR SIEVE 5A AT 24°C SHOWN WITH THE DATA OF UNION CARBIDE.

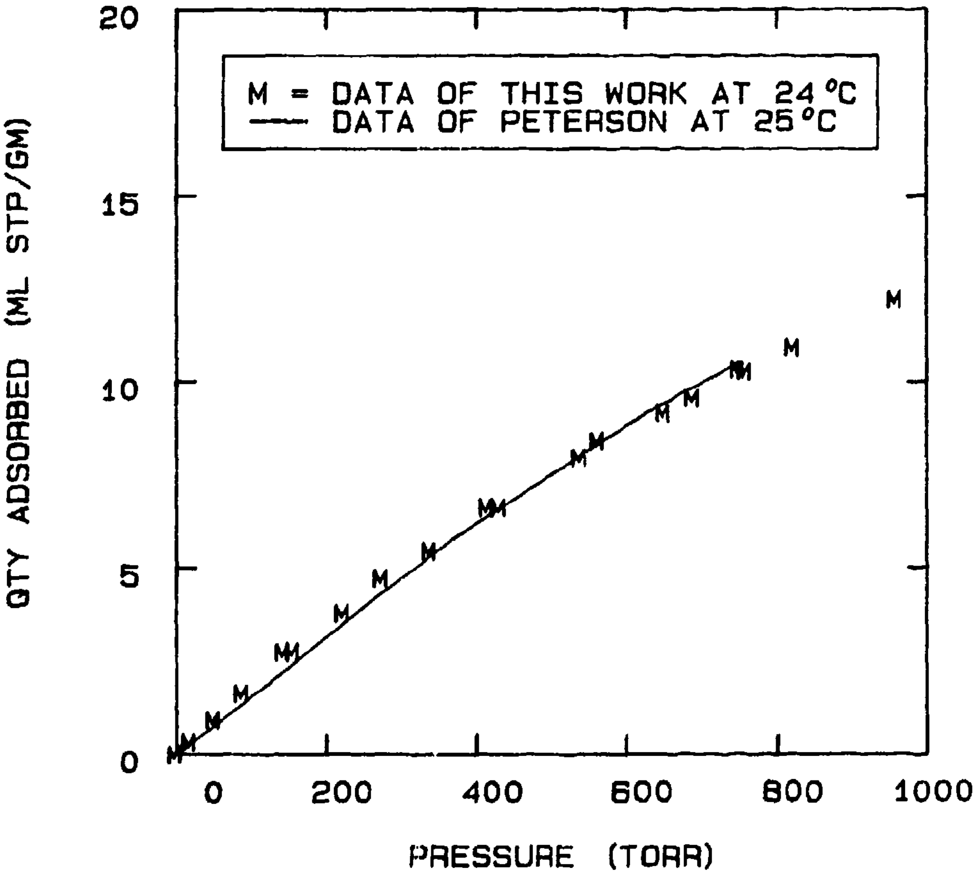

FIG 5-14. NITROGEN ISOTHERM ON MOLECULAR SIEVE 5A AT 24°C SHOWN WITH THE DATA PETERSON AT 25°C.

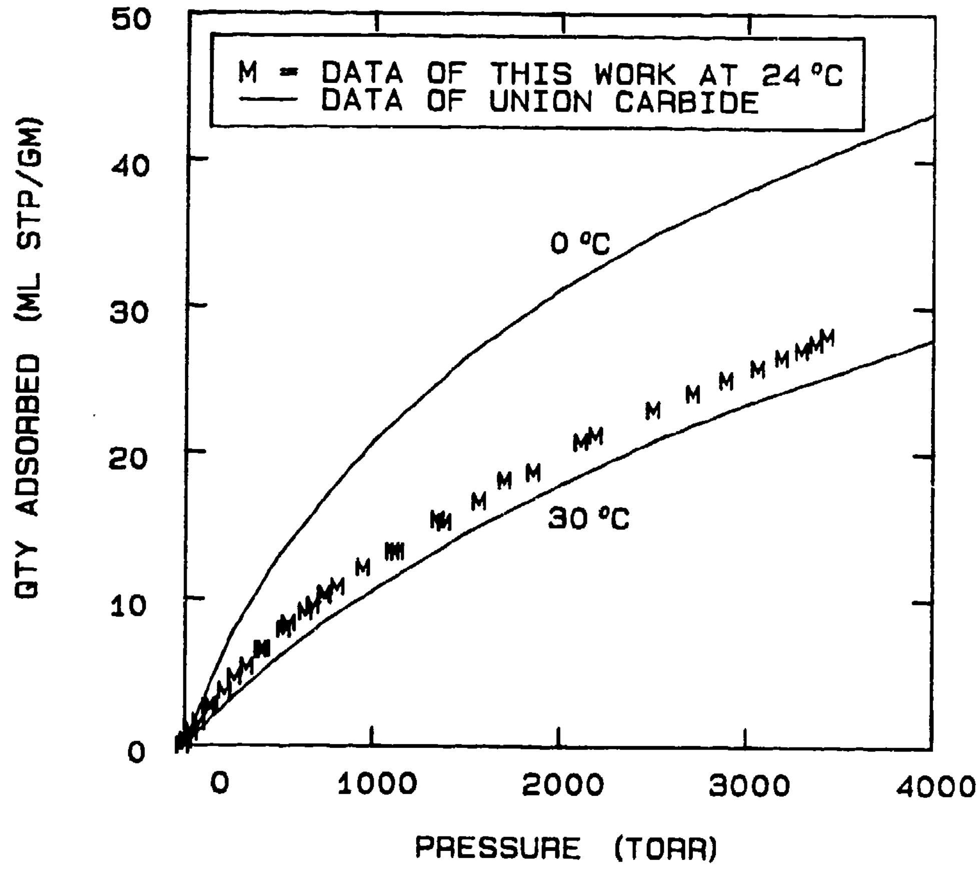

FIG 5-15. NITROGEN ISOTHERM ON MOLECULAR SIEVE 5A AT 24°C SHOWN WITH DATA OF UNION CARBIDE.

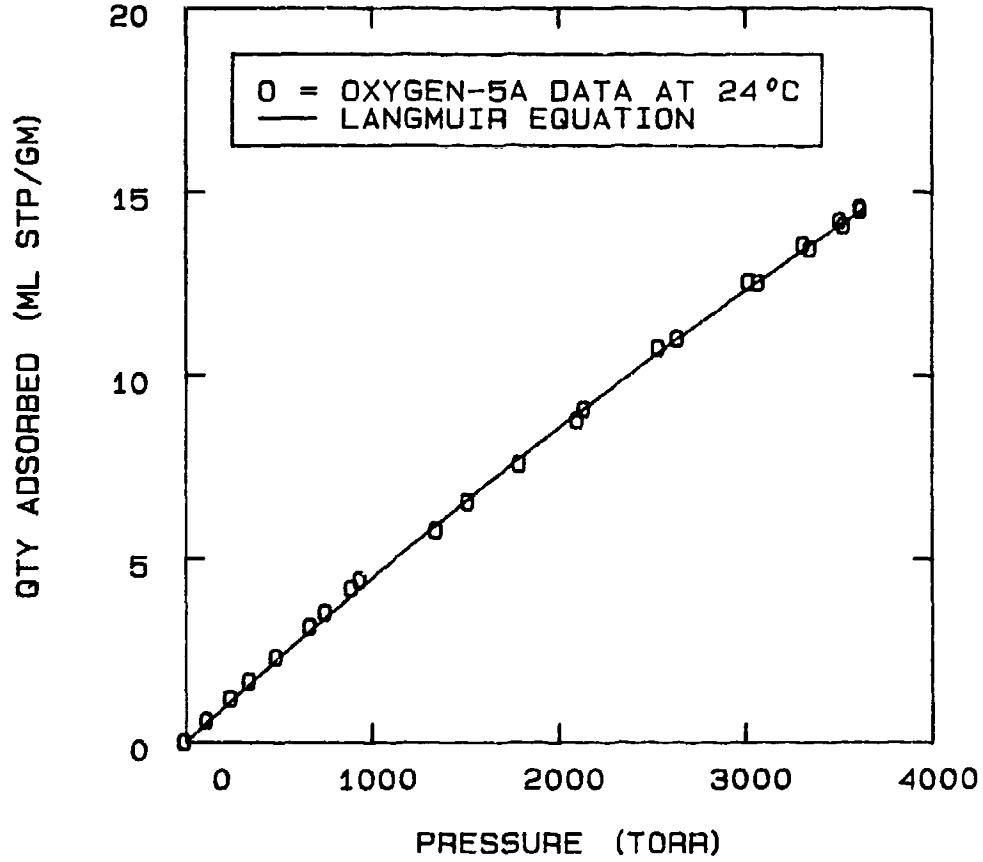

FIG 5-16. FITTING A LANGMUIR EQUATION TO THE OXYGEN-5A DATA AT 24°C.

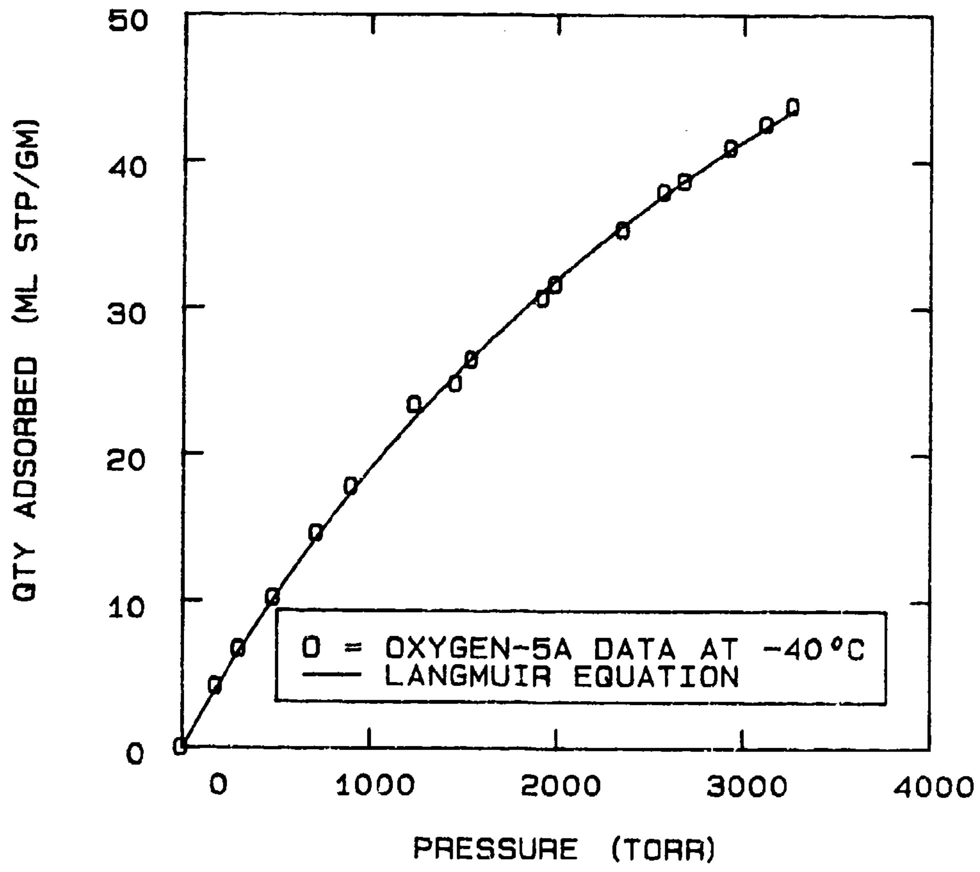

FIG 5-17. FITTING A LANGMUIR EQUATION TO THE OXYGEN-5A DATA AT -40°C.

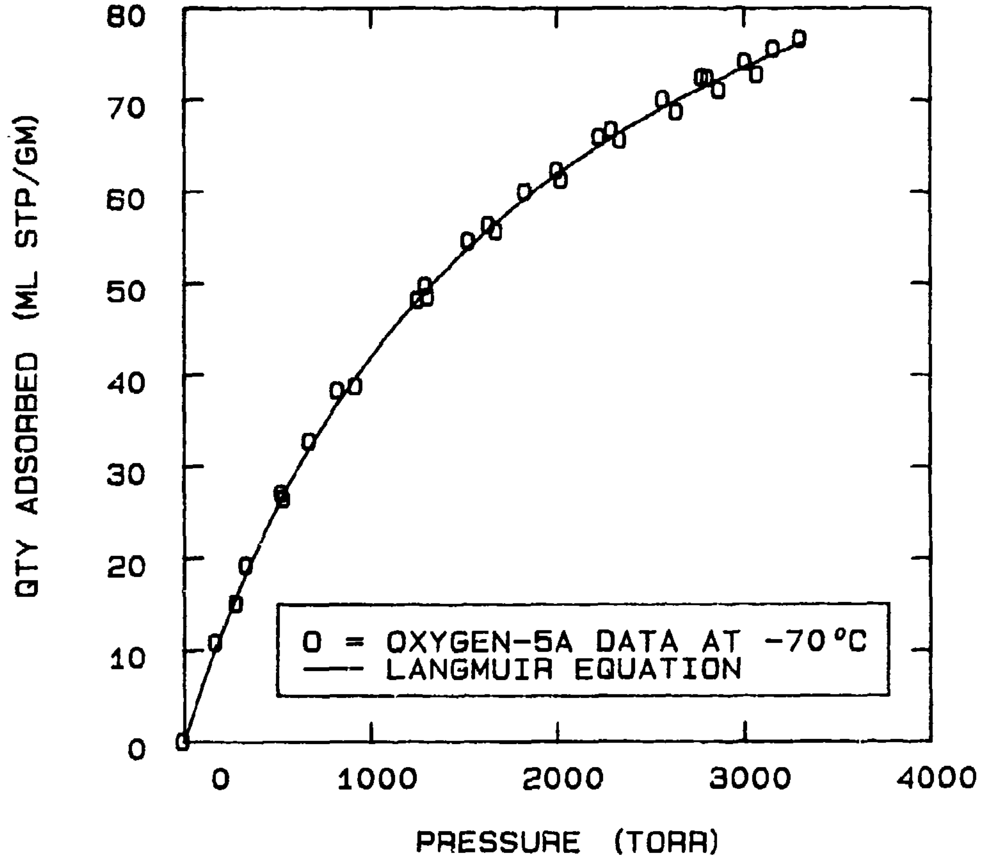

FIG 5-18. FITTING A LANGMUIR EQUATION TO THE OXYGEN-5A DATA AT −70°C.

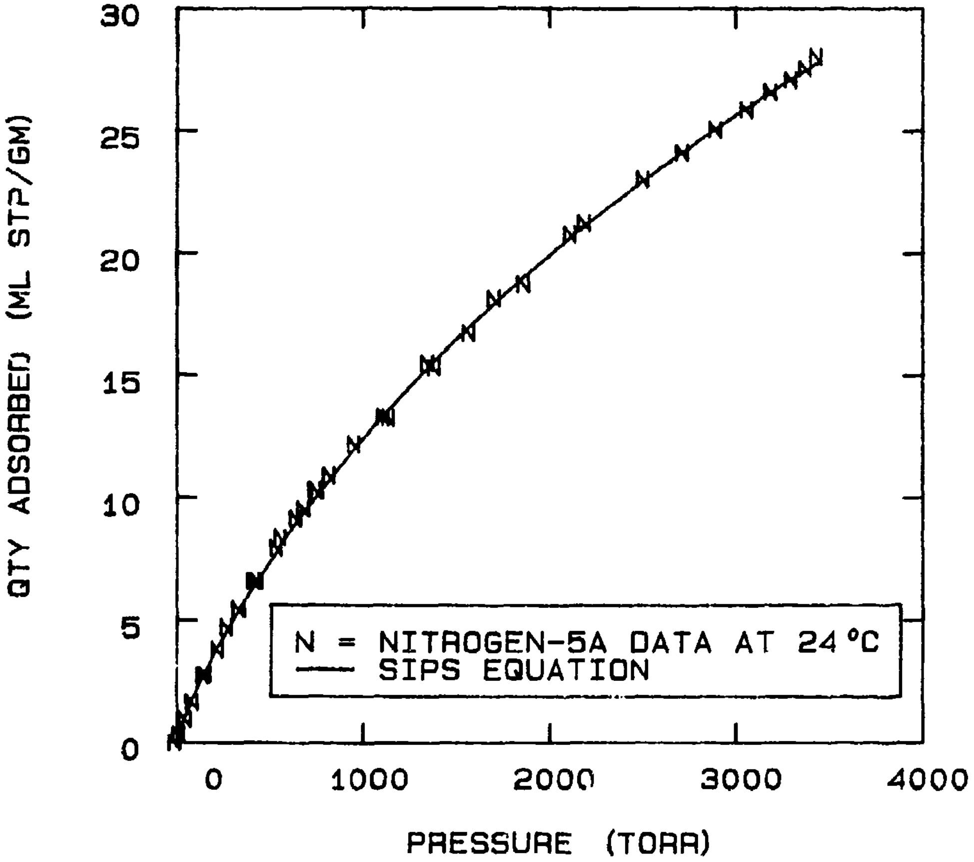

FIG 5-19. FITTING A SIPS EQUATION TO THE NITROGEN-5A DATA AT 24 °C.

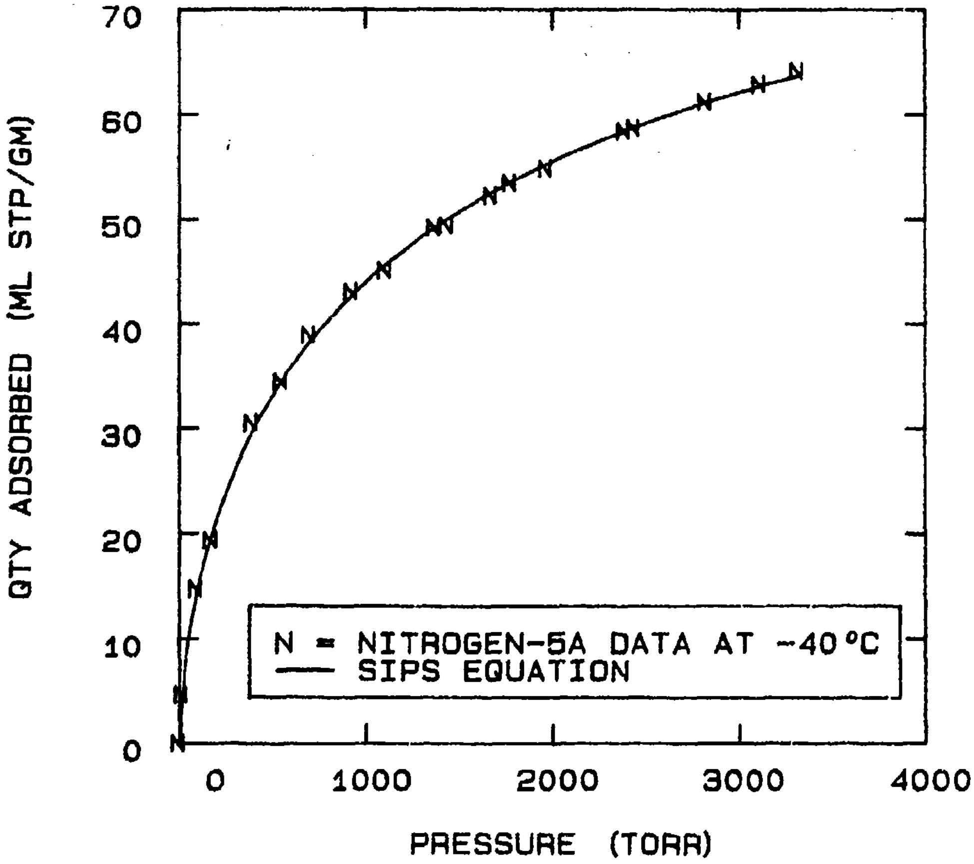

FIG 5-20. FITTING A SIPS EQUATION TO THE NITROGEN-5A DATA AT -40 °C.

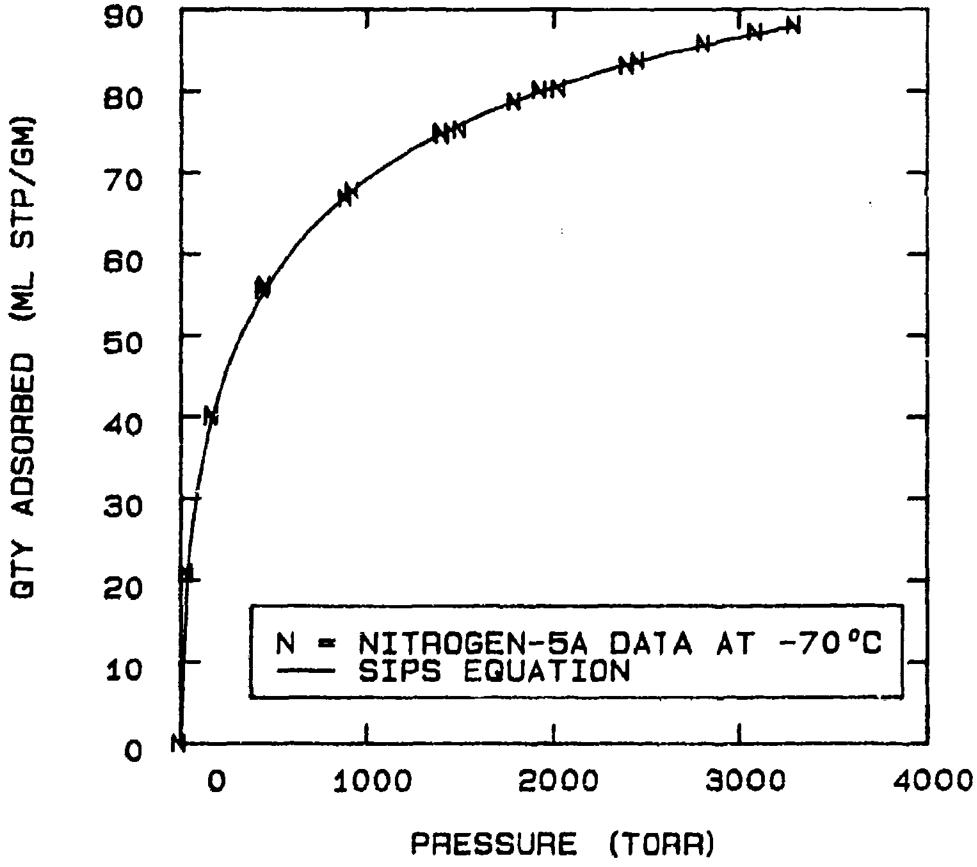

FIG 5-21. FITTING A SIPS EQUATION TO THE NITROGEN-5A DATA AT -70°C.

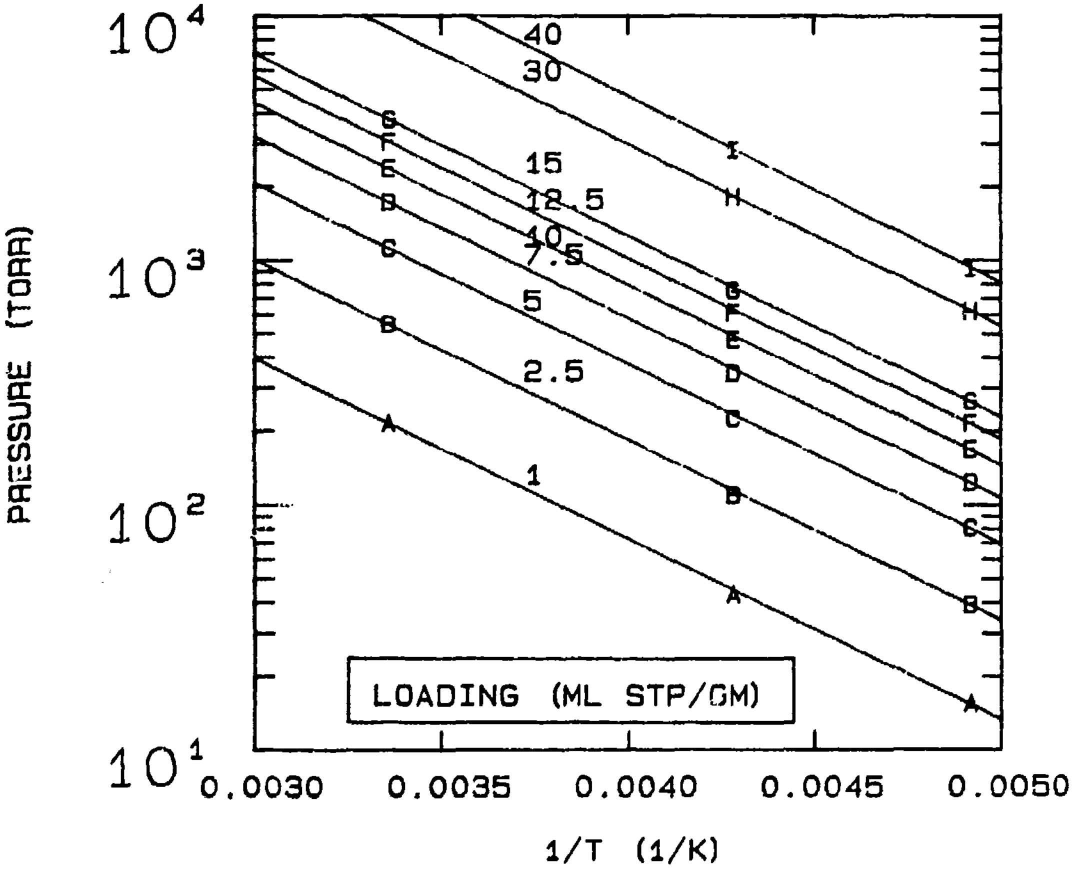

FIG 5-22. ISOSTERES FOR OXYGEN ON MOLECULAR SIEVE 5A.

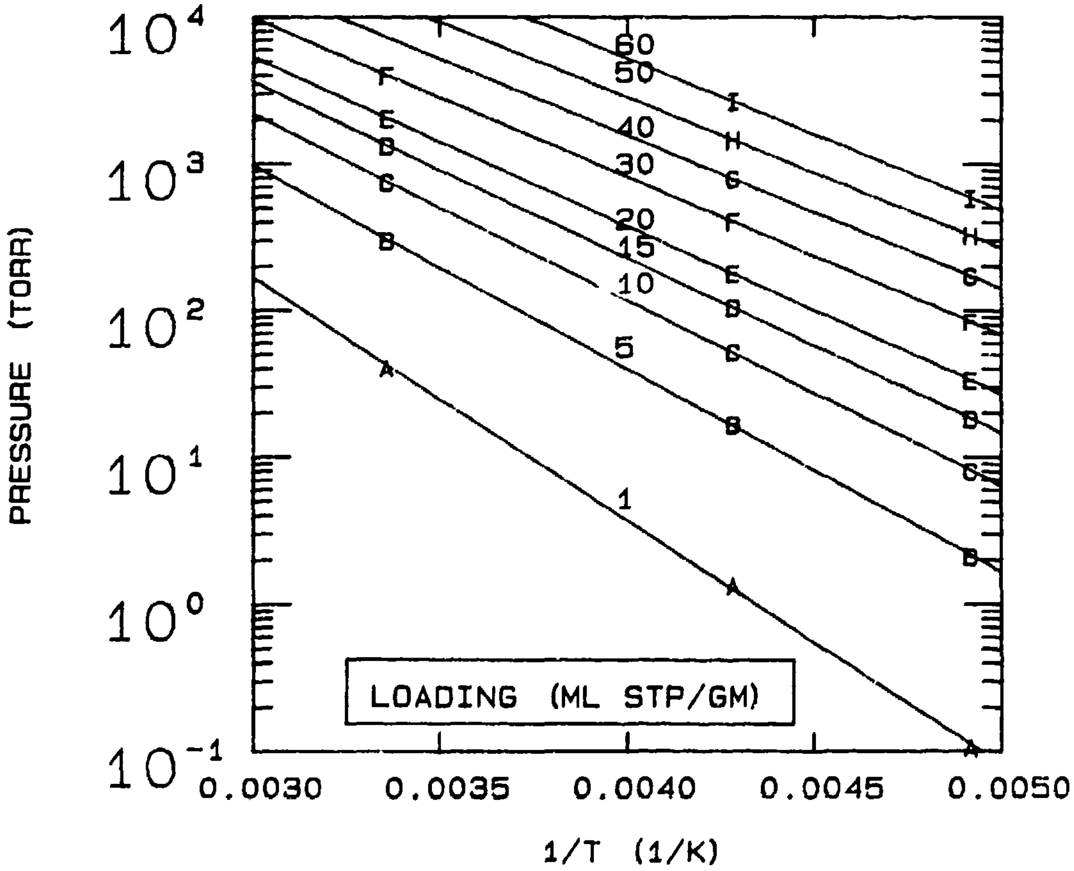

FIG 5-23. ISOSTERES FOR NITROGEN ON MOLECULAR SIEVE 5A.

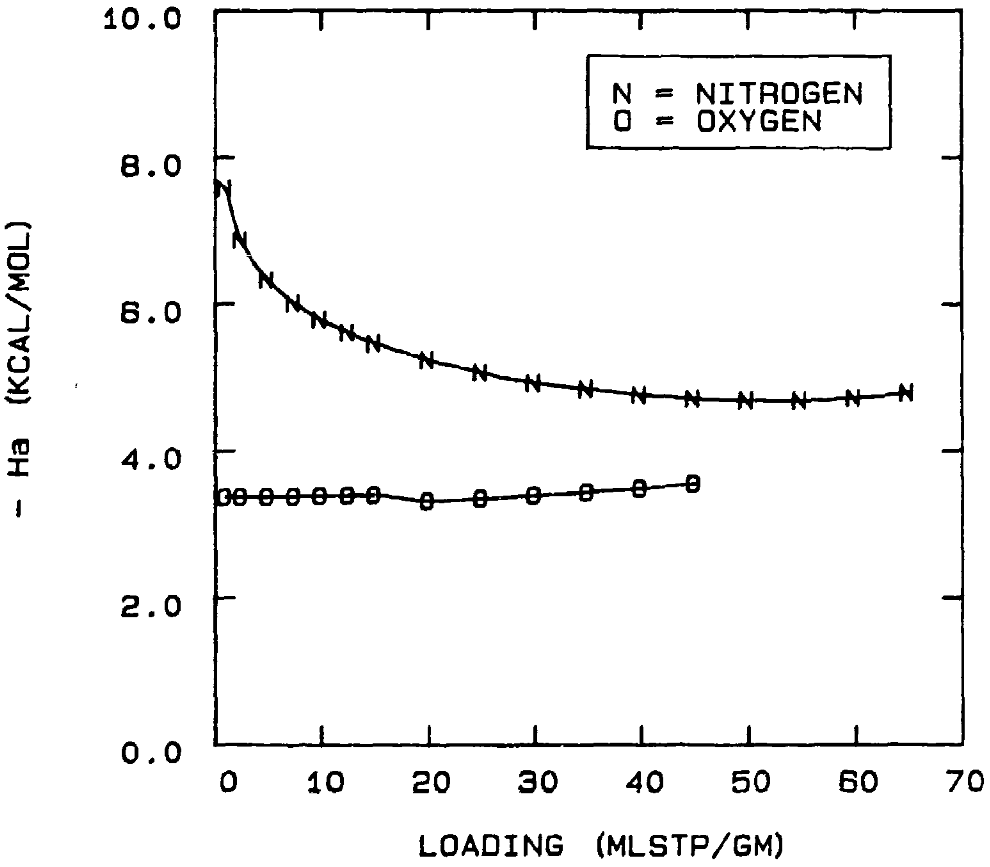

FIG 5-24. ISOSTERIC HEAT OF ADSORPTION FOR NITROGEN AND OXYGEN ON MOLECULAR SIEVE 5A.

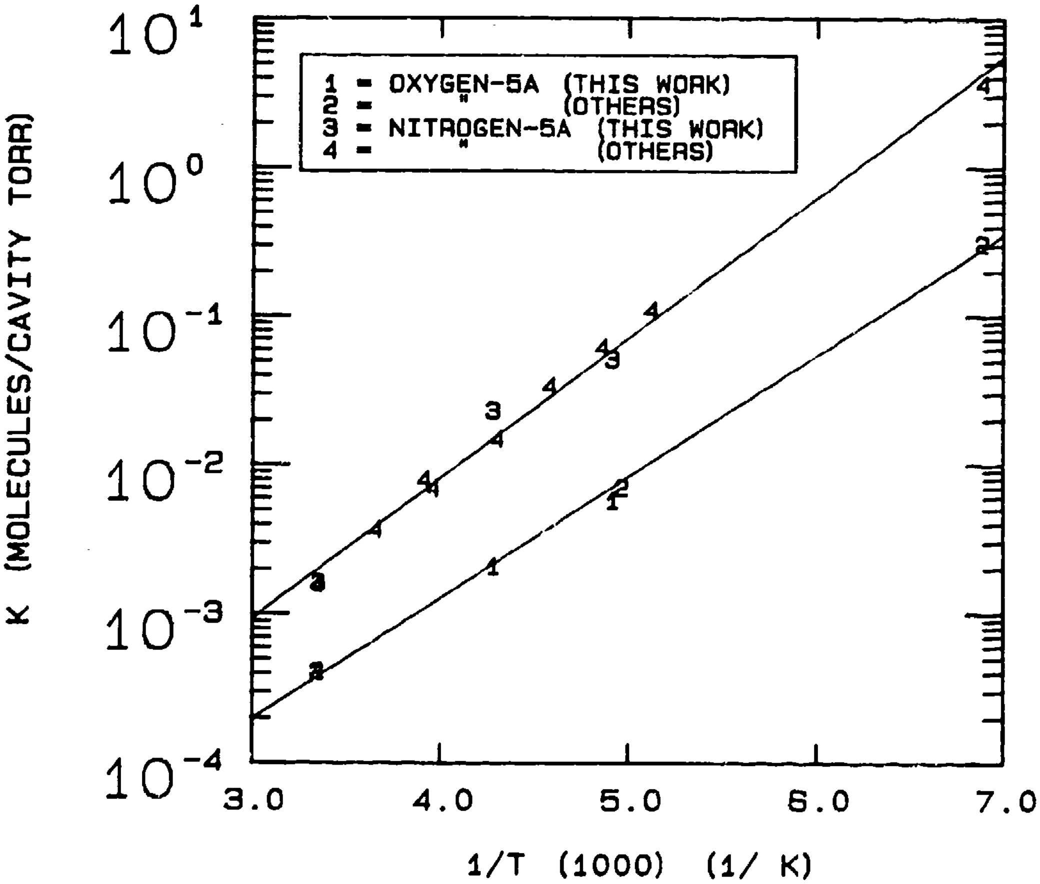

FIG 5-25. VANT HOFF PLOT SHOWING TEMPERATURE DEPENDENCE OF K.

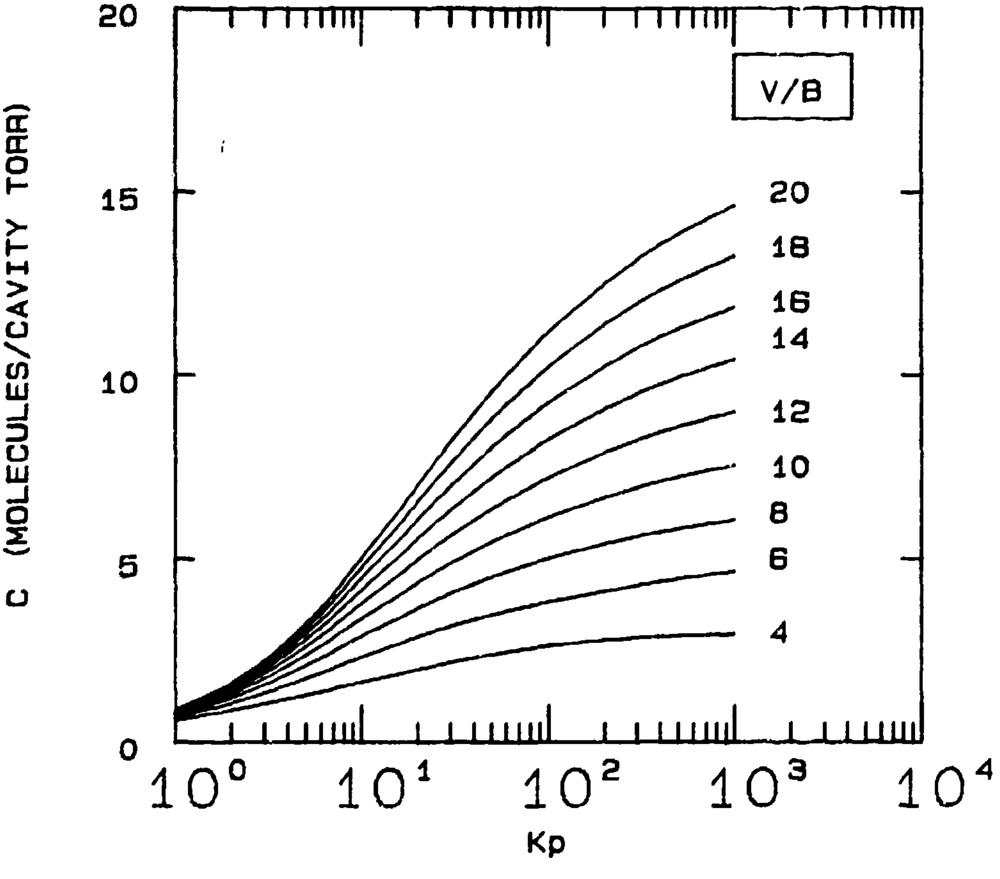

FIG 5-26. THEORETICAL EQUILIBRIUM CURVES CALCULATED USING THE STATISTICAL THERMODYNAMIC MODEL.

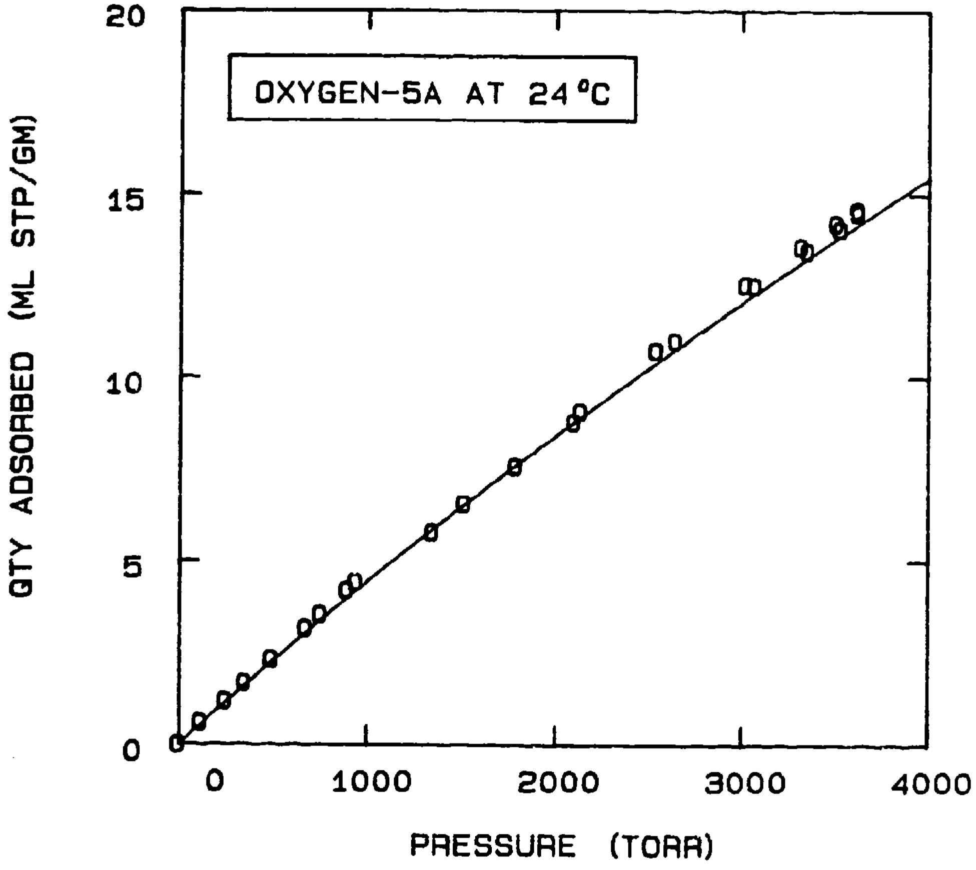

FIG 5-27. CORRELATION OF OXYGEN SORPTION ON MOLECULAR SIEVE 5A AT 24°C USING A STATISTICAL THERMODYNAMIC MODEL WHERE: K = 0.0004234, B = 38.8, AND m = 20.

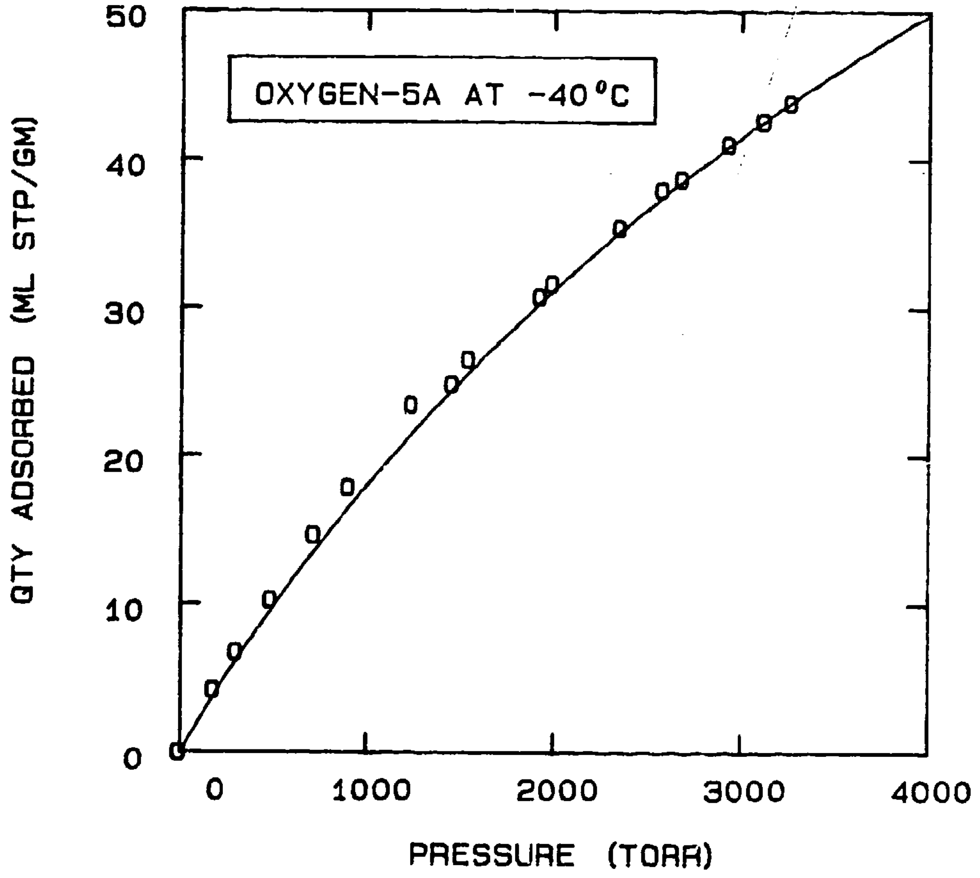

FIG 5-28. CORRELATION OF OXYGEN SORPTION ON MOLECULAR SIEVE 5A AT -40°C USING A STATISTICAL THERMODYNAMIC MODEL WHERE: K = 0.002031, B = 38.8, AND m = 20.

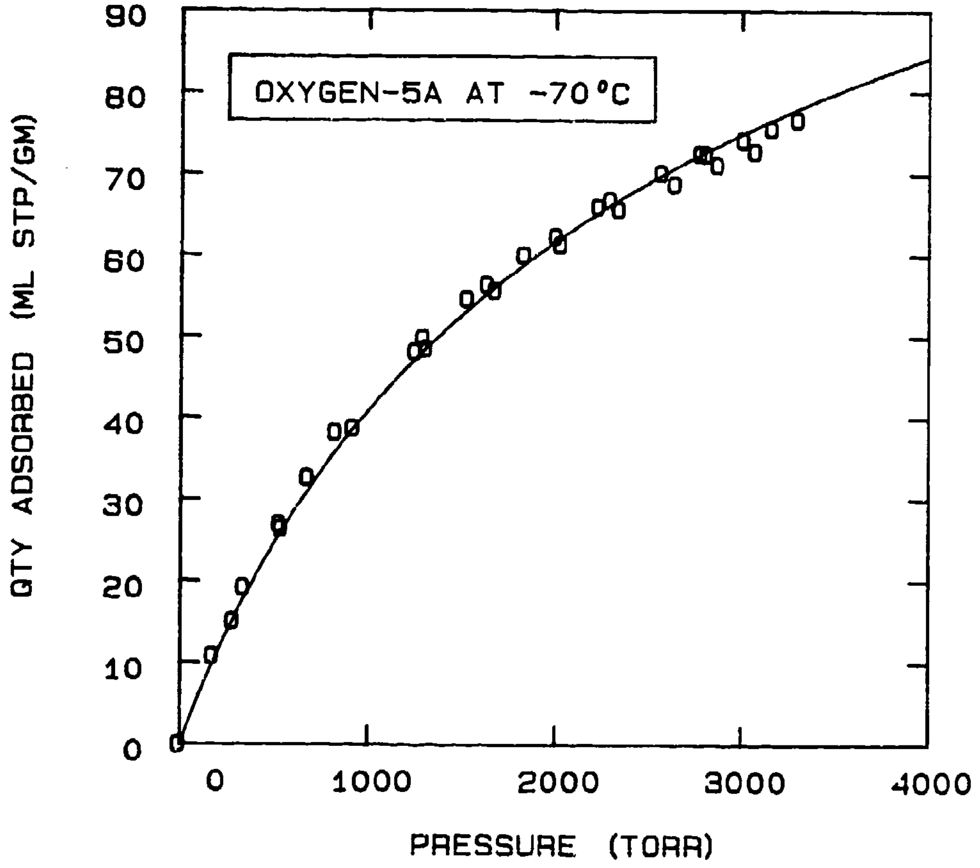

FIG 5-29. CORRELATION OF OXYGEN SORPTION ON MOLECULAR SIEVE 5A AT -70°C USING A STATISTICAL THERMODYNAMIC MODEL WHERE: K = 0.005952, B = 38.8, m = 20.

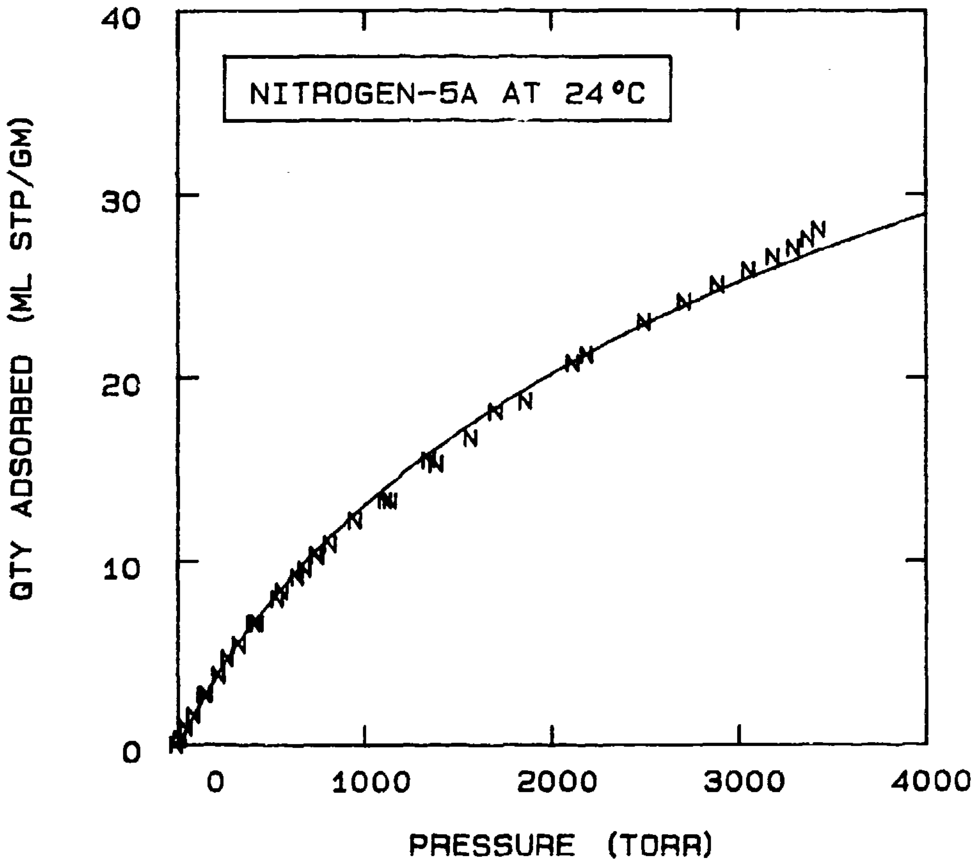

FIG 5-30. CORRELATION OF NITROGEN SORPTION ON MOLECULAR SIEVE 5A AT 24°C USING A STATISTICAL THERMODYNAMIC MODEL WHERE: K=0.001902, B=97, AND m=8.

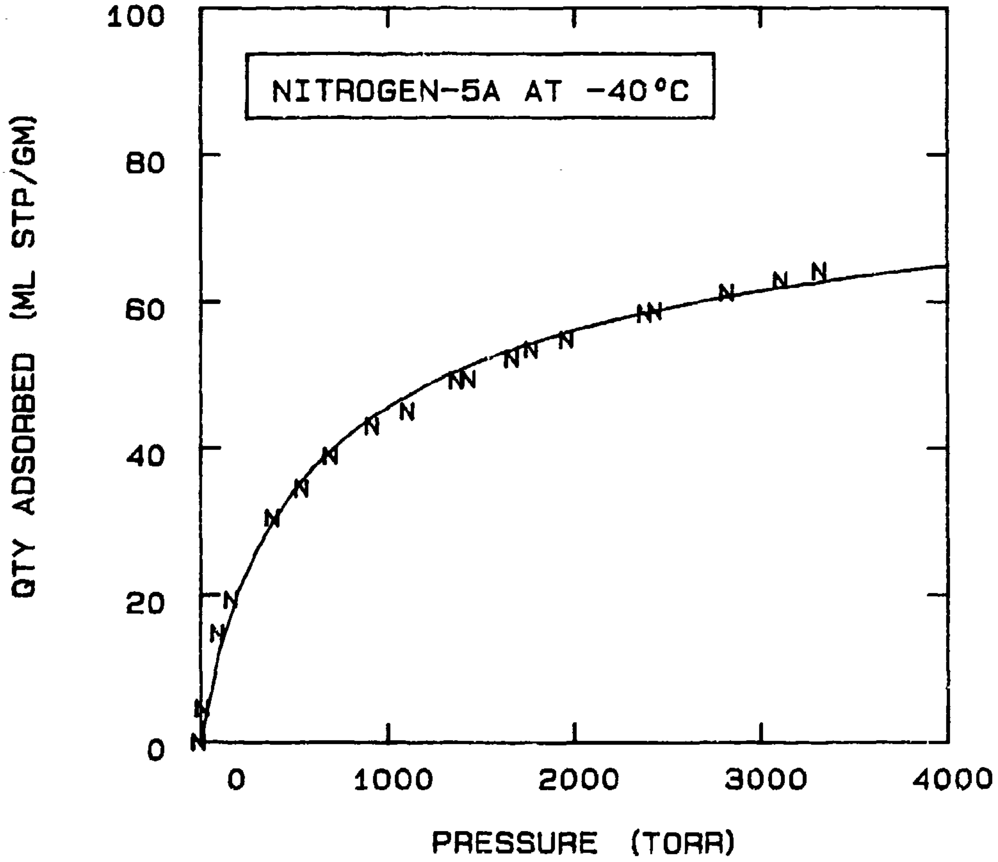

FIG 5-31. CORRELATION OF NITROGEN SORPTION ON MOLECULAR SIEVE 5A AT -40°C USING A STATISTICAL THERMODYNAMIC MODEL WHERE: K=0.01557, B=76, AND m=10.

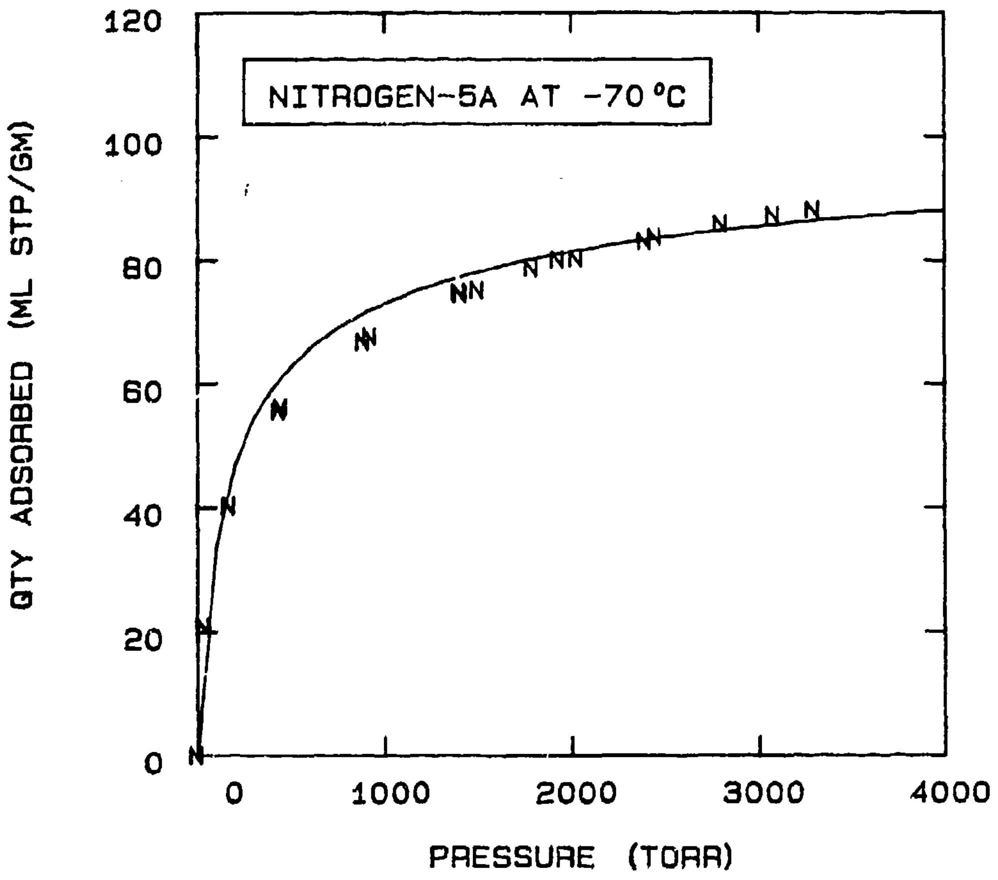

FIG 5-32. CORRELATION OF NITROGEN SORPTION ON MOLECULAR SIEVE 5A AT -70 °C USING A STATISTICAL THERMODYNAMIC MODEL WHERE: K=0.06585, B=67, AND m=11.

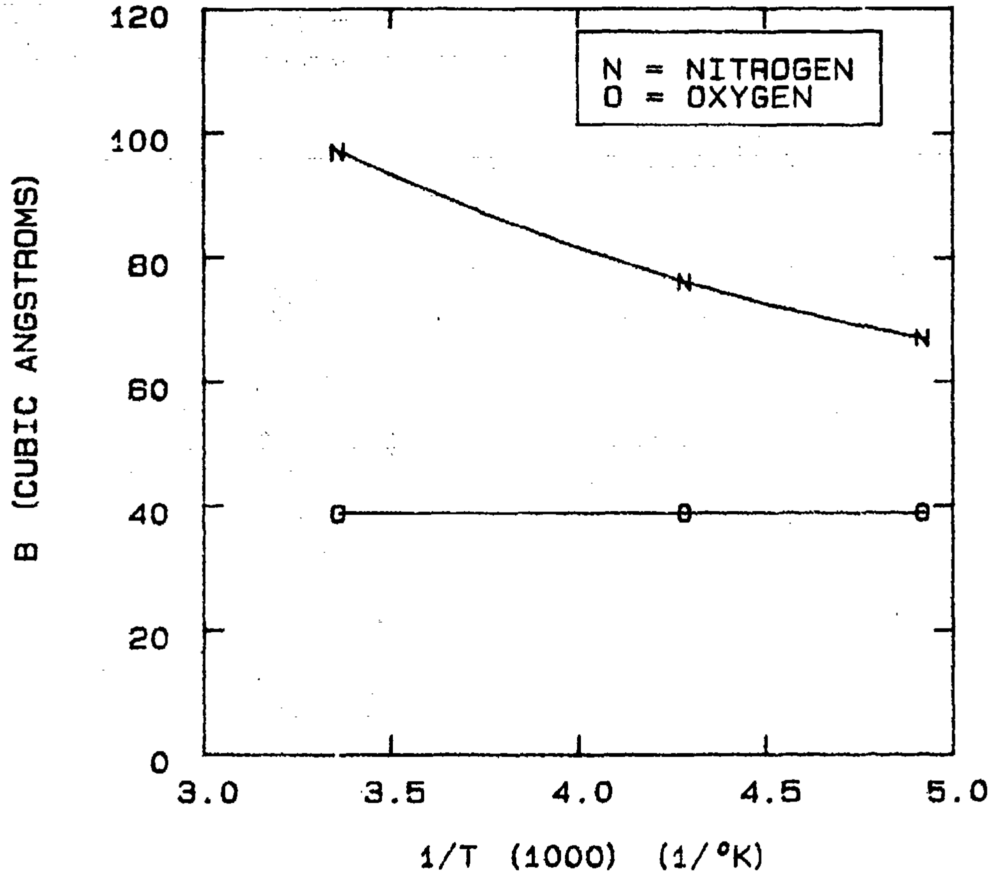

FIG 5-33. TEMPERATURE DEPENDENCE OF THE APPARENT EFFECTIVE MOLECULAR VOLUME FOR PURE NITROGEN AND OXYGEN ON MOLECULAR SIEVE 5A.

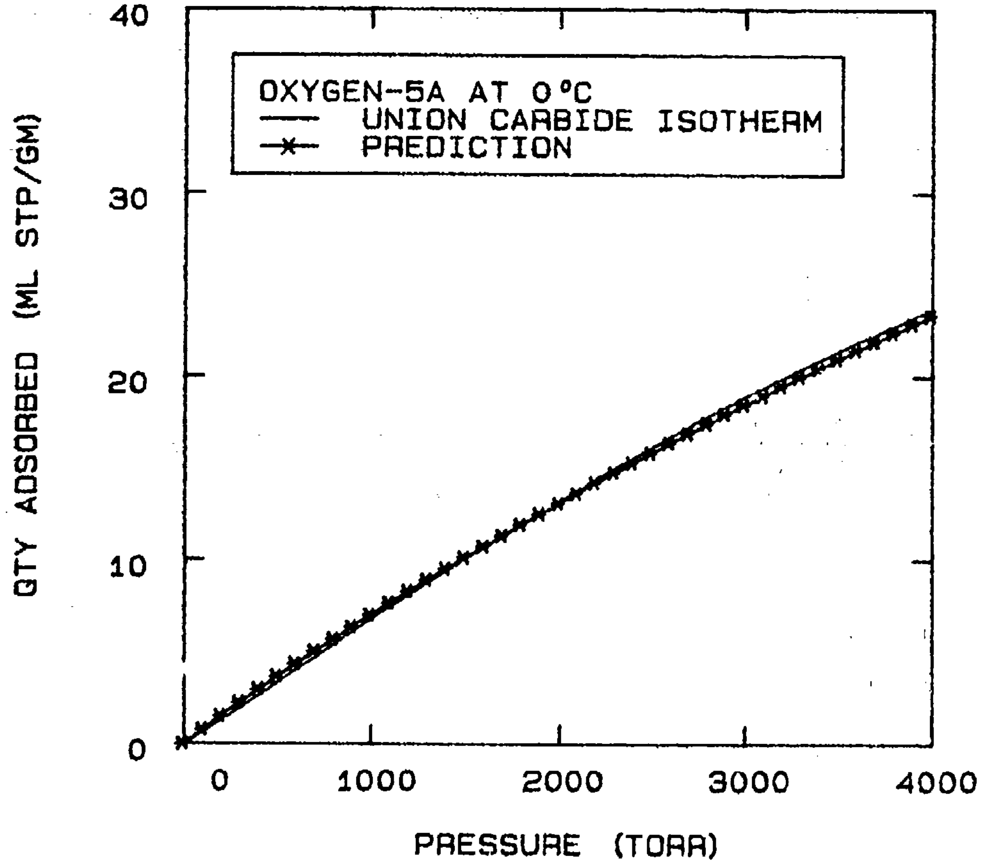

FIG 5-34. PREDICTION OF UNION CARBIDE DATA FOR OXYGEN-5A SORPTION AT 0°C USING A STATISTICAL THERMODYNAMIC MODEL WHERE: K=0.0006969, B=38.8, m=20.

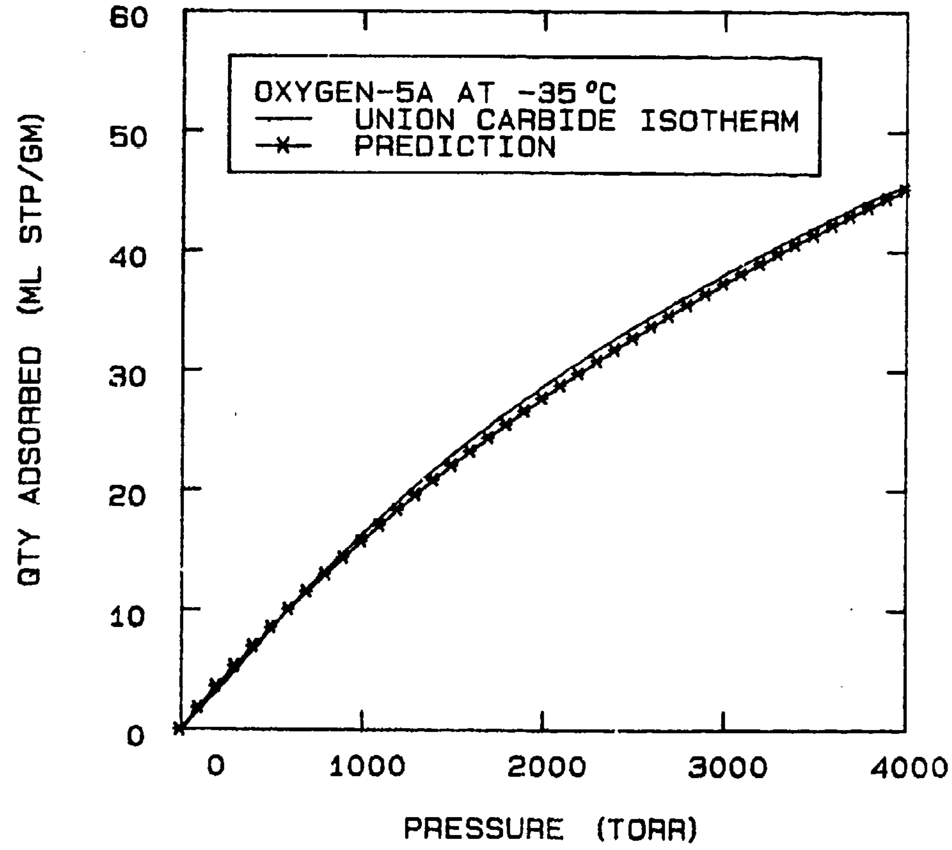

FIG 5-35. PREDICTION OF UNION CARBIDE DATA FOR OXYGEN-5A SORPTION AT -35°C USING A STATISTICAL THERMODYNAMIC MODEL WHERE: K=0.001735, B=38.8, m=20.

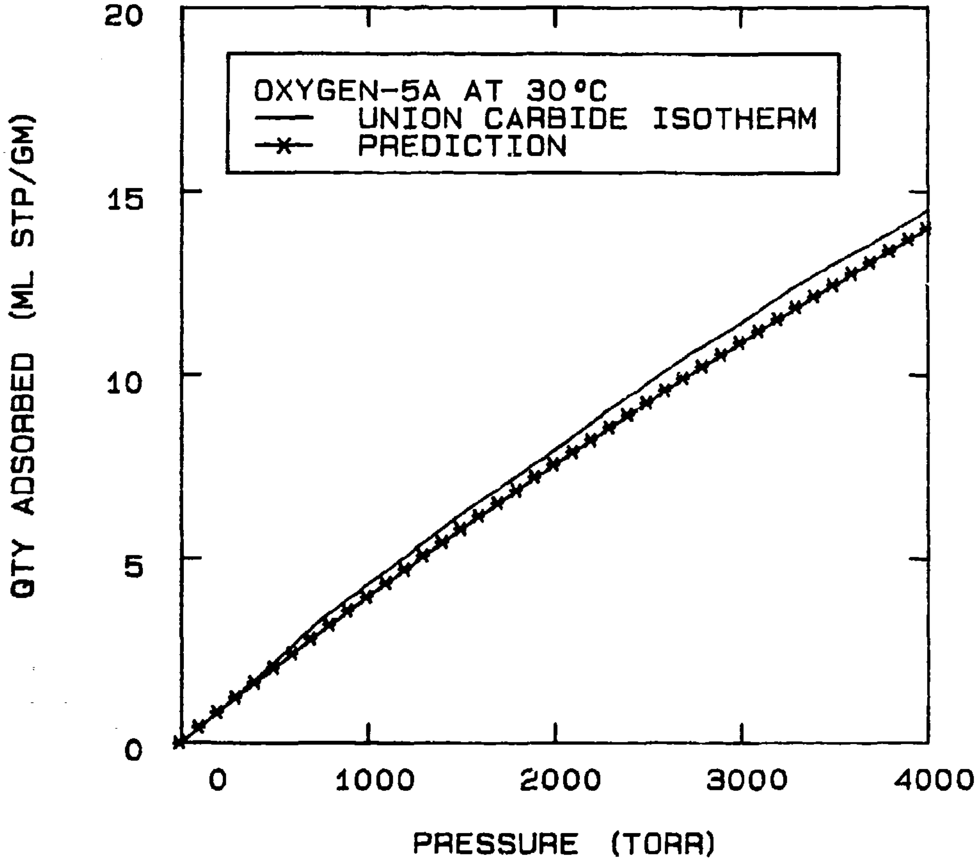

FIG 5-36. PREDICTION OF UNION CARBIDE DATA FOR OXYGEN-5A SORPTION AT 30°C USING A STATISTICAL THERMODYNAMIC MODEL WHERE: K=0.0003771, B=38.8, m=20.

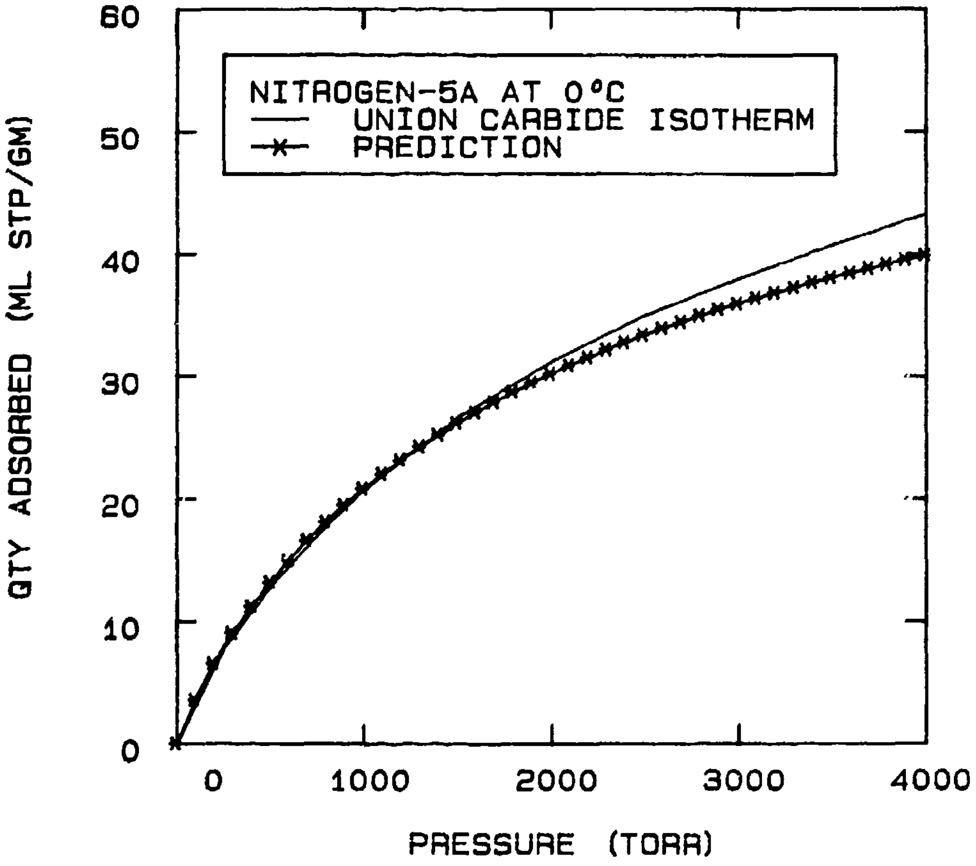

FIG 5-37. PREDICTION OF UNION CARBIDE DATA FOR NITROGEN-5A SORPTION AT 0°C USING A STATISTICAL THERMODYNAMIC MODEL WHERE: $K=0.003711$, $B=89.3$, $m=8$.

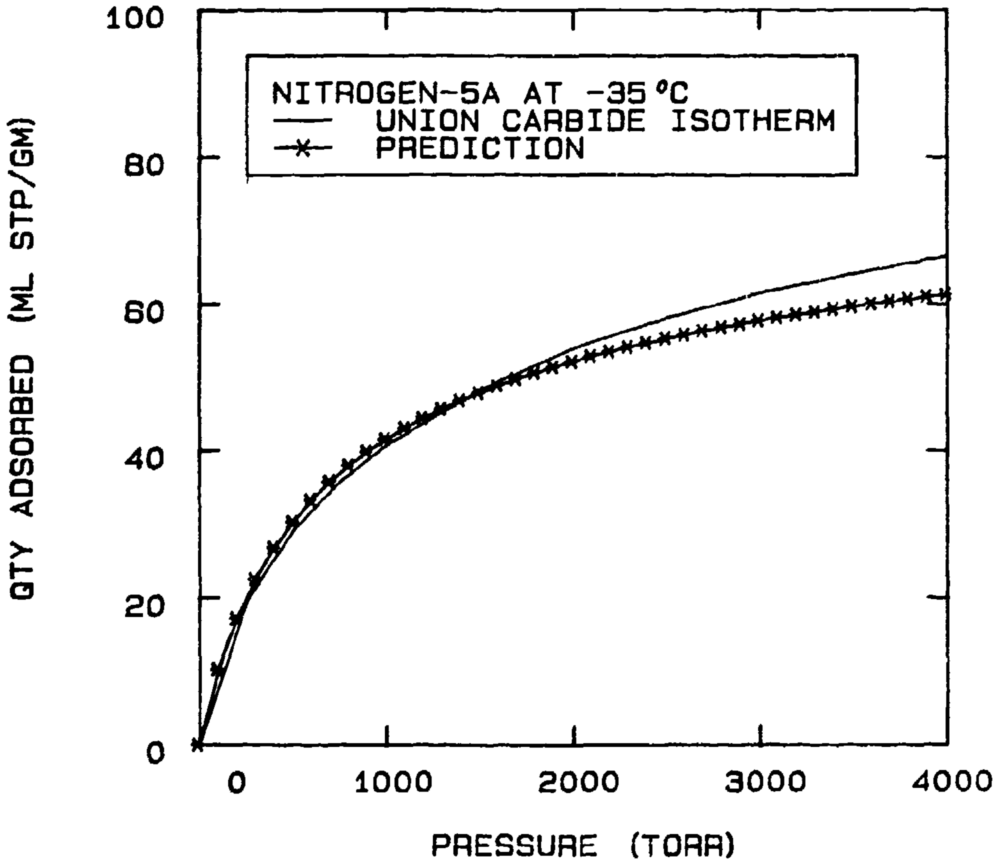

FIG 5-38. PREDICTION OF UNION CARBIDE DATA FOR NITROGEN-5A SORPTION AT -35 °C USING A STATISTICAL THERMODYNAMIC MODEL WHERE: $K=0.01261$, $B=77.6$, $m=10$.

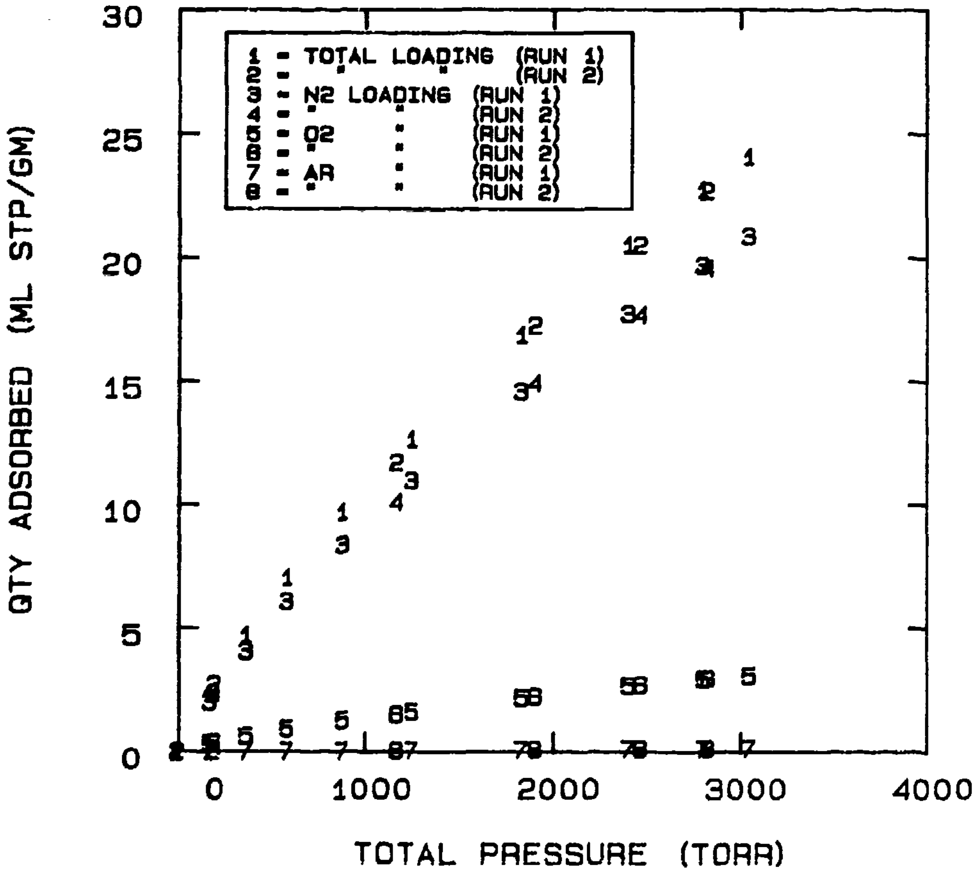

FIG 5-39. AIR-5A AT 24 °C WHERE THE TOTAL MOLAR RATIO OF NITROGEN, OXYGEN, AND ARGON WITHIN THE SYSTEM IS CONSTANT AT 78.14 : 20.92 : 0.94, RESPECTIVELY.

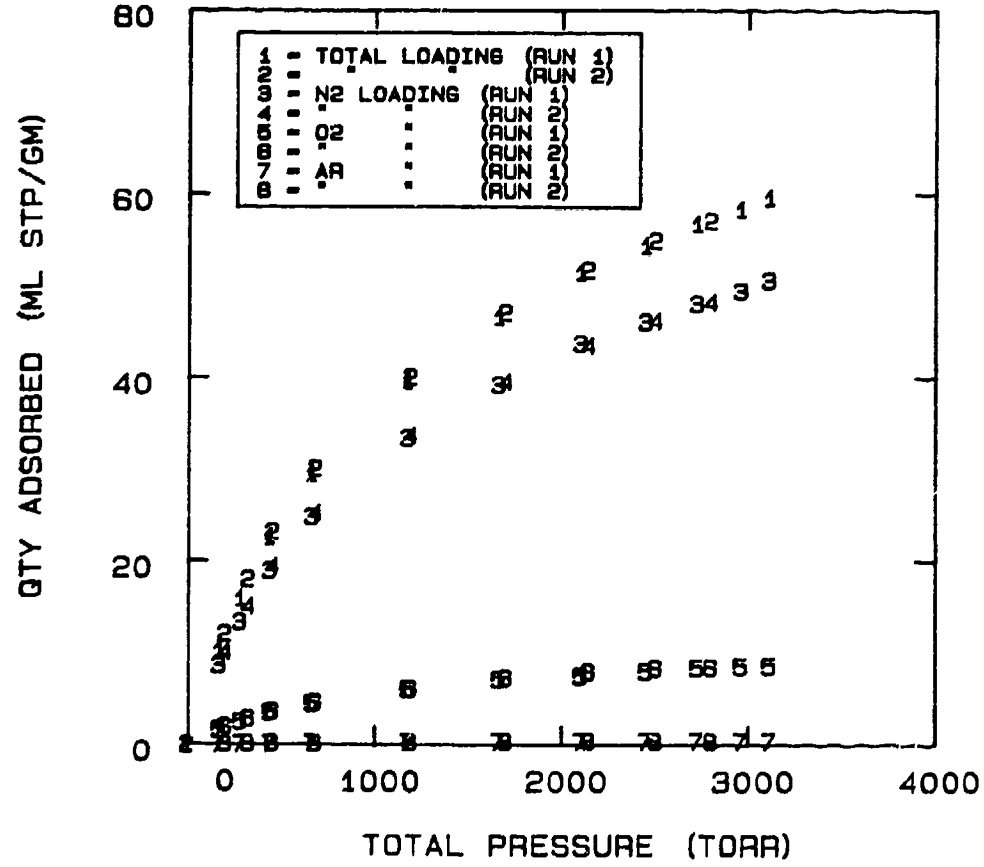

FIG 5-40. AIR-5A AT -40°C WHERE THE TOTAL MOLAR RATIO OF NITROGEN, OXYGEN, AND ARGON WITHIN THE SYSTEM IS CONSTANT AT 78.14 : 20.92 : 0.94, RESPECTIVELY.

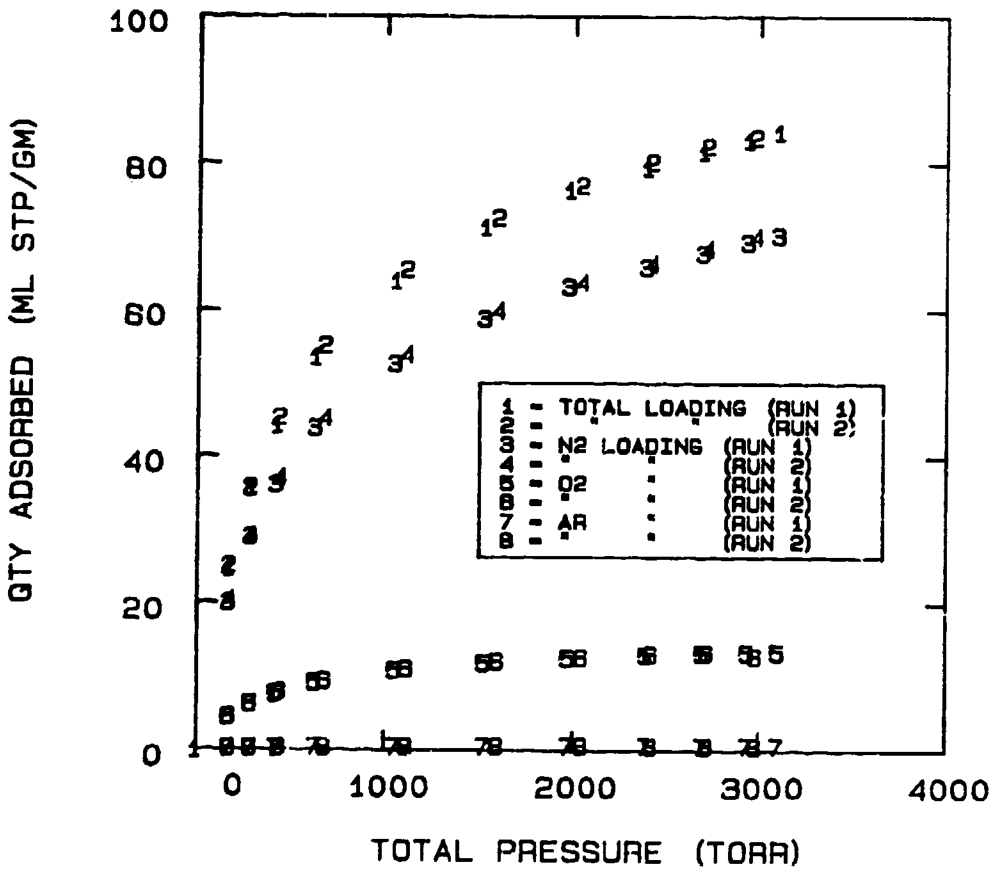

FIG 5-41. AIR-5A AT -70°C WHERE THE TOTAL MOLAR RATIO OF NITROGEN, OXYGEN, AND ARGON WITHIN THE SYSTEM IS CONSTANT AT 78.14 : 20.92 : 0.94, RESPECTIVELY.

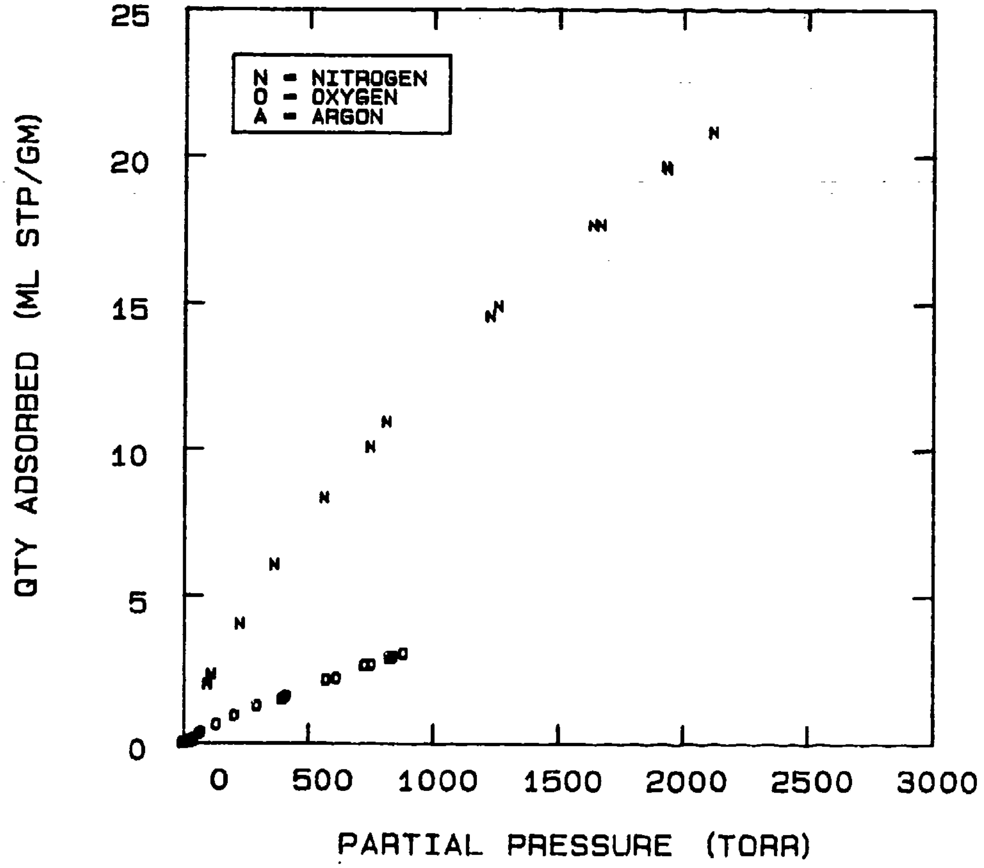

FIG 5-42. MULTICOMPONENT DATA FOR THE SYSTEM AIR-5A AT 24°C.

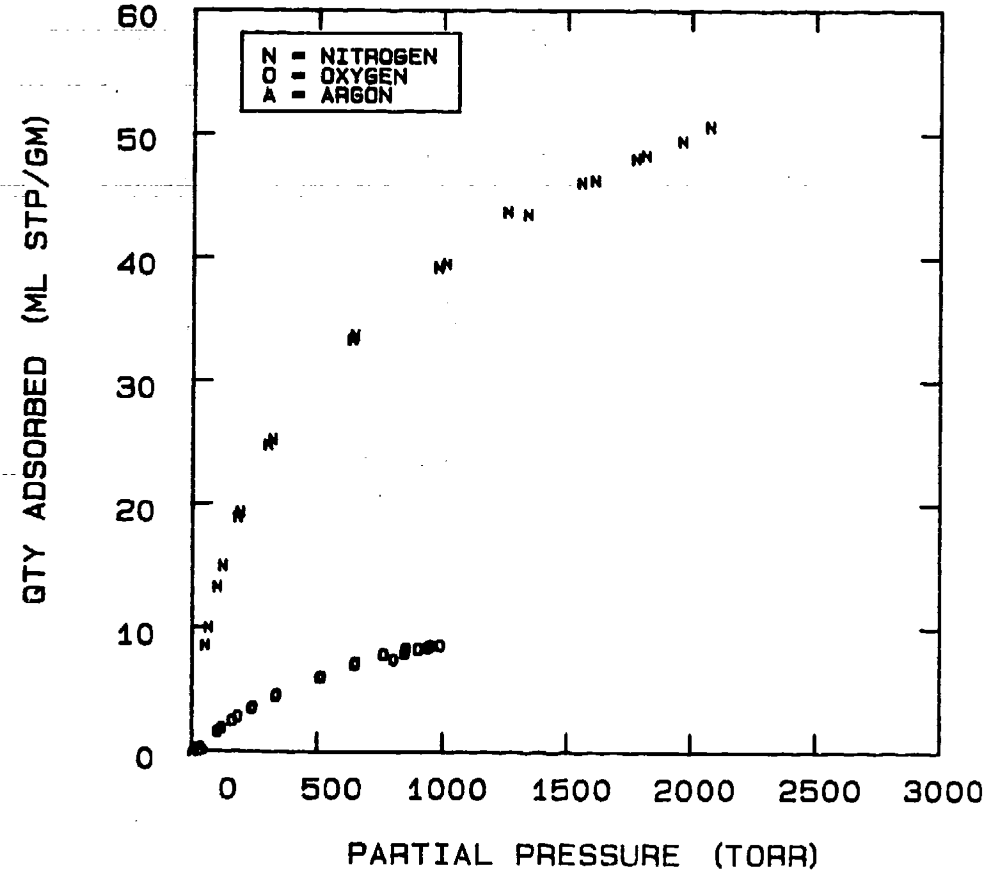

FIG 5-43. MULTICOMPONENT DATA FOR THE SYSTEM AIR-5A AT -40 °C.

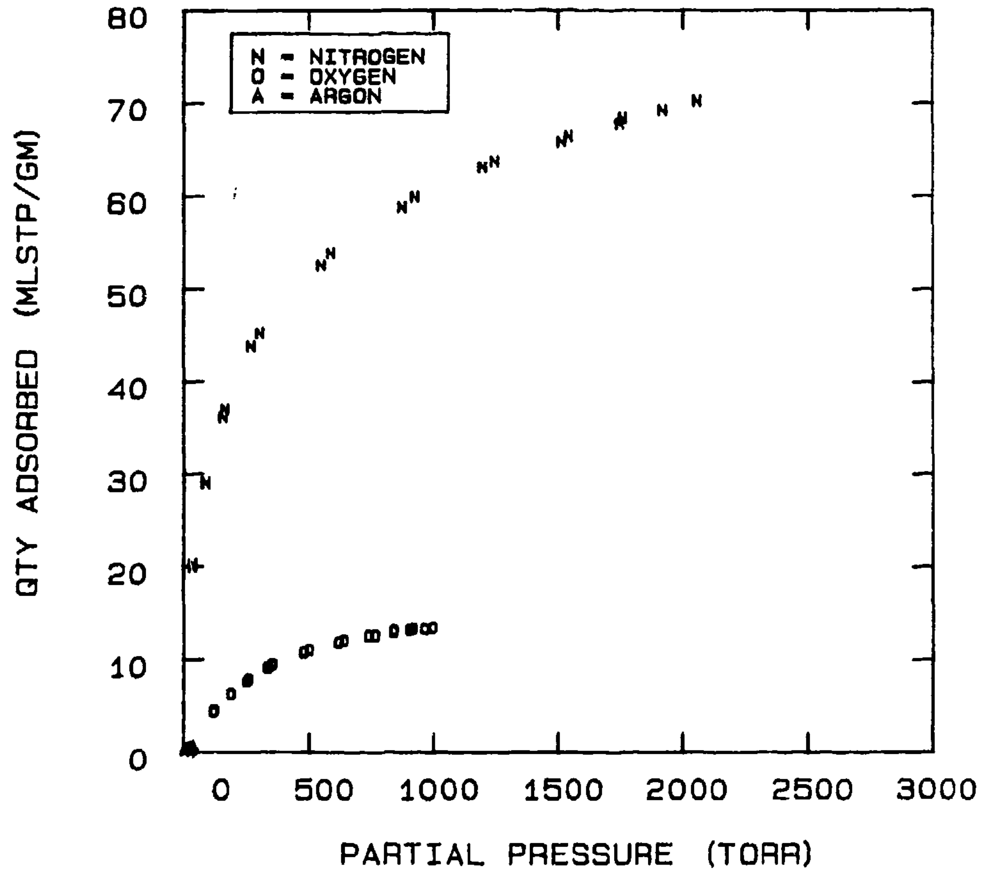

FIG 5-44. MULTICOMPONENT DATA FOR THE SYSTEM AIR-5A AT -70°C.

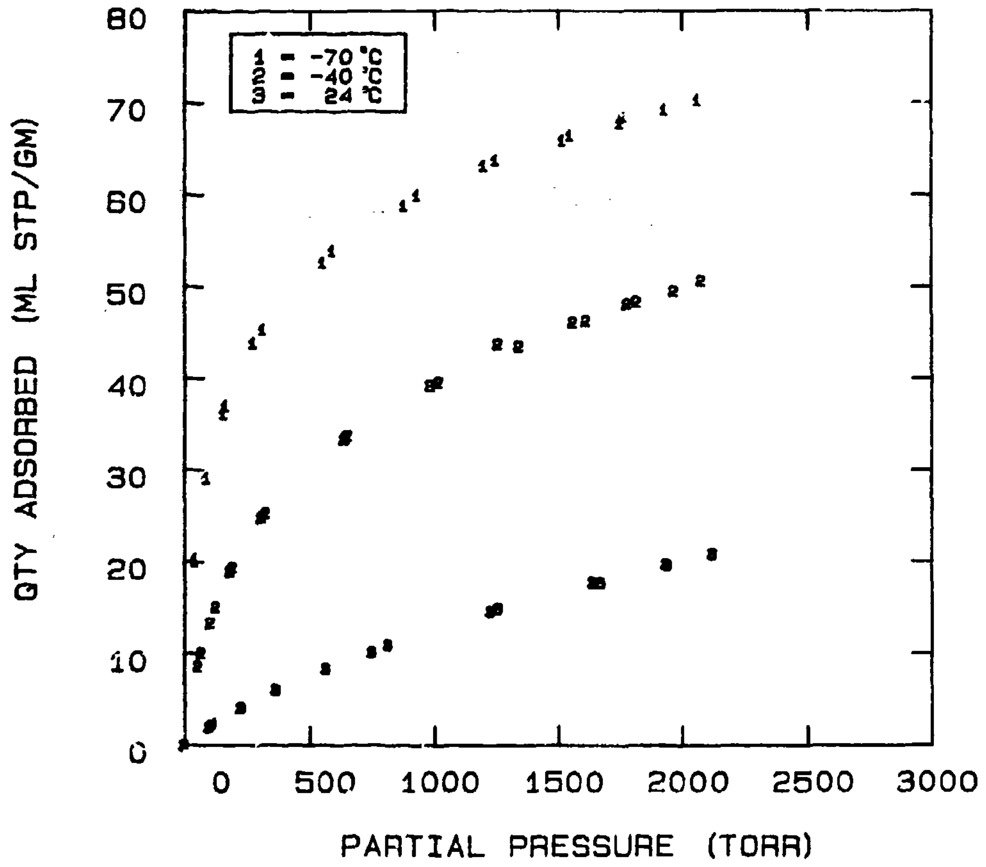

FIG 5-45. NITROGEN LOADING AT 24, -40, AND -70°C FOR THE AIR-5A SYSTEM.

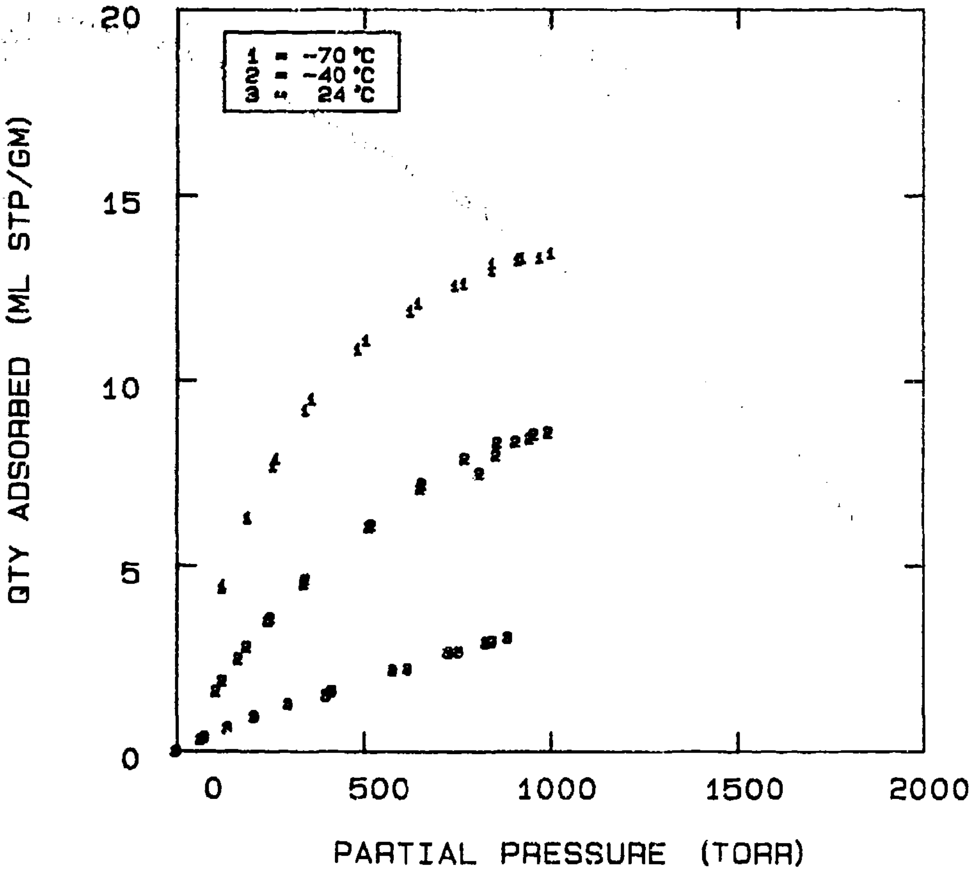

FIG 5-46. OXYGEN LOADING AT 24, -40, AND -70°C FOR THE AIR-5A SYSTEM.

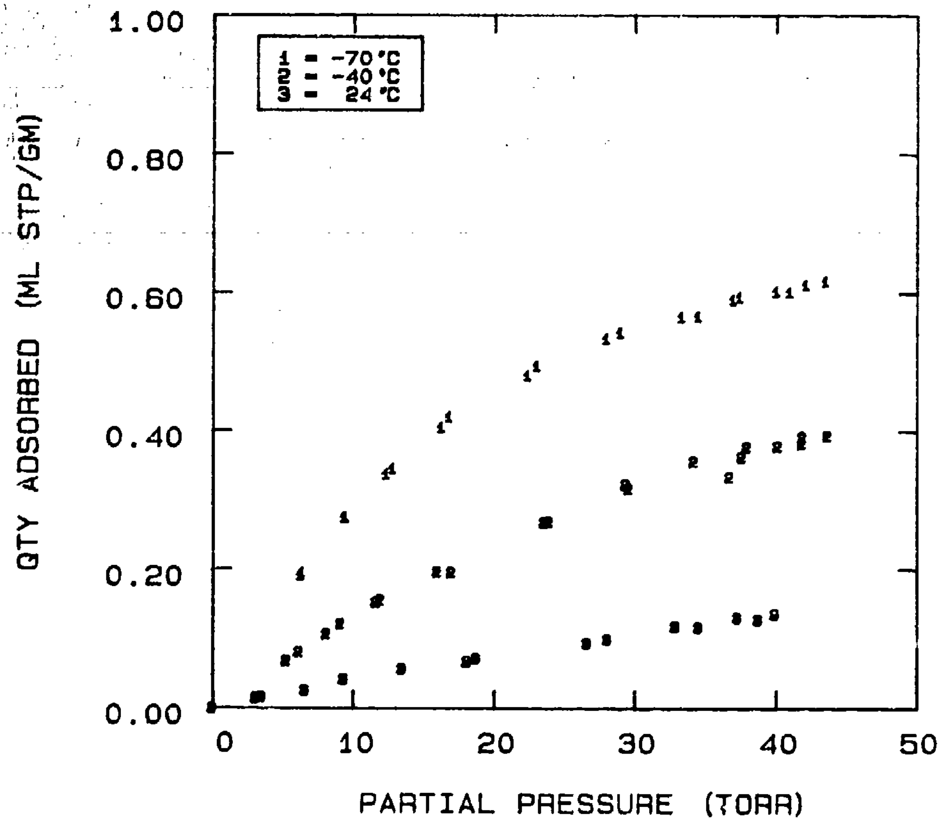

FIG 5-47. ARGON LOADING AT 24, -40, AND -70°C FOR THE AIR-5A SYSTEM.

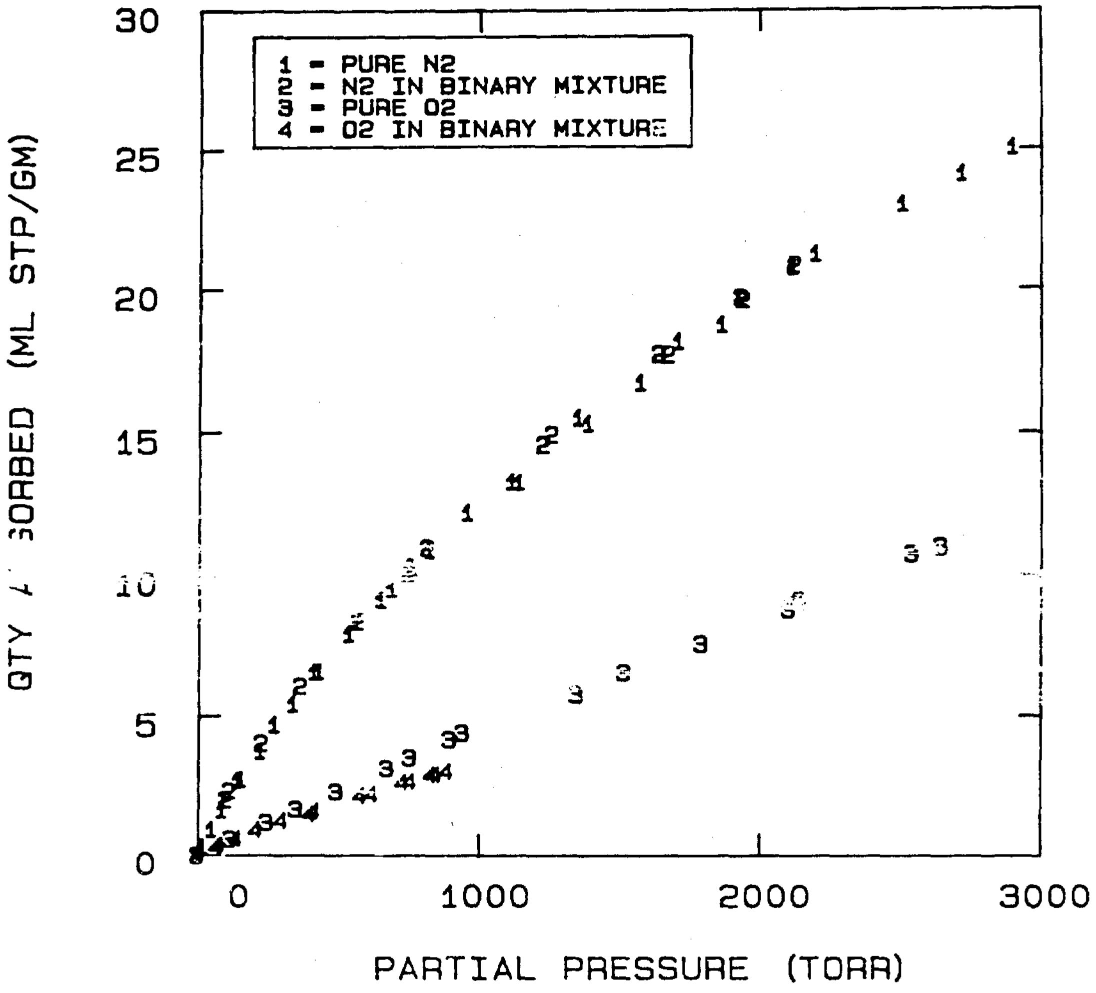

FIG 5-48. PURE AND MULTICOMPONENT DATA OF NITROGEN AND OXYGEN ON MOLECULAR SIEVE 5A AT 24°C.

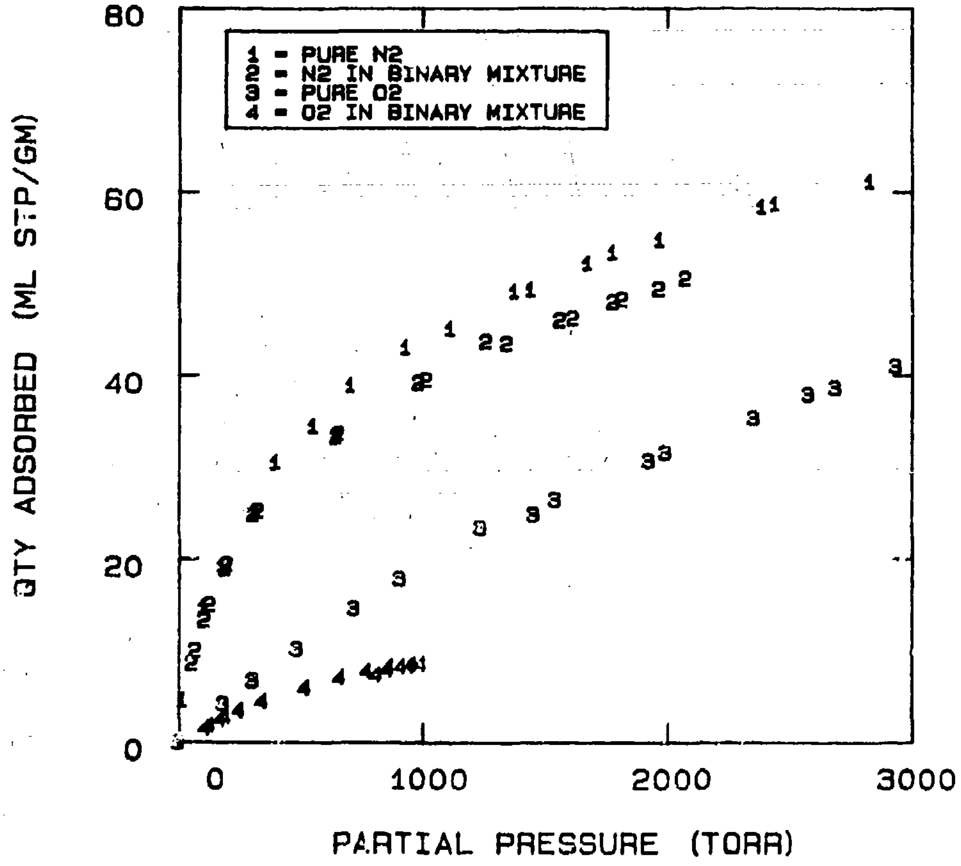

FIG 5-49. PURE AND MULTICOMPONENT DATA OF NITROGEN AND OXYGEN ON MOLECULAR SIEVE 5A AT -40°C.

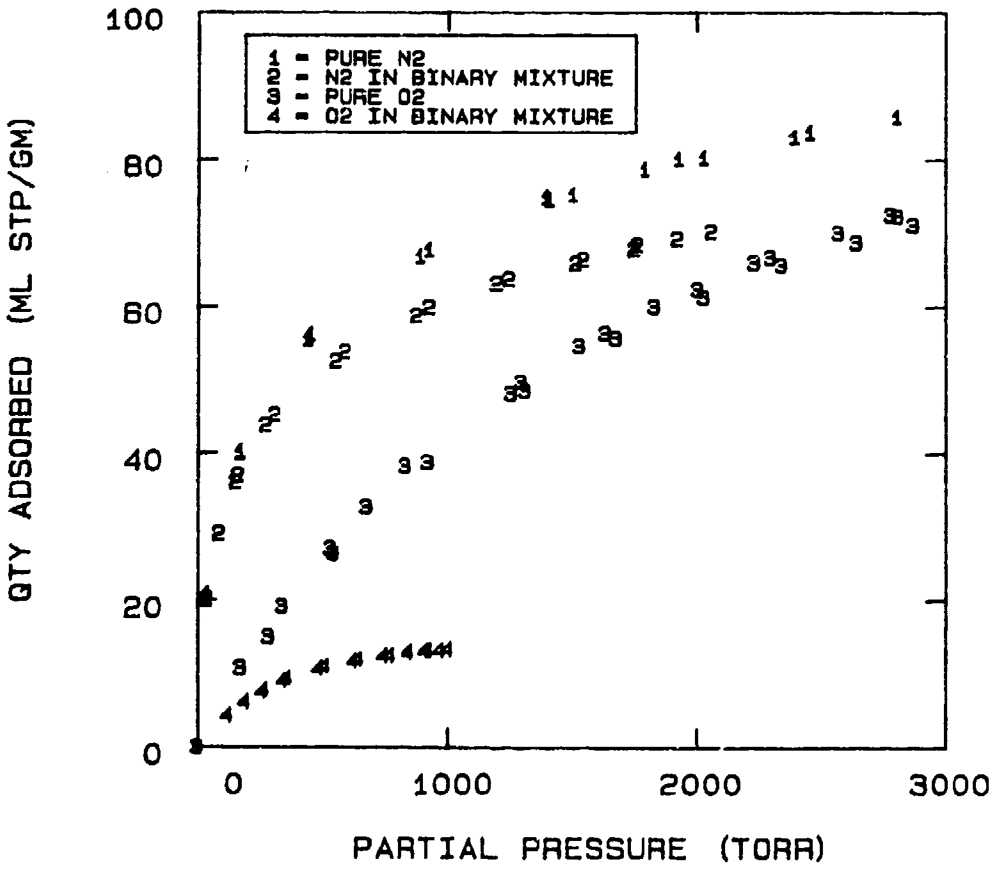

FIG 5-50. PURE AND MULTICOMPONENT DATA OF NITROGEN AND OXYGEN ON MOLECULAR SIEVE 5A AT -70°C.

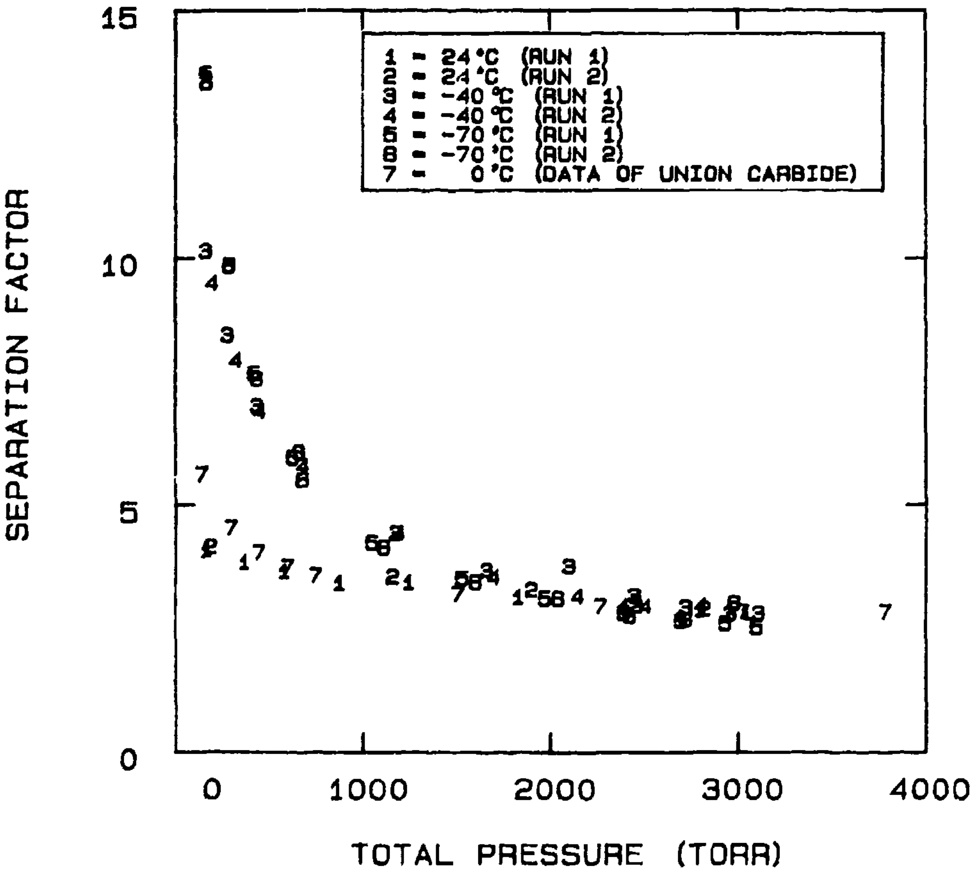

FIG 5-51. SEPARATION FACTORS FOR THE BINARY MIXTURE OF NITROGEN AND OXYGEN ON MOLECULAR SIEVE 5A.

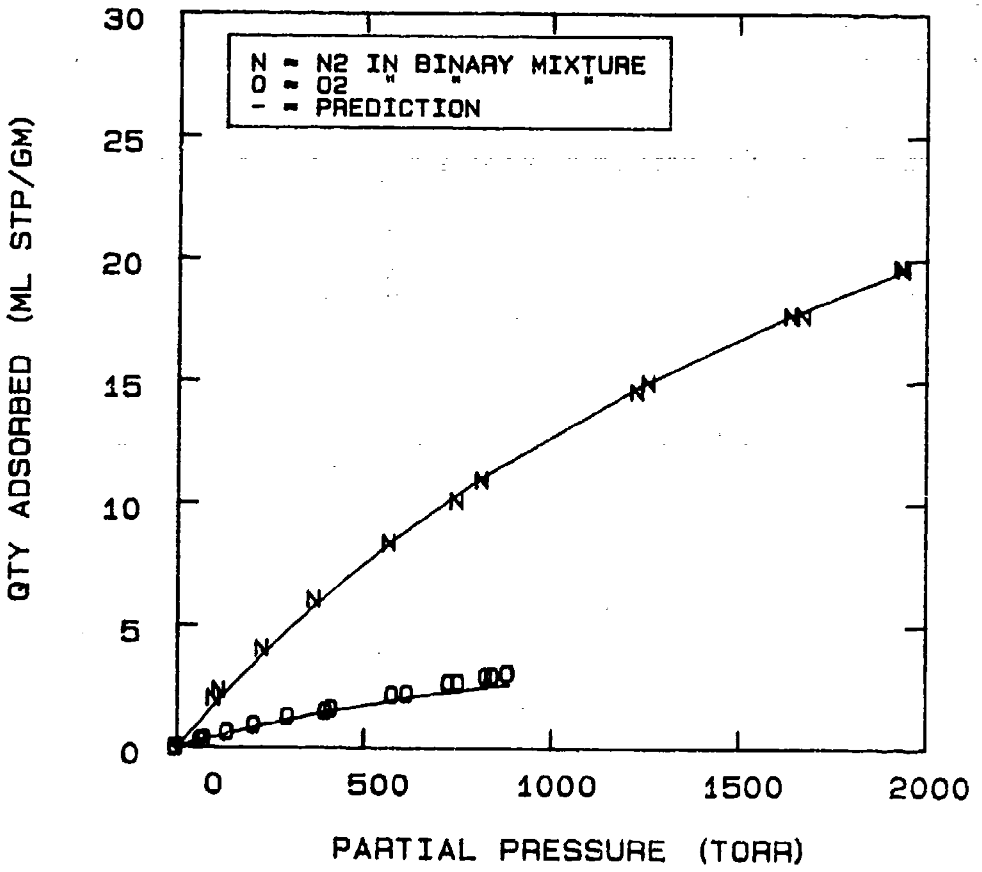

FIG 5-52. PREDICTION OF NITROGEN-OXYGEN ADSORPTION ON MOLECULAR SIEVE 5A AT 24°C USING A STATISTICAL THERMODYNAMIC MODEL WITH PURE COMPONENT PARAMETERS.

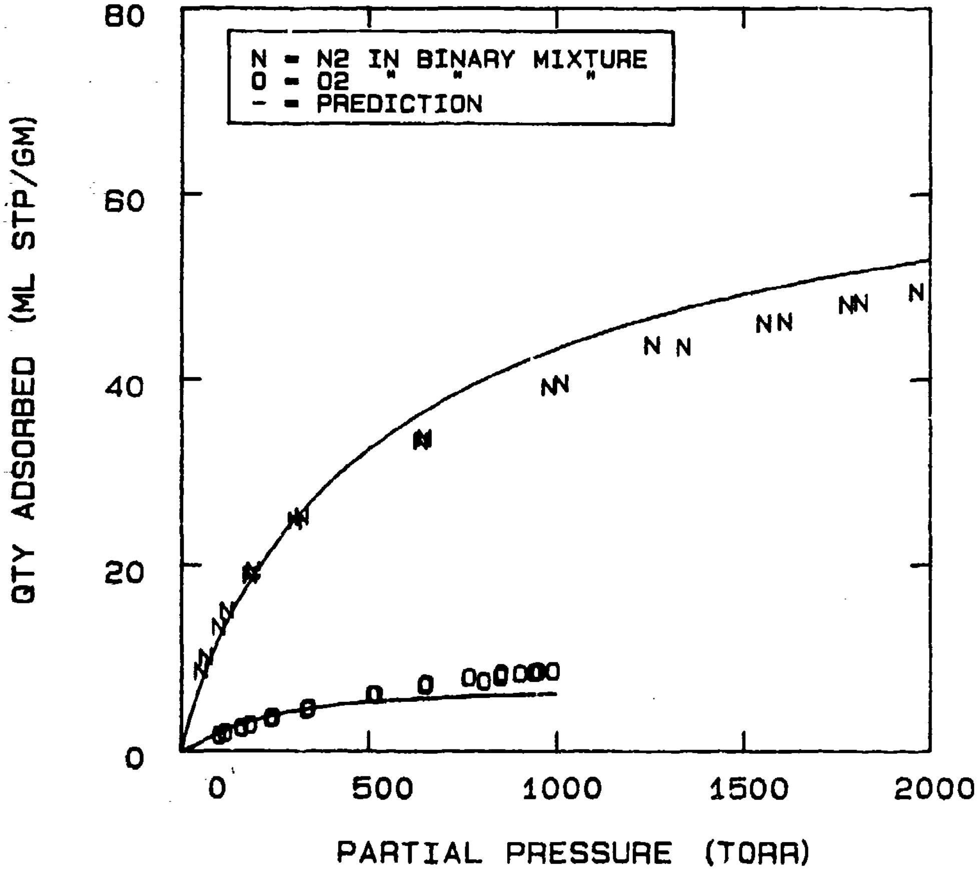

FIG 5-53. PREDICTION OF NITROGEN-OXYGEN ADSORPTION ON MOLECULAR SIEVE 5A AT -40°C USING A STATISTICAL THERMODYNAMIC MODEL WITH PURE COMPONENT PARAMETERS.

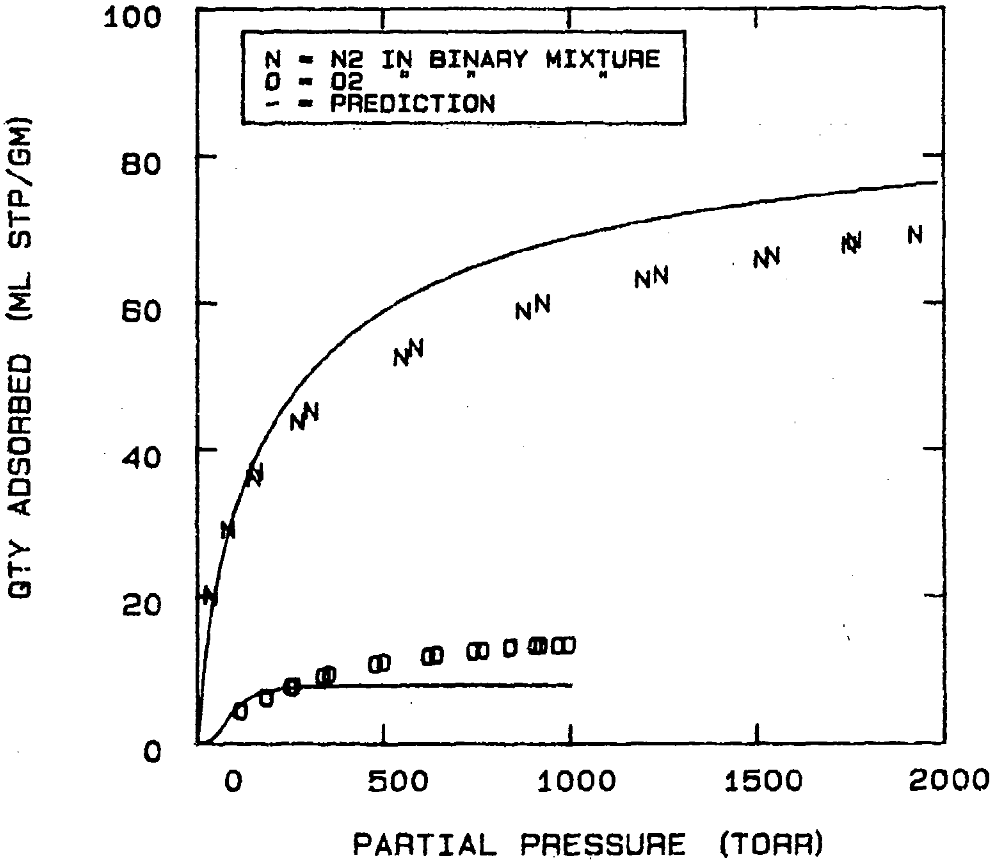

FIG 5-54. PREDICTION OF NITROGEN-OXYGEN ADSORPTION ON MOLECULAR SIEVE 5A AT -70°C USING A STATISTICAL THERMODYNAMIC MODEL WITH PURE COMPONENT PARAMETERS.

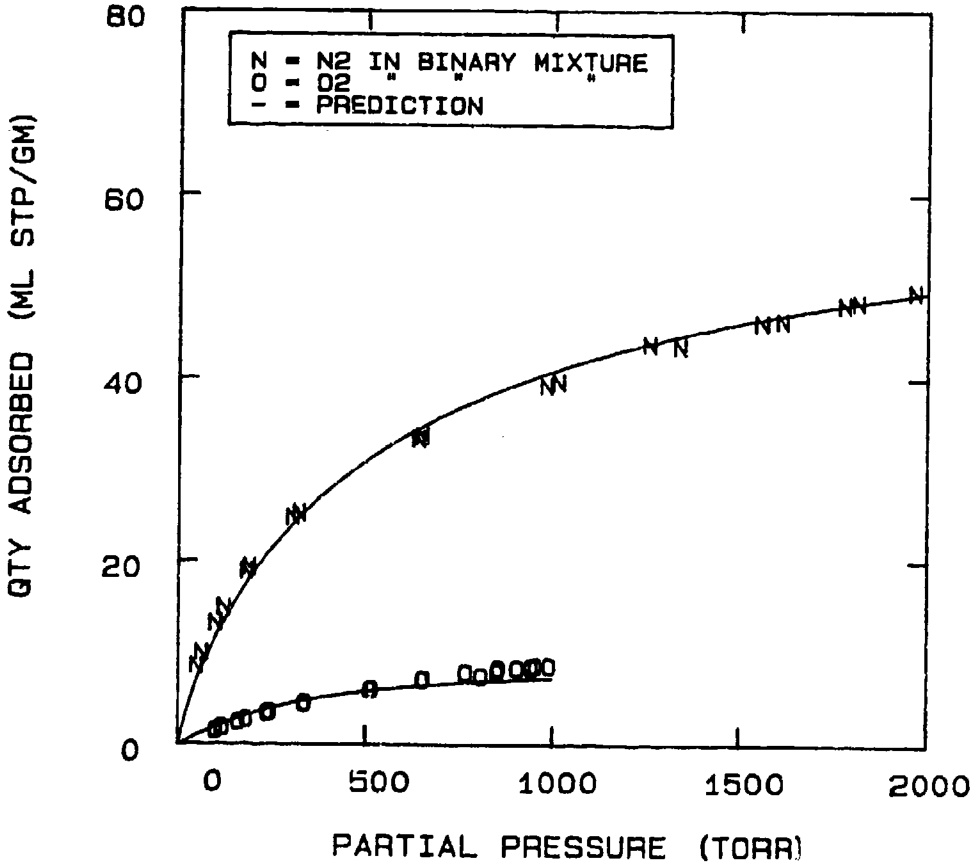

FIG 5-55. PREDICTION OF N2-O2 SORPTION AT -40°C USING A STATISTICAL THERMODYNAMIC MODEL WITH ADJUSTED EFFECTIVE MOLECULAR VOLUMES (BO2 = 28, BN2 = 82.5) .

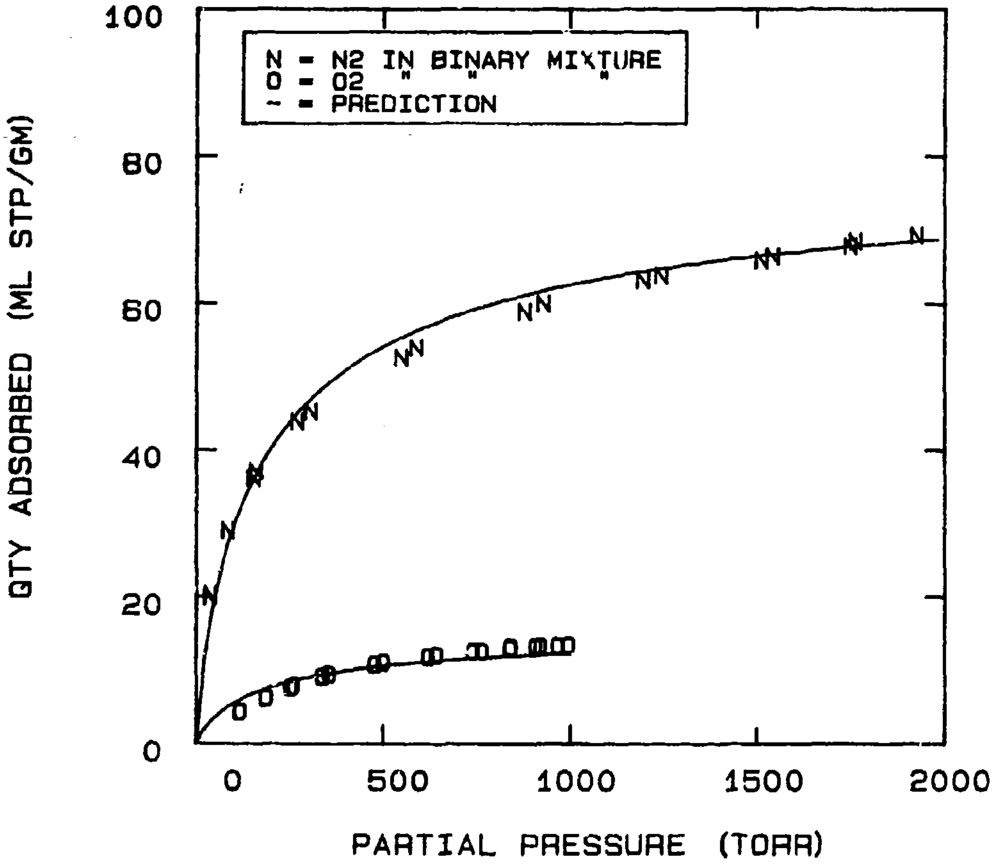

FIG 5-56. PREDICTION OF N2-O2 SORPTION AT -70 °C USING A STATISTICAL THERMODYNAMIC MODEL WITH ADJUSTED EFFECTIVE MOLECULAR VOLUMES (BO2 = 25, BN2 = 74).

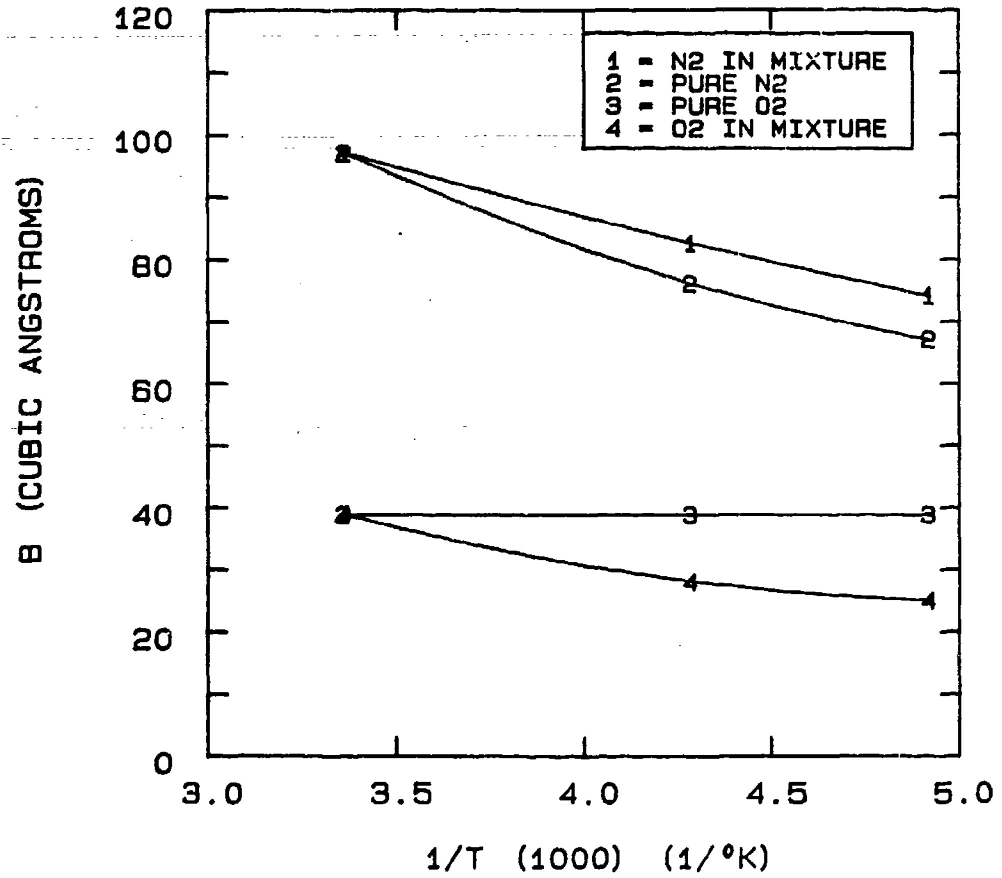

FIG 5-57. APPARENT EFFECTIVE MOLECULAR VOLUME FOR N2 AND O2 AS PURE COMPONENTS AND IN A N2-O2-AR MIXTURE WITH TOTAL MOLAR RATIO OF 78.14 : 20.92 : 0.94 .

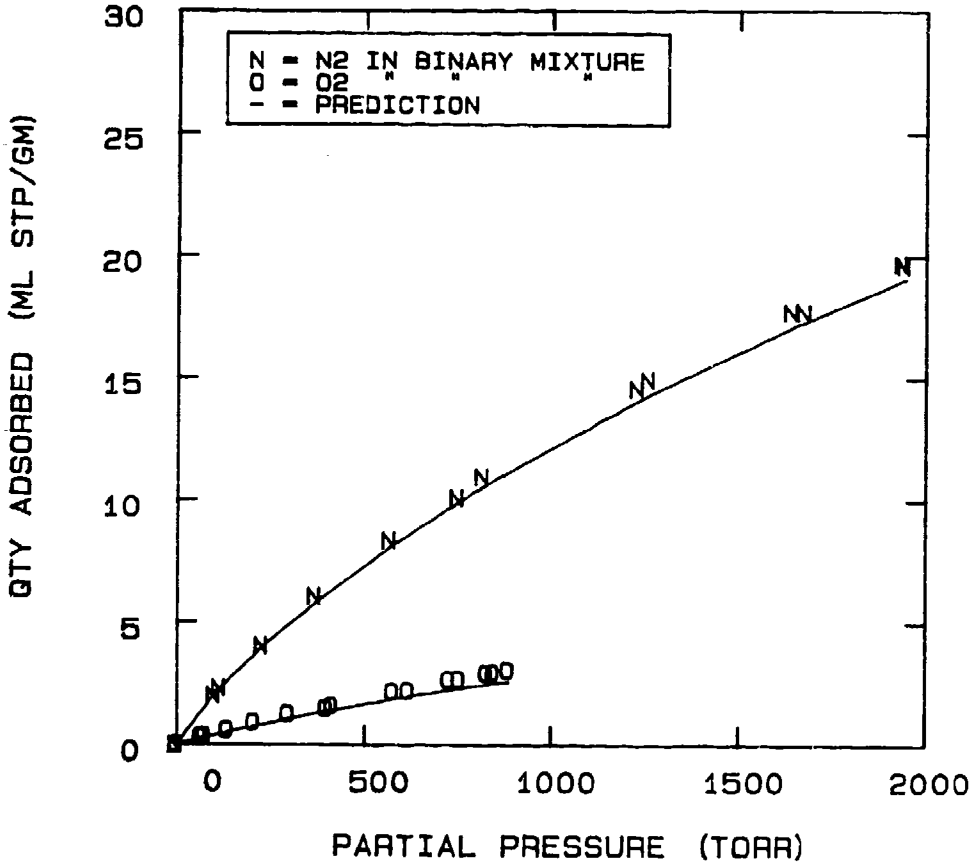

FIG 5-58. PREDICTION OF N2-O2 SORPTION ON MOLECULAR SIEVE 5A AT 24 °C USING THE IDEAL ADSORBED SOLUTION THEORY.

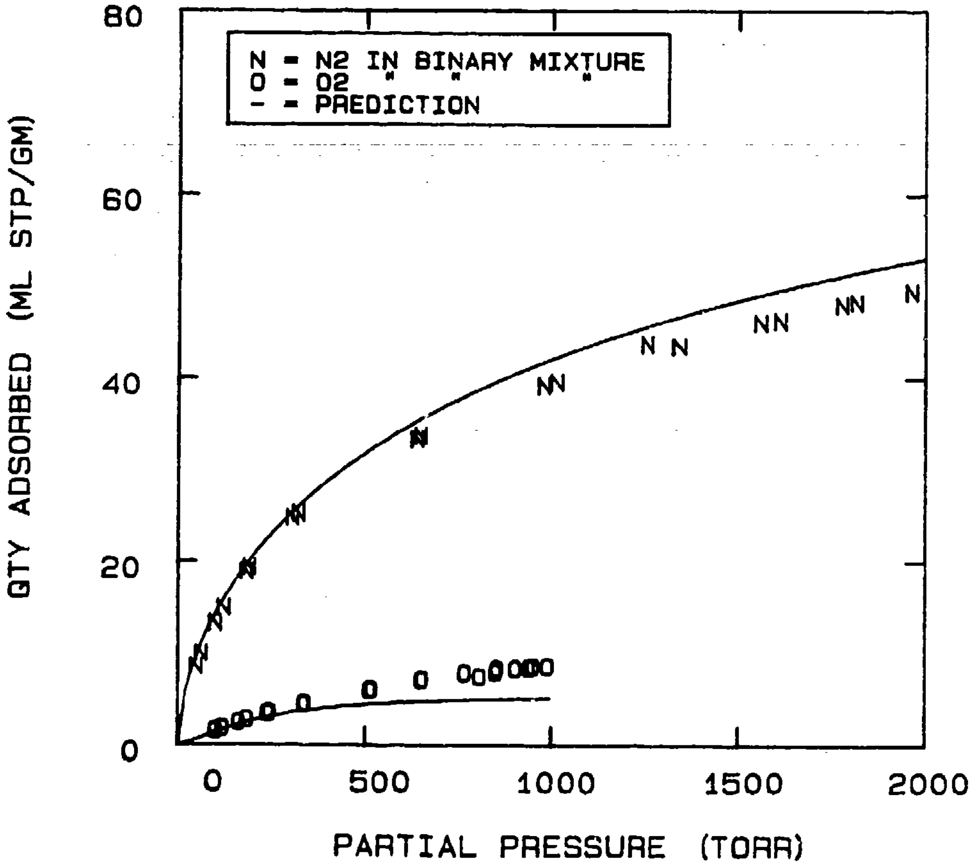

FIG 5-59. PREDICTION OF N2-O2 SORPTION ON MOLECULAR SIEVE 5A AT -40 °C USING THE IDEAL ADSORBED SOLUTION THEORY.

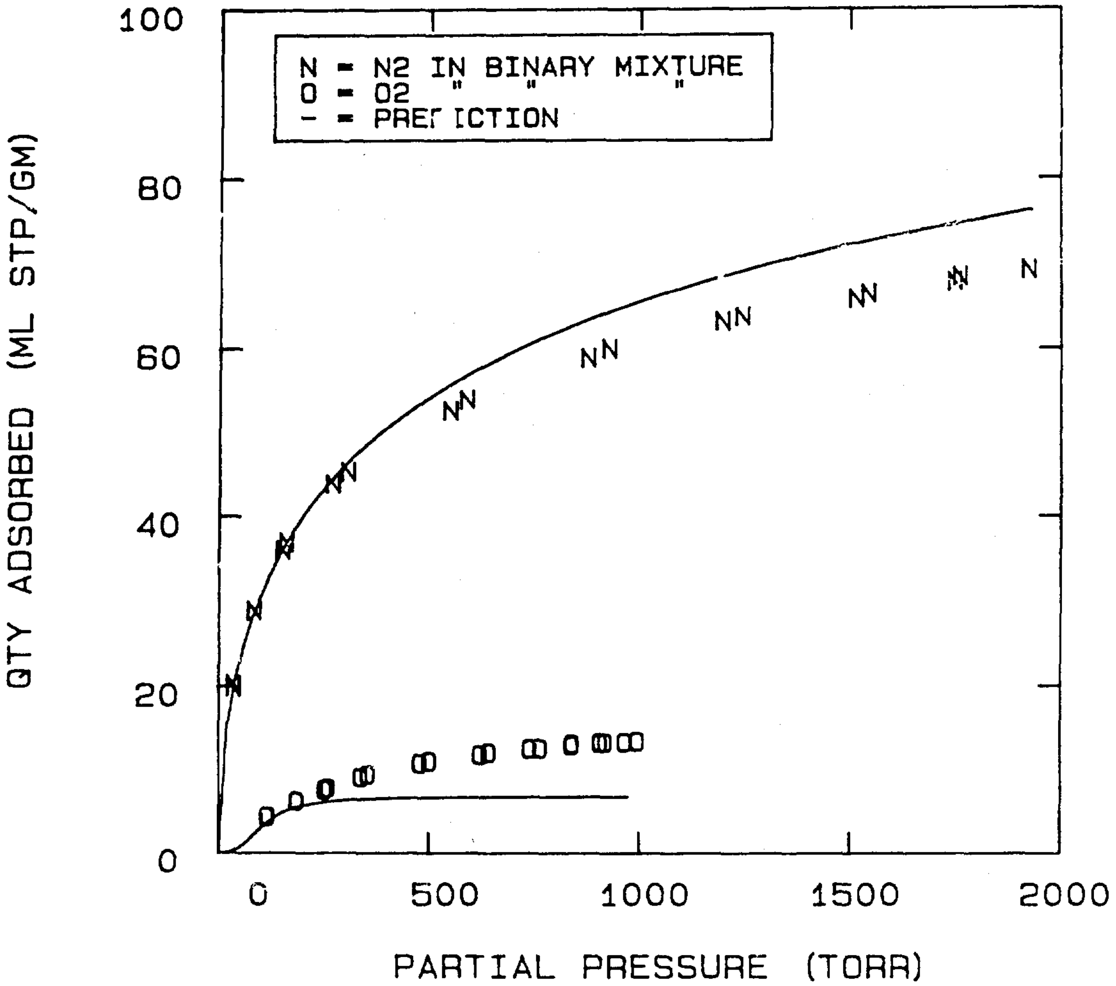

FIG 5-60. PREDICTION OF N2-O2 SORPTION ON MOLECULAR SIEVE 5A AT -70°C USING THE IDEAL ADSORBED SOLUTION THEORY.

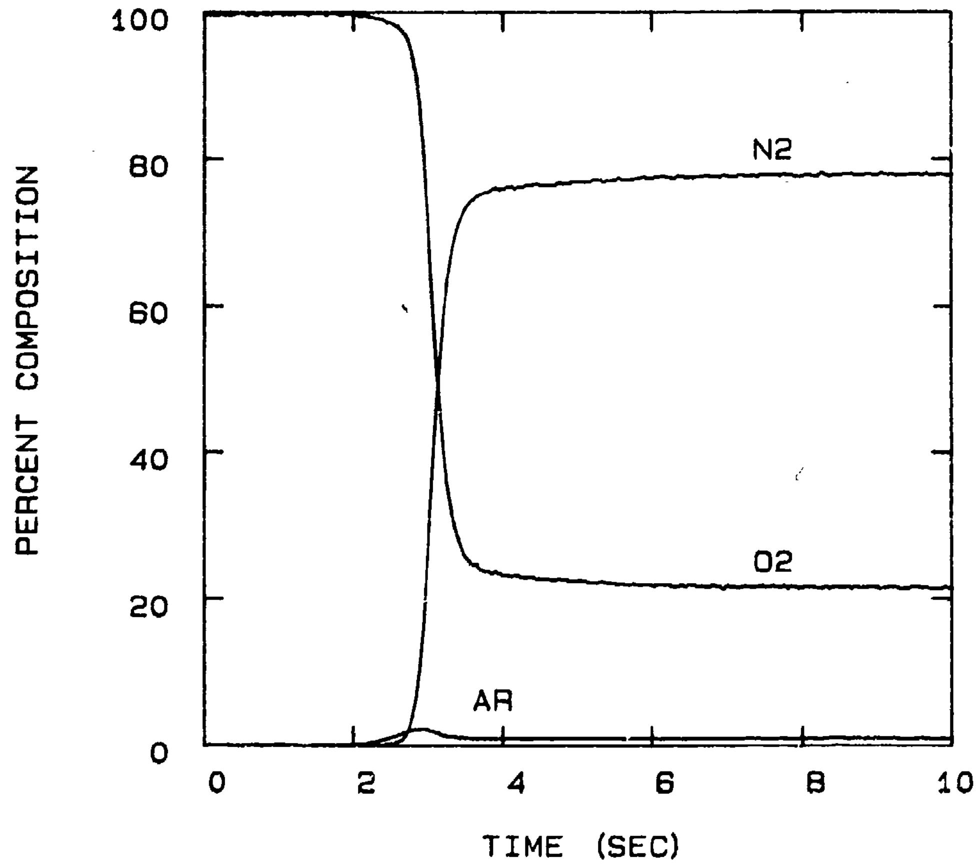

FIG 5-61. RUN 102021 : COLUMN NITROGEN BREAKTHROUGH AT 24°C, 25 SLPM, AND BED PRESSURE OF 25 PSIA.

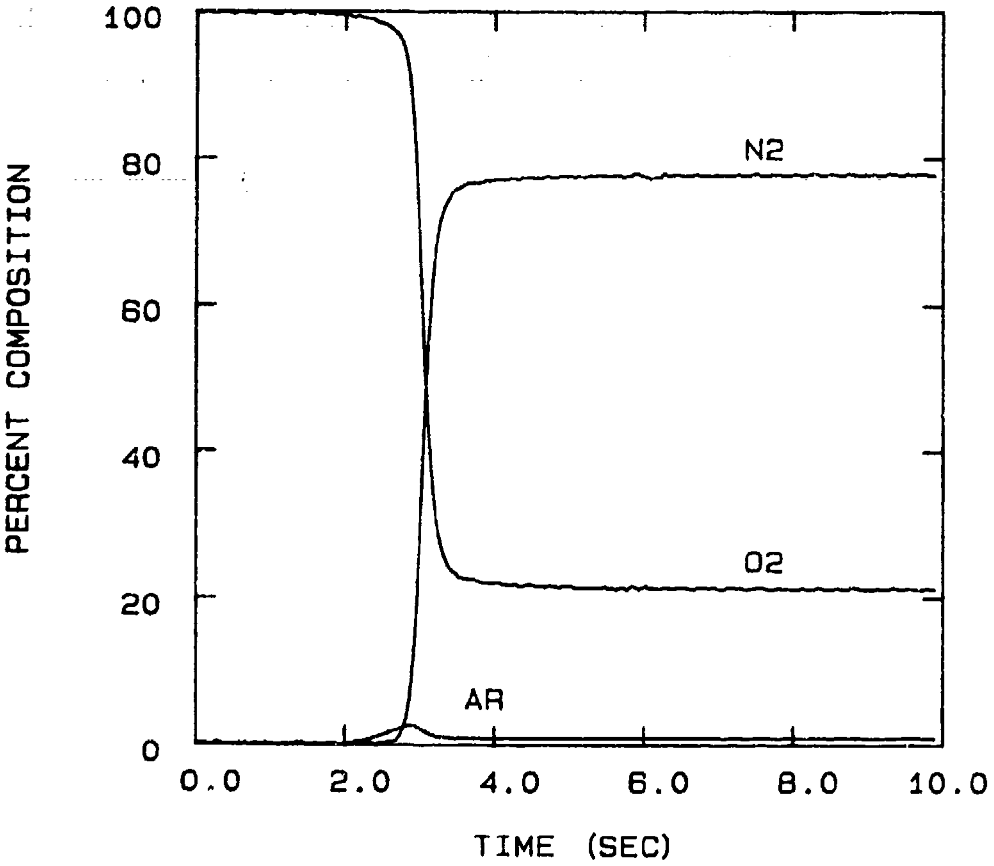

FIG 5-62. RUN 102712 : COLUMN NITROGEN BREAKTHROUGH AT 24°C, 25 SLPM, AND BED PRESSURE OF APPROXIMATELY 18.5 PSIA.

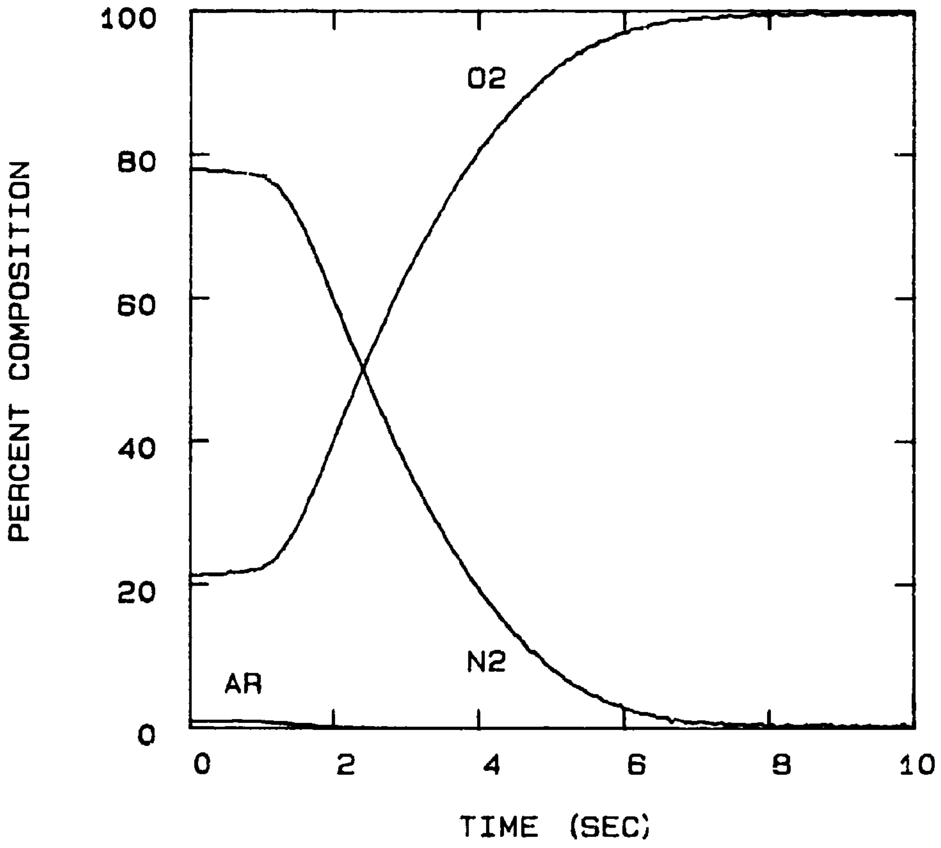

FIG 5-63. RUN 102023 : COLUMN OXYGEN BREAKTHROUGH AT 24°C, 25 SLPM, AND BED PRESSURE OF 25 PSIA.

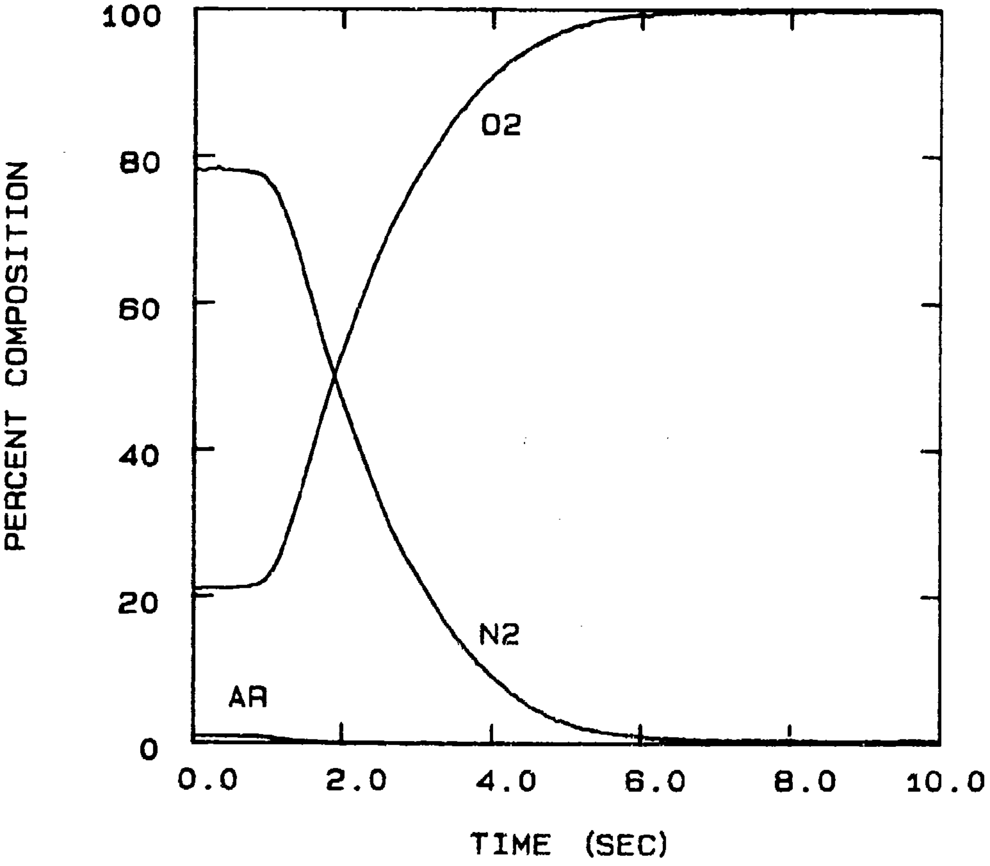

FIG 5-64. RUN 102714 : COLUMN OXYGEN BREAKTHROUGH AT 24°C, 25 SLPM, AND BED PRESSURE OF APPROXIMATELY 18.5 PSIA.

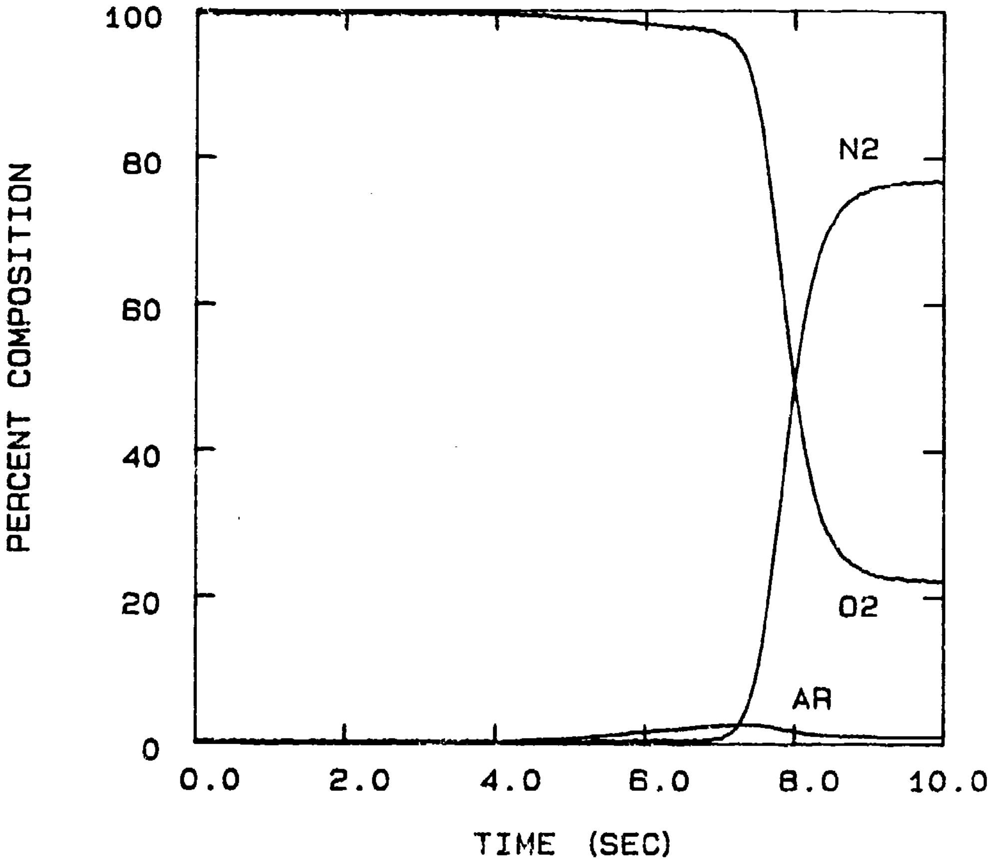

FIG 5-65. RUN 110407 : COLUMN NITROGEN BREAKTHROUGH AT -40°C, 25 SLPM, AND BED PRESSURE OF 25 PSIA.

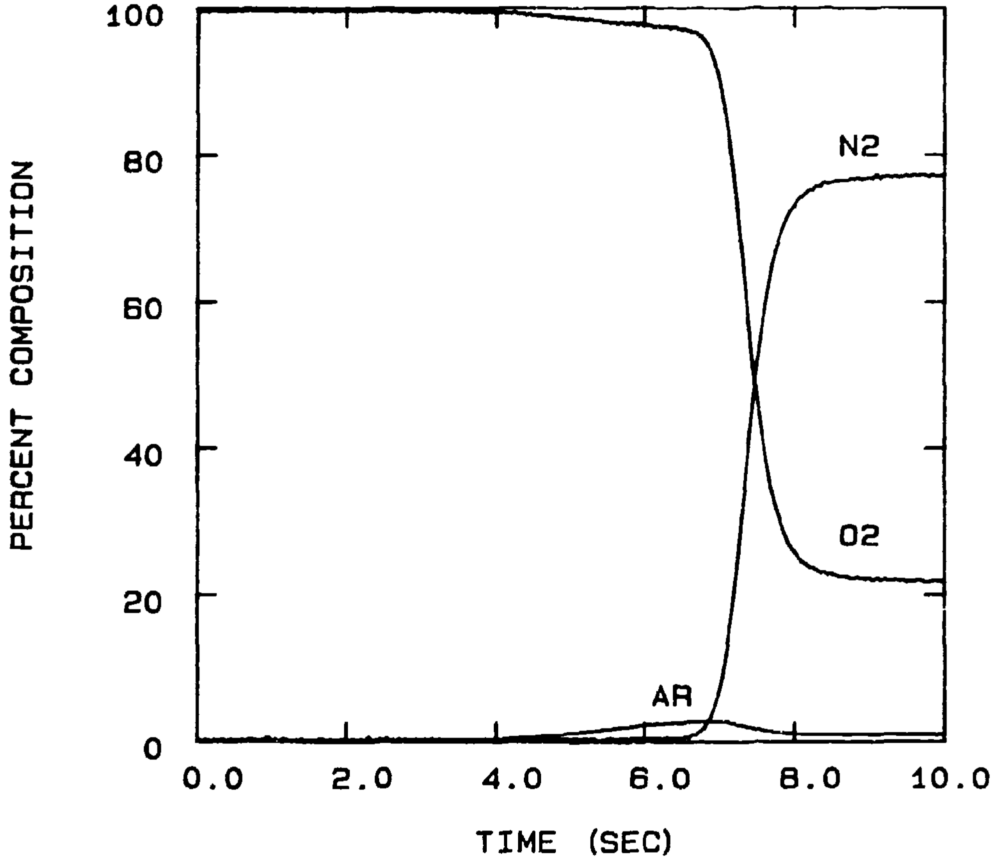

FIG 5-66. RUN 110413 : COLUMN NITROGEN BREAKTHROUGH AT -40°C, 25 SLPM, AND BED PRESSURE OF APPROXIMATELY 18.5 PSIA.

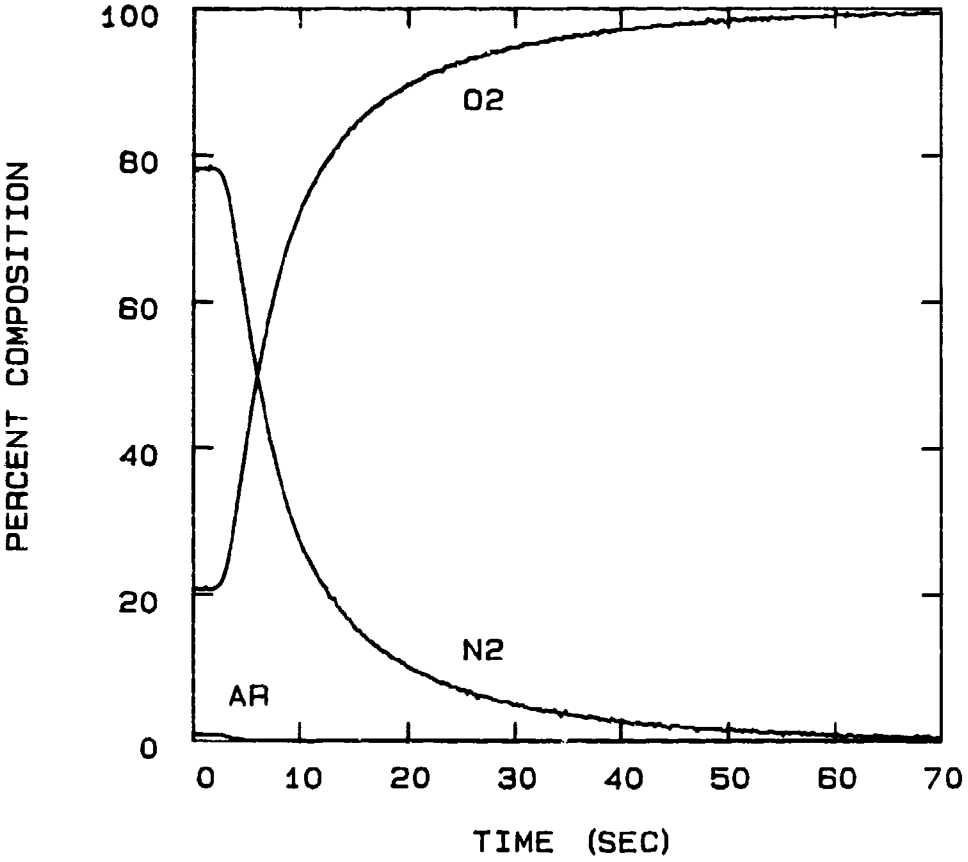

FIG 5-67. RUN 110408 : COLUMN OXYGEN BREAKTHROUGH AT -40°C, 25 SLPM, AND BED PRESSURE OF 25 PSIA.

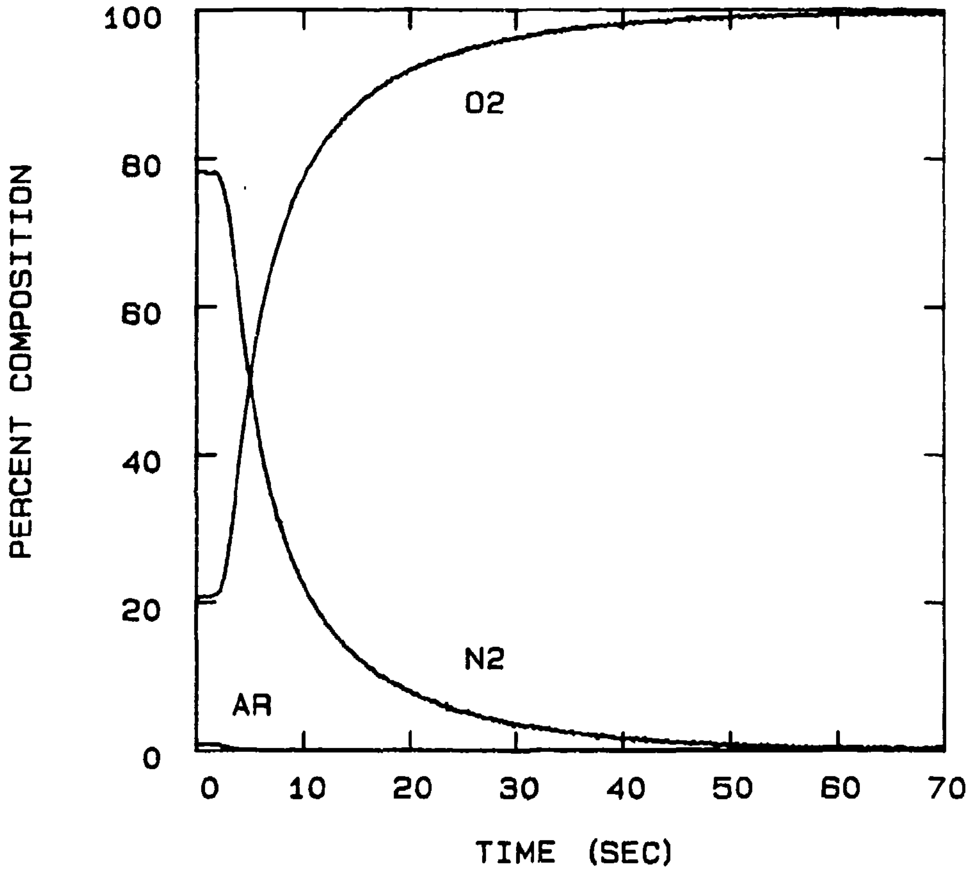

FIG 5-68. RUN 110412 : COLUMN OXYGEN BREAKTHROUGH AT -40°C, 25 SLPM, AND BED PRESSURE OF APPROXIMATELY 18.5 PSIA.

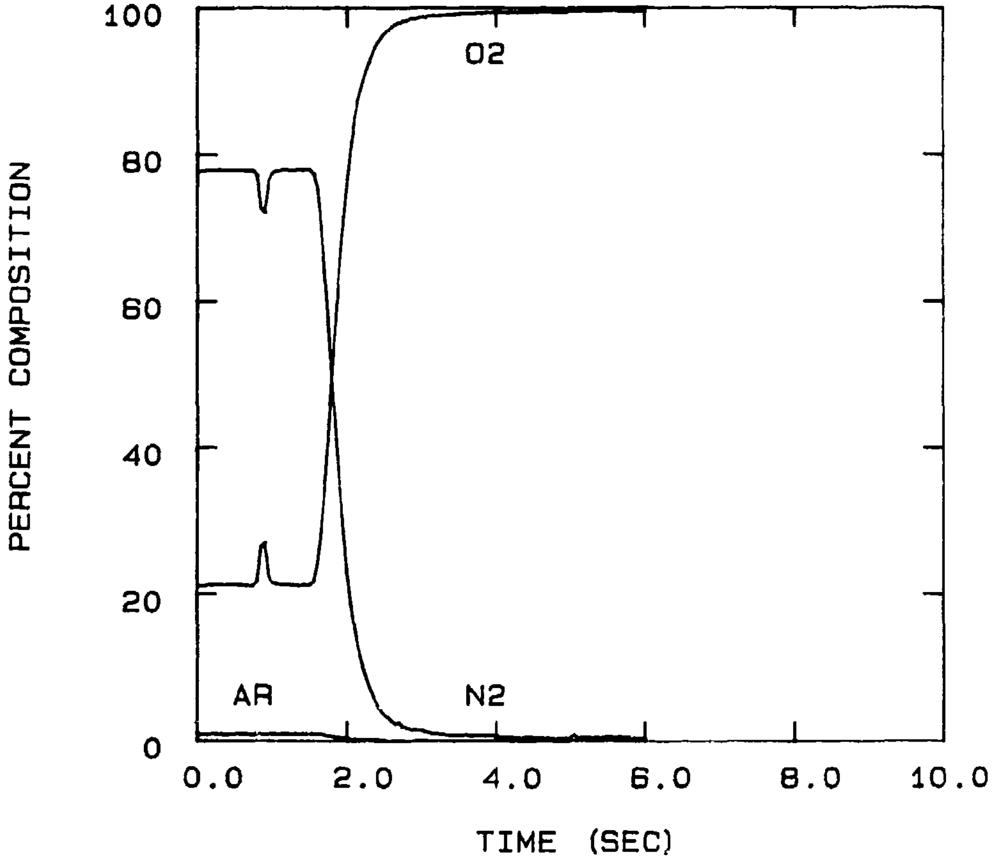

FIG 5-69. RUN 102709 : MEASUREMENT OF DISTANCE/ VELOCITY LAG TIME AT 25 SLPM.

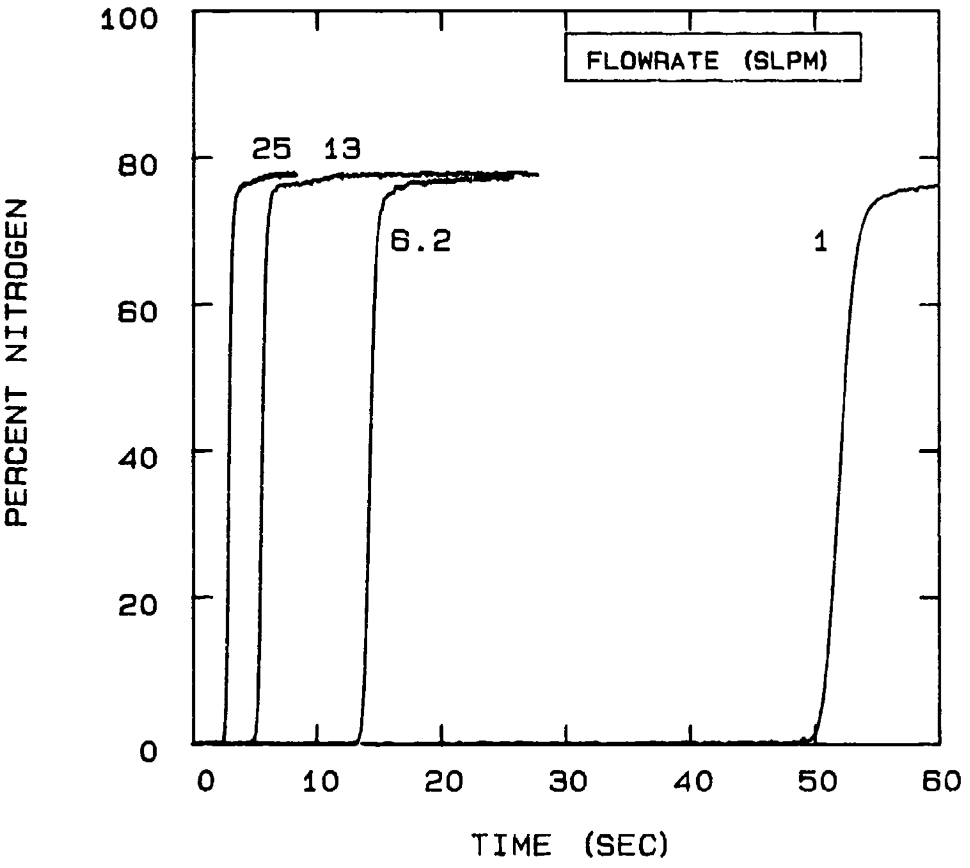

FIG 5-70. DEPENDENCE OF NITROGEN BREAKTHROUGH ON FLOWRATE AT 24°C AND BED PRESSURE OF 25 PSIA.

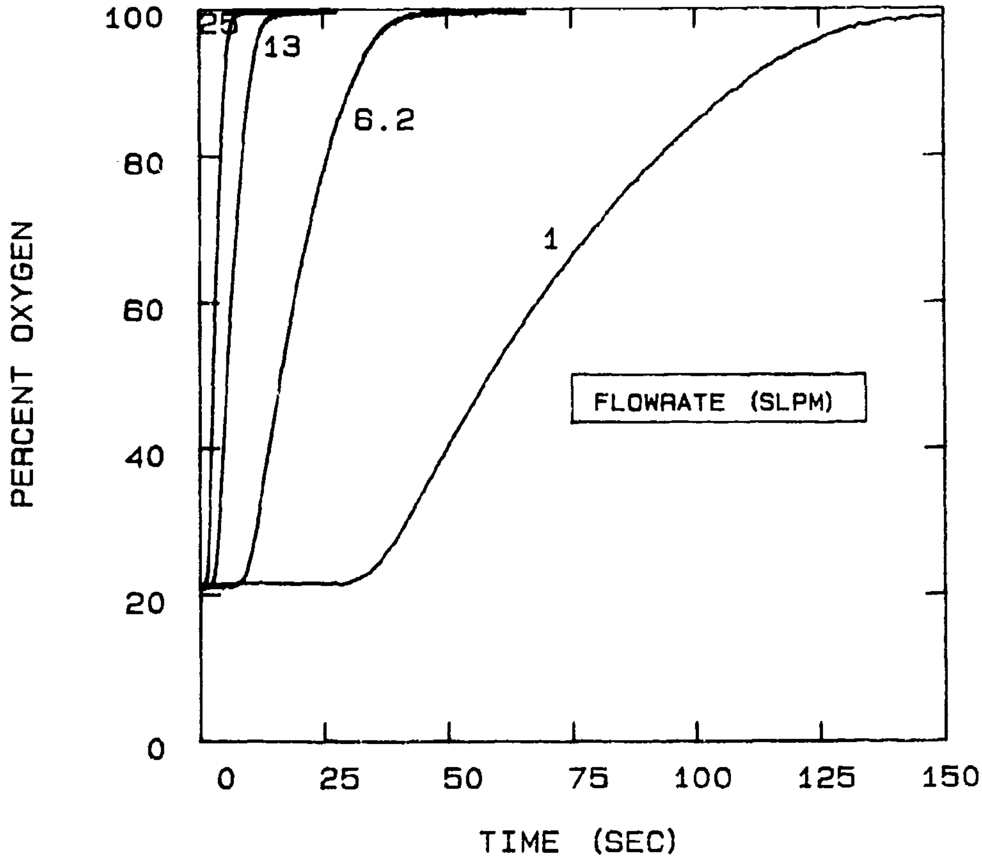

FIG 5-71. DEPENDENCE OF OXYGEN BREAKTHROUGH ON FLOWRATE AT 24°C AND BED PRESSURE OF 25 PSIA.

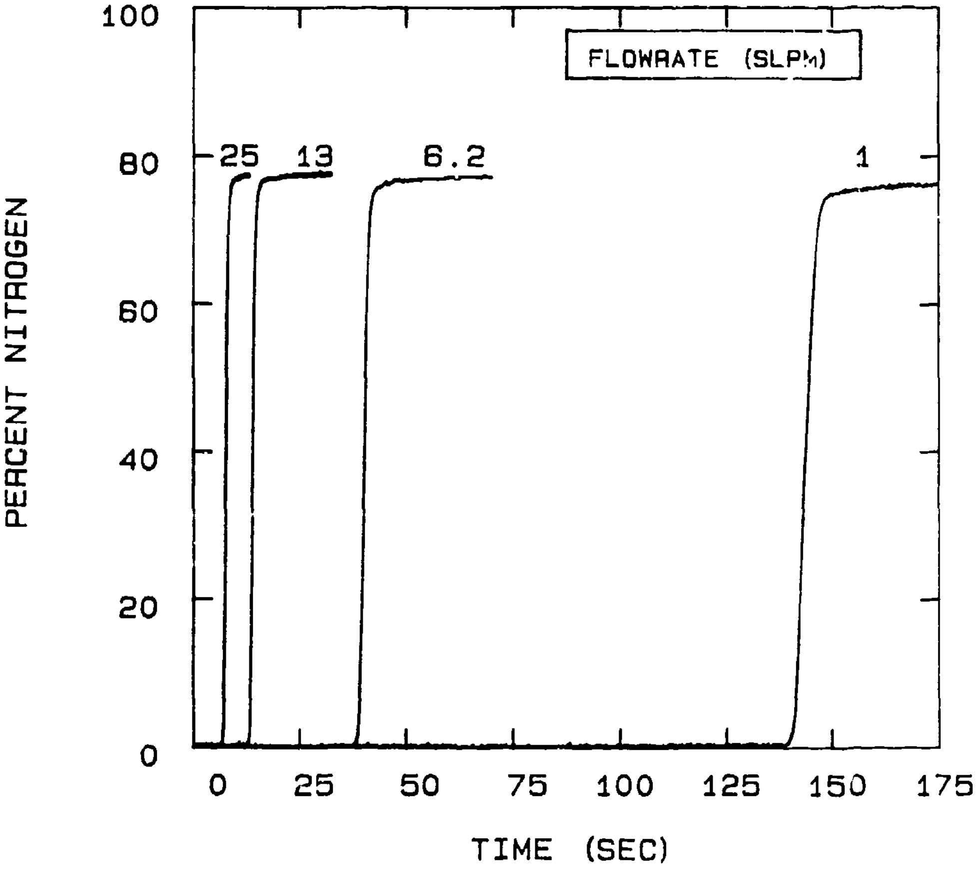

FIG 5-72. DEPENDENCE OF NITROGEN BREAKTHROUGH ON FLOWRATE AT -40°C AND BED PRESSURE OF 25 PSIA.

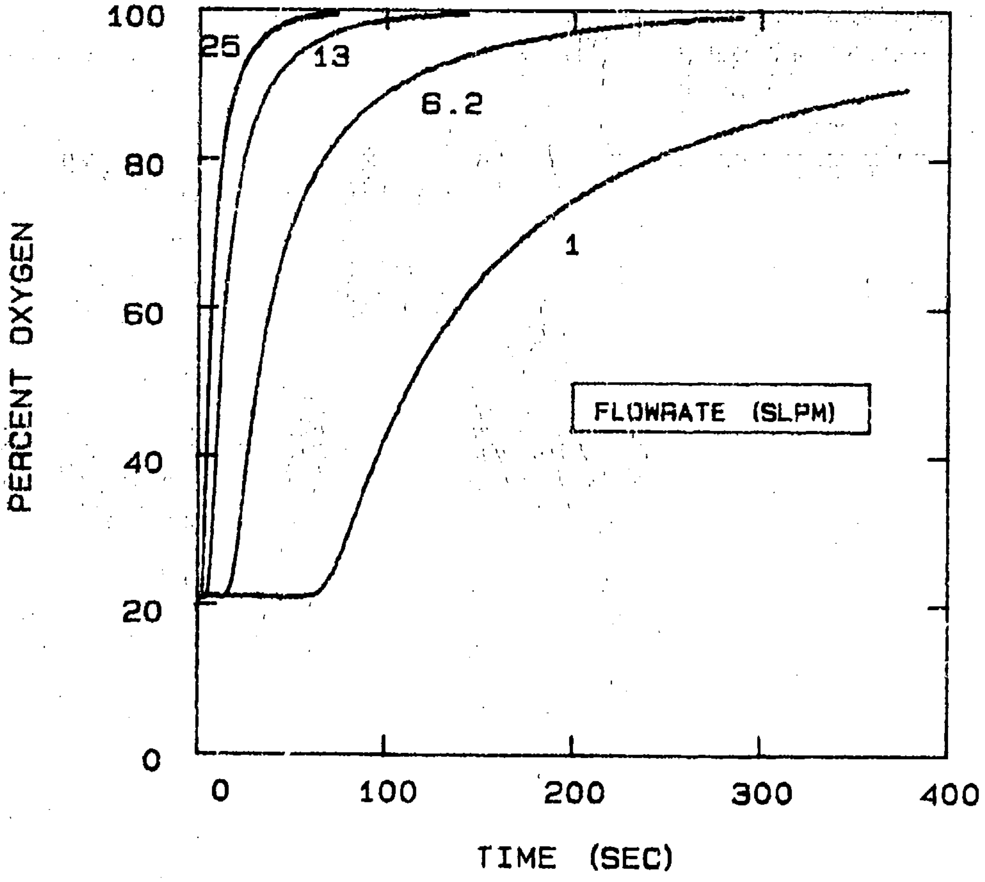

FIG 5-73. DEPENDENCE OF OXYGEN BREAKTHROUGH ON FLOWRATE AT -40°C AND BED PRESSURE OF 25 PSIA.

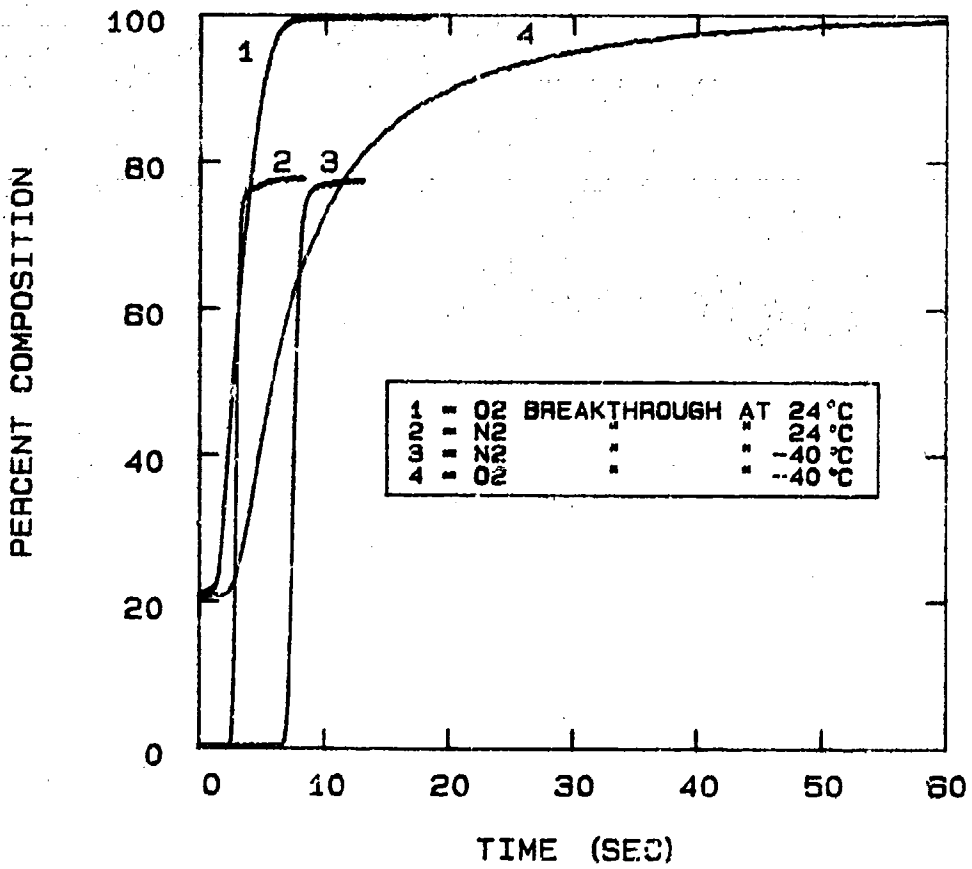

FIG 5-74. EFFECT OF TEMPERATURE ON NITROGEN AND OXYGEN BREAKTHROUGH FOR A FLOWRATE OF 25 SLPM AND BED PRESSURE OF 25 PSIA.

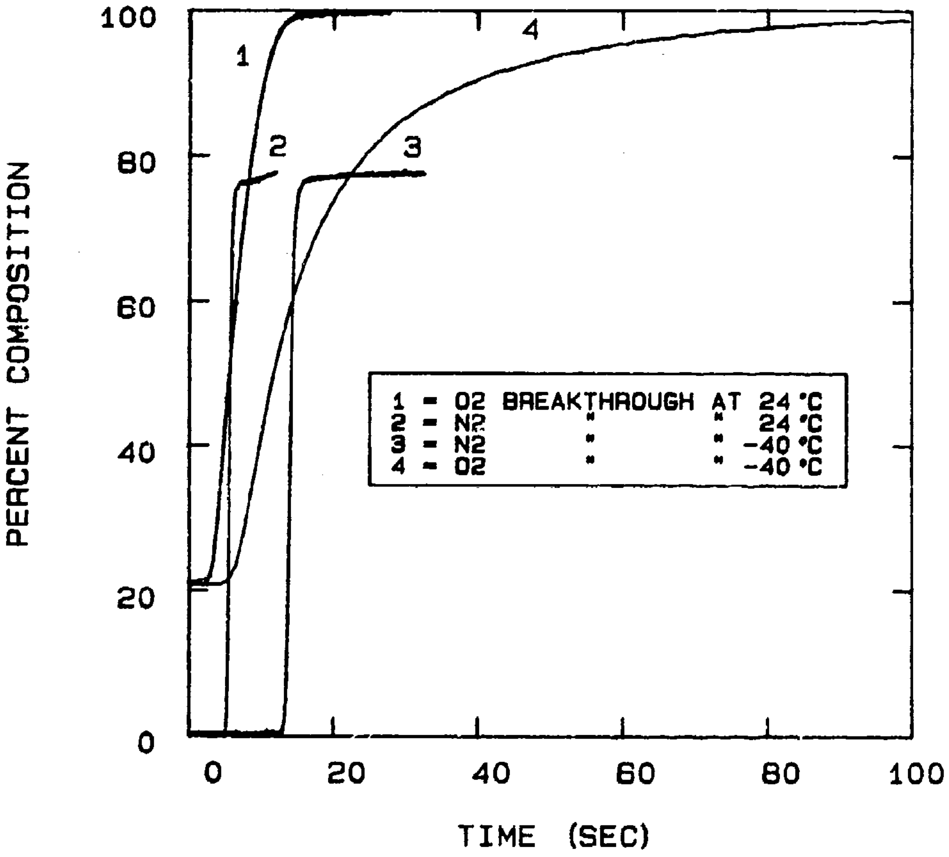

FIG 5-75. EFFECT OF TEMPERATURE ON NITROGEN AND OXYGEN BREAKTHROUGH FOR A FLOWRATE OF 13 SLPM AND BED PRESSURE OF 25 PSIA.

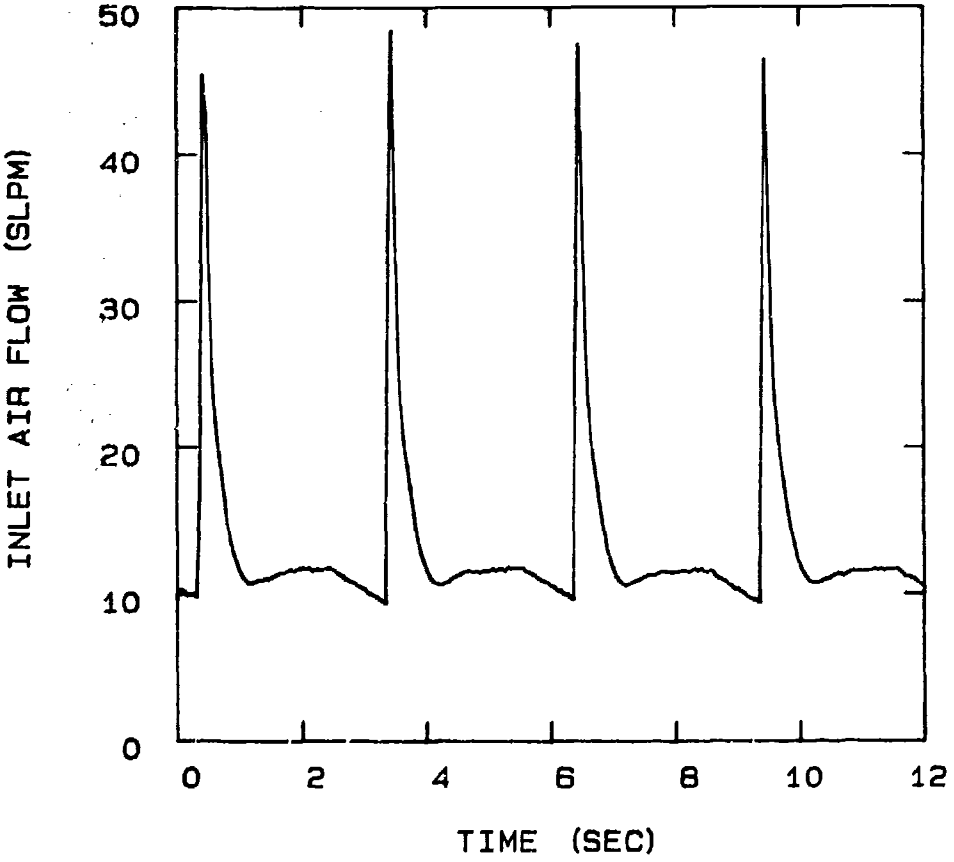

FIG 5-76. AIR FLOW INTO THE PSA UNIT OPERATING AT 24°C AND CONFIGURED FOR A 2 STEP CYCLE, 6 SEC. CYCLE TIME, 0.020" PURGE ORIFICE, AND 100 SCCM PRODUCT FLOW.

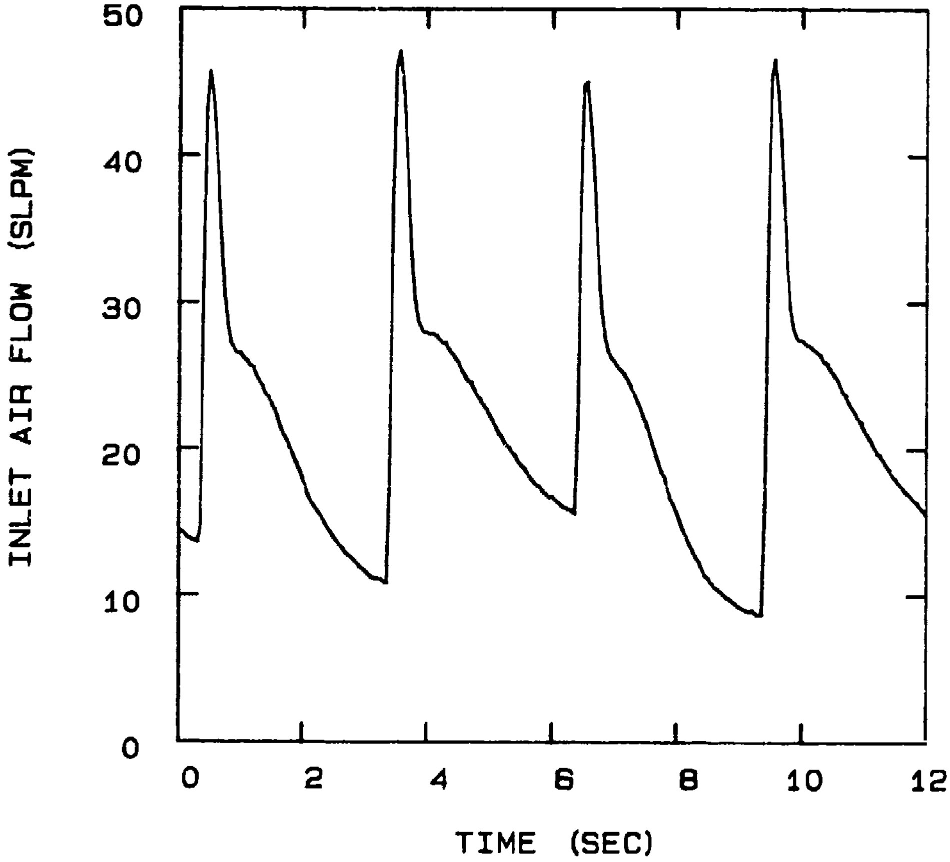

FIG 5-77. AIR FLOW INTO THE PSA UNIT OPERATING AT -40 °C AND CONFIGURED FOR A 2 STEP CYCLE, 6 SEC. CYCLE TIME, 0.020" PURGE ORIFICE, AND 100 SCCM PRODUCT FLOW.

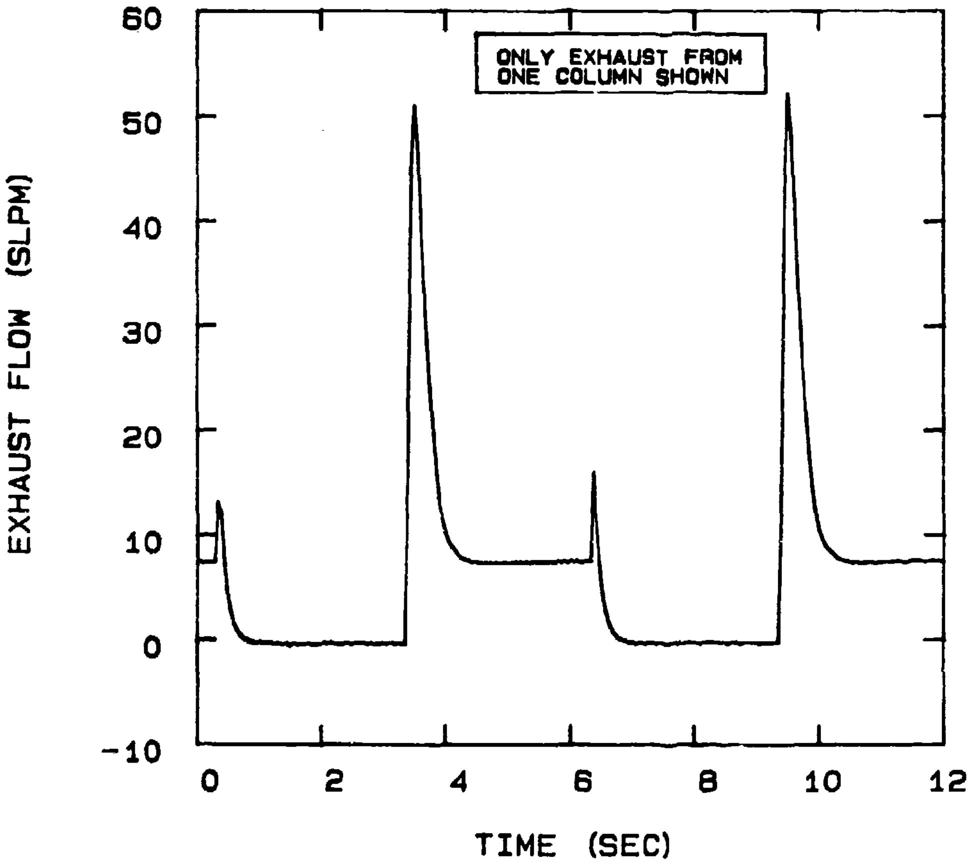

FIG 5-78. EXHAUST FLOW FROM THE PSA UNIT OPERATING AT 24°C AND CONFIGURED FOR A 2 STEP CYCLE, 6 SEC. CYCLE TIME, 0.020" PURGE ORIFICE, AND 100 SCCM PRODUCT FLOW.

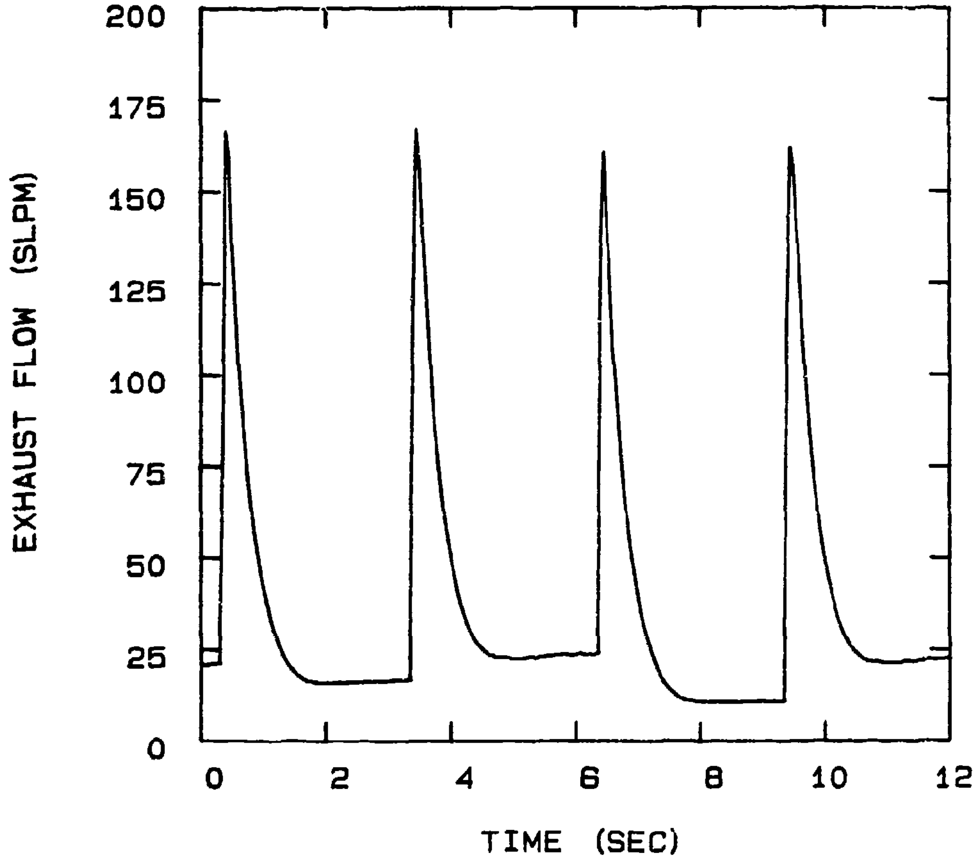

FIG 5-79. EXHAUST FLOW FROM THE PSA UNIT OPERATING AT -40°C AND CONFIGURED FOR A 2 STEP CYCLE, 6 SEC. CYCLE TIME, 0.020" PURGE ORIFICE, AND 100 SCCM PRODUCT FLOW.

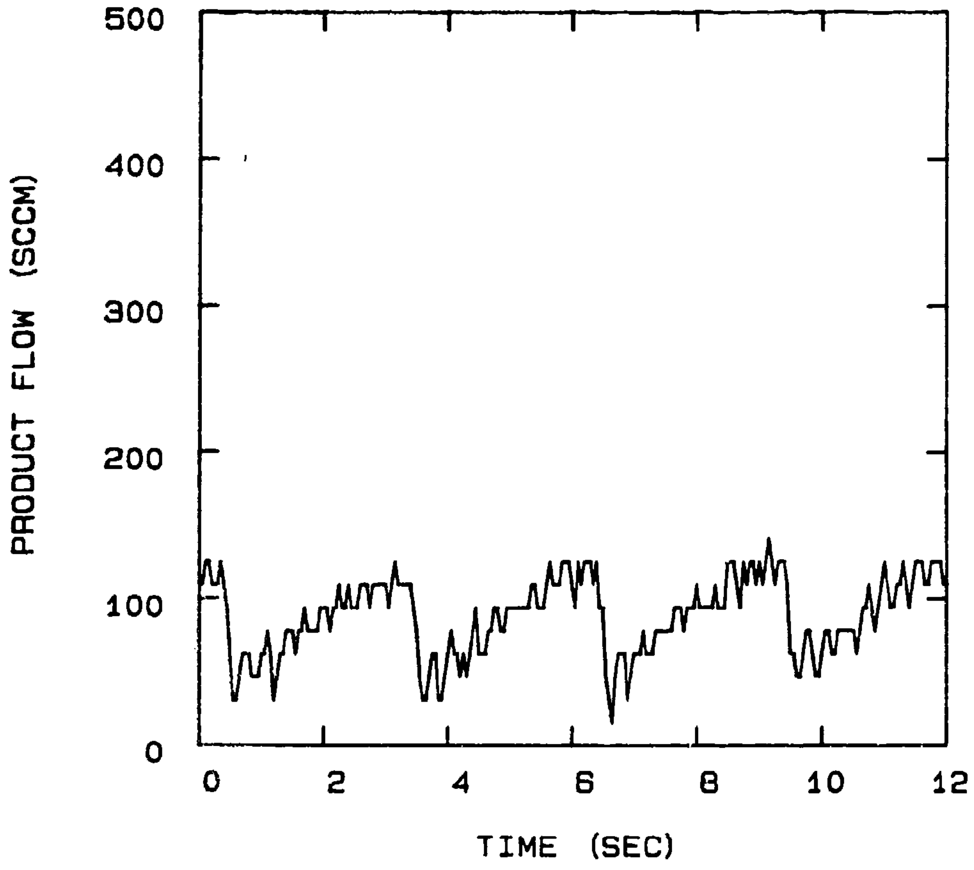

FIG 5-80. PRODUCT FLOW FROM THE PSA UNIT OPERATING AT 24°C AND CONFIGURED FOR A 2 STEP CYCLE, 6 SEC CYCLE TIME, 0.020" PURGE ORIFICE, AND 100 SCCM PRODUCT FLOW.

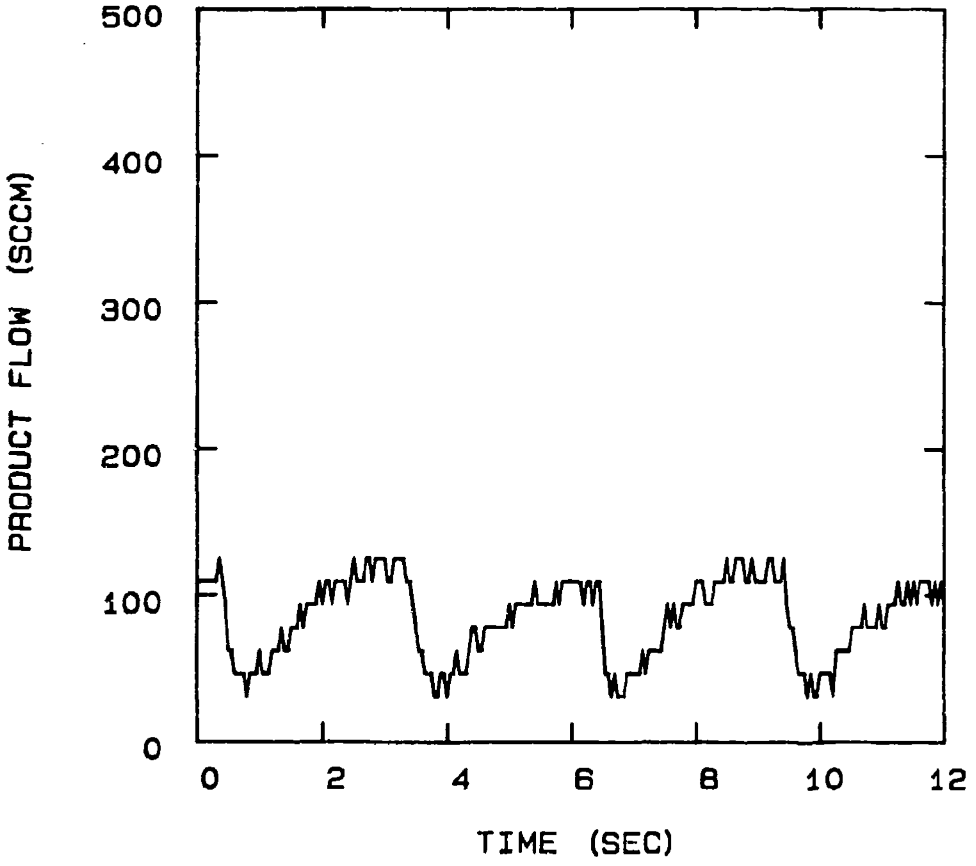

FIG 5-81. PRODUCT FLOW FROM THE PSA UNIT OPERATING AT -40°C AND CONFIGURED FOR A 2 STEP CYCLE, 6 SEC CYCLE TIME, 0.020" PURGE ORIFICE, AND 100 SCCM PRODUCT FLOW.

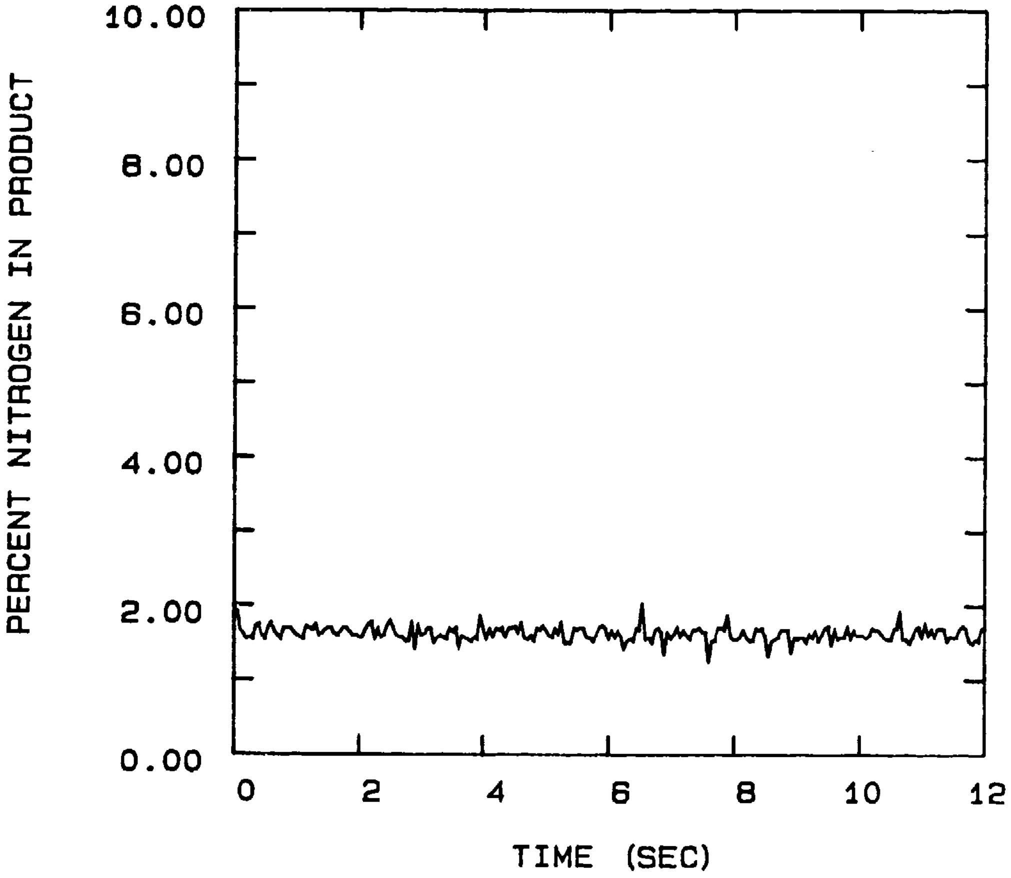

FIG 5-82. PRODUCT N2 FROM THE PSA UNIT OPERATING AT 24 °C AND CONFIGURED FOR A 2 STEP CYCLE, 6 SEC. CYCLE TIME, 0.020" PURGE ORIFICE, AND 100 SCCM PRODUCT FLOW.

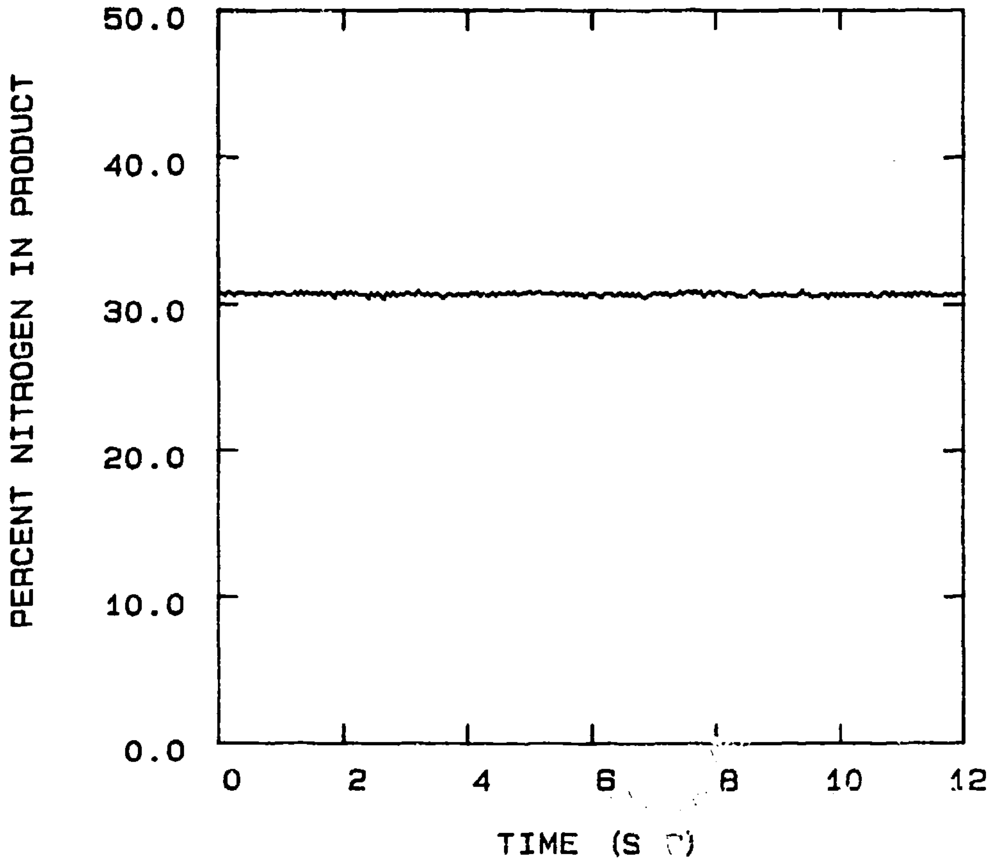

FIG 5-83. PRODUCT N2 FROM THE PSA UNIT OPERATING AT -40°C AND CONFIGURED FOR A 2 STEP CYCLE, 6 SEC. CYCLE TIME, 0.020" PURGE ORIFICE, AND 100 SCCM PRODUCT FLOW.

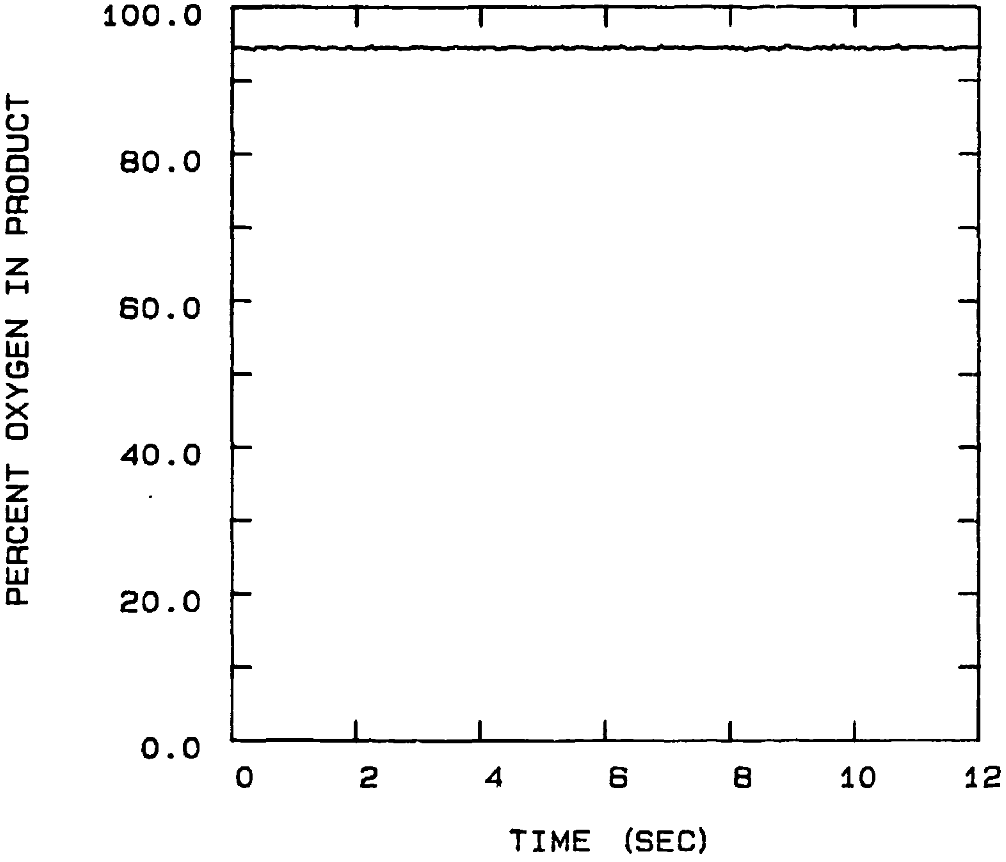

FIG 5-84. PRODUCT O2 FROM THE PSA UNIT OPERATING AT 24°C AND CONFIGURED FOR A 2 STEP CYCLE, 6 SEC. CYCLE TIME, 0.020" PURGE ORIFICE, AND 100 SCCM PRODUCT FLOW.

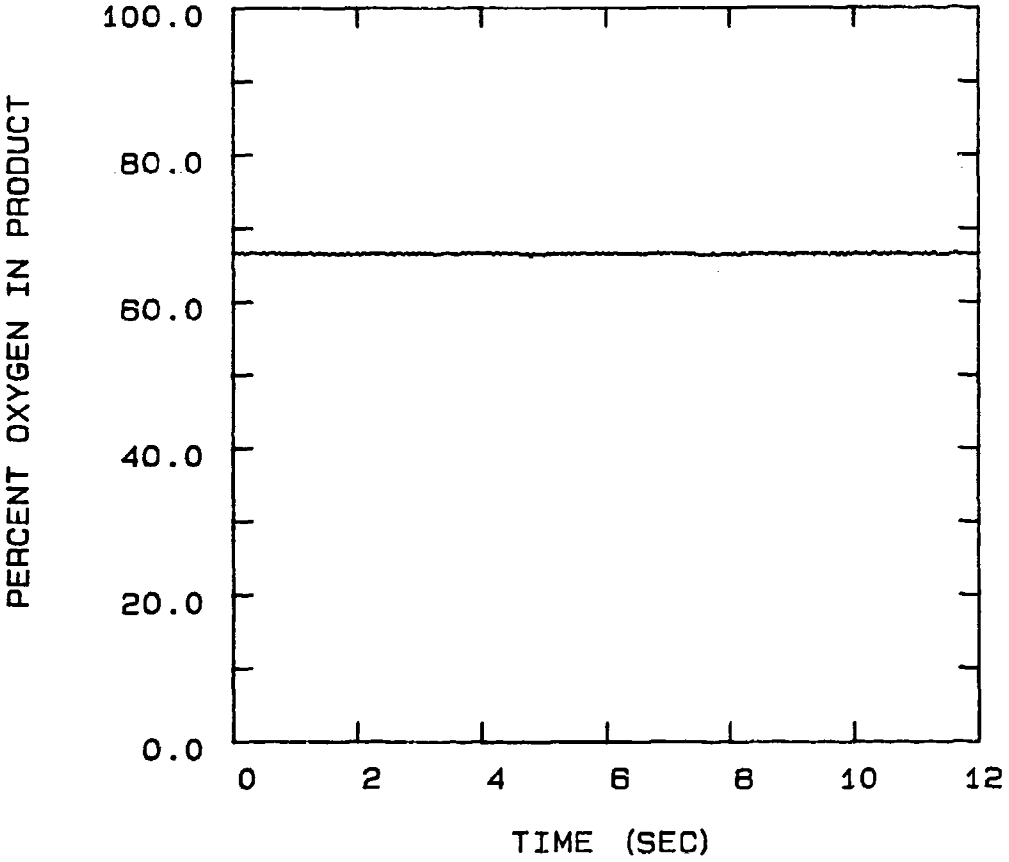

FIG 5-85. PRODUCT O2 FROM THE PSA UNIT OPERATING AT -40°C AND CONFIGURED FOR A 2 STEP CYCLE, 6 SEC. CYCLE TIME, 0.020" PURGE ORIFICE, AND 100 SCCM PRODUCT FLOW.

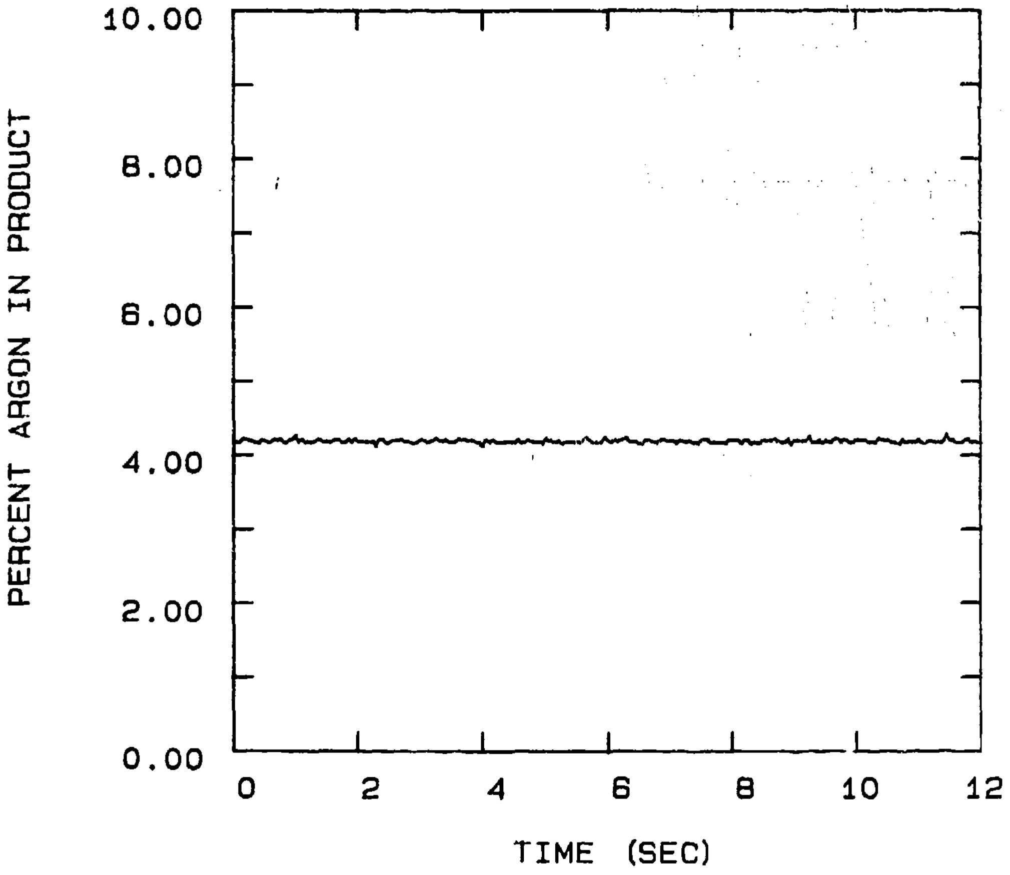

FIG 5-86. PRODUCT AR FROM THE PSA UNIT OPERATING AT 24 °C AND CONFIGURED FOR A 2 STEP CYCLE, 6 SEC. CYCLE TIME, 0.020" PURGE ORIFICE, AND 100 SCCM PRODUCT FLOW.

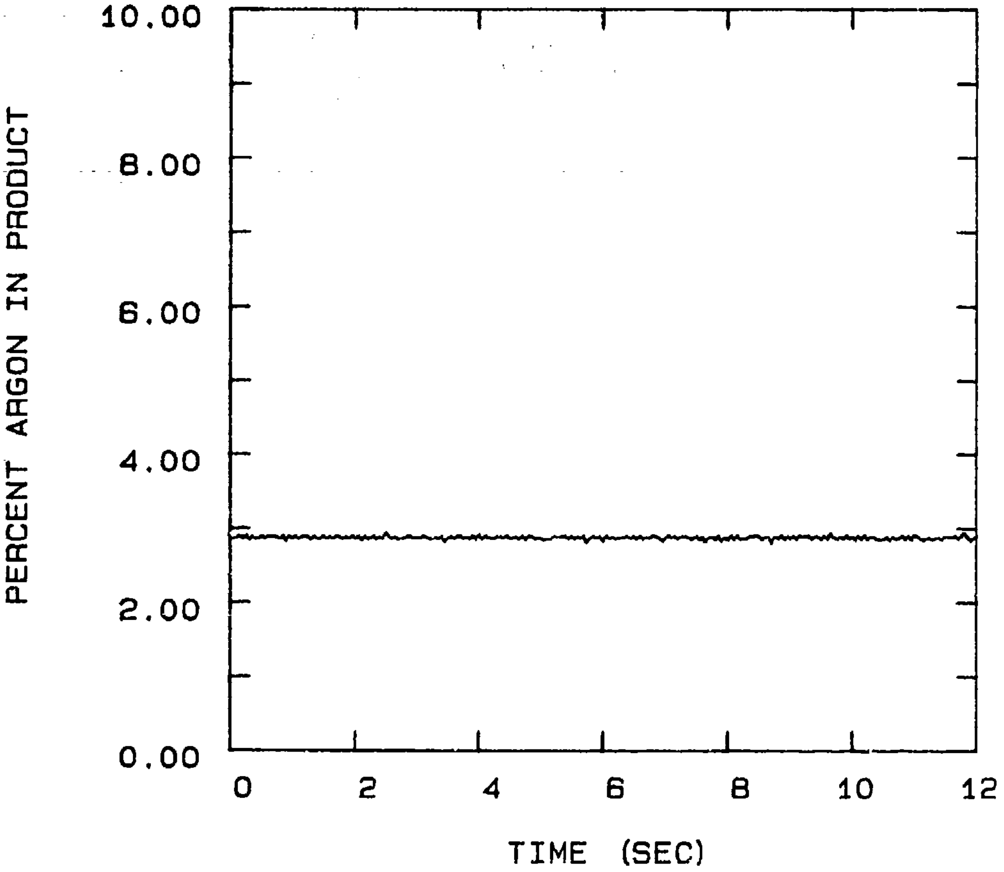

FIG 5-87. PRODUCT AR FROM THE PSA UNIT OPERATING AT -40°C AND CONFIGURED FOR A 2 STEP CYCLE, 6 SEC. CYCLE TIME, 0.020" PURGE ORIFICE, AND 100 SCCM PRODUCT FLOW.

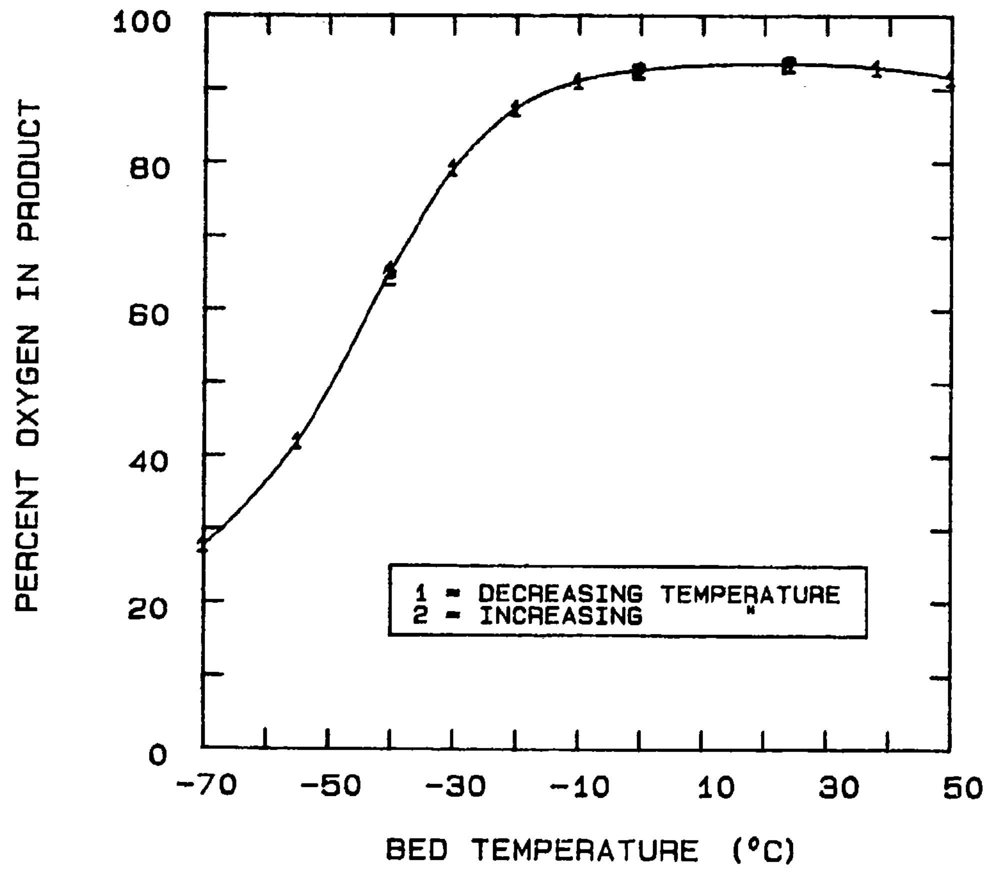

FIG 5-88. EFFECT OF BED TEMPERATURE ON A PSA UNIT CONFIGURED FOR A 2 STEP CYCLE, 6 SEC. CYCLE TIME, 0.020" PURGE ORIFICE, AND 100 SCCM PRODUCT FLOWRATE.

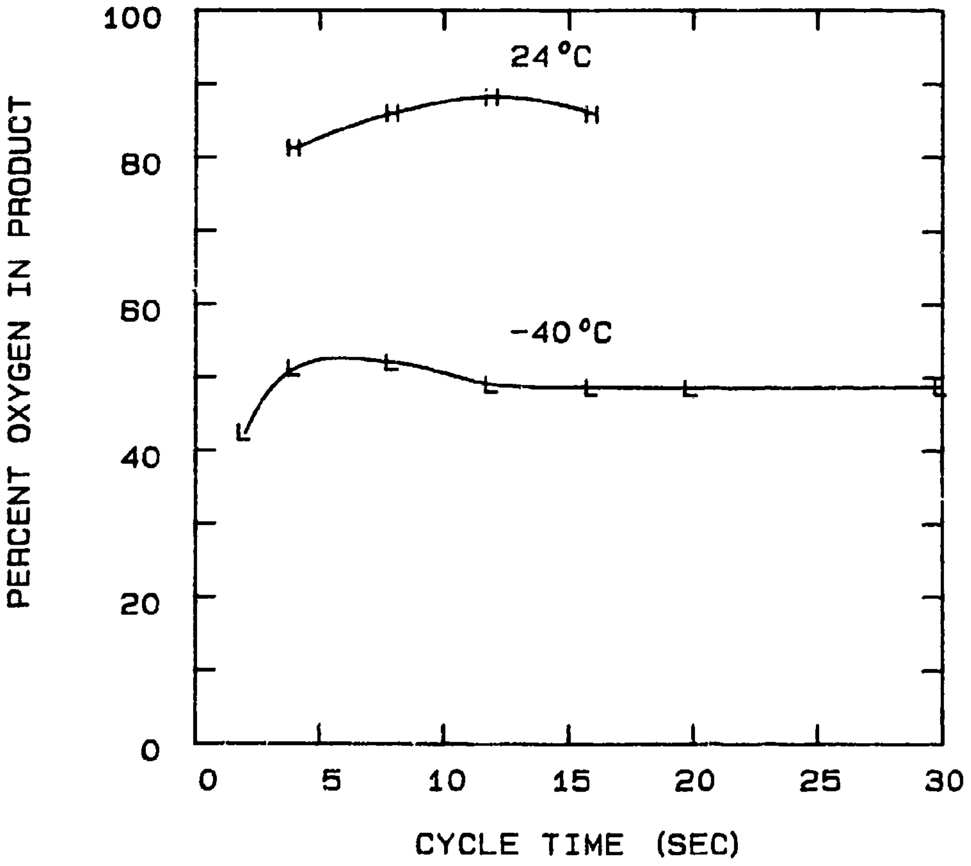

FIG 5-89. EFFECT OF CYCLE TIME AND TEMPERATURE ON THE PSA UNIT CONFIGURED FOR 2 STEPS/CYCLE, 0.010" PURGE ORIFICE, AND 100 SCCM PRODUCT FLOW.

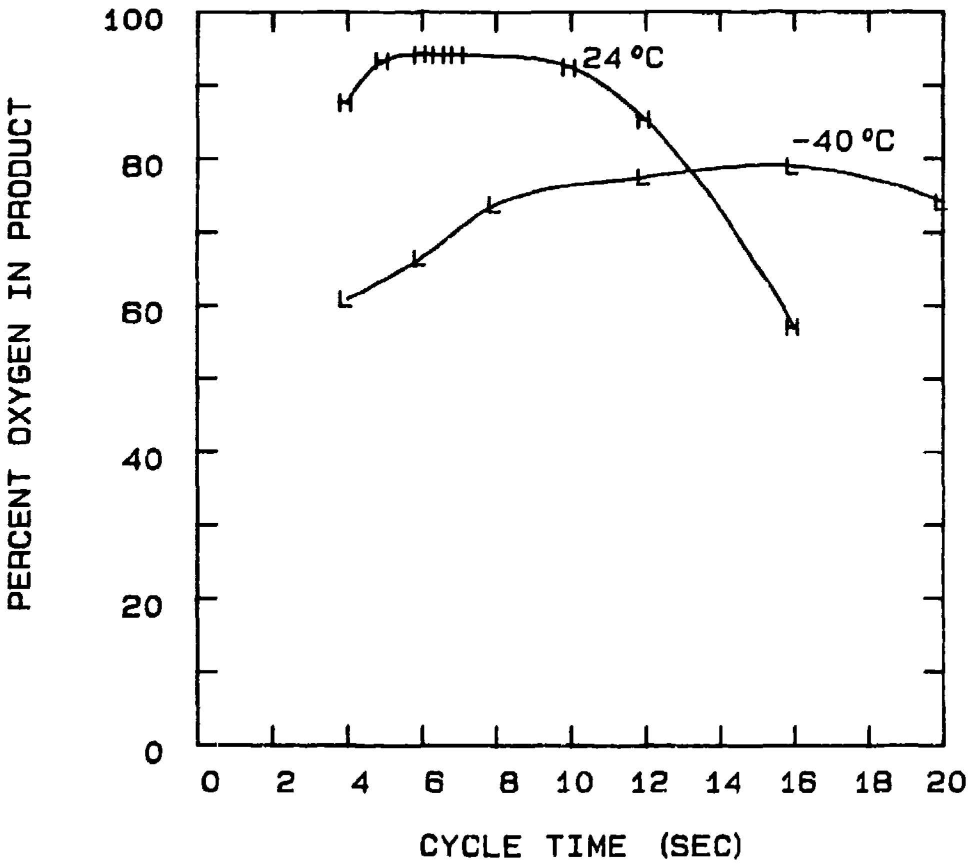

FIG 5-90. EFFECT OF CYCLE TIME AND TEMPERATURE ON THE PSA UNIT CONFIGURED FOR 2 STEPS/CYCLE, 0.020" PURGE ORIFICE, AND 100 SCCM PRODUCT FLOW.

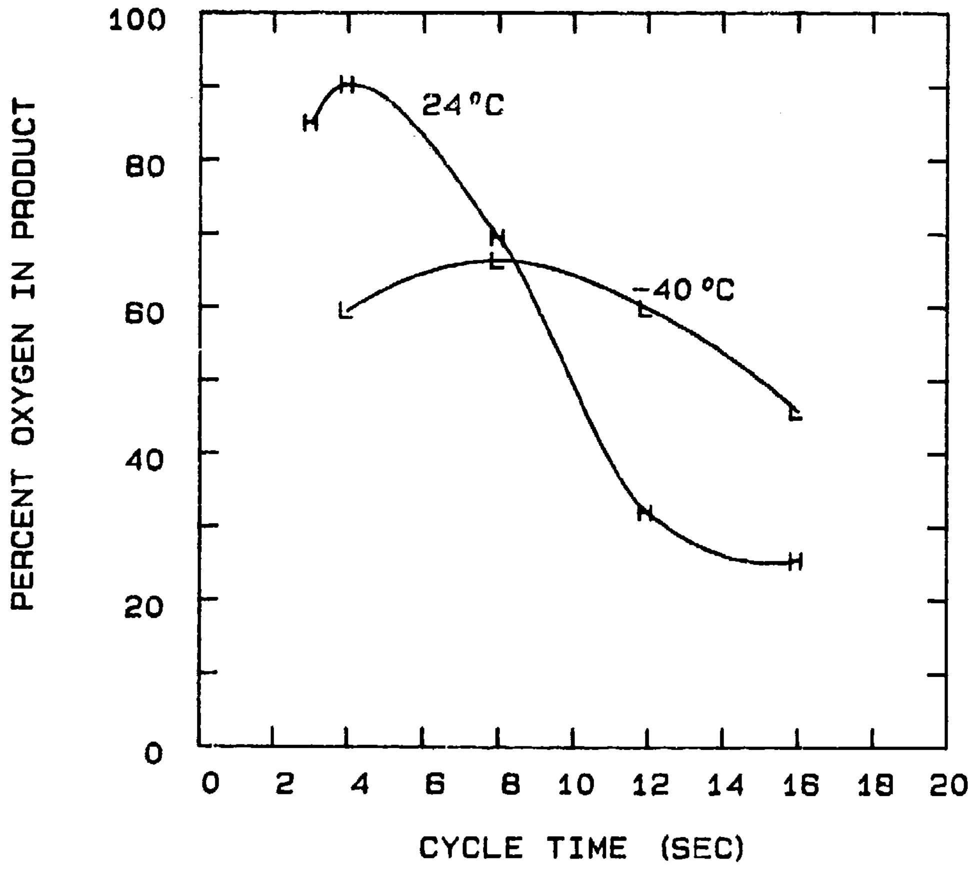

FIG 5-91. EFFECT OF CYCLE TIME AND TEMPERATURE ON THE PSA UNIT CONFIGURED FOR 2 STEPS/CYCLE, 0.029" PURGE ORIFICE, AND 100 SCCM PRODUCT FLOW.

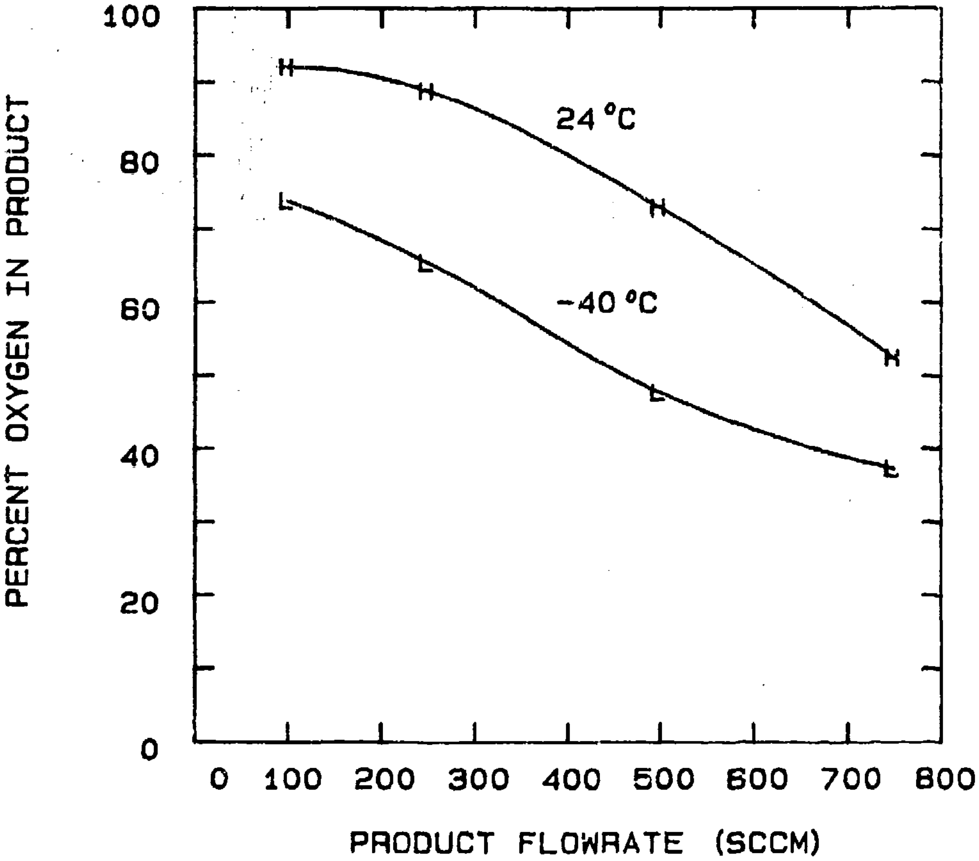

FIG 5-92. EFFECT OF PRODUCT FLOWRATE AND TEMPERATURE ON THE PSA UNIT CONFIGURED FOR 2 STEPS/CYCLE, 8 SEC. CYCLE TIME, AND 0.020" PURGE ORIFICE.

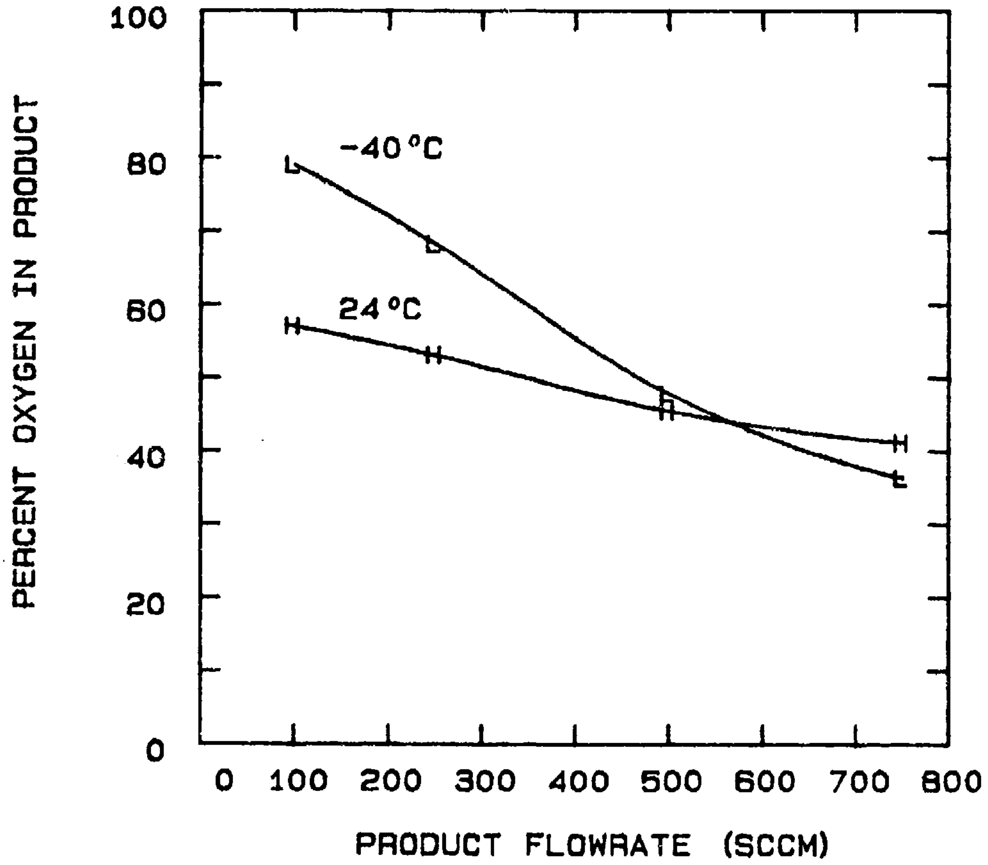

FIG 5-93. EFFECT OF PRODUCT FLOWRATE AND TEMPERATURE ON THE PSA UNIT CONFIGURED FOR 2 STEPS/CYCLE, 18 SEC. CYCLE TIME, AND 0.020" ORIFICE.

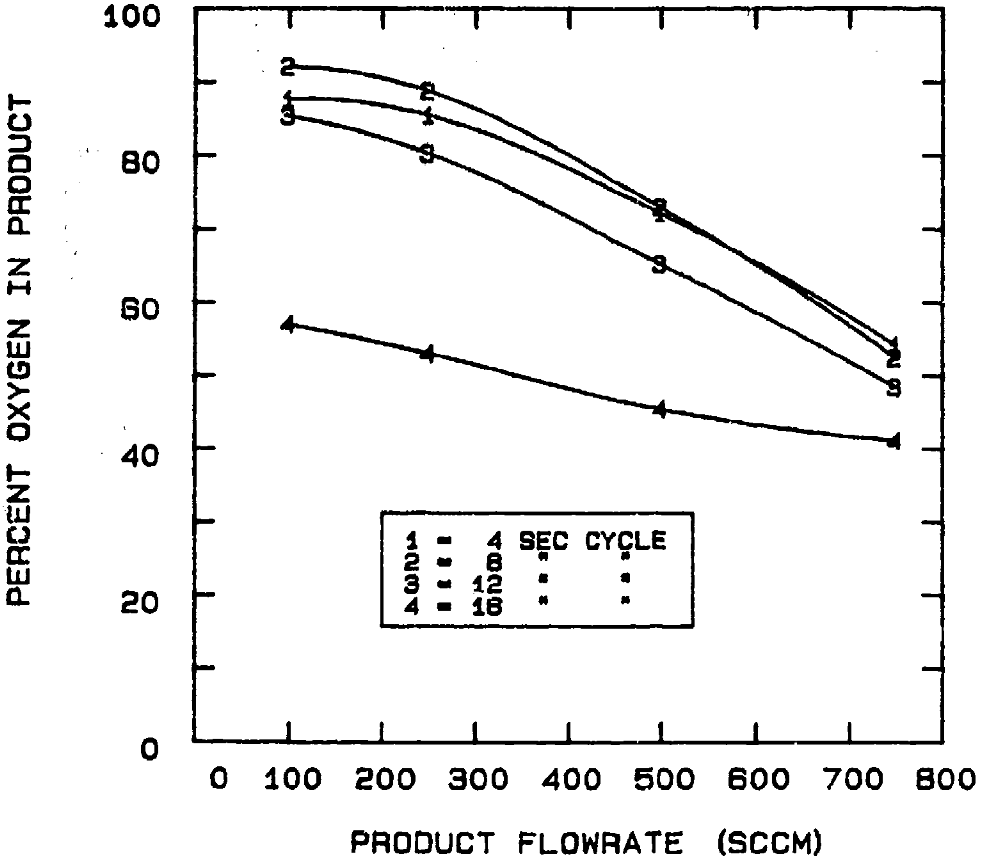

FIG 5-84. EFFECT OF PRODUCT FLOWRATE AND CYCLE TIME ON THE PSA UNIT OPERATING AT 24°C AND CONFIGURED FOR 2 STEPS/CYCLE AND 0.020" PURGE ORIFICE.

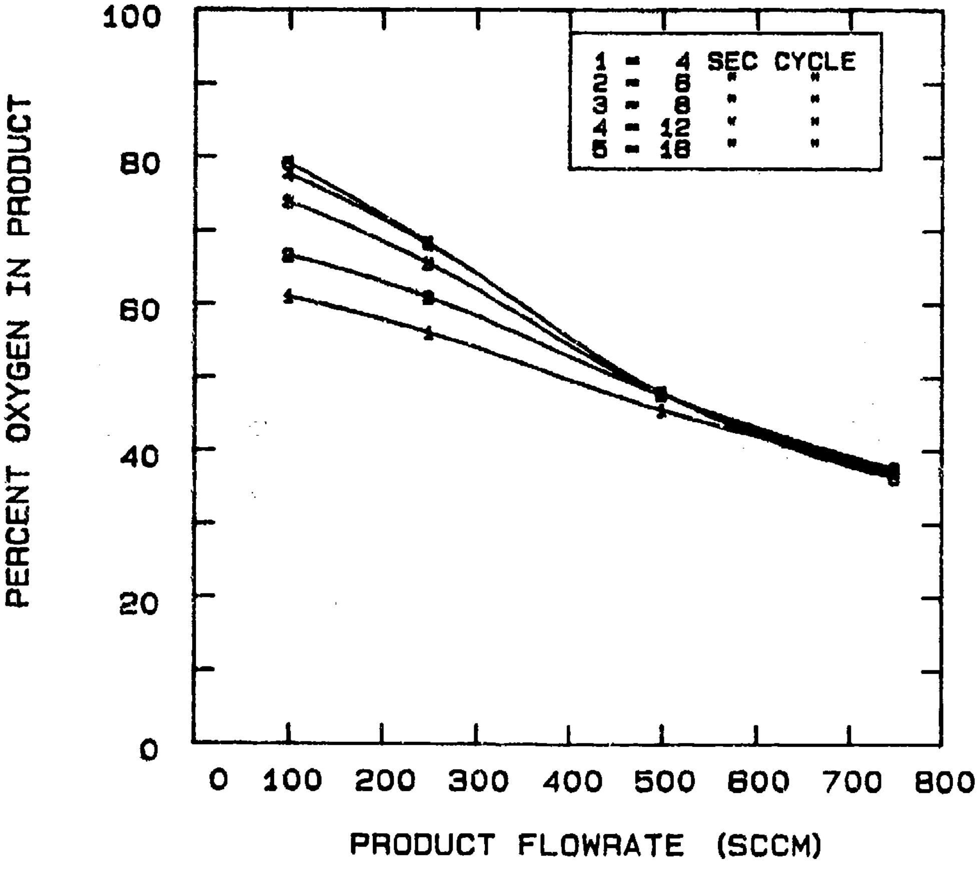

FIG 5-85. EFFECT OF PRODUCT FLOWRATE AND CYCLE TIME ON THE PSA UNIT OPERATING AT -40°C AND CONFIGURED FOR 2 STEPS/CYCLE AND 0.020" PURGE ORIFICE.

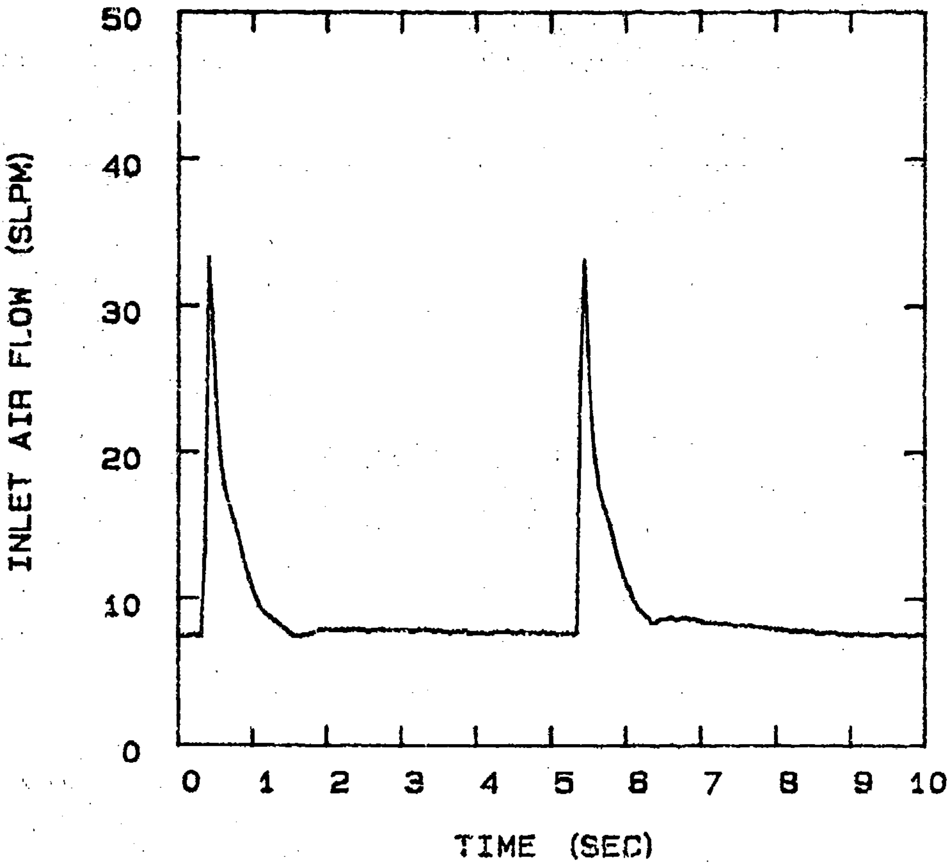

FIG 5-86. INLET FLOW FOR PSA UNIT CONFIGURATION: 24°C, 6 STEP CYCLE (1SEC, 3SEC, 1SEC), 10 SEC CYCLE TIME, 0.020" PURGE ORIFICE AND 100 SCCM PRODUCT FLOW.

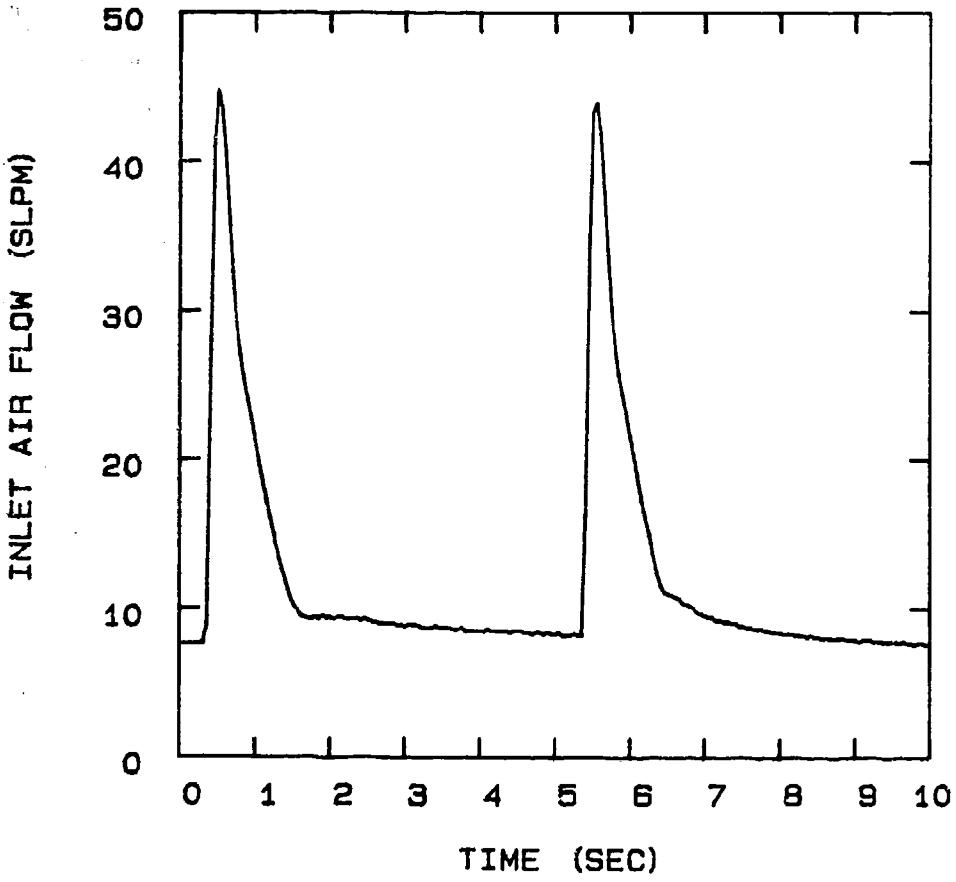

FIG 5-97. INLET FLOW FOR PSA UNIT CONFIGURATION:
-40 °C, 6 STEP CYCLE (1SEC, 3SEC, 1SEC), 10 SEC CYCLE TIME,
0.020" PURGE ORIFICE AND 100 SCCM PRODUCT FLOW.

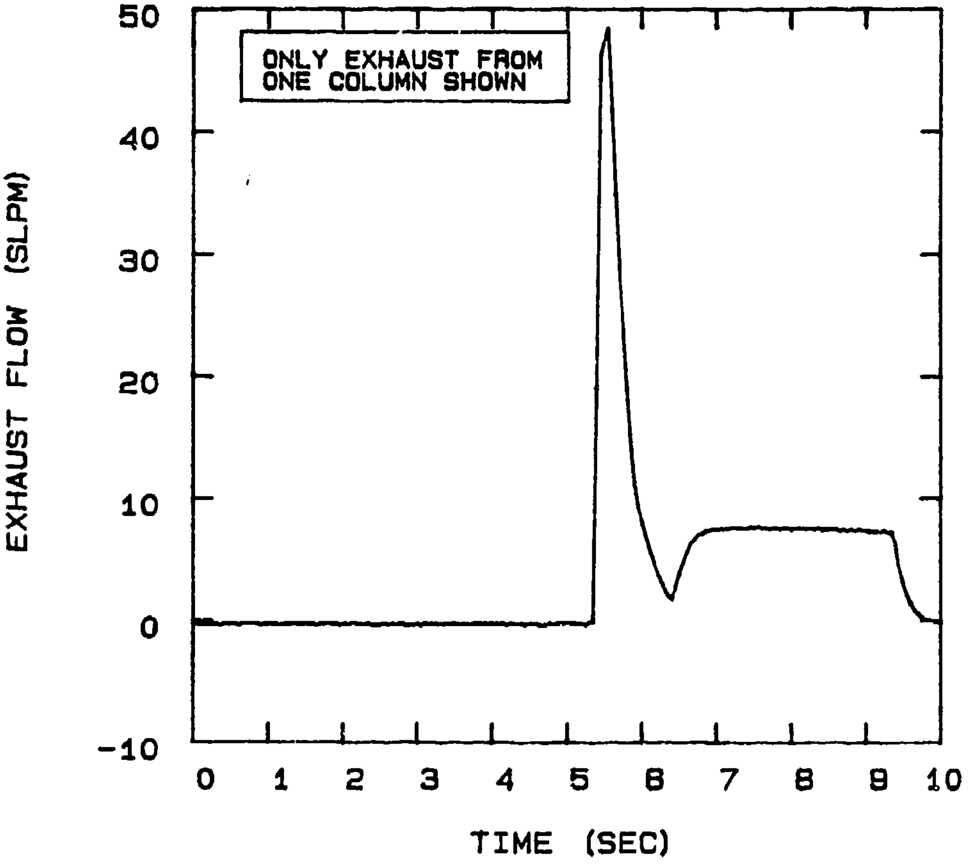

FIG 5-98. EXHAUST FLOW FOR PSA UNIT CONFIGURATION: 24 °C, 6 STEP CYCLE (1SEC, 3SEC, 1SEC), 10SEC CYCLE TIME, 0.020" PURGE ORIFICE, AND 100 SCCM PRODUCT FLOW.

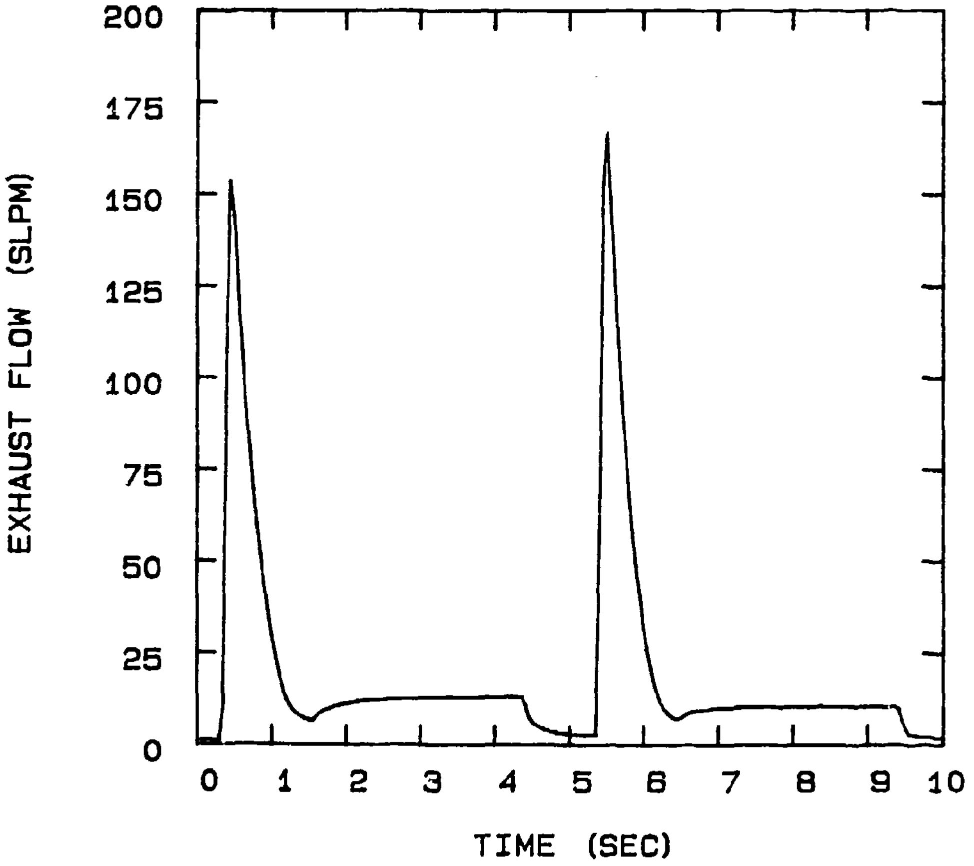

FIG 5-99. EXHAUST FLOW FOR PSA UNIT CONFIGURATION:
-40°C, 6 STEP CYCLE (1SEC, 3SEC, 1SEC), 10 SEC CYCLE TIME,
0.020" PURGE ORIFICE, AND 100 SCCM PRODUCT FLOW.

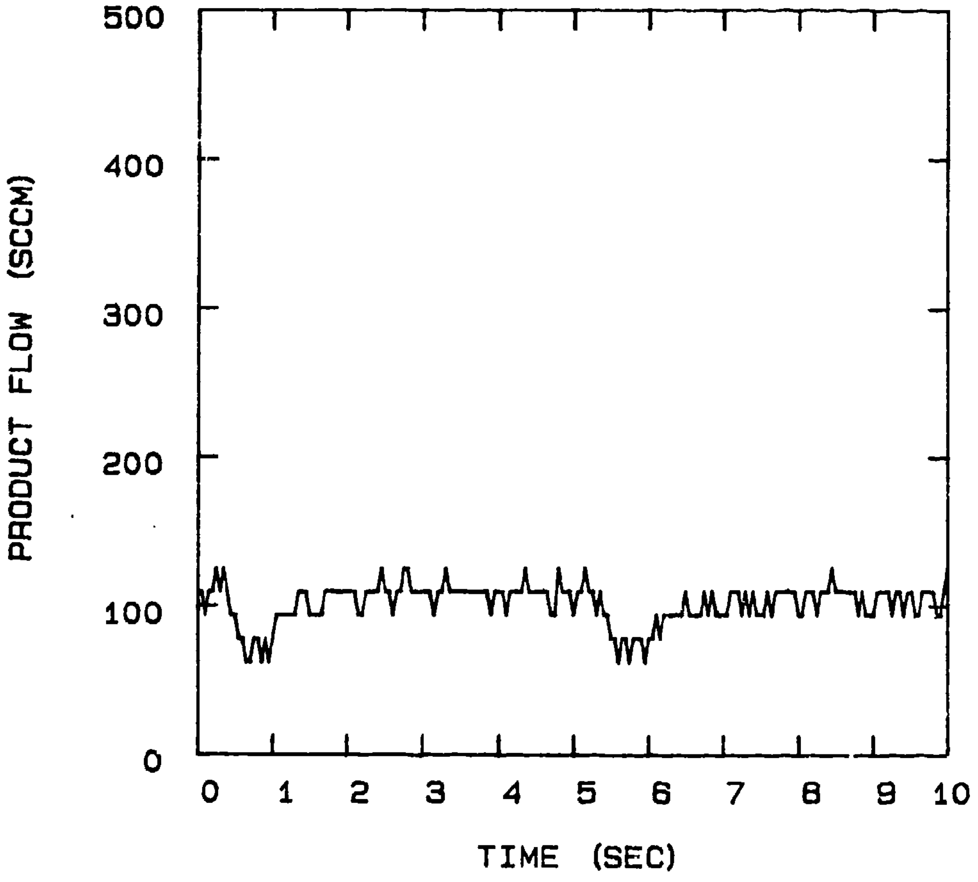

FIG 5-100. PRODUCT FLOW FOR PSA UNIT CONFIGURATION: 24°C, 6 STEP CYCLE (1SEC, 3SEC, 1SEC), 10 SEC CYCLE TIME, 0.020" PURGE ORIFICE, AND 100 SCCM PRODUCT FLOW.

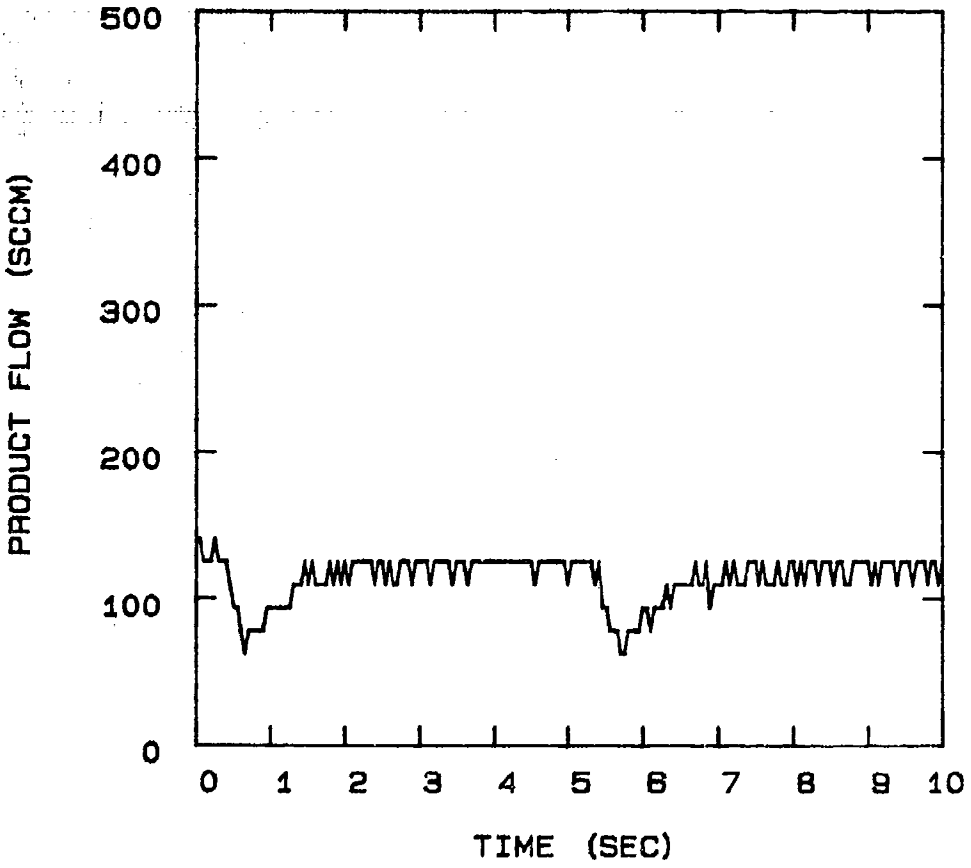

FIG 5-101. PRODUCT FLOW FOR PSA UNIT CONFIGURATION: -40°C, 6 STEP CYCLE (1SEC, 3SEC, 1SEC), 10 SEC CYCLE TIME, 0.020" PURGE ORIFICE, AND 100 SCCM PRODUCT FLOW.

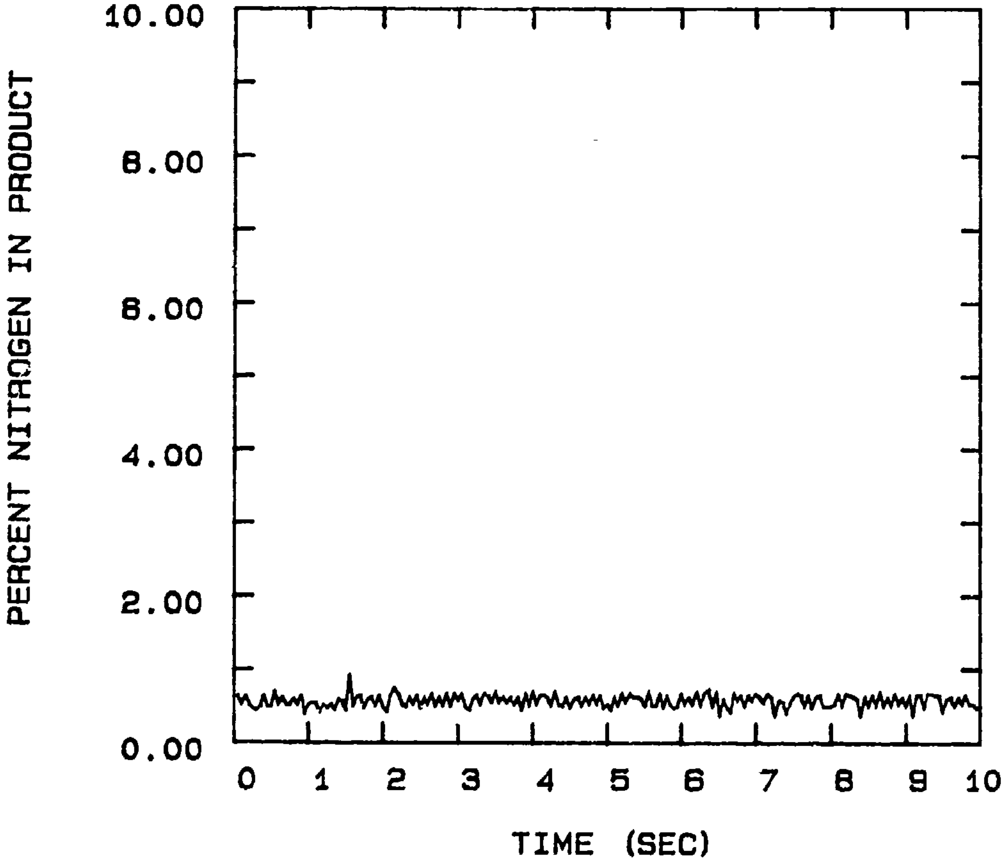

FIG 5-102. PRODUCT N2% FOR PSA UNIT CONFIGURATION: 24 °C, 6 STEP CYCLE (1SEC, 3SEC, 1SEC), 10 SEC CYCLE TIME, 0.020" PURGE ORIFICE, AND 100 SCCM PRODUCT FLOW.

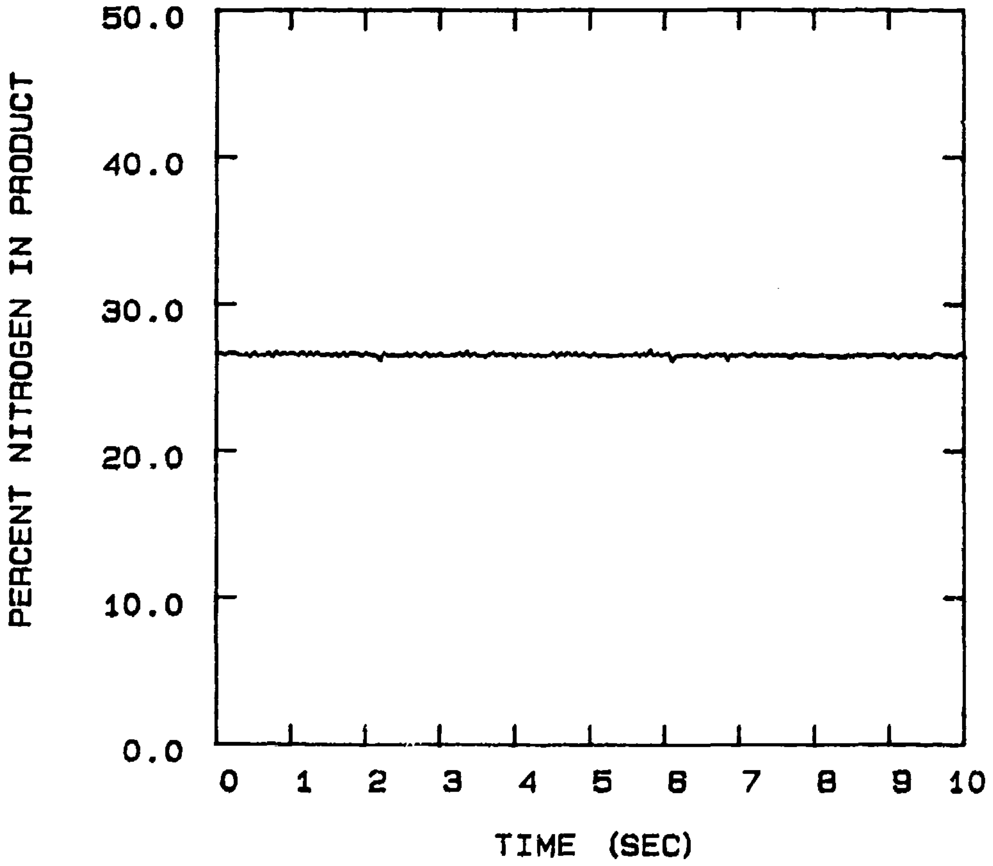

FIG 5-103. PRODUCT N2% FOR PSA UNIT CONFIGURATION: -40 °C, 6 STEP CYCLE (1SEC, 3SEC, 1SEC), 10 SEC CYCLE TIME, 0.020" PURGE ORIFICE, AND 100 SCCM PRODUCT FLOW.

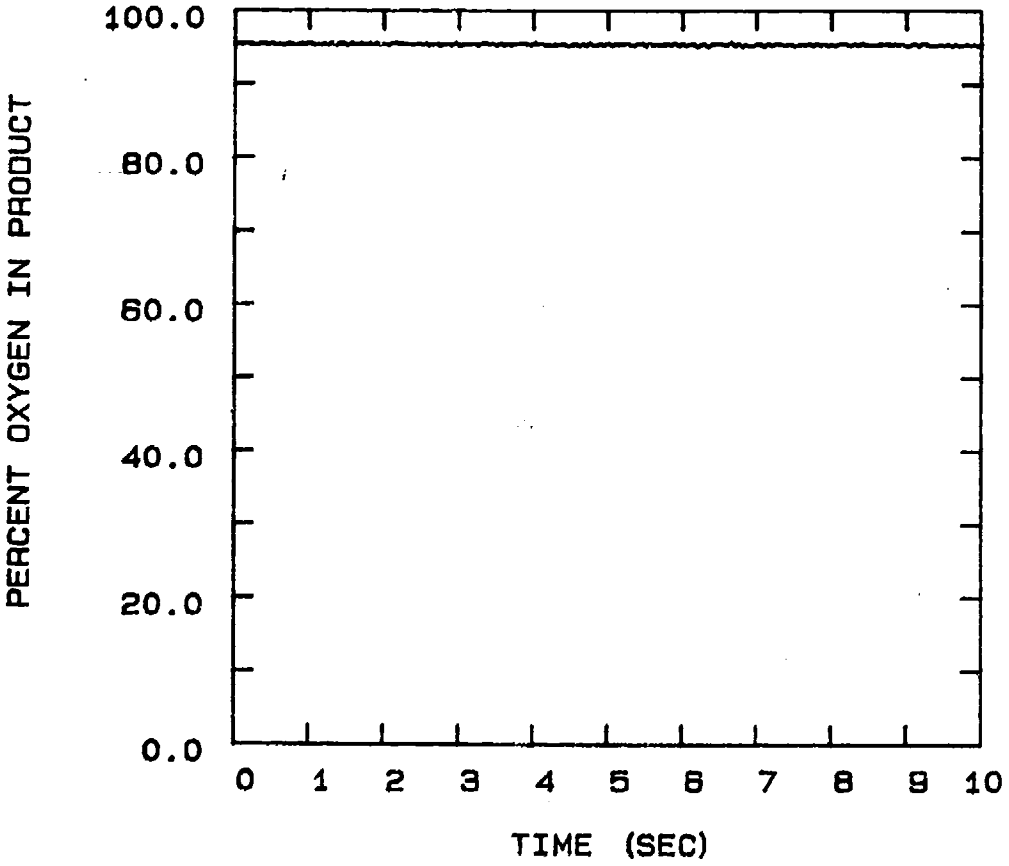

FIG 5-104. PRODUCT O2% FOR PSA UNIT CONFIGURATION: 24°C, 6 STEP CYCLE (1SEC, 3SEC, 1SEC), 10 SEC CYCLE TIME, 0.020" PURGE ORIFICE, AND 100 SCCM PRODUCT FLOW.

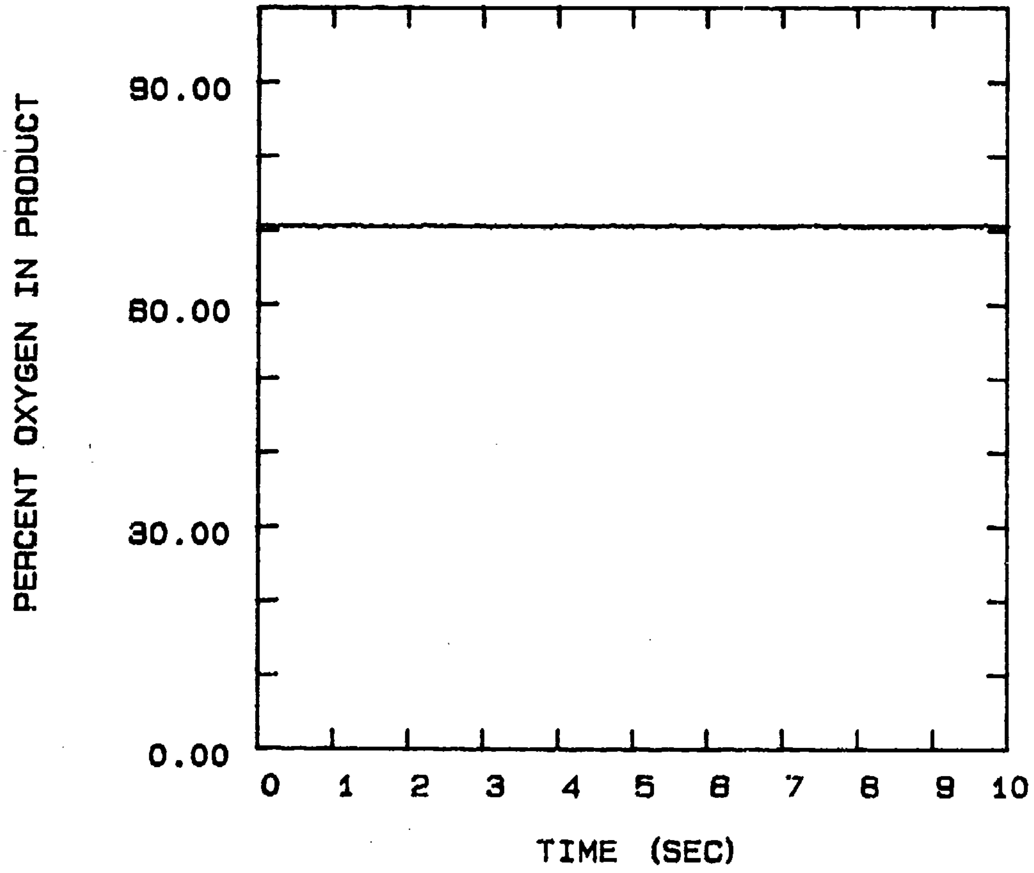

FIG 5-105. PRODUCT O2% FOR PSA UNIT CONFIGURATION: -40°C, 6 STEP CYCLE (1SEC, 3SEC, 1SEC), 10 SEC CYCLE TIME, 0.020" PURGE ORIFICE, AND 100 SCCM PRODUCT FLOW.

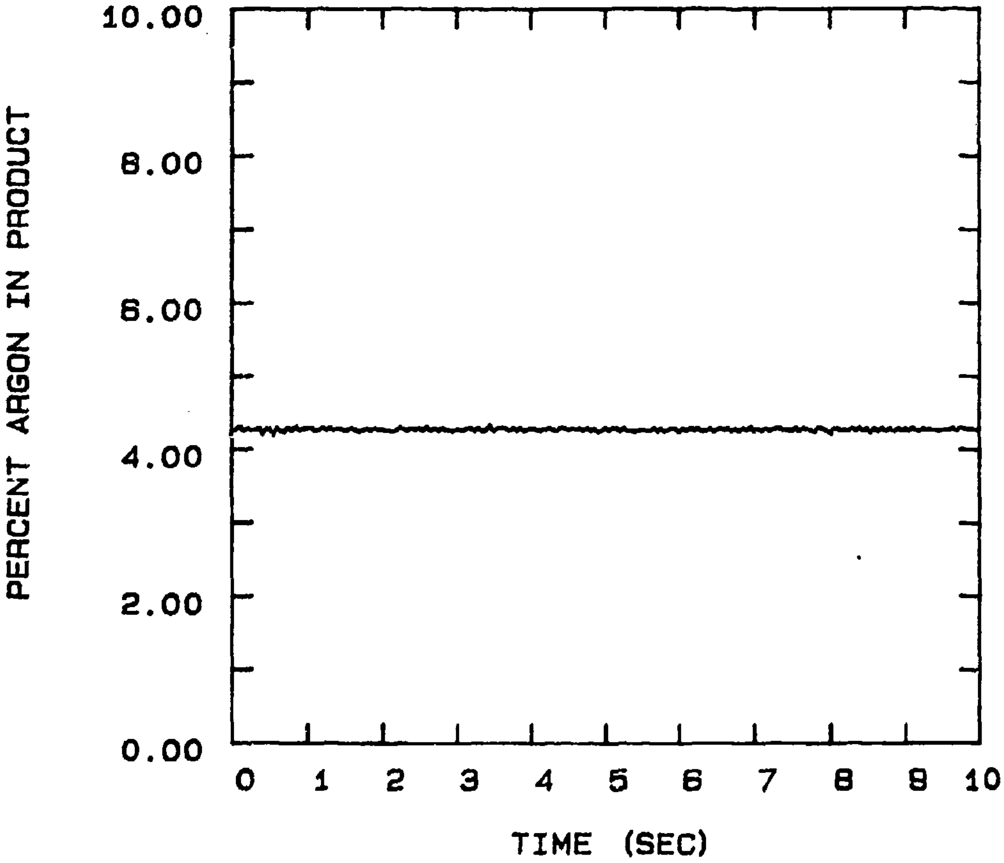

FIG 5-106. PRODUCT AR% FOR PSA UNIT CONFIGURATION: 24°C, 6 STEP CYCLE (1SEC, 3SEC, 1SEC), 10 SEC CYCLE TIME, 0.020" PURGE ORIFICE, AND 100 SCCM PRODUCT FLOW.

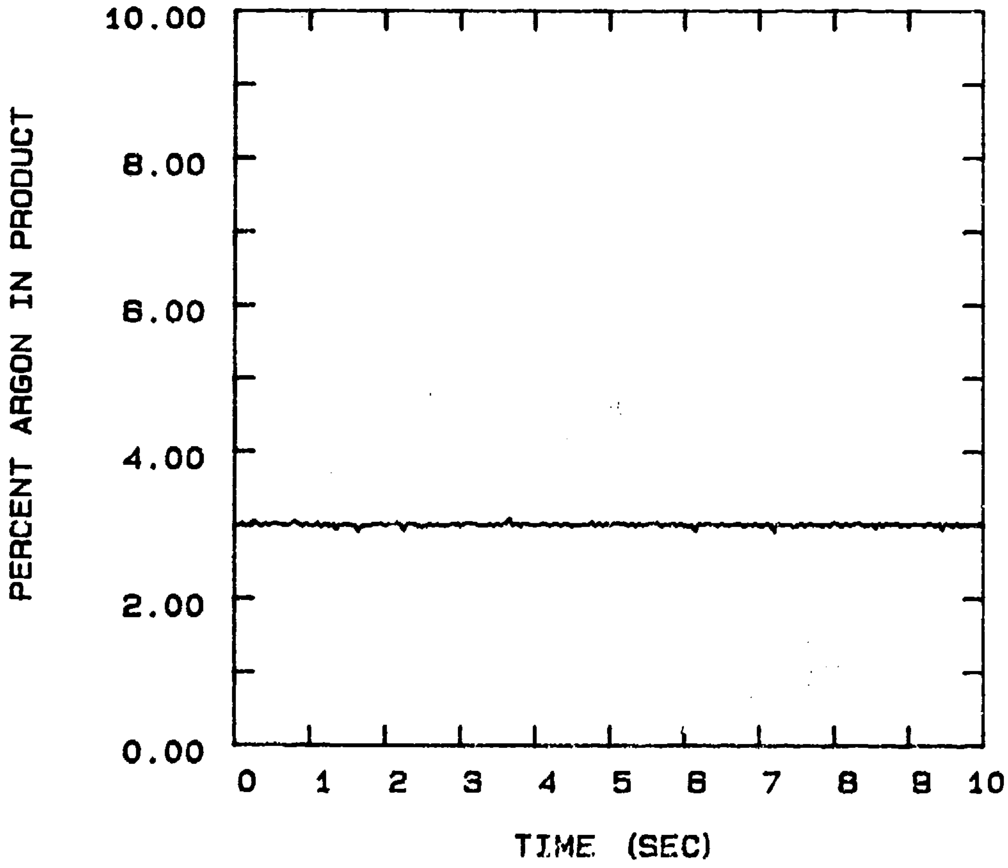

FIG 5-107. PRODUCT AR% FOR PSA UNIT CONFIGURATION:
-40°C, 6 STEP CYCLE (1SEC, 3SEC, 1SEC), 10 SEC CYCLE TIME,
0.020" PURGE ORIFICE, AND 100 SCCM PRODUCT FLOW.

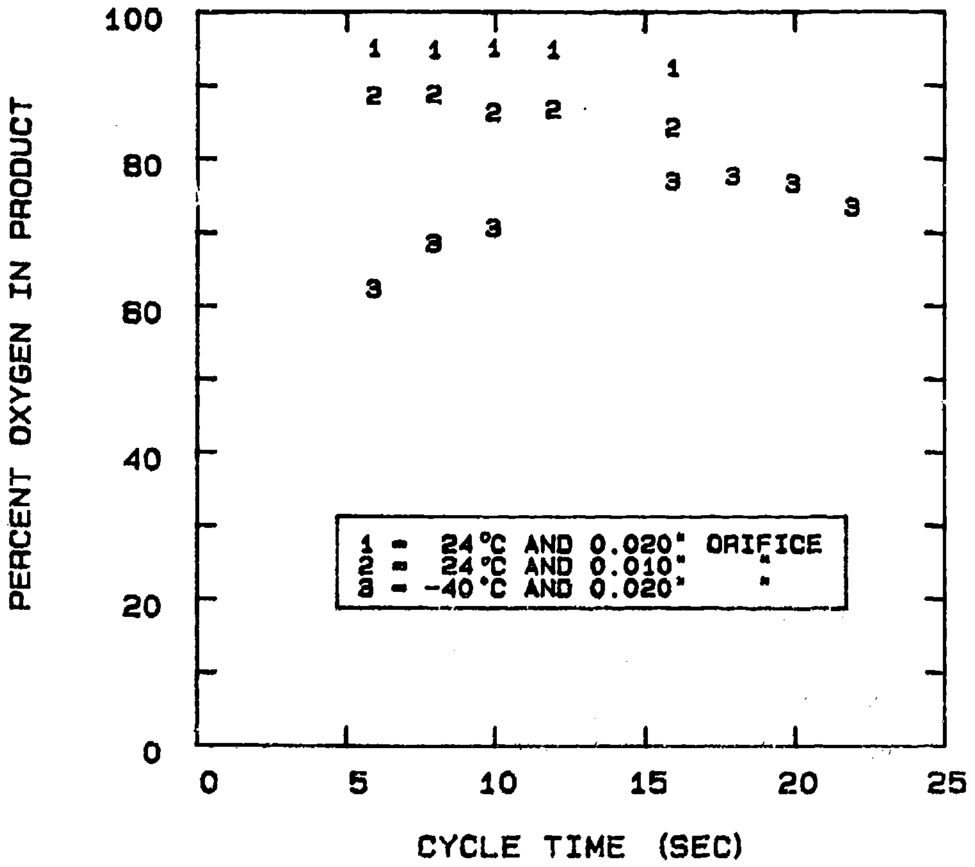

FIG 5-108. EFFECT OF CYCLE TIME AND TEMPERATURE ON THE PSA UNIT CONFIGURED FOR 8 STEP OPERATION AND 100 SCCM PRODUCT FLOW.

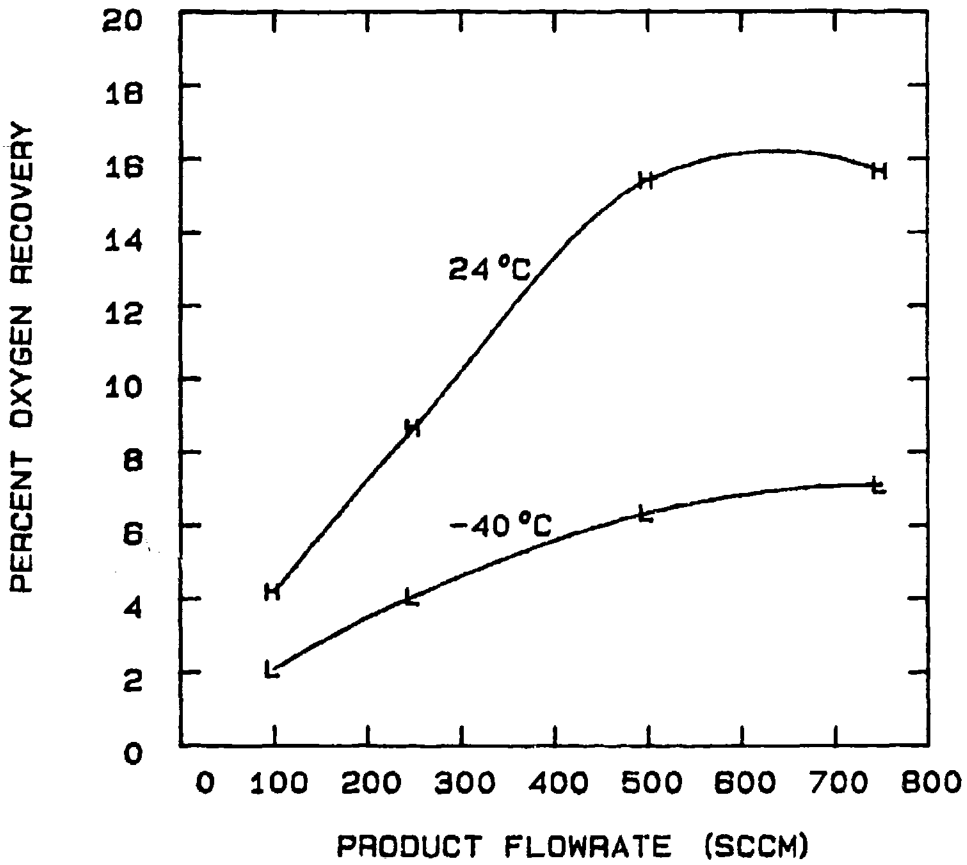

FIG 5-109. EFFECT OF PRODUCT FLOWRATE AND TEMPERATURE ON OXYGEN RECOVERY FOR A 2 STEP SYSTEM WITH A CYCLE TIME OF 8 SEC AND A 0.020" PURGE ORIFICE.

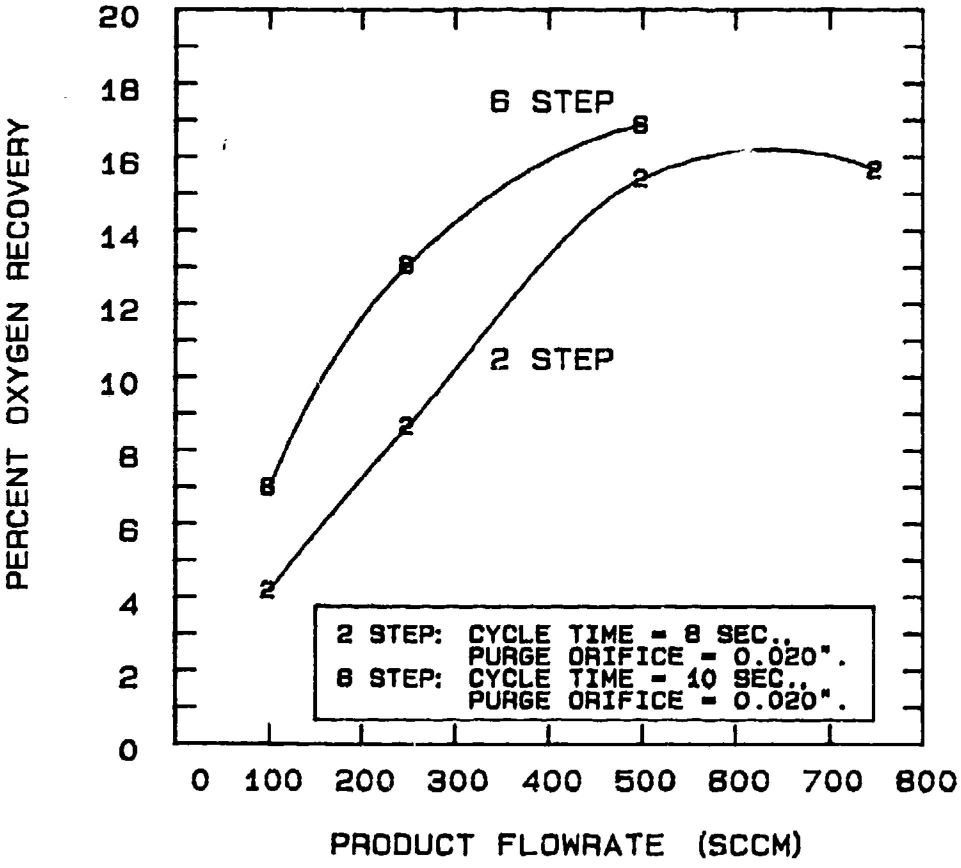

FIG 5-110. COMPARISON OF OXYGEN RECOVERY BETWEEN A 2 STEP AND 6 STEP SYSTEM OPERATING AT 24 °C.

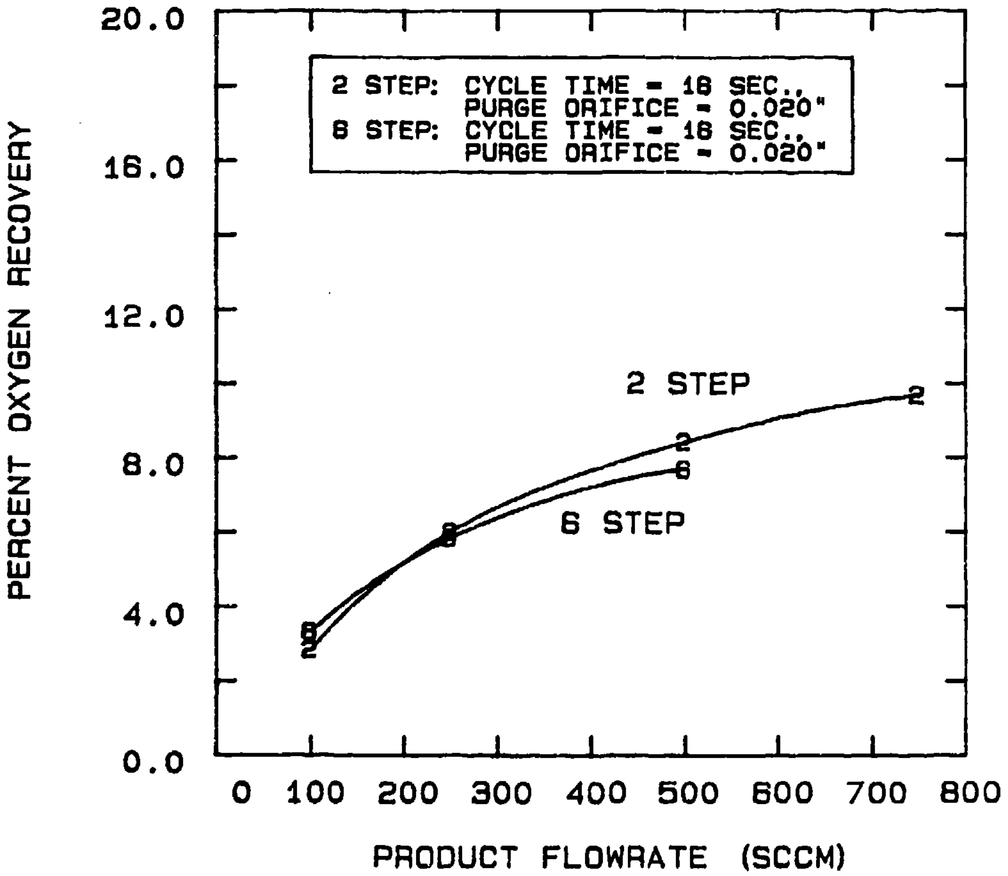

FIG 5-111. COMPARISON OF OXYGEN RECOVERY BETWEEN A 2 STEP AND 6 STEP SYSTEM OPERATING AT -40°C.

FIG 5-112. PREDICTION OF O2-N2 ADSORPTION ON MOLECULAR SIEVE 5A AT 24 C BASED ON THE DATA OF THIS WORK AND A STATISTICAL THERMODYNAMIC MODEL.

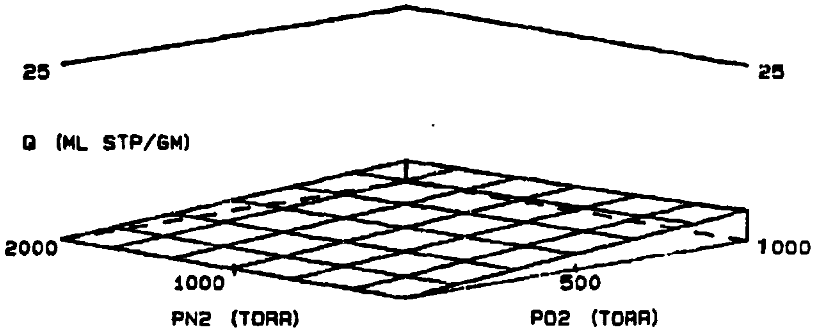

O2 COMPONENT LOADING

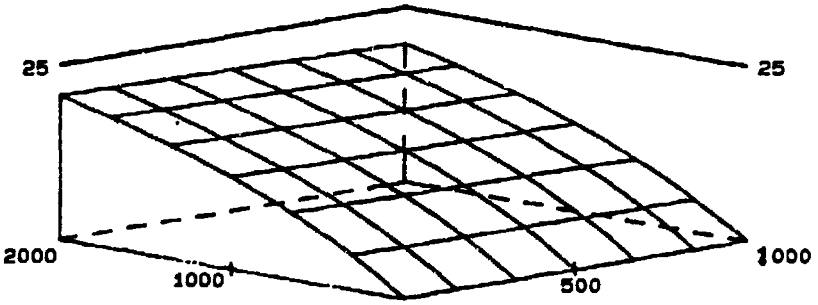

N2 COMPONENT LOADING

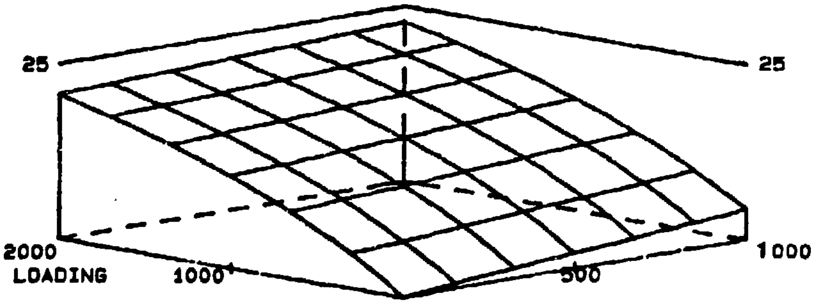

TOTAL LOADING

CHAPTER VI

CONCLUSIONS AND RECOMMENDATIONS

A. Conclusions

1. The pure component isotherms of nitrogen and oxygen on molecular sieve 5A were correlated by a statistical thermodynamic model.
2. The pure isotherm data of Union Carbide (69) were predicted with reasonable accuracy using a statistical thermodynamic model with parameters determined from the pure component isotherm data of this work.
3. The multicomponent isotherms for the nitrogen and oxygen on molecular sieve 5A were predicted at 24°C by a statistical thermodynamic model and the IAST theory using the pure component data of this model.
4. The surface of the molecular sieve 5A is energetically heterogeneous to the nitrogen molecule and homogeneous toward the oxygen molecule. This is evident by viewing the plot of Ha versus loading (See Figure 5-24).
5. The breakthrough data taken at 24 and -40°C shows that the length of the mass transfer front during adsorption ,i.e. nitrogen breakthrough experiments, remains nearly constant. On the contrary, the length of the mass transfer front during desorption,i.e. oxygen breakthrough, is much greater at -40°C.

A decrease in the rate of diffusion of the nitrogen molecules during desorption may account for the reduced performance of PSA systems at lower temperatures.

6. Optimum performance of a PSA system at -40°C requires lengthening of the cycle time. The optimum cycle times for the six step and two step system are nearly the same. Slightly higher oxygen product concentrations and oxygen recoveries were observed for six step system in comparison to the two step.
7. The separation factor for nitrogen-oxygen is constant above 1000 Torr and temperature dependent below 1000 Torr where it is inversely proportional to the temperature.
8. There is no improvement in the separation of argon at -40°C.
9. At 24°C the O2-N2-5A system may be considered ideal.

B. Recommendations

1. The nonideality of the binary mixture of nitrogen and oxygen at low temperature should be investigated to determine the nature of the interaction of these molecules. Possibly, an extension to existing models could be used to predict sorption at these lower temperatures.
2. The effect of the argon in the multicomponent mixture with nitrogen and oxygen should be investigated to ensure the validity of neglecting argon in the present analysis.
3. The PSA unit used in this study should be run at -40°C to determine if greater oxygen concentrations can be achieved by optimization of the purge flow through use of a automatic flow controller.
4. Additional experimentation and analysis of the breakthrough curves at -40°C should conducted to determine the underlying causes of the significantly longer nitrogen desorption.
5. Futher studies comparing the two step and the six step cycle should be undertaken.

APPENDIX

A NOMENCLATURE

B OPERATING PROCEDURE

C DATA AND CALCULATIONS

APPENDIX A

NOMENCLATURE

A = area

a = activity for an ideal gas (p/kT)

a_s = number of cavities with s sorbate molecules

B = effective molecular volume (cu. Angstroms)

c = sorbate concentration (molecules/cavity)

C = canonical ensemble partition function

D = zeolitic diffusivity (cm. sq./sec)

D_o = " " at zero concentration

D'_o = constant in units of (molecules)(cm.sq.)/(cavity)(sec)

D'_* = pre-exponential factor (molecules)(cm.sq.)/(cavity)(sec)

E = diffusional activation energy

G = Gibbs free energy

H = enthalpy

Ha = isosteric heat of adsorption

K = Henry's Law constant (c=Kp) (molecules/cavity/Torr)

Ko = pre-exponential factor giving temperature dependence of K (molecules/cavity) (dyne/cm.sq.)

k = Boltzmann's constant

m = maximum number of molecules per cavity (saturation limit) ($m \leq V/B$)

m_t = mass of sorbate adsorbed or desorbed during time, t

m = mass adsorbed or desorbed when time approaches infinity.

M = number of cavities

N = total number of sorbate molecules in the system

N = average number of molecules in the macroscopic system

n = number of molecules adsorbed by a crystal

P = total pressure

P_H = high pressure

P_L = low pressure

p = partial pressure

q(s) = site partition function

Q = subsystem of grand partition functions

qc = limiting isosteric heat of sorption at zero concentration

r = equivalent radius of a zeolite crystal

R = universal gas constant

r_i = position vector in the Sutherland potential

S = entropy

s = number of sorbate molecules occluded in a cavity

T = temperature, ^oK

t = dummmy variable

U = internal energy

U_s = potential energy for the subsystem

V_a = volume of the adsorbate

V_g = volume of the adsorbate in the gas phase

V = volume of the zeolite type A alpha cavity (776 cu. Angstroms)

$Z(s)$ = configuration integral for a system of s sorbate molecules in one molecular sieve 5A cavity

$Z(i,j)$ = configuration integral for a system of i molecules of species A and j molecules of species B within a molecular sieve 5A cavity

α = separation factor

ε = void fraction

θ = fractional coverage

$\lambda = \exp(\mu / kT)$

μ = chemical potential

σ, ξ = molecular constants in the potential energy function

τ = charge

ϕ = angle between the axis of the quadrupole and the line between the centers of the two molecules

ω = polarizability

Π = spreading pressure

Subscripts

A = component A

B = component B

i = number of molecules of species A

j = number of molecules of species B

APPENDIX B

OPERATING PROCEDURES

A. Brief Description of the Pure Component Apparatus Operating Procedure

(1) Regenerate the adsorbent by heating to a temperature of 350°C while applying a vacuum of < 1 Torr for twelve hours. Close valve (V4), set the temperature controller on the environmental test chamber (T) and allow the sample to stabilize at the desired experimental temperature (See Fig. 4-6).

(2) Open valve (V2) to permit the gaseous adsorbate (pure nitrogen or oxygen) to enter the previously evacuated charge chamber (C2).

(3) Close valve (V2) and annotate the temperature and initial pressure of the charge chamber (C2).

(4) Ensure the adsorbent temperature (T1) is stable at the desired temperature of the experiment.

(5) Inject a portion of the gaseous adsorbate from the charge chamber (C2) into the sample chamber (C1) by slightly opening valve (V3).

(6) Monitor the sample chamber (C1) pressure through use of the strip chart recorder (S) to determine when equilibrium has been reached. In this work equilibrium required a minimum of six to eight hours for each data point.

(7) Annotate the final pressure in the charge chamber (C2) and the equilibrium pressure in the sample chamber (C1).

(8) The above procedure is repeated until the equilibrium pressure within the sample chamber (C1) reaches the high limit of the

calibrated range of the pressure transducers.

B. Brief Description of the Multicomponent Apparatus Operating Procedure

(1) Follow step (1) through (6) as shown in the operating procedure for the pure component apparatus but use valve (V1) to draw vacuum on the sample chamber (C1) during the regeneration step (See Fig. 4-8). Air is permitted to enter the charge volume (C2).

(2) Monitor the pressure in the sample chamber (C1) to determine when equilibrium has been attained.

(3) Evacuate the MGA sampling volume (SV) by placing valve (V6) in the proper position.

(4) Evacuate the MGA sampling probe (PR) by proper positioning of valves (V5 and V6).

(5) Annotate the pressure in the sample chamber (C1) at equilibrium. Open valve (V1) momentarily to draw a small sample of gas from the sample chamber (C1) into the MGA sampling volume (SV).

(6) Annotate the pressure in the sample chamber (C1) immediately after the gas sample has been removed.

(7) Open valve (V5) to allow the gas sample to enter the gas sampling probe (PR) and the MGA for analysis.

(8) Evacuate the sampling volume (SV) and the MGA gas sampling probe (PR) by positioning valves (V5 and V6).

(9) Repeat the above procedure to obtain other data points.

C. Brief Description of the PSA Unit Operating Procedure

(1) Edit the data file XBASE.DAT to set the experimental configuration and the number of data channels.

(2) Install the proper purge orifice for the desired configuration.

(3) Set the inlet air regulator at 25 psia.

(4) Ensure all data channels give the proper outputs and the calibration factors for each channel are correct.

(5) Begin the experiment by running the main control program TT.FOR .

(6) Set the product flow rate.

(7) After a stable oxygen concentration is observed in the product flow depress the "line feed" key on the VT-54 terminal to begin the data collection process.

(8) The data is displayed to the screen of the VT-54 in engineering units and stored on a floppy diskette in A/D counts.

APPENDIX C

DATA AND CALCULATIONS

Table 17. Nitrogen-5A at 24°C (Run 1).

Pressure (Torr)	Quantity Adsorbed (ml STP/gm)
18	0.325
50	0.940
88	1.645
156	2.769
223	3.794
339	5.454
432	6.617
539	7.949
651	9.158
690	9.567
759	10.282
823	10.905
959	12.196
1143	13.266
1391	15.310
1577	16.731
1867	18.727
2198	21.237
2720	24.110
3067	25.863
3305	27.072
3439	28.041

Table 18. Nitrogen-5A at 24°C (Run 2)

Pressure (Torr)	Quantity Adsorbed (ml STP/gm)
143	2.742
274	4.724
415	6.606
563	8.382
750	10.316
1117	13.287
1355	15.502
1712	18.148
2120	20.779
2508	23.017
2901	25.039
3196	26.575
3382	27.541

Table 19. Nitrogen-5A at -40°C (Run 1)

Pressure (Torr)	Quantity Adsorbed (ml STP/gm)
18	4.651
100	14.812
395	30.593
703	38.982
929	43.107
1443	49.376
1970	54.838
2441	58.716
2829	61.189
3118	62.898
3320	64.144

Table 20. Nitrogen-5A at $-40^{o}C$ (Run 1 Desorption)

Pressure (Torr)	Quantity Adsorbed (ml STP/gm)
2389	58.409
1779	53.469
1376	49.241

Table 21. Nitrogen-5A at $-40^{o}C$ (Run 2)

Pressure (Torr)	Quantity Adsorbed (ml STP/gm)
175	19.402
553	34.532
1112	45.126
1676	52.256

Table 22. Nitrogen-5A at $-70^{o}C$ (Run 1)

Pressure (Torr)	Quantity Adsorbed (ml STP/gm)
38	20.927
174	40.319
454	56.236
931	67.720
1505	75.246
2032	80.253
2457	83.693
2808	85.847
3087	87.232
3299	88.081

Table 23. Nitrogen-5A at -70°C (Run 1 Desorption)

Pressure (Torr)	Quantity Adsorbed (ml STP/gm)
2400	83.123
1795	78.697
1412	74.574

Table 24. Nitrogen-5A at -70°C (Run 2)

Pressure (Torr)	Quantity Adsorbed (ml STP/gm)
36	20.783
172	40.084
444	55.645
895	66.879
1402	74.896
1934	80.104

Table 25. Oxygen-5A at 24°C (Run 1)

Pressure (Torr)	Quantity Adsorbed (ml STP/gm)
249	1.194
495	2.318
757	3.544
945	4.417
1520	6.545
2141	9.065
2544	10.736
3025	12.528
3320	13.560
3511	14.197
3620	14.561

Table 26. Oxygen-5A at 24°C (Run 2)

Pressure (Torr)	Quantity Adsorbed (ml STP/gm)
119	0.604
352	1.684
677	3.166
899	4.195
1350	5.760
1795	7.558
2105	8.769
2648	10.988
3074	12.492
3356	13.447
3532	14.054
3625	14.476

Table 27. Oxygen-5A at -40°C (Run 1)

Pressure (Torr)	Quantity Adsorbed (ml STP/gm)
183	4.228
307	6.799
488	10.282
720	14.657
905	17.863
1458	24.837
1929	30.717
2358	35.353
2689	38.660
2937	40.979
3124	42.560
3268	43.812

Table 28. Oxygen-5A at -40°C (Run 1 Desorption)

Pressure (Torr)	Quantity Adsorbed (ml STP/gm)
2581	37.932
1996	31.620
1546	26.480
1241	23.426

Table 29. Oxygen-5A at -70°C (Run 1)

Pressure (Torr)	Quantity Adsorbed (ml STP/gm)
176	10.826
342	19.252
532	27.040
682	32.742
833	38.275
1257	48.164
1639	56.334
2007	62.263
2301	66.689
2575	70.033
2782	72.437
3015	74.090
3165	75.512
3305	76.575

Table 30. Oxygen-5A at -70°C (Run 1 Desorption)

Pressure (Torr)	Quantity Adsorbed (ml STP/gm)
2813	72.341
2234	65.919
1836	60.002
1531	54.598
1298	49.760

Table 31. Oxygen-5A at -70°C (Run 2)

Pressure (Torr)	Quantity Adsorbed (ml STP/gm)
285	15.083
543	26.459
926	38.772
1314	48.513
1681	55.664
2032	61.240
2340	65.601
2648	68.700
2875	71.043
3077	72.724

Table 32. Isosteric heat of adsorption for oxygen

Quantity Adsorbed (ml STP/gm)	- Ha (cal/mol)
1.0	3371
2.5	3372
5.0	3378
7.5	3382
10.0	3387
12.5	3392
15.0	3398
20.0	3317
25.0	3352
30.0	3392
35.0	3438
40.0	3490
45.0	3551

Table 33. Isosteric heat of adsorption for nitrogen

Quantity Adsorbed (ml STP/gm)	- Ha (cal/mol)
1.0	7578
2.5	6871
5.0	6333
7.5	6016
10.0	5791
12.5	5615
15.0	5471
20.0	5244
25.0	5068
30.0	4927
35.0	4842
40.0	4764
45.0	4710
50.0	4683
55.0	4683
60.0	4715
65.0	4787

Table 34. Air-5A at 24°C (Run 1) (Total Loading)

Total Pressure (Torr)	Total Quantity Adsorbed (ml STP/gm)
169	2.356
372	4.727
585	7.072
882	9.713
1252	12.651
1836	16.860
2405	20.507
2803	22.745
3051	24.048

Table 35. Air-5A at 24°C (Run 1) (Nitrogen Loading)

Total Pressure (Torr)	Quantity Nitrogen Adsorbed (ml STP/gm)
169	2.024
372	4.068
585	6.092
882	8.373
1252	10.962
1836	14.581
2405	17.715
2803	19.679
3051	20.845

Table 36. Air-5A at 24°C (Run 1) (Oxygen Loading)

Total Pressure (Torr)	Quantity Oxygen Adsorbed (ml STP/gm)
169	0.319
372	0.633
585	0.938
882	1.283
1252	1.617
1836	2.185
2405	2.674
2803	2.935
3051	3.067

Table 37. Air-5A at 24°C (Run 1) (Argon Loading)

Total Pressure (Torr)	Quantity Argon Adsorbed (ml STP/gm)
169	0.014
372	0.026
585	0.042
882	0.057
1252	0.072
1836	0.094
2405	0.118
2803	0.131
3051	0.136

Table 38. Air-5A at -40°C (Run 1) (Total Loading)

Total Pressure (Torr)	Total Quantity Adsorbed (ml STP/gm)
168	10.325
280	15.960
444	22.664
666	29.558
1184	39.684
1670	46.584
2110	51.516
2457	54.410
2731	56.748
2968	58.392
3118	59.615

Table 39. Air-5A at -40°C (Run 1) (Nitrogen Loading)

Total Pressure (Torr)	Quantity Nitrogen Adsorbed (ml STP/gm)
168	8.629
280	13.351
444	18.985
666	24.838
1184	33.375
1670	39.189
2110	43.697
2457	46.078
2731	48.033
2968	49.462
3118	50.634

Table 40. Air-5A at -40°C (Run 1) (Oxygen Loading)

Total Pressure (Torr)	Quantity Oxygen Adsorbed (ml STP/gm)
168	1.626
280	2.501
444	3.526
666	4.522
1184	6.041
1670	7.080
2110	7.485
2457	7.968
2731	8.336
2968	8.538
3118	8.588

Table 41. Air-5A at -40°C (Run 1) (Argon Loading)

Total Pressure (Torr)	Quantity Argon Adsorbed (ml STP/gm)
168	0.069
280	0.107
444	0.153
666	0.197
1184	0.268
1670	0.316
2110	0.333
2457	0.363
2731	0.378
2968	0.391
3118	0.393

Table 42. Air-5A at -70°C (Run 1) (Total Loading)

Total Pressure (Torr)	Total Quantity Adsorbed (ml STP/gm)
168	24.632
290	35.617
427	44.188
634	53.462
1060	63.913
1536	71.236
1981	76.284
2400	79.439
2705	81.648
2943	83.142

Table 43. Air-5A at -70°C (Run 1) (Nitrogen Loading)

Total Pressure (Torr)	Quantity Nitrogen Adsorbed (ml STP/gm)
168	20.030
290	29.048
427	36.146
634	43.859
1060	52.596
1536	58.827
1981	63.152
2400	65.877
2705	67.803
2943	69.217

Table 44. Air-5A at -70 C°(Run 1) (Oxygen Loading)

Total Pressure (Torr)	Quantity Oxygen Adsorbed (ml STP/gm)
168	4.415
290	6.295
427	7.704
634	9.198
1060	10.837
1536	11.875
1981	12.568
2400	12.973
2705	13.243
2943	13.315

Table 45. Air-5A at -70°C (Run 1) (Argon Loading)

Total Pressure (Torr)	Quantity Argon Adsorbed (ml STP/gm)
168	0.192
290	0.275
427	0.338
634	0.405
1060	0.480
1536	0.533
1981	0.565
2400	0.590
2705	0.602
2943	0.611

Table 46. Air-5A at 24°C (Run 2) (Total Loading)

Total Pressure (Torr)	Total Quantity Adsorbed (ml STP/gm)
194	2.736
1169	11.691
1908	17.247
2467	20.497
2829	22.678

Table 47. Air-5A at 24°C (Run 2) (Nitrogen Loading)

Total Pressure (Torr)	Quantity Nitrogen Adsorbed (ml STP/gm)
194	2.351
1169	10.108
1908	14.917
2467	17.685
2829	19.598

Table 48. Air-5A at 24°C (Run 2) (Oxygen Loading)

Total Pressure (Torr)	Quantity Oxygen Adsorbed (ml STP/gm)
194	0.369
1169	1.516
1908	2.231
2467	2.695
2829	2.952

Table 49. Air-5A at 24°C (Run 2) (Argon Loading)

Total Pressure (Torr)	Quantity Argon Adsorbed (ml STP/gm)
194	0.016
1169	0.067
1908	0.099
2467	0.117
2829	0.128

Table 50. Air-5A at -40°C (Run 2) (Total Loading)

Total Pressure (Torr)	Total Quantity Adsorbed (ml STP/gm)
199	12.048
325	18.012
458	23.163
687	30.087
1200	40.048
1707	47.059
2151	51.723
2513	54.953
2808	57.098

Table 51. Air-5A at -40°C (Run 2) (Nitrogen Loading)

Total Pressure (Torr)	Quantity Nitrogen Adsorbed (ml STP/gm)
199	10.060
325	15.062
458	19.410
687	25.263
1200	33.695
1707	39.537
2151	43.485
2513	46.255
2808	48.283

Table 52. Air-5A at -40°C (Run 2) (Oxygen Loading)

Total Pressure (Torr)	Quantity Oxygen Adsorbed (ml STP/gm)
199	1.907
325	2.828
458	3.598
687	4.629
1200	6.084
1707	7.199
2151	7.882
2513	8.320
2808	8.433

Table 53. Air-5A at $-40^{o}C$ (Run 2) (Argon Loading)

Total Pressure (Torr)	Quantity Argon Adsorbed (ml STP/gm)
199	0.081
325	0.122
458	0.156
687	0.196
1200	0.269
1707	0.323
2151	0.356
2513	0.377
2808	0.382

Table 54. Air-5A at $-70^{o}C$ (Run 2) (Total Loading)

Total Pressure (Torr)	Total Quantity Adsorbed (ml STP/gm)
171	25.049
289	35.728
443	45.251
688	55.163
1122	65.464
1608	72.520
2053	76.911
2431	80.141
2731	82.298

Table 55. Air-5A at -70°C (Run 2) (Nitrogen Loading)

Total Pressure (Torr)	Quantity Nitrogen Adsorbed (ml STP/gm)
171	20.363
289	29.131
443	37.020
688	45.240
1122	53.892
1608	59.895
2053	63.736
2431	66.398
2731	68.394

Table 56. Air-5A at -70°C (Run 2) (Oxygen Loading)

Total Pressure (Torr)	Quantity Oxygen Adsorbed (ml STP/gm)
171	4.491
289	6.321
443	7.885
688	9.503
1122	11.079
1608	12.082
2053	12.609
2431	13.148
2731	13.303

Table 57. Air-5A at -70°C (Run 2) (Argon Loading)

Total Pressure (Torr)	Quantity Argon Adsorbed (ml STP/gm)
171	0.195
289	0.276
443	0.346
688	0.420
1122	0.494
1608	0.542
2053	0.566
2431	0.594
2731	0.601

```
************************************************************************
VOLUME.RES
G.W.MILLER
USAF SCHOOL OF AEROSPACE MEDICINE
CREW TECHNOLOGY DIVISION
BROOKS AFB,TEXAS


DETERMINATION OF SAMPLE TRUE VOLUME AND
TRUE DENSITY BY HELIUM DISPLACEMENT

SAMPLE: UNION CARBIDE MOLECULAR SIEVE 5A (20X40 MESH) AT 297.15K


NUMBER OF DATA POINTS: 20
SAMPLE WEIGHT (GM)= 32.8
VOLUME OF SAMPLE CHAMBER (ML)=170.0
VOLUME OF THE CHARGE CHAMBER (ML)=158.6


POINT NO:  1
INITIAL PRESSURE (TORR)= 1500.
FINAL PRESSURE (TORR)=  750.
MOLES ADDED (GM MOL*10**3)= 12.838
CALCULATED TOTAL VOLUME (ML)= 317.20
CALCULATED SAMPLE CHAMBER VOLUME (ML)= 158.60
CALCULATED SAMPLE VOLUME (ML)=  11.40


POINT NO:  2
INITIAL PRESSURE (TORR)= 2000.
FINAL PRESSURE (TORR)= 1008.
MOLES ADDED (GM MOL*10**3)= 17.117
CALCULATED TOTAL VOLUME (ML)= 314.68
CALCULATED SAMPLE CHAMBER VOLUME (ML)= 156.08
CALCULATED SAMPLE VOLUME (ML)=  13.92


POINT NO:  3
INITIAL PRESSURE (TORR)= 2500.
FINAL PRESSURE (TORR)= 1246.
MOLES ADDED (GM MOL*10**3)= 21.396
CALCULATED TOTAL VOLUME (ML)= 318.22
CALCULATED SAMPLE CHAMBER VOLUME (ML)= 159.62
CALCULATED SAMPLE VOLUME (ML)=  10.38


POINT NO:  4
```

```
INITIAL PRESSURE (TORR)= 3000.
FINAL PRESSURE (TORR)= 1495.
MOLES ADDED (GM MOL*10**3)= 25.676
CALCULATED TOTAL VOLUME (ML)= 318.26
CALCULATED SAMPLE CHAMBER VOLUME (ML)= 159.66
CALCULATED SAMPLE VOLUME (ML)=  10.34


POINT NO:  5
INITIAL PRESSURE (TORR)= 3500.
FINAL PRESSURE (TORR)= 1743.
MOLES ADDED (GM MOL*10**3)= 29.955
CALCULATED TOTAL VOLUME (ML)= 318.47
CALCULATED SAMPLE CHAMBER VOLUME (ML)= 159.87
CALCULATED SAMPLE VOLUME (ML)=  10.13


POINT NO:  6
INITIAL PRESSURE (TORR)= 1500.
FINAL PRESSURE (TORR)=  750.
MOLES ADDED (GM MOL*10**3)= 12.838
CALCULATED TOTAL VOLUME (ML)= 317.20
CALCULATED SAMPLE CHAMBER VOLUME (ML)= 158.60
CALCULATED SAMPLE VOLUME (ML)=  11.40


POINT NO:  7
INITIAL PRESSURE (TORR)= 2000.
FINAL PRESSURE (TORR)=  998.
MOLES ADDED (GM MOL*10**3)= 17.117
CALCULATED TOTAL VOLUME (ML)= 317.84
CALCULATED SAMPLE CHAMBER VOLUME (ML)= 159.24
CALCULATED SAMPLE VOLUME (ML)=  10.76


POINT NO:  8
INITIAL PRESSURE (TORR)= 2500.
FINAL PRESSURE (TORR)= 1241.
MOLES ADDED (GM MOL*10**3)= 21.396
CALCULATED TOTAL VOLUME (ML)= 319.50
CALCULATED SAMPLE CHAMBER VOLUME (ML)= 160.90
CALCULATED SAMPLE VOLUME (ML)=   9.10


POINT NO:  9
INITIAL PRESSURE (TORR)= 3000.
FINAL PRESSURE (TORR)= 1495.
MOLES ADDED (GM MOL*10**3)= 25.676
CALCULATED TOTAL VOLUME (ML)= 318.26
```

```
CALCULATED SAMPLE CHAMBER VOLUME (ML)= 159.66
CALCULATED SAMPLE VOLUME (ML)=  10.34


POINT NO: 10
INITIAL PRESSURE (TORR)= 3500.
FINAL PRESSURE (TORR)= 1748.
MOLES ADDED (GM MOL*10**3)= 29.955
CALCULATED TOTAL VOLUME (ML)= 317.56
CALCULATED SAMPLE CHAMBER VOLUME (ML)= 158.96
CALCULATED SAMPLE VOLUME (ML)=  11.04


POINT NO: 11
INITIAL PRESSURE (TORR)= 1500.
FINAL PRESSURE (TORR)=  750.
MOLES ADDED (GM MOL*10**3)= 12.838
CALCULATED TOTAL VOLUME (ML)= 317.20
CALCULATED SAMPLE CHAMBER VOLUME (ML)= 158.60
CALCULATED SAMPLE VOLUME (ML)=  11.40


POINT NO: 12
INITIAL PRESSURE (TORR)= 2000.
FINAL PRESSURE (TORR)=  998.
MOLES ADDED (GM MOL*10**3)= 17.117
CALCULATED TOTAL VOLUME (ML)= 317.84
CALCULATED SAMPLE CHAMBER VOLUME (ML)= 159.24
CALCULATED SAMPLE VOLUME (ML)=  10.76


POINT NO: 13
INITIAL PRESSURE (TORR)= 2500.
FINAL PRESSURE (TORR)= 1246.
MOLES ADDED (GM MOL*10**3)= 21.396
CALCULATED TOTAL VOLUME (ML)= 318.22
CALCULATED SAMPLE CHAMBER VOLUME (ML)= 159.62
CALCULATED SAMPLE VOLUME (ML)=  10.38


POINT NO: 14
INITIAL PRESSURE (TORR)= 3000.
FINAL PRESSURE (TORR)= 1499.
MOLES ADDED (GM MOL*10**3)= 25.676
CALCULATED TOTAL VOLUME (ML)= 317.41
CALCULATED SAMPLE CHAMBER VOLUME (ML)= 158.81
CALCULATED SAMPLE VOLUME (ML)=  11.19
```

```
POINT NO: 15
INITIAL PRESSURE (TORR)= 3500.
FINAL PRESSURE (TORR)= 1748.
MOLES ADDED (GM MOL*10**3)= 29.955
CALCULATED TOTAL VOLUME (ML)= 317.56
CALCULATED SAMPLE CHAMBER VOLUME (ML)= 158.96
CALCULATED SAMPLE VOLUME (ML)=  11.04

POINT NO: 16
INITIAL PRESSURE (TORR)= 1500.
FINAL PRESSURE (TORR)=  752.
MOLES ADDED (GM MOL*10**3)= 12.838
CALCULATED TOTAL VOLUME (ML)= 316.36
CALCULATED SAMPLE CHAMBER VOLUME (ML)= 157.76
CALCULATED SAMPLE VOLUME (ML)=  12.24

POINT NO: 17
INITIAL PRESSURE (TORR)= 2000.
FINAL PRESSURE (TORR)= 1003.
MOLES ADDED (GM MOL*10**3)= 17.117
CALCULATED TOTAL VOLUME (ML)= 316.25
CALCULATED SAMPLE CHAMBER VOLUME (ML)= 157.65
CALCULATED SAMPLE VOLUME (ML)=  12.35

POINT NO: 18
INITIAL PRESSURE (TORR)= 2500.
FINAL PRESSURE (TORR)= 1246.
MOLES ADDED (GM MOL*10**3)= 21.396
CALCULATED TOTAL VOLUME (ML)= 318.22
CALCULATED SAMPLE CHAMBER VOLUME (ML)= 159.62
CALCULATED SAMPLE VOLUME (ML)=  10.38

POINT NO: 19
INITIAL PRESSURE (TORR)= 3000.
FINAL PRESSURE (TORR)= 1500.
MOLES ADDED (GM MOL*10**3)= 25.676
CALCULATED TOTAL VOLUME (ML)= 317.20
CALCULATED SAMPLE CHAMBER VOLUME (ML)= 158.60
CALCULATED SAMPLE VOLUME (ML)=  11.40

POINT NO: 20
INITIAL PRESSURE (TORR)= 3500.
FINAL PRESSURE (TORR)= 1748.
MOLES ADDED (GM MOL*10**3)= 29.955
```

```
CALCULATED TOTAL VOLUME (ML)= 317.56
CALCULATED SAMPLE CHAMBER VOLUME (ML)= 158.96
CALCULATED SAMPLE VOLUME (ML)=  11.04




MEAN SAMPLE VOLUME (ML)=  11.05
STANDARD DEVIATION (ML)= 1.0004
SAMPLE VOLUME WITH 95% CONFIDENCE INTERVAL (ML)= 11.05 PLUS OR MINUS 0.47
SAMPLE DENSITY (GM/ML)=   2.97
```

```
*************************************************************************
C   N2241.FOR
C   EQUILIBRIUM ADSORPTION PROGRAM
C   GEORGE MILLER
C   23 JULY 83
    DIMENSION PCHAR1(100),TCHARC(100),TSAMPC(100),PFINAL(100)
    DIMENSION XMOLTO(100),XMOLIN(100),XMOLGA(100),XMOLAD(100)
    DIMENSION VSTP(100),VOLWT(100),PCHAR2(100),Z1(100)
    DIMENSION Z2(100),Z3(100)
    OPEN(UNIT=1,NAME='N2241.GPH',TYPE='NEW',DISPOSE='SAVE')
    OPEN(UNIT=7,NAME='N2241.RES',TYPE='NEW',DISPOSE='SAVE')
C   PCHAR1=INITIAL CHARGE CHAMBER PRESSURE (TORR)
C   PCHAR2=FINAL CHARGE CHAMBER PRESSURE (TORR)
C   Z1=INITIAL CHARGE CHAMBER PRESSURE Z FACTOR
C   Z2=FINAL CHARGE CHAMBER PRESSURE Z FACTOR
C   Z3=EQUILIBRIUM Z FACTOR
C   TCHARC=TEMP IN THE CHARGE CHAMBER (DEG C)
C   TSAMPC=TEMP IN THE SAMPLE CHAMBER (DEG C)
C   PFINAL=FINAL PRESSURE IN THE SAMPLE CHAMBER (TORR)
C   XMOLTO=TOTAL MOLES ADDED (GM MOL)
C   XMOLIN=MOLES ADDED (GM MOL)
C   XMOLGA=MOLES IN GAS PHASE (GM MOL)
C   XMOLAD=MOLES ADSORBED (GM MOL)
C   VSTP=VOLUME ADSORBED (ML STP)
C   VOLWT=VOLUME ADSORBED(ML STP)/WEIGHT OF SAMPLE (GM)
C   SAMWT=SAMPLE WEIGHT (GM)
C   VCHARC=VOLUME OF THE CHARGE CHAMBER (ML)
C   VSAMPC=VOLUME OF THE SAMPLE CHAMBER (ML)
C   VSAMPL=VOLUME OF SAMPLE (ML)
C   VSAMPT=TRUE DEAD VOLUME IN SAMPLE CHAMBER (ML)
    NDATA=22
    SAMWT=32.8
    R=82.057
    VCHARC=158.6
    VSAMPC=170.0
```

```
      VSAMPL=11.05
      VSAMPT=VSAMPC-VSAMPL
C
C         INPUT:EXPERIMENT NO.1
C
      PCHAR1(1)=759.
      PCHAR1(2)=691.
      PCHAR1(3)=554.
      PCHAR1(4)=760.
      PCHAR1(5)=499.
      PCHAR1(6)=759.
      PCHAR1(7)=855.
      PCHAR1(8)=900.
      PCHAR1(9)=1000.
      PCHAR1(10)=827.4
      PCHAR1(11)=1298.
      PCHAR1(12)=1292.7
      PCHAR1(13)=1546.3
      PCHAR1(14)=1551.4
      PCHAR1(15)=2063.4
      PCHAR1(16)=2322.
      PCHAR1(17)=2580.6
      PCHAR1(18)=3097.7
      PCHAR1(19)=3873.4
      PCHAR1(20)=3847.6
      PCHAR1(21)=3878.6
      PCHAR1(22)=3873.4

C
      PCHAR2(1)=686.
      PCHAR2(2)=553.
      PCHAR2(3)=395.
      PCHAR2(4)=499.
      PCHAR2(5)=256.
      PCHAR2(6)=357.
      PCHAR2(7)=562.
      PCHAR2(8)=564.
      PCHAR2(9)=680.
      PCHAR2(10)=718.8
      PCHAR2(11)=1106.7
      PCHAR2(12)=1122.2
      PCHAR2(13)=1189.4
      PCHAR2(14)=1184.3
      PCHAR2(15)=1463.5
      PCHAR2(16)=1892.8
      PCHAR2(17)=1949.6
      PCHAR2(18)=2337.5
      PCHAR2(19)=2859.8
      PCHAR2(20)=3201.1
```

```
      PCHAR2(21)=3433.9
      PCHAR2(22)=3573.5
C
      PFINAL(1)=17.5
      PFINAL(2)=50.
      PFINAL(3)=88.
      PFINAL(4)=156.
      PFINAL(5)=223.
      PFINAL(6)=339.
      PFINAL(7)=432.
      PFINAL(8)=539.
      PFINAL(9)=651.
      PFINAL(10)=690.
      PFINAL(11)=759.
      PFINAL(12)=823.
      PFINAL(13)=959.
      PFINAL(14)=1142.9
      PFINAL(15)=1391.1
      PFINAL(16)=1577.3
      PFINAL(17)=1866.9
      PFINAL(18)=2197.9
      PFINAL(19)=2720.2
      PFINAL(20)=3066.7
      PFINAL(21)=3304.6
      PFINAL(22)=3439.
C
      TCHARC(1)=24.
      TCHARC(2)=25.
      TCHARC(3)=25.
      TCHARC(4)=25.
      TCHARC(5)=25.
      TCHARC(6)=25.
      TCHARC(7)=25.
      TCHARC(8)=25.
      TCHARC(9)=25.
      TCHARC(10)=23.
      TCHARC(11)=24.
      TCHARC(12)=24.
      TCHARC(13)=24.
      TCHARC(14)=24.
      TCHARC(15)=25.
      TCHARC(16)=24.
      TCHARC(17)=24.
      TCHARC(18)=24.
      TCHARC(19)=24.
      TCHARC(20)=24.
      TCHARC(21)=24.
      TCHARC(22)=24.
C
```

```
      TSAMPC(1)=25.
      TSAMPC(2)=25.
      TSAMPC(3)=25.
      TSAMPC(4)=25.
      TSAMPC(5)=25.
      TSAMPC(6)=24.
      TSAMPC(7)=24.
      TSAMPC(8)=24.
      TSAMPC(9)=24.
      TSAMPC(10)=24.
      TSAMPC(11)=24.
      TSAMPC(12)=24.
      TSAMPC(13)=24.
      TSAMPC(14)=24.
      TSAMPC(15)=24.
      TSAMPC(16)=24.
      TSAMPC(17)=24.
      TSAMPC(18)=24.
      TSAMPC(19)=24.
      TSAMPC(20)=24.
      TSAMPC(21)=24.
      TSAMPC(22)=24.
C
      DO100 J=1,NDATA
      TCHARC(J)=TCHARC(J)+273.15
      TSAMPC(J)=TSAMPC(J)+273.15
  100 CONTINUE
      TOTAL=0.
      DO101 J=1,NDATA
      Z1(J)=(-2.565068585E-07*PCHAR1(J))+ 1.00000
      XMOL1=((PCHAR1(J)/760.)*VCHARC)/(R*TCHARC(J)*Z1(J))
      Z2(J)=(-2.565068585E-07*PCHAR2(J))+ 1.00000
      XMOL2=((PCHAR2(J)/760.)*VCHARC)/(R*TCHARC(J)*Z2(J))
      XMOLIN(J)=XMOL1-XMOL2
      XMOLTO(J)=TOTAL+XMOLIN(J)
      TOTAL=XMOLTO(J)
      Z3(J)=(-2.565068585E-07*PFINAL(J))+ 1.00000
      XMOLGA(J)=((PFINAL(J)/760.)*VSAMPT)/(R*TSAMPC(J)*Z3(J))
      XMOLAD(J)=XMOLTO(J)-XMOLGA(J)
      VSTP(J)=XMOLAD(J)*R*273.15
      VOLWT(J)=VSTP(J)/SAMWT
  101 CONTINUE
      DO103 J=1,NDATA
      XMOLIN(J)=XMOLIN(J)*1000.
      XMOLTO(J)=XMOLTO(J)*1000.
      XMOLGA(J)=XMOLGA(J)*1000.
      XMOLAD(J)=XMOLAD(J)*1000.
  103 CONTINUE
      WRITE(7,15)
```

```
15  FORMAT(///,1X,'G.W.MILLER')
    WRITE(7,18)
18  FORMAT(1X,'USAF SCHOOL OF AEROSPACE MEDICINE')
    WRITE(7,19)
19  FORMAT(1X,'CREW TECHNOLOGY DIVISION')
    WRITE(7,20)
20  FORMAT(1X,'BROOKS AFB,TEXAS')
    WRITE(7,16)
16  FORMAT(//,1X,'ADSORPTION ISOTHERM EXPERIMENT NO.1')
    WRITE(7,1)
1   FORMAT(1X,'NITROGEN ON UNION CARBIDE MOLECULAR SIEVE 5A (20X40
     1MESH) AT 24 DEG C')
    WRITE(7,2)NDATA
2   FORMAT(//,1X,'NUMBER OF DATA POINTS=',I3)
    WRITE(7,3) SAMWT
3   FORMAT(1X,'SAMPLE WEIGHT (GM)=',F6.1)
    WRITE(7,4) VCHARC
4   FORMAT(1X,'VOLUME OF CHARGE CHAMBER (ML)=',F6.1)
    WRITE(7,5) VSAMPC
5   FORMAT(1X,'VOLUME OF SAMPLE CHAMBER W/O ZEOLITE (ML)=',F6.1)
    WRITE(7,6) VSAMPL
6   FORMAT(1X,'TRUE VOLUME OF SAMPLE (ML)=',F6.2)
    WRITE(7,7) VSAMPT
7   FORMAT(1X,'TRUE DEAD VOLUME OF SAMPLE CHAMBER (ML)=',F6.1)
    DO105 J=1,NDATA
    WRITE(7,8)J
8   FORMAT(//,1X,'POINT NO:',I3)
    WRITE(7,500) PCHAR1(J),XMOLIN(J)
500 FORMAT(1X,'INITIAL CHARGE PRES (TORR)=',F7.1,4X,'MOLES ADDED (G
     1M MOL*10**3)=',F9.4)
    WRITE(7,501) PCHAR2(J),XMOLTO(J)
501 FORMAT(1X,'FINAL CHARGE PRES (TORR)=',F7.1,6X,'TOTAL MOLES (GM
     1 MOL*10**3)=',F9.4)
    WRITE(7,502) TCHARC(J),XMOLGA(J)
502 FORMAT(1X,'CHARGE CHAMBER TEMP(K)=',F7.2,8X,'MOLES IN GAS PHASE
     1(GM MOL*10**3)=',F9.4)
    WRITE(7,11) PFINAL(J),XMOLAD(J)
11  FORMAT(1X,'EQUILIBRIUM PRES (TORR)=',F7.1,7X,'MOLES ADSORBED (G
     1M MOL*10**3)=',F9.4)
    WRITE(7,12) TSAMPC(J),VSTP(J)
12  FORMAT(1X,'SAMPLE CHAMBER TEMP(K)=',F7.2,8X,'VOLUME ADSORBED (M
     1L) S.T.P.=',F9.4)
    WRITE(7,13) Z1(J),Z3(J)
13  FORMAT(1X,'INITIAL CHARGE PRES Z=',F8.5,8X,'EQUILIBRIUM PRES Z=
     1',F8.5)
    WRITE(7,600) Z2(J),VOLWT(J)
600 FORMAT(1X,'FINAL CHARGE PRES Z=',F8.5,10X,'(ML)S.T.P./GM OF ZEO
     1LITE=',F8.3)
105 CONTINUE
```

```
      DO666 J=1,NDATA
      WRITE(1,667) PFINAL(J),VOLWT(J)
  667 FORMAT(F7.0,3X,F8.3)
  666 CONTINUE
      STOP
      END
```

```
***********************************************************************
N2241.RES
G.W.MILLER
USAF SCHOOL OF AEROSPACE MEDICINE
CREW TECHNOLOGY DIVISION
BROOKS AFB,TEXAS

ADSORPTION ISOTHERM EXPERIMENT NO.1
NITROGEN ON UNION CARBIDE MOLECULAR SIEVE 5A (20X40 MESH) AT 24 DEG C
NUMBER OF DATA POINTS= 22
SAMPLE WEIGHT (GM)=  32.8
VOLUME OF CHARGE CHAMBER (ML)= 158.6
VOLUME OF SAMPLE CHAMBER W/O ZEOLITE (ML)= 170.0
TRUE VOLUME OF SAMPLE (ML)= 11.05
TRUE DEAD VOLUME OF SAMPLE CHAMBER (ML)= 158.9

POINT NO:  1
INITIAL CHARGE PRES (TORR)= 759   MOLES ADDED (GM MOL*10**3)=0.6250
FINAL CHARGE PRES (TORR)= 686.0   TOTAL MOLES (GM MOL*10**3)=0.6250
CHARGE CHAMBER TEMP(K)= 297.15    MOLES IN GAS PHASE(GM MOL*10**3)=0.1496
EQUILIBRIUM PRES (TORR)= 17.5     MOLES ADSORBED (GM MOL*10**3)=0.4754
SAMPLE CHAMBER TEMP(K)= 298.15    VOLUME ADSORBED (ML) S.T.P.=10.6556
INITIAL CHARGE PRES Z= 0.99981    EQUILIBRIUM PRES Z= 1.00000
FINAL CHARGE PRES Z= 0.99982      (ML)S.T.P./GM OF ZEOLITE=0.325

POINT NO:  2
INITIAL CHARGE PRES (TORR)= 691   MOLES ADDED (GM MOL*10**3)=1.1775
FINAL CHARGE PRES (TORR)= 553.0   TOTAL MOLES (GM  MOL*10**3)=1.8025
CHARGE CHAMBER TEMP (K)= 298.15   MOLES IN GAS PHASE(GM MOL*10**3)=0.4274
EQUILIBRIUM PRES (TORR)= 50.0     MOLES ADSORBED (GM MOL*10**3)=1.3751
SAMPLE CHAMBER TEMP (K)= 298.15   VOLUME ADSORBED (ML) S.T.P.=30.8203
INITIAL CHARGE PRES Z= 0.99982    EQUILIBRIUM PRES Z=0.99999
FINAL CHARGE PRES Z= 0.99986      (ML)S.T.P./GM OF ZEOLITE=0.940

POINT NO:  3
INITIAL CHARGE PRES (TORR)= 554   MOLES ADDED(GM MOL*10**3)=1.3566
FINAL CHARGE PRES (TORR)= 395.0   TOTAL MOLES(GM MOL*10**3)=3.1591
CHARGE CHAMBER TEMP (K)= 298.15   MOLES IN GAS PHASE(GM MOL*10**3)=0.7523
EQUILIBRIUM PRES (TORR)= 88.0     MOLES ADSORBED(GM MOL*10**3)=2.4068
SAMPLE CHAMBER TEMP (K)= 298.15   VOLUME ADSORBED(ML)S.T.P.=53.9449
INITIAL CHARGE PRES Z= 0.99986    EQUILIBRIUM PRES Z=0.99998
```

```
FINAL CHARGE PRES Z= 0.99990       (ML)S.T.P./GM OF ZEOLITE=1.645

POINT NO:  4
INITIAL CHARGE PRES (TORR)= 760   MOLES ADDED(GM MOL*10**3)=2.2270
FINAL CHARGE PRES (TORR)= 499.0   TOTAL MOLES (GM MOL*10**3)=5.3861
CHARGE CHAMBER TEMP (K)= 298.15   MOLES IN GAS PHASE(GM MOL*10**3)=1.3336
EQUILIBRIUM PRES (TORR)=156.0     MOLES ADSORBED(GM MOL*10**3)=4.0524
SAMPLE CHAMBER TEMP (K)= 298.15   VOLUME ADSORBED(ML)S.T.P.=90.8304
INITIAL CHARGE PRES Z= 0.99981    EQUILIBRIUM PRES Z=0.99996
FINAL CHARGE PRES Z= 0.99987      (ML)S.T.P./GM OF ZEOLITE=2.769

POINT NO:  5
INITIAL CHARGE PRES (TORR)= 499   MOLES ADDED(GM MOL*10**3)=2.0731
FINAL CHARGE PRES (TORR)= 256.0   TOTAL MOLES (GM MOL*10**3)=7.4592
CHARGE CHAMBER TEMP (K)= 298.15   MOLES IN GAS PHASE(GM MOL*10**3)=1.9065
EQUILIBRIUM PRES (TORR)= 223.0    MOLES ADSORBED(GM MOL*10**3)=5.5528
SAMPLE CHAMBER TEMP (K)= 298.15   VOLUME ADSORBED(ML)S.T.P.=124.4586
INITIAL CHARGE PRES Z= 0.99987    EQUILIBRIUM PRES Z=0.99994
FINAL CHARGE PRES Z= 0.99993      (ML)S.T.P./GM OF ZEOLITE=3.794

POINT NO:  6
INITIAL CHARGE PRES (TORR)= 759   MOLES ADDED(GM MOL*10**3)=3.4300
FINAL CHARGE PRES (TORR)= 357.0   TOTAL MOLES(GM MOL*10**3)=10.8892
CHARGE CHAMBER TEMP (K)= 298.15   MOLES IN GAS PHASE(GM MOL*10**3)=2.9080
EQUILIBRIUM PRES (TORR)= 339.0    MOLES ADSORBED (GM MOL*10**3)=7.9812
SAMPLE CHAMBER TEMP (K)= 297.15   VOLUME ADSORBED (ML) S.T.P.=178.8891
INITIAL CHARGE PRES Z= 0.99981    EQUILIBRIUM PRES Z=0.99991
FINAL CHARGE PRES Z= 0.99991      (ML)S.T.P./GM OF ZEOLITE=5.454

POINT NO:  7
INITIAL CHARGE PRES (TORR)= 855   MOLES ADDED(GM MOL*10**3)=2.5001
FINAL CHARGE PRES (TORR)= 562.0   TOTAL MOLES (GM MOL*10**3)=13.3893
CHARGE CHAMBER TEMP (K)= 298.15   MOLES IN GAS PHASE(GM MOL*10**3)=3.7058
EQUILIBRIUM PRES (TORR)= 432.0    MOLES ADSORBED(GM MOL*10**3)=9.6835
SAMPLE CHAMBER TEMP (K)= 297.15   VOLUME ADSORBED(ML)S.T.P.=217.0439
INITIAL CHARGE PRES Z= 0.99978    EQUILIBRIUM PRES Z=0.99989
FINAL CHARGE PRES Z= 0.99986      (ML)S.T.P./GM OF ZEOLITE=6.617

POINT NO:  8
INITIAL CHARGE PRES (TORR)= 900   MOLES ADDED (GM MOL*10**3)=   2.8671
FINAL CHARGE PRES (TORR)= 564.0   TOTAL MOLES (GM  MOL*10**3)=  16.2564
CHARGE CHAMBER TEMP(K)= 298.15    MOLES IN GAS PHASE(GM MOL*10**3)=4.6239
EQUILIBRIUM PRES (TORR)= 539.0    MOLES ADSORBED (GM MOL*10**3)=  11.6325
SAMPLE CHAMBER TEMP(K)= 297.15    VOLUME ADSORBED (ML) S.T.P.= 260.7303
INITIAL CHARGE PRES Z= 0.99977    EQUILIBRIUM PRES Z= 0.99986
FINAL CHARGE PRES Z= 0.99986      (ML)S.T.P./GM OF ZEOLITE=   7.949

POINT NO:  9
INITIAL CHARGE PRES(TORR)= 1000   MOLES ADDED (GM MOL*10**3)=   2.7307
```

```
FINAL CHARGE PRES (TORR)= 680.0  TOTAL MOLES (GM  MOL*10**3)=  18.9871
CHARGE CHAMBER TEMP(K)= 298.15   MOLES IN GAS PHASE(GM MOL*10**3)=5.5848
EQUILIBRIUM PRES (TORR)= 651.0   MOLES ADSORBED (GM MOL*10**3)=  13.4023
SAMPLE CHAMBER TEMP(K)= 297.15   VOLUME ADSORBED (ML) S.T.P.= 300.3973
INITIAL CHARGE PRES Z= 0.99974   EQUILIBRIUM PRES Z= 0.99983
FINAL CHARGE PRES Z= 0.99983     (ML)S.T.P./GM OF ZEOLITE=   9.158

POINT NO: 10
INITIAL CHARGE PRES (TORR)= 827  MOLES ADDED (GM MOL*10**3)=   0.9330
FINAL CHARGE PRES (TORR)= 718.8  TOTAL MOLES (GM  MOL*10**3)=  19.9201
CHARGE CHAMBER TEMP(K)= 296.15   MOLES IN GAS PHASE(GM MOL*10**3)=5.9195
EQUILIBRIUM PRES (TORR)= 690.0   MOLES ADSORBED (GM MOL*10**3)=  14.0006
SAMPLE CHAMBER TEMP(K)= 297.15   VOLUME ADSORBED (ML) S.T.P.= 313.8082
INITIAL CHARGE PRES Z= 0.99979   EQUILIBRIUM PRES Z= 0.99982
FINAL CHARGE PRES Z= 0.99982     (ML)S.T.P./GM OF ZEOLITE=   9.567

POINT NO: 11
INITIAL CHARGE PRES(TORR)= 1298  MOLES ADDED (GM MOL*10**3)=   1.6383
FINAL CHARGE PRES(TORR)= 1106.7  TOTAL MOLES (GM  MOL*10**3)=  21.5583
CHARGE CHAMBER TEMP(K)= 297.15   MOLES IN GAS PHASE(GM MOL*10**3)=6.5115
EQUILIBRIUM PRES (TORR)= 759.0   MOLES ADSORBED (GM MOL*10**3)=  15.0468
SAMPLE CHAMBER TEMP(K)= 297.15   VOLUME ADSORBED (ML) S.T.P.= 337.2574
INITIAL CHARGE PRES Z= 0.99967   EQUILIBRIUM PRES Z= 0.99981
FINAL CHARGE PRES Z= 0.99972     (ML)S.T.P./GM OF ZEOLITE=  10.282

POINT NO: 12
INITIAL CHARGE PRES(TORR)= 1292  MOLES ADDED (GM MOL*10**3)=   1.4601
FINAL CHARGE PRES (TORR)= 1122.2 TOTAL MOLES (GM  MOL*10**3)=  23.0185
CHARGE CHAMBER TEMP(K)= 297.15   MOLES IN GAS PHASE(GM MOL*10**3)=7.0607
EQUILIBRIUM PRES (TORR)=  823.0  MOLES ADSORBED (GM MOL*10**3)=  15.9578
SAMPLE CHAMBER TEMP(K)= 297.15   VOLUME ADSORBED (ML) S.T.P.= 357.6755
INITIAL CHARGE PRES Z= 0.99967   EQUILIBRIUM PRES Z= 0.99979
FINAL CHARGE PRES Z= 0.99971     (ML)S.T.P./GM OF ZEOLITE=  10.905

POINT NO: 13
INITIAL CHARGE PRES(TORR)= 1546  MOLES ADDED (GM MOL*10**3)=   3.0567
FINAL CHARGE PRES (TORR)= 1189.4 TOTAL MOLES (GM  MOL*10**3)=  26.0751
CHARGE CHAMBER TEMP(K)= 297.15   MOLES IN GAS PHASE(GM MOL*10**3)=8.2277
EQUILIBRIUM PRES (TORR)= 959.0   MOLES ADSORBED (GM MOL*10**3)=  17.8474
SAMPLE CHAMBER TEMP(K)= 297.15   VOLUME ADSORBED (ML) S.T.P.= 400.0292
INITIAL CHARGE PRES Z= 0.99960   EQUILIBRIUM PRES Z= 0.99975
FINAL CHARGE PRES Z= 0.99969     (ML)S.T.P./GM OF ZEOLITE=  12.196

POINT NO: 14
INITIAL CHARGE PRES(TORR)= 1551  MOLES ADDED (GM MOL*10**3)=   3.1440
FINAL CHARGE PRES (TORR)= 1184.3 TOTAL MOLES (GM  MOL*10**3)=  29.2192
CHARGE CHAMBER TEMP(K)= 297.15   MOLES IN GAS PHASE(GM MOL*10**3)=9.8060
EQUILIBRIUM PRES (TORR)= 1142.9  MOLES ADSORBED (GM MOL*10**3)=  19.4132
SAMPLE CHAMBER TEMP(K)= 297.15   VOLUME ADSORBED (ML) S.T.P.= 435.1248
```

```
INITIAL CHARGE PRES Z= 0.99960   EQUILIBRIUM PRES Z= 0.99971
FINAL CHARGE PRES Z= 0.99970     (ML)S.T.P./GM OF ZEOLITE=  13.266

POINT NO: 15
 INITIAL CHARGE PRES(TORR)= 2063  MOLES ADDED (GM MOL*10**3)=   5.1217
FINAL CHARGE PRES (TORR)= 1463.5 TOTAL MOLES (GM  MOL*10**3)=  34.3408
CHARGE CHAMBER TEMP(K)=298.15    MOLES IN GAS PHASE (GMOL*10**3)=11.9363
EQUILIBRIUM PRES (TORR)= 1391.1  MOLES ADSORBED (GM MOL*10**3)=  22.4046
SAMPLE CHAMBER TEMP(K)= 297.15   VOLUME ADSORBED (ML) S.T.P.= 502.1730
INITIAL CHARGE PRES Z= 0.99947   EQUILIBRIUM PRES Z= 0.99964
FINAL CHARGE PRES Z= 0.99962     (ML)S.T.P./GM OF ZEOLITE=  15.310

POINT NO: 16
INITIAL CHARGE PRES(TORR)= 2322  MOLES ADDED (GM MOL*10**3)=   3.6773
FINAL CHARGE PRES (TORR)= 1892.8 TOTAL MOLES (GM  MOL*10**3)=  38.0181
CHARGE CHAMBER TEMP(K)= 297.15   MOLES IN GAS PHASE(GMOL*10**3)=13.5346
EQUILIBRIUM PRES (TORR)= 1577.3  MOLES ADSORBED (GM MOL*10**3)=  24.4835
SAMPLE CHAMBER TEMP(K)= 297.15   VOLUME ADSORBED (ML) S.T.P.= 548.7704
INITIAL CHARGE PRES Z= 0.99940   EQUILIBRIUM PRES Z= 0.99960
FINAL CHARGE PRES Z= 0.99951     (ML)S.T.P./GM OF ZEOLITE=  16.731

POINT NO: 17
INITIAL CHARGE PRES(TORR)= 2580  MOLES ADDED (GM MOL*10**3)=   5.4067
FINAL CHARGE PRES(TORR)=1949.6   TOTAL MOLES (GM MOL*10**3)=  43.4248
CHARGE CHAMBER TEMP(K)=297.15    MOLES IN GAS PHASE(GMOL*10**3)=16.0208
EQUILIBRIUM PRES(TORR)=1866.9    MOLES ADSORBED (GM MOL*10**3)=  27.4040
SAMPLE CHAMBER TEMP(K)=297.15    VOLUME ADSORBED (ML) S.T.P.= 614.2301
INITIAL CHARGE PRES Z=0.99934    EQUILIBRIUM PRES Z= 0.99952
FINAL CHARGE PRES Z=0.99950      (ML)S.T.P./GM OF ZEOLITE=  18.727


POINT NO: 18
INITIAL CHARGE PRES(TORR)= 3097  MOLES ADDED (GM MOL*10**3)=   6.5153
FINAL CHARGE PRES (TORR)= 2337.5 TOTAL MOLES (GM  MOL*10**3)=  49.9401
CHARGE CHAMBER TEMP(K)= 297.15   MOLES IN GAS PHASE(GMOL*10**3)=18.8629
EQUILIBRIUM PRES (TORR)= 2197.9  MOLES ADSORBED (GM MOL*10**3)=  31.0772
SAMPLE CHAMBER TEMP(K)= 297.15   VOLUME ADSORBED (ML) S.T.P.= 696.5603
INITIAL CHARGE PRES Z= 0.99921   EQUILIBRIUM PRES Z= 0.99944
FINAL CHARGE PRES Z= 0.99940     (ML)S.T.P./GM OF ZEOLITE=  21.237


POINT NO: 19
INITIAL CHARGE PRES(TORR)= 3873  MOLES ADDED (GM MOL*10**3)=   8.6899
FINAL CHARGE PRES (TORR)= 2859.8 TOTAL MOLES (GM  MOL*10**3)=  58.6300
CHARGE CHAMBER TEMP(K)= 297.15   MOLES IN GAS PHASE(GMOL*10**3)=23.3485
EQUILIBRIUM PRES (TORR)= 2720.2  MOLES ADSORBED (GM MOL*10**3)=  35.2815
SAMPLE CHAMBER TEMP(K)= 297.15   VOLUME ADSORBED (ML) S.T.P.= 790.7943
INITIAL CHARGE PRES Z= 0.99901   EQUILIBRIUM PRES Z= 0.99930
FINAL CHARGE PRES Z= 0.99927     (ML)S.T.P./GM OF ZEOLITE=  24.110
```

```
POINT NO: 20
INITIAL CHARGE PRES(TORR)= 3847  MOLES ADDED (GM MOL*10**3)=   5.5431
FINAL CHARGE PRES (TORR)= 3201.1 TOTAL MOLES (GM  MOL*10**3)=  64.1731
CHARGE CHAMBER TEMP(K)= 297.15   MOLES IN GAS PHASE(GMOL*10**3)=26.3250
EQUILIBRIUM PRES (TORR)= 3066.7  MOLES ADSORBED (GM MOL*10**3)=  37.8481
SAMPLE CHAMBER TEMP(K)= 297.15   VOLUME ADSORBED (ML) S.T.P.= 848.3221
INITIAL CHARGE PRES Z= 0.99901   EQUILIBRIUM PRES Z= 0.99921
FINAL CHARGE PRES Z= 0.99918     (ML)S.T.P./GM OF ZEOLITE=  25.863


POINT NO: 21
INITIAL CHARGE PRES (TORR)= 3878 MOLES ADDED (GMOL*10**3)=   3.8131
FINAL CHARGE PRES (TORR)= 3433.9 TOTAL MOLES (GMOL*10**3)=  67.9862
CHARGE CHAMBER TEMP(K)= 297.15   MOLES IN GAS PHASE(GMOL*10**3)=28.3689
EQUILIBRIUM PRES (TORR)= 3304.6  MOLES ADSORBED (GMOL*10**3)= 39.6173
SAMPLE CHAMBER TEMP(K)= 297.15   VOLUME ADSORBED (ML) S.T.P.= 887.9771
INITIAL CHARGE PRES Z= 0.99901   EQUILIBRIUM PRES Z= 0.99915
FINAL CHARGE PRES Z= 0.99912     (ML)S.T.P./GM OF ZEOLITE=  27.072


POINT NO: 22
INITIAL CHARGE PRES (TORR)= 3873 MOLES ADDED (GM MOL*10**3)=   2.5716
FINAL CHARGE PRES (TORR)= 3573.5 TOTAL MOLES (GM  MOL*10**3)=  70.5578
CHARGE CHAMBER TEMP(K)= 297.15   MOLES IN GAS PHASE(GMOL*10**3)=29.5237
EQUILIBRIUM PRES (TORR)= 3439.0  MOLES ADSORBED (GM MOL*10**3)= 41.0341
SAMPLE CHAMBER TEMP(K)= 297.15   VOLUME ADSORBED (ML) S.T.P.= 919.7330
INITIAL CHARGE PRES Z= 0.99901   EQUILIBRIUM PRES Z= 0.99912
FINAL CHARGE PRES Z= 0.99908     (ML)S.T.P./GM OF ZEOLITE=  28.041
```

```
*********************************************************************
C    T241.FOR
C    TERNARY EQUILIBRIUM ADSORPTION PROGRAM (AIR AT 24 C)
C    G.W. MILLER
C    8 AUG 83
     DIMENSION PCHAR1(100),TCHARC(100),TSAMPC(100),PFINAL(100)
     DIMENSION XMOLTO(100),XMOLIN(100),XMOLGA(100),XMOLAD(100)
     DIMENSION VSTP(100),VOLWT(100),PCHAR2(100),Z1(100)
     DIMENSION Z2(100),Z3(100),XN2MGA(100),XO2MGA(100),XARMGA(100)
     DIMENSION Z4(100),TN2SAM(100),TO2SAM(100),TARSAM(100)
     DIMENSION XN2ADD(100),XO2ADD(100),XARADD(100)
     DIMENSION XN2GAS(100),XO2GAS(100),XARGAS(100)
     DIMENSION XN2ADS(100),XO2ADS(100),XARADS(100)
     DIMENSION VOLN2(100),VOLO2(100),VOLAR(100)
     DIMENSION VOWTN2(100),VOWTO2(100),VOWTAR(100)
     DIMENSION PMGAVO(100),XMOLRE(100),XN2REM(100)
     DIMENSION XO2REM(100),XARREM(100),SEPFAC(100)
     DIMENSION XMFO2A(100),XMFARA(100),XMFN2A(100)
C
```

```
      OPEN(UNIT=1,NAME='TAI241.DAT',TYPE='NEW',DISPOSE='SAVE')
      OPEN(UNIT=2,NAME='TN2241.DAT',TYPE='NEW',DISPOSE='SAVE')
      OPEN(UNIT=3,NAME='TO2241.DAT',TYPE='NEW',DISPOSE='SAVE')
      OPEN(UNIT=4,NAME='TAR241.DAT',TYPE='NEW',DISPOSE='SAVE')
      OPEN(UNIT=5,NAME='SEP241.DAT',TYPE='NEW',DISPOSE='SAVE')
      OPEN(UNIT=7,NAME='T241.RES',TYPE='NEW',DISPOSE='SAVE')
C
C     INPUT DATA FROM EXPERIMENT
C
C     SAMWT=SAMPLE WEIGHT (GM)
C     VCHARC=VOLUME OF THE CHARGE CHAMBER (ML)
C     VSAMPC=VOLUME OF THE SAMPLE CHAMBER (ML)
C     VSAMPL=VOLUME OF SAMPLE (ML)
C     VSAMPT=TRUE DEAD VOLUME IN SAMPLE CHAMBER (ML)
C     VOLMGA=VOLUME OF THE MGA SAMPLE CHAMBER (ML)
C     PCHAR1=INITIAL CHARGE CHAMBER PRESSURE (TORR)
C     PCHAR2=FINAL CHARGE CHAMBER PRESSURE (TORR)
C     TCHARC=TEMP IN THE CHARGE CHAMBER (DEG C)
C     TSAMPC=TEMP IN THE SAMPLE CHAMBER (DEG C)
C     PFINAL=EQUILIBRIUM PRESSURE IN THE SAMPLE CHAMBER (TORR)
C     XN2MGA=MOLE FRACTION OF NITROGEN IN THE MGA SAMPLE VOLUME
C     XO2MGA=MOLE FRACTION OF OXYGEN IN THE MGA SAMPLE VOLUME
C     XARMGA=MOLE FRACTION OF ARGON IN THE MGA SAMPLE VOLUME
C     PMGAVO=FINAL PRESSURE OF THE MGA SAMPLE VOLUME (TORR)
C
C     CALCULATED VALUES
C
C     Z1=INITIAL CHARGE CHAMBER PRESSURE Z FACTOR
C     Z2=FINAL CHARGE CHAMBER PRESSURE Z FACTOR
C     Z3=EQUILIBRIUM PRESSURE Z FACTOR
C     Z4=MGA SAMPLE VOLUME Z FACTOR
C     XMOLTO=TOTAL MOLES IN SAMPLE CHAMBER (GM MOL)
C     TN2SAM=TOTAL MOLES OF NITROGEN IN THE SAMPLE CHAMBER (GM MOL)
C     TO2SAM=TOTAL MOLES OF OXYGEN IN THE SAMPLE CHAMBER (GM MOL)
C     TARSAM=TOTAL MOLES OF ARGON IN THE SAMPLE CHAMBER (GM MOL)
C     XMOLIN=MOLES ADDED (GM MOL)
C     XN2ADD=MOLES OF NITROGEN ADDED (GM MOL)
C     XO2ADD=MOLES OF OXYGEN ADDED (GM MOL)
C     XARADD=MOLES OF ARGON ADDED (GM MOL)
C     XMOLGA=MOLES IN GAS PHASE (GM MOL)
C     XN2GAS=MOLES OF NITROGEN IN THE GAS PHASE (GM MOL)
C     XO2GAS=MOLES OF OXYGEN IN THE GAS PHASE (GM MOL)
C     XARGAS=MOLES OF ARGON IN THE GAS PHASE (GM MOL)
C     XMOLAD=MOLES ADSORBED (GM MOL)
C     XN2ADS=MOLES OF NITROGEN ADSORBED (GM MOL)
C     XO2ADS=MOLES OF OXYGEN ADSORBED (GM MOL)
C     XARADS=MOLES OF ARGON ADSORBED (GM MOL)
C     XMFN2A=MOLE FRACTION OF NITROGEN ADSORBED
C     XMFO2A=MOLE FRACTION OF OXYGEN ADSORBED
```

```
C     XMFARA=MOLE FRACTION OF ARGON ADSORBED
C     VSTP=VOLUME ADSORBED (ML STP)
C     VOLN2=VOLUME OF NITROGEN ADSORBED (ML STP)
C     VOLO2=VOLUME OF OXYGEN ADSORBED (ML STP)
C     VOLAR=VOLUME OF ARGON ADSORBED (ML STP)
C     VOLWT=VOLUME ADSORBED(ML STP)/WEIGHT OF SAMPLE (GM)
C     VOWTN2=VOLUME NITROGEN ADSORBED (ML STP)/WEIGHT OF SAMPLE (GM)
C     VOWTO2=VOLUME OXYGEN ADSORBED (ML STP)/WEIGHT OF SAMPLE (GM)
C     VOWTAR=VOLUME ARGON ADSORBED (ML STP)/WEIGHT OF SAMPLE (GM)
C     SEPFAC=SEPARATION FACTOR BETWEEN NITROGEN AND OXYGEN NEGLECTING
C     ARGON.
C
      NDATA=9
      SAMWT=32.8
      R=82.057
      VCHARC=158.6
      VSAMPC=170.0
      VSAMPL=11.05
      VSAMPT=VSAMPC-VSAMPL
      VOLMGA=12.9484
      AIRN2=0.7814
      AIRO2=0.2092
      AIRAR=0.0094
C
C         INPUT:EXPERIMENT NO.4
C
      PCHAR1(1)=763.
      PCHAR1(2)=1034.3
      PCHAR1(3)=1789.3
      PCHAR1(4)=2311.6
      PCHAR1(5)=2802.9
      PCHAR1(6)=3351.1
      PCHAR1(7)=3868.3
      PCHAR1(8)=3868.3
      PCHAR1(9)=3868.3
C
      PCHAR2(1)=189.
      PCHAR2(2)=413.7
      PCHAR2(3)=1142.9
      PCHAR2(4)=1520.4
      PCHAR2(5)=1856.6
      PCHAR2(6)=1949.6
      PCHAR2(7)=2534.
      PCHAR2(8)=2901.2
      PCHAR2(9)=3180.5
C
      PFINAL(1)=169.
      PFINAL(2)=372.
      PFINAL(3)=585.
```

```
      PFINAL(4)=882.
      PFINAL(5)=1251.5
      PFINAL(6)=1835.9
      PFINAL(7)=2404.7
      PFINAL(8)=2802.9
      PFINAL(9)=3051.2
C
      TCHARC(1)=25.
      TCHARC(2)=24.
      TCHARC(3)=25.
      TCHARC(4)=24.
      TCHARC(5)=25.
      TCHARC(6)=24.
      TCHARC(7)=24.
      TCHARC(8)=24.
      TCHARC(9)=24.
C
      TSAMPC(1)=24.
      TSAMPC(2)=25.
      TSAMPC(3)=24.
      TSAMPC(4)=25.
      TSAMPC(5)=24.
      TSAMPC(6)=24.
      TSAMPC(7)=24.
      TSAMPC(8)=24.
      TSAMPC(9)=24.
C
      XN2MGA(1)=0.5973
          XN2MGA(2)=0.6157
      XN2MGA(3)=0.6289
      XN2MGA(4)=0.6457
      XN2MGA(5)=0.6536
      XN2MGA(6)=0.6705
      XN2MGA(7)=0.6832
      XN2MGA(8)=0.6906
      XN2MGA(9)=0.6962
C
      XO2MGA(1)=0.3847
      XO2MGA(2)=0.3666
      XO2MGA(3)=0.3551
      XO2MGA(4)=0.3390
      XO2MGA(5)=0.3314
      XO2MGA(6)=0.3150
      XO2MGA(7)=0.3031
      XO2MGA(8)=0.2961
      XO2MGA(9)=0.2907
C
      XARMGA(1)=0.0180
      XARMGA(2)=0.0177
```

```
      XARMGA(3)=0.0160
      XARMGA(4)=0.0153
      XARMGA(5)=0.0150
      XARMGA(6)=0.0145
      XARMGA(7)=0.0137
      XARMGA(8)=0.0133
      XARMGA(9)=0.0131
C
      PMGAVO(1)=164.
      PMGAVO(2)=359.
      PMGAVO(3)=564.
      PMGAVO(4)=847.
      PMGAVO(5)=1205.
      PMGAVO(6)=1753.1
      PMGAVO(7)=2291.
      PMGAVO(8)=2663.3
      PMGAVO(9)=2890.9
C
      DO100 J=1,NDATA
      TCHARC(J)=TCHARC(J)+273.15
      TSAMPC(J)=TSAMPC(J)+273.15
100   CONTINUE
      TOTAL=0.
      TOTN2=0.
      TOTO2=0.
      TOTAR=0.
C
      DO101 J=1,NDATA
      Z1(J)=(-4.204836514E-07*PCHAR1(J))+ 1.00000
          XMOL1=((PCHAR1(J)/760.)*VCHARC)/(R*TCHARC(J)*Z1(J))
      Z2(J)=(-4.204836514E-07*PCHAR2(J))+ 1.00000
      XMOL2=((PCHAR2(J)/760.)*VCHARC)/(R*TCHARC(J)*Z2(J))
      XMOLIN(J)=XMOL1-XMOL2
      XMOLTO(J)=TOTAL+XMOLIN(J)
      TOTAL=XMOLTO(J)
          XN2ADD(J)=AIRN2*XMOLIN(J)
          XO2ADD(J)=AIRO2*XMOLIN(J)
          XARADD(J)=AIRAR*XMOLIN(J)
      TN2SAM(J)=TOTN2+XN2ADD(J)
      TOTN2=TN2SAM(J)
      TO2SAM(J)=TOTO2+XO2ADD(J)
      TOTO2=TO2SAM(J)
      TARSAM(J)=TOTAR+XARADD(J)
      TOTAR=TARSAM(J)
      ZPURN2=(-2.565068585E-07*PFINAL(J))+ 1.00000
      ZPURO2=(-8.333328077E-07*PFINAL(J))+ 1.00000
      ZPURAR=(-8.617667817E-07*PFINAL(J))+ 1.00000
      Z3(J)=(ZPURN2*XN2MGA(J))+(ZPURO2*XO2MGA(J))+(ZPURAR*XARMGA(J))
      XMOLGA(J)=((PFINAL(J)/760.)*VSAMPT)/(R*TSAMPC(J)*Z3(J))
```

```
      XN2GAS(J)=XMOLGA(J)*XN2MGA(J)
      XO2GAS(J)=XMOLGA(J)*XO2MGA(J)
      XARGAS(J)=XMOLGA(J)*XARMGA(J)
          XMOLAD(J)=XMOLTO(J)-XMOLGA(J)
      XN2ADS(J)=TN2SAM(J)-XN2GAS(J)
      XO2ADS(J)=TO2SAM(J)-XO2GAS(J)
      XARADS(J)=TARSAM(J)-XARGAS(J)
      XMFN2A(J)=XN2ADS(J)/XMOLAD(J)
      XMFO2A(J)=XO2ADS(J)/XMOLAD(J)
      XMFARA(J)=XARADS(J)/XMOLAD(J)
      VSTP(J)=XMOLAD(J)*R*273.15
      VOLN2(J)=XN2ADS(J)*R*273.15
      VOLO2(J)=XO2ADS(J)*R*273.15
      VOLAR(J)=XARADS(J)*R*273.15
      VOLWT(J)=VSTP(J)/SAMWT
      VOWTN2(J)=VOLN2(J)/SAMWT
      VOWTO2(J)=VOLO2(J)/SAMWT
      VOWTAR(J)=VOLAR(J)/SAMWT
      ZPURN2=(-2.565068585E-07*PMGAVO(J))+ 1.00000
      ZPURO2=(-8.333328077E-07*PMGAVO(J))+ 1.00000
      ZPURAR=(-8.617667817E-07*PMGAVO(J))+ 1.00000
      Z4(J)=(ZPURN2*XN2MGA(J))+(ZPURO2*XO2MGA(J))+(ZPURAR*XARMGA(J))
      XMOLRE(J)=((PMGAVO(J)/760.)*VOLMGA)/(R*TSAMPC(J)*Z4(J))
      XN2REM(J)=XN2MGA(J)*XMOLRE(J)
      XO2REM(J)=XO2MGA(J)*XMOLRE(J)
      XARREM(J)=XARMGA(J)*XMOLRE(J)
      TOTAL=TOTAL-XMOLRE(J)
      TOTN2=TOTN2-XN2REM(J)
      TOTO2=TOTO2-XO2REM(J)
      TOTAR=TOTAR-XARREM(J)
      XX1=XO2MGA(J)+XARMGA(J)
      XX2=XMFO2A(J)+XMFARA(J)
      SEPFAC(J)=(XMFN2A(J)*XX1)/(XN2MGA(J)*XX2)
  101 CONTINUE
      DO103 J=1,NDATA
      XMOLIN(J)=XMOLIN(J)*1000.
      XMOLTO(J)=XMOLTO(J)*1000.
      XMOLGA(J)=XMOLGA(J)*1000.
      XMOLAD(J)=XMOLAD(J)*1000.
      TN2SAM(J)=TN2SAM(J)*1000.
      TO2SAM(J)=TO2SAM(J)*1000.
      TARSAM(J)=TARSAM(J)*1000.
      XN2ADD(J)=XN2ADD(J)*1000.
      XO2ADD(J)=XO2ADD(J)*1000.
      XARADD(J)=XARADD(J)*1000.
      XN2GAS(J)=XN2GAS(J)*1000.
      XO2GAS(J)=XO2GAS(J)*1000.
      XARGAS(J)=XARGAS(J)*1000.
      XN2ADS(J)=XN2ADS(J)*1000.
```

```
      XO2ADS(J)=XO2ADS(J)*1000.
      XARADS(J)=XARADS(J)*1000.
      XMOLRE(J)=XMOLRE(J)*1000.
      XN2REM(J)=XN2REM(J)*1000.
      XO2REM(J)=XO2REM(J)*1000.
      XARREM(J)=XARREM(J)*1000.
103   CONTINUE
      WRITE(7,15)
15    FORMAT(/,1X,'G.W.MILLER')
      WRITE(7,18)
18    FORMAT(1X,'USAF SCHOOL OF AEROSPACE MEDICINE')
      WRITE(7,19)
19    FORMAT(1X,'CREW TECHNOLOGY DIVISION')
      WRITE(7,20)
20    FORMAT(1X,'BROOKS AFB,TEXAS')
      WRITE(7,16)
16    FORMAT(//,1X,'ADSORPTION ISOTHERM EXPFRIMENT NO.5')
      WRITE(7,1)
1         FORMAT(1X,'AIR ON UNION CARBIDE ZEOLITE 5A (20X40 MESH) AT 24 D
     1EG C')
      WRITE(7,2)NDATA
2     FORMAT(//,1X,'NUMBER OF DATA POINTS=',I3)
      WRITE(7,3) SAMWT
3     FORMAT(1X,'SAMPLE WEIGHT (GM)=',F6.1)
      WRITE(7,4) VCHARC
4     FORMAT(1X,'VOLUME OF CHARGE CHAMBER (ML)=',F6.1)
      WRITE(7,5) VSAMPC
5     FORMAT(1X,'VOLUME OF SAMPLE CHAMBER W/O ZEOLITE (ML)=',F6.1)
      WRITE(7,6) VSAMPL
      WRITE(7,33) VOLMGA
33    FORMAT(1X,'MGA SAMPLE VOLUME (ML)=',F6.2)
6     FORMAT(1X,'TRUE VOLUME OF SAMPLE (ML)=',F6.2)
      WRITE(7,7) VSAMPT
7     FORMAT(1X,'TRUE DEAD VOLUME OF SAMPLE CHAMBER (ML)=',F6.1)
      WRITE(7,850) AIRN2
850   FORMAT(1X,'MOLE FRACTION OF NITROGEN IN THE BOTTLED AIR=',F7.4)
      WRITE(7,851) AIRO2
851   FORMAT(1X,'MOLE FRACTION OF OXYGEN IN THE BOTTLED AIR=',F7.4)
      WRITE(7,852) AIRAR
852   FORMAT(1X,'MOLE FRACTION OF ARGON IN THE BOTTLED AIR=',F7.4)
      WRITE(7,300)
300   FORMAT(//,1X,'**********************************************')
      WRITE(7,301)
301   FORMAT(1X,'**********************************************')
      DO105 J=1,NDATA
      WRITE(7,8)J
8     FORMAT(//,1X,'POINT NO:',I3,/)
      WRITE(7,333)
333   FORMAT(1X,'INPUT:',/)
```

```
      WRITE(7,700) PCHAR1(J)
  700 FORMAT(1X,'INITIAL CHARGE PRESSURE (TORR)=',F7.1)
      WRITE(7,701) PCHAR2(J)
  701 FORMAT(1X,'FINAL CHARGE PRESSURE (TORR)=',F7.1)
      WRITE(7,702) TCHARC(J)
  702 FORMAT(1X,'TEMPERATURE OF THE CHARGE CHAMBER (K)=',F7.2)
      WRITE(7,706) PFINAL(J)
  706 FORMAT(1X,'EQUILIBRIUM PRESSURE (TORR)=',F7.1)
      WRITE(7,707) TSAMPC(J)
  707 FORMAT(1X,'TEMPERATURE OF THE SAMPLE CHAMBER (K)=',F7.2)
      WRITE(7,708) XN2MGA(J)
  708 FORMAT(1X,'MOLE FRACTION NITROGEN IN THE MGA SAMPLE=',1X,F6.4)
      WRITE(7,709) XO2MGA(J)
  709 FORMAT(1X,'MOLE FRACTION OXYGEN IN THE MGA SAMPLE=',1X,F6.4)
      WRITE(7,710) XARMGA(J)
  710 FORMAT(1X,'MOLE FRACTION ARGON IN THE MGA SAMPLE=',1X,F6.4)
      WRITE(7,711) PMGAVO(J)
  711 FORMAT(1X,'MGA SAMPLE VOLUME PRESSURE (TORR)=',F7.1)
      WRITE(7,712)
  712 FORMAT(//,1X,'OUTPUT:',/)
      WRITE(7,713) Z1(J)
  713 FORMAT(1X,'INITIAL CHARGE PRESSURE Z=',F8.5)
      WRITE(7,714) Z2(J)
  714 FORMAT(1X,'FINAL CHARGE PRESSURE Z=',F8.5)
      WRITE(7,715) Z3(J)
  715 FORMAT(1X,'EQUILIBRIUM PRESSURE Z=',F8.5)
      WRITE(7,716) Z4(J)
  716 FORMAT(1X,'MGA SAMPLE CHAMBER Z=',F8.5,/)
      WRITE(7,717) XN2ADD(J)
  717 FORMAT(1X,'MOLES OF NITROGEN ADDED (GM MOL*10**3)=',F10.4)
      WRITE(7,718) XO2ADD(J)
  718 FORMAT(1X,'MOLES OF OXYGEN ADDED (GM MOL*10**3)=',F10.4)
      WRITE(7,719) XARADD(J)
  719 FORMAT(1X,'MOLES OF ARGON ADDED (GM MOL*10**3)=',F10.4)
      WRITE(7,720) XMOLIN(J)
  720 FORMAT(1X,'TOTAL MOLES ADDED (GM MOL*10**3)=',F10.4,/)
      WRITE(7,721) TN2SAM(J)
  721 FORMAT(1X,'TOTAL MOLES OF NITROGEN IN THE SAMPLE CHAMBER (GM MO
     1L*10**3)=',F10.4)
      WRITE(7,722) TO2SAM(J)
  722 FORMAT(1X,'TOTAL MOLES OF OXYGEN IN THE SAMPLE CHAMBER (GM MOL*
     110**3)=',F10.4)
      WRITE(7,723) TARSAM(J)
  723 FORMAT(1X,'TOTAL MOLES OF ARGON IN THE SAMPLE CHAMBER (GM MOL*1
     10**3)=',F10.4)
      WRITE(7,724) XMOLTO(J)
  724 FORMAT(1X,'TOTAL MOLES IN THE SAMPLE CHAMBER (GM MOL*10**3)=',F
     110.4,/)
      WRITE(7,725) XN2GAS(J)
```

```
725 FORMAT(1X,'MOLES OF NITROGEN IN THE GAS PHASE (GM MOL*10**3)=',
     1F10.4)
    WRITE(7,726) XO2GAS(J)
726 FORMAT(1X,'MOLES OF OXYGEN IN THE GAS PHASE (GM MOL*10**3)=',F1
     10.4)
    WRITE(7,727) XARGAS(J)
727 FORMAT(1X,'MOLES OF ARGON IN THE GAS PHASE (GM MOL*10**3)=',F10
     1.4)
    WRITE(7,728) XMOLGA(J)
728 FORMAT(1X,'TOTAL MOLES IN THE GAS PHASE (GM MOL*10**3)=',F10.4)
    WRITE(7,450) XN2MGA(J)
450 FORMAT(1X,'MOLE FRACTION OF NITROGEN IN THE GAS PHASE=',2X,F6.4
     1)
    WRITE(7,451) XO2MGA(J)
451 FORMAT(1X,'MOLE FRACTION OF OXYGEN IN THE GAS PHASE=',2X,F6.4)
    WRITE(7,452) XARMGA(J)
452 FORMAT(1X,'MOLE FRACTION OF ARGON IN THE GAS PHASE=',2X,F6.4,/)
    WRITE(7,729) XN2ADS(J)
729 FORMAT(1X,'MOLES OF NITROGEN ADSORBED (GM MOL*10**3)=',F10.4)
    WRITE(7,730) XO2ADS(J)
730 FORMAT(1X,'MOLES OF OXYGEN ADSORBED (GM MOL*10**3)=',F10.4)
    WRITE(7,731) XARADS(J)
731 FORMAT(1X,'MOLES OF ARGON ADSORBED (GM MOL*10**3)=',F10.4)
    WRITE(7,732) XMOLAD(J)
732 FORMAT(1X,'TOTAL MOLES ADSORBED (GM MOL*10**3)=',F10.4)
    WRITE(7,453) XMFN2A(J)
453 FORMAT(1X,'MOLE FRACTION OF NITROGEN ADSORBED=',2X,F6.4)
    WRITE(7,454) XMFO2A(J)
454 FORMAT(1X,'MOLE FRACTION OF OXYGEN ADSORBED=',2X,F6.4)
    WRITE(7,455) XMFARA(J)
455 FORMAT(1X,'MOLE FRACTION OF ARGON ADSORBED=',2X,F6.4,/)
    WRITE(7,733) VOLN2(J)
733 FORMAT(1X,'VOLUME OF NITROGEN ADSORBED (ML STP)=',F10.3)
    WRITE(7,734) VOLO2(J)
734 FORMAT(1X,'VOLUME OF OXYGEN ADSORBED (ML STP)=',F10.3)
    WRITE(7,735) VOLAR(J)
735 FORMAT(1X,'VOLUME OF ARGON ADSORBED (ML STP)=',F10.3)
    WRITE(7,736) VSTP(J)
736 FORMAT(1X,'TOTAL VOLUME ADSORBED (ML STP)=',F10.3,/)
    WRITE(7,737) VOWTN2(J)
737 FORMAT(1X,'VOLUME OF NITROGEN ADSORBED (ML STP/GM)=',F9.3)
    WRITE(7,750) VOWTO2(J)
750 FORMAT(1X,'VOLUME OF OXYGEN ADSORBED (ML STP/GM)=',F9.3)
    WRITE(7,751) VOWTAR(J)
751 FORMAT(1X,'VOLUME OF ARGON ADSORBED (ML STP/GM)=',F9.3)
    WRITE(7,752) VOLWT(J)
752 FORMAT(1X,'TOTAL VOLUME ADSORBED (ML STP/GM)=',F9.3,/)
    WRITE(7,753) XN2REM(J)
753 FORMAT(1X,'MOLES OF NITROGEN REMOVED BY THE MGA (GM MOL*10**3)=
```

```
     1',F10.5)
    WRITE(7,754) XO2REM(J)
754 FORMAT(1X,'MOLES OF OXYGEN REMOVED BY THE MGA (GM MOL*10**3)=',
     1F10.5)
    WRITE(7,755) XARREM(J)
755 FORMAT(1X,'MOLES OF ARGON REMOVED BY THE MGA (GM MOL*10**3)=',F
     110.5)
    WRITE(7,756) XMOLRE(J)
756 FORMAT(1X,'TOTAL MOLES REMOVED BY THE MGA (GM MOL*10**3)=',F10.
     15)
    WRITE(7,777) SEPFAC(J)
777 FORMAT(/,1X,'SEPARATION FACTOR BETWEEN NITROGEN AND OXYGEN=',F7
     1.3)
    WRITE(7,757)
757 FORMAT(//,1X,'***********************************************')
    WRITE(7,320)
320 FORMAT(1X,'***********************************************')
105 CONTINUE
    DO555 J=1,NDATA
    WRITE(1,551) PFINAL(J),VOLWT(J)
551 FORMAT(F7.0,3X,F8.3)
555 CONTINUE
    DO556 J=1,NDATA
    WRITE(2,551) PFINAL(J),VOWTN2(J)
556 CONTINUE
    DO557 J=1,NDATA
    WRITE(3,551) PFINAL(J),VOWTO2(J)
557 CONTINUE
    DO558 J=1,NDATA
    WRITE(4,551) PFINAL(J),VOWTAR(J)
558 CONTINUE
    DO559 J=1,NDATA
    WRITE(5,551) PFINAL(J),SEPFAC(J)
559 CONTINUE
    STOP
    END
```

```
************************************************************************
 T241.RES
 G.W:MILLER
 USAF SCHOOL OF AEROSPACE MEDICINE
 CREW TECHNOLOGY DIVISION
 BROOKS AFB,TEXAS


 ADSORPTION ISOTHERM EXPERIMENT NO.5
 AIR ON UNION CARBIDE ZEOLITE 5A (20X40 MESH) AT 24 DEG C
```

```
NUMBER OF DATA POINTS=  9
SAMPLE WEIGHT (GM)=  32.8
VOLUME OF CHARGE CHAMBER (ML)= 158.6
VOLUME OF SAMPLE CHAMBER W/O ZEOLITE (ML)= 170.0
TRUE VOLUME OF SAMPLE (ML)= 11.05
MGA SAMPLE VOLUME (ML)= 12.95
TRUE DEAD VOLUME OF SAMPLE CHAMBER (ML)= 158.9
MOLE FRACTION OF NITROGEN IN THE BOTTLED AIR= 0.7814
MOLE FRACTION OF OXYGEN IN THE BOTTLED AIR= 0.2092
MOLE FRACTION OF ARGON IN THE BOTTLED AIR= 0.0094

POINT NO:  1
INPUT:
INITIAL CHARGE PRESSURE (TORR)=  763.0
FINAL CHARGE PRESSURE (TORR)=  189.0
TEMPERATURE OF THE CHARGE CHAMBER (K)= 298.15
EQUILIBRIUM PRESSURE (TORR)=  169.0
TEMPERATURE OF THE SAMPLE CHAMBER (K)= 297.15
MOLE FRACTION NITROGEN IN THE MGA SAMPLE= 0.5973
MOLE FRACTION OXYGEN IN THE MGA SAMPLE= 0.3847
MOLE FRACTION ARGON IN THE MGA SAMPLE= 0.0180
MGA SAMPLE VOLUME PRESSURE (TORR)=  164.0

OUTPUT:
INITIAL CHARGE PRESSURE Z= 0.99968
FINAL CHARGE PRESSURE Z= 0.99992
EQUILIBRIUM PRESSURE Z= 0.99992
MGA SAMPLE CHAMBER Z= 0.99992

MOLES OF NITROGEN ADDED (GM MOL*10**3)=     3.8274
MOLES OF OXYGEN ADDED (GM MOL*10**3)=    1.0247
MOLES OF ARGON ADDED (GM MOL*10**3)=    0.0460
TOTAL MOLES ADDED (GM MOL*10**3)=    4.8981

TOTAL MOLES OF NITROGEN IN THE SAMPLE CHAMBER (GM MOL*10**3)= 3.8274
TOTAL MOLES OF OXYGEN IN THE SAMPLE CHAMBER (GM MOL*10**3) = 1.0247
TOTAL MOLES OF ARGON IN THE SAMPLE CHAMBER (GM MOL*10**3) = 0.0460
TOTAL MOLES IN THE SAMPLE CHAMBER (GM MOL*10**3)=    4.8981

MOLES OF NITROGEN IN THE GAS PHASE (GM MOL*10**3)=    0.8659
MOLES OF OXYGEN IN THE GAS PHASE (GM MOL*10**3)=    0.5577
MOLES OF ARGON IN THE GAS PHASE (GM MOL*10**3)=    0.0261
TOTAL MOLES IN THE GAS PHASE (GM MOL*10**3)=    1.4497
MOLE FRACTION OF NITROGEN IN THE GAS PHASE=  0.5973
MOLE FRACTION OF OXYGEN IN THE GAS PHASE=  0.3847
MOLE FRACTION OF ARGON IN THE GAS PHASE=  0.0180

MOLES OF NITROGEN ADSORBED (GM MOL*10**3)=    2.9614
MOLES OF OXYGEN ADSORBED (GM MOL*10**3)=    0.4670
```

```
MOLES OF ARGON ADSORBED (GM MOL*10**3)=    0.0199
TOTAL MOLES ADSORBED (GM MOL*10**3)=    3.4484
MOLE FRACTION OF NITROGEN ADSORBED= 0.8588
MOLE FRACTION OF OXYGEN ADSORBED= 0.1354
MOLE FRACTION OF ARGON ADSORBED= 0.0058

VOLUME OF NITROGEN ADSORBED (ML STP)=    66.377
VOLUME OF OXYGEN ADSORBED (ML STP)=    10.467
VOLUME OF ARGON ADSORBED (ML STP)=    0.447
TOTAL VOLUME ADSORBED (ML STP)=    77.291

VOLUME OF NITROGEN ADSORBED (ML STP/GM)=    2.024
VOLUME OF OXYGEN ADSORBED (ML STP/GM)=    0.319
VOLUME OF ARGON ADSORBED (ML STP/GM)=    0.014
TOTAL VOLUME ADSORBED (ML STP/GM)=    2.356

MOLES OF NITROGEN REMOVED BY THE MGA (GM MOL*10**3)=   0.06845
MOLES OF OXYGEN REMOVED BY THE MGA (GM MOL*10**3)=   0.04409
MOLES OF ARGON REMOVED BY THE MGA (GM MOL*10**3)=   0.00206
TOTAL MOLES REMOVED BY THE MGA (GM MOL*10**3)=   0.11460

SEPARATION FACTOR BETWEEN NITROGEN AND OXYGEN=  4.100

POINT NO:  2
INPUT:
INITIAL CHARGE PRESSURE (TORR)= 1034.3
FINAL CHARGE PRESSURE (TORR)=  413.7
TEMPERATURE OF THE CHARGE CHAMBER (K)= 297.15
EQUILIBRIUM PRESSURE (TORR)=  372.0
TEMPERATURE OF THE SAMPLE CHAMBER (K)= 298.15
MOLE FRACTION NITROGEN IN THE MGA SAMPLE= 0.6157
MOLE FRACTION OXYGEN IN THE MGA SAMPLE= 0.3666
MOLE FRACTION ARGON IN THE MGA SAMPLE= 0.0177
MGA SAMPLE VOLUME PRESSURE (TORR)=  359.0

OUTPUT:
INITIAL CHARGE PRESSURE Z= 0.99957
FINAL CHARGE PRESSURE Z= 0.99983
EQUILIBRIUM PRESSURE Z= 0.99982
MGA SAMPLE CHAMBER Z= 0.99983

MOLES OF NITROGEN ADDED (GM MOL*10**3)=    4.1529
MOLES OF OXYGEN ADDED (GM MOL*10**3)=    1.1118
MOLES OF ARGON ADDED (GM MOL*10**3)=    0.0500
TOTAL MOLES ADDED (GM MOL*10**3)=    5.3146

TOTAL MOLES OF NITROGEN IN THE SAMPLE CHAMBER (GM MOL*10**3)= 7.9118
TOTAL MOLES OF OXYGEN IN THE SAMPLE CHAMBER (GM MOL*10**3)=  2.0924
TOTAL MOLES OF ARGON IN THE SAMPLE CHAMBER (GM MOL*10**3)=  0.0939
```

```
TOTAL MOLES IN THE SAMPLE CHAMBER (GM MOL*10**3)=   10.0981

MOLES OF NITROGEN IN THE GAS PHASE (GM MOL*10**3)=    1.9583
MOLES OF OXYGEN IN THE GAS PHASE (GM MOL*10**3)=    1.1660
MOLES OF ARGON IN THE GAS PHASE (GM MOL*10**3)=    0.0563
TOTAL MOLES IN THE GAS PHASE (GM MOL*10**3)=    3.1807
MOLE FRACTION OF NITROGEN IN THE GAS PHASE=  0.6157
MOLE FRACTION OF OXYGEN IN THE GAS PHASE=  0.3666
MOLE FRACTION OF ARGON IN THE GAS PHASE=  0.0177

MOLES OF NITROGEN ADSORBED (GM MOL*10**3)=    5.9534
MOLES OF OXYGEN ADSORBED (GM MOL*10**3)=    0.9264
MOLES OF ARGON ADSORBED (GM MOL*10**3)=    0.0376
TOTAL MOLES ADSORBED (GM MOL*10**3)=    6.9175
MOLE FRACTION OF NITROGEN ADSORBED=  0.8606
MOLE FRACTION OF OXYGEN ADSORBED=  0.1339
MOLE FRACTION OF ARGON ADSORBED=  0.0054

VOLUME OF NITROGEN ADSORBED (ML STP)=   133.440
VOLUME OF OXYGEN ADSORBED (ML STP)=    20.764
VOLUME OF ARGON ADSORBED (ML STP)=     0.844
TOTAL VOLUME ADSORBED (ML STP)=   155.047

VOLUME OF NITROGEN ADSORBED (ML STP/GM)=    4.068
VOLUME OF OXYGEN ADSORBED (ML STP/GM)=    0.633
VOLUME OF ARGON ADSORBED (ML STP/GM)=    0.026
TOTAL VOLUME ADSORBED (ML STP/GM)=    4.727

MOLES OF NITROGEN REMOVED BY THE MGA (GM MOL*10**3)=   0.15395
MOLES OF OXYGEN REMOVED BY THE MGA (GM MOL*10**3)=   0.09167
MOLES OF ARGON REMOVED BY THE MGA (GM MOL*10**3)=   0.00443
TOTAL MOLES REMOVED BY THE MGA (GM MOL*10**3)=   0.25005

SEPARATION FACTOR BETWEEN NITROGEN AND OXYGEN=  3.855

POINT NO:  3
INPUT:
INITIAL CHARGE PRESSURE (TORR)= 1789.3
FINAL CHARGE PRESSURE (TORR)= 1142.9
TEMPERATURE OF THE CHARGE CHAMBER (K)= 298.15
EQUILIBRIUM PRESSURE (TORR)=  585.0
TEMPERATURE OF THE SAMPLE CHAMBER (K)= 297.15
MOLE FRACTION NITROGEN IN THE MGA SAMPLE= 0.6289
MOLE FRACTION OXYGEN IN THE MGA SAMPLE= 0.3551
MOLE FRACTION ARGON IN THE MGA SAMPLE= 0.0160
MGA SAMPLE VOLUME PRESSURE (TORR)=  564.0

OUTPUT:
INITIAL CHARGE PRESSURE Z= 0.99925
```

```
FINAL CHARGE PRESSURE Z= 0.99952
EQUILIBRIUM PRESSURE Z= 0.99972
MGA SAMPLE CHAMBER Z= 0.99973

MOLES OF NITROGEN ADDED (GM MOL*10**3)=    4.3137
MOLES OF OXYGEN ADDED (GM MOL*10**3)=    1.1549
MOLES OF ARGON ADDED (GM MOL*10**3)=    0.0519
TOTAL MOLES ADDED (GM MOL*10**3)=    5.5205

TOTAL MOLES OF NITROGEN IN THE SAMPLE CHAMBER (GM MOL*10**3)= 12.0715
TOTAL MOLES OF OXYGEN IN THE SAMPLE CHAMBER (GM MOL*10**3)=  3.1556
TOTAL MOLES OF ARGON IN THE SAMPLE CHAMBER (GM MOL*10**3)=  0.1414
TOTAL MOLES IN THE SAMPLE CHAMBER (GM MOL*10**3)=   15.3685

MOLES OF NITROGEN IN THE GAS PHASE (GM MOL*10**3)=    3.1566
MOLES OF OXYGEN IN THE GAS PHASE (GM MOL*10**3)=    1.7823
MOLES OF ARGON IN THE GAS PHASE (GM MOL*10**3)=    0.0803
TOTAL MOLES IN THE GAS PHASE (GM MOL*10**3)=    5.0192
MOLE FRACTION OF NITROGEN IN THE GAS PHASE=  0.6289
MOLE FRACTION OF OXYGEN IN THE GAS PHASE=  0.3551
MOLE FRACTION OF ARGON IN THE GAS PHASE=  0.0160

MOLES OF NITROGEN ADSORBED (GM MOL*10**3)=    8.9150
MOLES OF OXYGEN ADSORBED (GM MOL*10**3)=    1.3733
MOLES OF ARGON ADSORBED (GM MOL*10**3)=    0.0611
TOTAL MOLES ADSORBED (GM MOL*10**3)=   10.3494
MOLE FRACTION OF NITROGEN ADSORBED=  0.8614
MOLE FRACTION OF OXYGEN ADSORBED=  0.1327
MOLE FRACTION OF ARGON ADSORBED=  0.0059

VOLUME OF NITROGEN ADSORBED (ML STP)=   199.819
VOLUME OF OXYGEN ADSORBED (ML STP)=    30.782
VOLUME OF ARGON ADSORBED (ML STP)=     1.369
TOTAL VOLUME ADSORBED (ML STP)=   231.970

VOLUME OF NITROGEN ADSORBED (ML STP/GM)=     6.092
VOLUME OF OXYGEN ADSORBED (ML STP/GM)=     0.938
VOLUME OF ARGON ADSORBED (ML STP/GM)=     0.042
TOTAL VOLUME ADSORBED (ML STP/GM)=     7.072

MOLES OF NITROGEN REMOVED BY THE MGA (GM MOL*10**3)=    0.24791
MOLES OF OXYGEN REMOVED BY THE MGA (GM MOL*10**3)=    0.13998
MOLES OF ARGON REMOVED BY THE MGA (GM MOL*10**3)=    0.00631
TOTAL MOLES REMOVED BY THE MGA (GM MOL*10**3)=    0.39419

SEPARATION FACTOR BETWEEN NITROGEN AND OXYGEN=  3.667

POINT NO:  4
INPUT:
```

```
INITIAL CHARGE PRESSURE (TORR)= 2311.6
FINAL CHARGE PRESSURE (TORR)= 1520.4
TEMPERATURE OF THE CHARGE CHAMBER (K)= 297.15
EQUILIBRIUM PRESSURE (TORR)=  882.0
TEMPERATURE OF THE SAMPLE CHAMBER (K)= 298.15
MOLE FRACTION NITROGEN IN THE MGA SAMPLE= 0.6457
MOLE FRACTION OXYGEN IN THE MGA SAMPLE= 0.3390
MOLE FRACTION ARGON IN THE MGA SAMPLE= 0.0153
MGA SAMPLE VOLUME PRESSURE (TORR)=  847.0

OUTPUT:
INITIAL CHARGE PRESSURE Z= 0.99903
FINAL CHARGE PRESSURE Z= 0.99936
EQUILIBRIUM PRESSURE Z= 0.99959
MGA SAMPLE CHAMBER Z= 0.99961

MOLES OF NITROGEN ADDED (GM MOL*10**3)=    5.2998
MOLES OF OXYGEN ADDED (GM MOL*10**3)=    1.4189
MOLES OF ARGON ADDED (GM MOL*10**3)=    0.0638
TOTAL MOLES ADDED (GM MOL*10**3)=    6.7824

TOTAL MOLES OF NITROGEN IN THE SAMPLE CHAMBER (GM MOL*10**3)= 17.1234
TOTAL MOLES OF OXYGEN IN THE SAMPLE CHAMBER (GM MOL*10**3)=  4.4345
TOTAL MOLES OF ARGON IN THE SAMPLE CHAMBER (GM MOL*10**3)=  0.1989
TOTAL MOLES IN THE SAMPLE CHAMBER (GM MOL*10**3)=   21.7568

MOLES OF NITROGEN IN THE GAS PHASE (GM MOL*10**3)=    4.8705
MOLES OF OXYGEN IN THE GAS PHASE (GM MOL*10**3)=    2.5571
MOLES OF ARGON IN THE GAS PHASE (GM MOL*10**3)=    0.1154
TOTAL MOLES IN THE GAS PHASE (GM MOL*10**3)=    7.5430
MOLE FRACTION OF NITROGEN IN THE GAS PHASE=  0.6457
MOLE FRACTION OF OXYGEN IN THE GAS PHASE=  0.3390
MOLE FRACTION OF ARGON IN THE GAS PHASE=  0.0153

MOLES OF NITROGEN ADSORBED (GM MOL*10**3)=   12.2529
MOLES OF OXYGEN ADSORBED (GM MOL*10**3)=    1.8775
MOLES OF ARGON ADSORBED (GM MOL*10**3)=    0.0834
TOTAL MOLES ADSORBED (GM MOL*10**3)=   14.2138
MOLE FRACTION OF NITROGEN ADSORBED=  0.8620
MOLE FRACTION OF OXYGEN ADSORBED=  0.1321
MOLE FRACTION OF ARGON ADSORBED=  0.0059

VOLUME OF NITROGEN ADSORBED (ML STP)=   274.635
VOLUME OF OXYGEN ADSORBED (ML STP)=    42.081
VOLUME OF ARGON ADSORBED (ML STP)=     1.870
TOTAL VOLUME ADSORBED (ML STP)=   318.586

VOLUME OF NITROGEN ADSORBED (ML STP/GM)=    8.373
VOLUME OF OXYGEN ADSORBED (ML STP/GM)=    1.283
```

```
VOLUME OF ARGON ADSORBED (ML STP/GM)=    0.057
TOTAL VOLUME ADSORBED (ML STP/GM)=    9.713

MOLES OF NITROGEN REMOVED BY THE MGA (GM MOL*10**3)=   0.38101
MOLES OF OXYGEN REMOVED BY THE MGA (GM MOL*10**3)=   0.20003
MOLES OF ARGON REMOVED BY THE MGA (GM MOL*10**3)=   0.00903
TOTAL MOLES REMOVED BY THE MGA (GM MOL*10**3)=   0.59007

SEPARATION FACTOR BETWEEN NITROGEN AND OXYGEN=  3.429

POINT NO:  5
INPUT:
INITIAL CHARGE PRESSURE (TORR)= 2802.9
FINAL CHARGE PRESSURE (TORR)= 1856.6
TEMPERATURE OF THE CHARGE CHAMBER (K)= 298.15
EQUILIBRIUM PRESSURE (TORR)= 1251.5
TEMPERATURE OF THE SAMPLE CHAMBER (K)= 297.15
MOLE FRACTION NITROGEN IN THE MGA SAMPLE= 0.6536
MOLE FRACTION OXYGEN IN THE MGA SAMPLE= 0.3314
MOLE FRACTION ARGON IN THE MGA SAMPLE= 0.0150
MGA SAMPLE VOLUME PRESSURE (TORR)= 1205.0

OUTPUT:
INITIAL CHARGE PRESSURE Z= 0.99882
FINAL CHARGE PRESSURE Z= 0.99922
EQUILIBRIUM PRESSURE Z= 0.99943
MGA SAMPLE CHAMBER Z= 0.99945

MOLES OF NITROGEN ADDED (GM MOL*10**3)=    6.3196
MOLES OF OXYGEN ADDED (GM MOL*10**3)=    1.6919
MOLES OF ARGON ADDED (GM MOL*10**3)=    0.0760
TOTAL MOLES ADDED (GM MOL*10**3)=    8.0876

TOTAL MOLES OF NITROGEN IN THE SAMPLE CHAMBER (GM MOL*10**3)= 23.0620
TOTAL MOLES OF OXYGEN IN THE SAMPLE CHAMBER (GM MOL*10**3)=  5.9264
TOTAL MOLES OF ARGON IN THE SAMPLE CHAMBER (GM MOL*10**3)=  0.2658
TOTAL MOLES IN THE SAMPLE CHAMBER (GM MOL*10**3)=   29.2543

MOLES OF NITROGEN IN THE GAS PHASE (GM MOL*10**3)=    7.0202
MOLES OF OXYGEN IN THE GAS PHASE (GM MOL*10**3)=    3.5595
MOLES OF ARGON IN THE GAS PHASE (GM MOL*10**3)=    0.1611
TOTAL MOLES IN THE GAS PHASE (GM MOL*10**3)=   10.7408
MOLE FRACTION OF NITROGEN IN THE GAS PHASE=  0.6536
MOLE FRACTION OF OXYGEN IN THE GAS PHASE=  0.3314
MOLE FRACTION OF ARGON IN THE GAS PHASE=  0.0150

MOLES OF NITROGEN ADSORBED (GM MOL*10**3)=   16.0419
MOLES OF OXYGEN ADSORBED (GM MOL*10**3)=    2.3669
MOLES OF ARGON ADSORBED (GM MOL*10**3)=    0.1047
```

```
TOTAL MOLES ADSORBED (GM MOL*10**3)=   18.5135
MOLE FRACTION OF NITROGEN ADSORBED=  0.8665
MOLE FRACTION OF OXYGEN ADSORBED=  0.1278
MOLE FRACTION OF ARGON ADSORBED=  0.0057

VOLUME OF NITROGEN ADSORBED (ML STP)=   359.560
VOLUME OF OXYGEN ADSORBED (ML STP)=    53.052
VOLUME OF ARGON ADSORBED (ML STP)=     2.348
TOTAL VOLUME ADSORBED (ML STP)=   414.960

VOLUME OF NITROGEN ADSORBED (ML STP/GM)=   10.962
VOLUME OF OXYGEN ADSORBED (ML STP/GM)=    1.617
VOLUME OF ARGON ADSORBED (ML STP/GM)=    0.072
TOTAL VOLUME ADSORBED (ML STP/GM)=   12.651

MOLES OF NITROGEN REMOVED BY THE MGA (GM MOL*10**3)=   0.55062
MOLES OF OXYGEN REMOVED BY THE MGA (GM MOL*10**3)=   0.27918
MOLES OF ARGON REMOVED BY THE MGA (GM MOL*10**3)=   0.01264
TOTAL MOLES REMOVED BY THE MGA (GM MOL*10**3)=   0.84244

SEPARATION FACTOR BETWEEN NITROGEN AND OXYGEN=  3.440

POINT NO:  6
INPUT:
INITIAL CHARGE PRESSURE (TORR)= 3351.1
FINAL CHARGE PRESSURE (TORR)= 1949.6
TEMPERATURE OF THE CHARGE CHAMBER (K)= 297.15
EQUILIBRIUM PRESSURE (TORR)= 1835.9
TEMPERATURE OF THE SAMPLE CHAMBER (K)= 297.15
MOLE FRACTION NITROGEN IN THE MGA SAMPLE= 0.6705
MOLE FRACTION OXYGEN IN THE MGA SAMPLE= 0.3150
MOLE FRACTION ARGON IN THE MGA SAMPLE= 0.0145
MGA SAMPLE VOLUME PRESSURE (TORR)= 1753.1

OUTPUT:
INITIAL CHARGE PRESSURE Z= 0.99859
FINAL CHARGE PRESSURE Z= 0.99918
EQUILIBRIUM PRESSURE Z= 0.99918
MGA SAMPLE CHAMBER Z= 0.99922

MOLES OF NITROGEN ADDED (GM MOL*10**3)=     9.3936
MOLES OF OXYGEN ADDED (GM MOL*10**3)=    2.5149
MOLES OF ARGON ADDED (GM MOL*10**3)=    0.1130
TOTAL MOLES ADDED (GM MOL*10**3)=   12.0215

TOTAL MOLES OF NITROGEN IN THE SAMPLE CHAMBER (GM MOL*10**3)= 31.9050
TOTAL MOLES OF OXYGEN IN THE SAMPLE CHAMBER (GM MOL*10**3)=  8.1621
TOTAL MOLES OF ARGON IN THE SAMPLE CHAMBER (GM MOL*10**3)=  0.3662
TOTAL MOLES IN THE SAMPLE CHAMBER (GM MOL*10**3)=   40.4334
```

```
MOLES OF NITROGEN IN THE GAS PHASE (GM MOL*10**3)=   10.5672
MOLES OF OXYGEN IN THE GAS PHASE (GM MOL*10**3)=    4.9645
MOLES OF ARGON IN THE GAS PHASE (GM MOL*10**3)=    0.2285
TOTAL MOLES IN THE GAS PHASE (GM MOL*10**3)=   15.7602
MOLE FRACTION OF NITROGEN IN THE GAS PHASE=  0.6705
MOLE FRACTION OF OXYGEN IN THE GAS PHASE=  0.3150
MOLE FRACTION OF ARGON IN THE GAS PHASE=  0.0145

MOLES OF NITROGEN ADSORBED (GM MOL*10**3)=   21.3378
MOLES OF OXYGEN ADSORBED (GM MOL*10**3)=    3.1977
MOLES OF ARGON ADSORBED (GM MOL*10**3)=    0.1377
TOTAL MOLES ADSORBED (GM MOL*10**3)=   24.6732
MOLE FRACTION OF NITROGEN ADSORBED=  0.8648
MOLE FRACTION OF OXYGEN ADSORBED=  0.1296
MOLE FRACTION OF ARGON ADSORBED=  0.0056

VOLUME OF NITROGEN ADSORBED (ML STP)=   478.263
VOLUME OF OXYGEN ADSORBED (ML STP)=    71.673
VOLUME OF ARGON ADSORBED (ML STP)=    3.086
TOTAL VOLUME ADSORBED (ML STP)=   553.022

VOLUME OF NITROGEN ADSORBED (ML STP/GM)=   14.581
VOLUME OF OXYGEN ADSORBED (ML STP/GM)=    2.185
VOLUME OF ARGON ADSORBED (ML STP/GM)=    0.094
TOTAL VOLUME ADSORBED (ML STP/GM)=   16.860

MOLES OF NITROGEN REMOVED BY THE MGA (GM MOL*10**3)=   0.82197
MOLES OF OXYGEN REMOVED BY THE MGA (GM MOL*10**3)=   0.38616
MOLES OF ARGON REMOVED BY THE MGA (GM MOL*10**3)=   0.01778
TOTAL MOLES REMOVED BY THE MGA (GM MOL*10**3)=   1.22591

SEPARATION FACTOR BETWEEN NITROGEN AND OXYGEN=  3.144

POINT NO:  7
INPUT:
INITIAL CHARGE PRESSURE (TORR)= 3868.3
FINAL CHARGE PRESSURE (TORR)= 2534.0
TEMPERATURE OF THE CHARGE CHAMBER (K)= 297.15
EQUILIBRIUM PRESSURE (TORR)= 2404.7
TEMPERATURE OF THE SAMPLE CHAMBER (K)= 297.15
MOLE FRACTION NITROGEN IN THE MGA SAMPLE= 0.6832
MOLE FRACTION OXYGEN IN THE MGA SAMPLE= 0.3031
MOLE FRACTION ARGON IN THE MGA SAMPLE= 0.0137
MGA SAMPLE VOLUME PRESSURE (TORR)= 2291.0

OUTPUT:
INITIAL CHARGE PRESSURE Z= 0.99837
FINAL CHARGE PRESSURE Z= 0.99893
EQUILIBRIUM PRESSURE Z= 0.99894
```

```
MGA SAMPLE CHAMBER Z= 0.99899

MOLES OF NITROGEN ADDED (GM MOL*10**3)=    8.9474
MOLES OF OXYGEN ADDED (GM MOL*10**3)=    2.3954
MOLES OF ARGON ADDED (GM MOL*10**3)=    0.1076
TOTAL MOLES ADDED (GM MOL*10**3)=   11.4504

TOTAL MOLES OF NITROGEN IN THE SAMPLE CHAMBER (GM MOL*10**3)= 40.0304
TOTAL MOLES OF OXYGEN IN THE SAMPLE CHAMBER (GM MOL*10**3)= 10.1714
TOTAL MOLES OF ARGON IN THE SAMPLE CHAMBER (GM MOL*10**3)=  0.4561
TOTAL MOLES IN THE SAMPLE CHAMBER (GM MOL*10**3)=   50.6579

MOLES OF NITROGEN IN THE GAS PHASE (GM MOL*10**3)=   14.1066
MOLES OF OXYGEN IN THE GAS PHASE (GM MOL*10**3)=    6.2584
MOLES OF ARGON IN THE GAS PHASE (GM MOL*10**3)=    0.2829
TOTAL MOLES IN THE GAS PHASE (GM MOL*10**3)=  20.6479
MOLE FRACTION OF NITROGEN IN THE GAS PHASE=  0.6832
MOLE FRACTION OF OXYGEN IN THE GAS PHASE=  0.3031
MOLE FRACTION OF ARGON IN THE GAS PHASE=  0.0137

MOLES OF NITROGEN ADSORBED (GM MOL*10**3)=   25.9238
MOLES OF OXYGEN ADSORBED (GM MOL*10**3)=    3.9130
MOLES OF ARGON ADSORBED (GM MOL*10**3)=    0.1732
TOTAL MOLES ADSORBED (GM MOL*10**3)=   30.0100
MOLE FRACTION OF NITROGEN ADSORBED=  0.8638
MOLE FRACTION OF OXYGEN ADSORBED=  0.1304
MOLE FRACTION OF ARGON ADSORBED=  0.0058

VOLUME OF NITROGEN ADSORBED (ML STP)=   581.052
VOLUME OF OXYGEN ADSORBED (ML STP)=   87.706
VOLUME OF ARGON ADSORBED (ML STP)=    3.882
TOTAL VOLUME ADSORBED (ML STP)=  672.640

VOLUME OF NITROGEN ADSORBED (ML STP/GM)=   17.715
VOLUME OF OXYGEN ADSORBED (ML STP/GM)=    2.674
VOLUME OF ARGON ADSORBED (ML STP/GM)=    0.118
TOTAL VOLUME ADSORBED (ML STP/GM)=  20.507

MOLES OF NITROGEN REMOVED BY THE MGA (GM MOL*10**3)=   1.09477
MOLES OF OXYGEN REMOVED BY THE MGA (GM MOL*10**3)=   0.48569
MOLES OF ARGON REMOVED BY THE MGA (GM MOL*10**3)=   0.02195
TOTAL MOLES REMOVED BY THE MGA (GM MOL*10**3)=   1.60241

SEPARATION FACTOR BETWEEN NITROGEN AND OXYGEN=  2.942

POINT NO:  8
INPUT:
INITIAL CHARGE PRESSURE (TORR)= 3868.3
FINAL CHARGE PRESSURE (TORR)= 2901.2
```

```
TEMPERATURE OF THE CHARGE CHAMBER (K)= 297.15
EQUILIBRIUM PRESSURE (TORR)= 2802.9
TEMPERATURE OF THE SAMPLE CHAMBER (K)= 297.15
MOLE FRACTION NITROGEN IN THE MGA SAMPLE= 0.6906
MOLE FRACTION OXYGEN IN THE MGA SAMPLE= 0.2961
MOLE FRACTION ARGON IN THE MGA SAMPLE= 0.0133
MGA SAMPLE VOLUME PRESSURE (TORR)= 2663.3

OUTPUT:
INITIAL CHARGE PRESSURE Z= 0.99837
FINAL CHARGE PRESSURE Z= 0.99878
EQUILIBRIUM PRESSURE Z= 0.99878
MGA SAMPLE CHAMBER Z= 0.99884

MOLES OF NITROGEN ADDED (GM MOL*10**3)=    6.4860
MOLES OF OXYGEN ADDED (GM MOL*10**3)=    1.7365
MOLES OF ARGON ADDED (GM MOL*10**3)=    0.0780
TOTAL MOLES ADDED (GM MOL*10**3)=    8.3005

TOTAL MOLES OF NITROGEN IN THE SAMPLE CHAMBER (GM MOL*10**3)= 45.4217
TOTAL MOLES OF OXYGEN IN THE SAMPLE CHAMBER (GM MOL*10**3)=  11.4222
TOTAL MOLES OF ARGON IN THE SAMPLE CHAMBER (GM MOL*10**3)=  0.5121
TOTAL MOLES IN THE SAMPLE CHAMBER (GM MOL*10**3)=   57.3560

MOLES OF NITROGEN IN THE GAS PHASE (GM MOL*10**3)=   16.6234
MOLES OF OXYGEN IN THE GAS PHASE (GM MOL*10**3)=    7.1274
MOLES OF ARGON IN THE GAS PHASE (GM MOL*10**3)=    0.3201
TOTAL MOLES IN THE GAS PHASE (GM MOL*10**3)=   24.0710
MOLE FRACTION OF NITROGEN IN THE GAS PHASE=  0.6906
MOLE FRACTION OF OXYGEN IN THE GAS PHASE=  0.2961
MOLE FRACTION OF ARGON IN THE GAS PHASE=  0.0133

MOLES OF NITROGEN ADSORBED (GM MOL*10**3)=   28.7983
MOLES OF OXYGEN ADSORBED (GM MOL*10**3)=    4.2948
MOLES OF ARGON ADSORBED (GM MOL*10**3)=    0.1920
TOTAL MOLES ADSORBED (GM MOL*10**3)=   33.2851
MOLE FRACTION OF NITROGEN ADSORBED=  0.8652
MOLE FRACTION OF OXYGEN ADSORBED=  0.1290
MOLE FRACTION OF ARGON ADSORBED=  0.0058

VOLUME OF NITROGEN ADSORBED (ML STP)=   645.481
VOLUME OF OXYGEN ADSORBED (ML STP)=    96.263
VOLUME OF ARGON ADSORBED (ML STP)=    4.303
TOTAL VOLUME ADSORBED (ML STP)=   746.047

VOLUME OF NITROGEN ADSORBED (ML STP/GM)=   19.679
VOLUME OF OXYGEN ADSORBED (ML STP/GM)=    2.935
VOLUME OF ARGON ADSORBED (ML STP/GM)=    0.131
TOTAL VOLUME ADSORBED (ML STP/GM)=  22.745
```

```
MOLES OF NITROGEN REMOVED BY THE MGA (GM MOL*10**3)=   1.28665
MOLES OF OXYGEN REMOVED BY THE MGA (GM MOL*10**3)=   0.55166
MOLES OF ARGON REMOVED BY THE MGA (GM MOL*10**3)=   0.02478
TOTAL MOLES REMOVED BY THE MGA (GM MOL*10**3)=   1.86310

SEPARATION FACTOR BETWEEN NITROGEN AND OXYGEN=  2.876

POINT NO:  9
INPUT:
INITIAL CHARGE PRESSURE (TORR)= 3868.3
FINAL CHARGE PRESSURE (TORR)= 3180.5
TEMPERATURE OF THE CHARGE CHAMBER (K)= 297.15
EQUILIBRIUM PRESSURE (TO      3051.2
TEMPERATURE OF THE SAMPLE CHAMBER (K)= 297.15
MOLE FRACTION NITROGEN IN THE MGA SAMPLE= 0.6962
MOLE FRACTION OXYGEN IN THE MGA SAMPLE= 0.2907
MOLE FRACTION ARGON IN THE MGA SAMPLE= 0.0131
MGA SAMPLE VOLUME PRESSURE (TORR)= 2890.9

OUTPUT:
INITIAL CHARGE PRESSURE Z= 0.99837
FINAL CHARGE PRESSURE Z= 0.99866
EQUILIBRIUM PRESSURE Z= 0.99868
MGA SAMPLE CHAMBER Z= 0.99875

MOLES OF NITROGEN ADDED (GM MOL*10**3)=    4.6134
MOLES OF OXYGEN ADDED (GM MOL*10**3)=    1.2351
MOLES OF ARGON ADDED (GM MOL*10**3)=    0.0555
TOTAL MOLES ADDED (GM MOL*10**3)=    5.9040

TOTAL MOLES OF NITROGEN IN THE SAMPLE CHAMBER (GM MOL*10**3)= 48.7485
TOTAL MOLES OF OXYGEN IN THE SAMPLE CHAMBER (GM MOL*10**3)= 12.1057
TOTAL MOLES OF ARGON IN THE SAMPLE CHAMBER (GM MOL*10**3)=  0.5429
TOTAL MOLES IN THE SAMPLE CHAMBER (GM MOL*10**3)=   61.3970

MOLES OF NITROGEN IN THE GAS PHASE (GM MOL*10**3)=   18.2446
MOLES OF OXYGEN IN THE GAS PHASE (GM MOL*10**3)=    7.6181
MOLES OF ARGON IN THE GAS PHASE (GM MOL*10**3)=    0.3433
TOTAL MOLES IN THE GAS PHASE (GM MOL*10**3)=   26.2059
MOLE FRACTION OF NITROGEN IN THE GAS PHASE=  0.6962
MOLE FRACTION OF OXYGEN IN THE GAS PHASE=  0.2907
MOLE FRACTION OF ARGON IN THE GAS PHASE=  0.0131

MOLES OF NITROGEN ADSORBED (GM MOL*10**3)=   30.5039
MOLES OF OXYGEN ADSORBED (GM MOL*10**3)=    4.4876
MOLES OF ARGON ADSORBED (GM MOL*10**3)=    0.1996
TOTAL MOLES ADSORBED (GM MOL*10**3)=   35.1911
MOLE FRACTION OF NITROGEN ADSORBED=  0.8668
MOLE FRACTION OF OXYGEN ADSORBED=  0.1275
```

```
MOLE FRACTION OF ARGON ADSORBED=  0.0057

VOLUME OF NITROGEN ADSORBED (ML STP)=   683.711
VOLUME OF OXYGEN ADSORBED (ML STP)=   100.584
VOLUME OF ARGON ADSORBED (ML STP)=     4.473
TOTAL VOLUME ADSORBED (ML STP)=   788.768

VOLUME OF NITROGEN ADSORBED (ML STP/GM)=   20.845
VOLUME OF OXYGEN ADSORBED (ML STP/GM)=    3.067
VOLUME OF ARGON ADSORBED (ML STP/GM)=    0.136
TOTAL VOLUME ADSORBED (ML STP/GM)=   24.048

MOLES OF NITROGEN REMOVED BY THE MGA (GM MOL*10**3)=   1.40806
MOLES OF OXYGEN REMOVED BY THE MGA (GM MOL*10**3)=   0.58794
MOLES OF ARGON REMOVED BY THE MGA (GM MOL*10**3)=   0.02649
TOTAL MOLES REMOVED BY THE MGA (GM MOL*10**3)=   2.02249

SEPARATION FACTOR BETWEEN NITROGEN AND OXYGEN=  2.840
```

```
*********************************************************************
C       RUTHVE.FOR
C   PREDICTION OF PURE COMPONENT ISOTHERM DATA USING RUTHVEN'S EQN.
C
C   OWNER: G.W.MILLER
C   DATE:  20 FEB 84
C   FILENAME: RUTHVE.FOR
C
    IMPLICIT REAL * 8 (A-H,O-Z)
    DIMENSION C(40),XNUM(20),XDEN(20),XP(40)
    OPEN(UNIT=7,NAME='NEW.DAT',TYPE='NEW',DISPOSE='SAVE')
C
C   NOMENCLATURE:
C   C = AMOUNT ADSORBED [ML STP/GM(CRYSTAL+BINDER)]
C   XK=HENRY'S CONSTANT(MOLECULES/(CAVITY*TORR))
C   XP = PRESSURE (TORR)
C   B = EFFECTIVE MOLECULAR VOLUME OR VAN DER WAALS COVOLUME (A**3)
C   V = CAVITY VOLUME (A**3)
C   M = MAXIMUM NO. OF MOLECULES/CAVITY (LESS THAN OR EQUAL TO V/B)
C
C   INPUT:
C
    XK= 0.01261D00
    B = 77.63D00
    V = 776.0D00
    M = 10
C
C   CALCULATIONS:
C
```

```
      XPP = 0.0
      DO500 II=1,40
      XP(II) = XPP + 100.
      XPP = XP(II)
      XKP = XK * XPP
      XNUSUM = 0.0
      XDESUM = 0.0
      XNUM(1) = XKP
      XDEN(1) = 1. + XKP
      DO100 I=2,M
      L = I
      XNUM1 = (XKP**L) * (( 1.- ((L*B)/V))**L)
      PFACT1 = 1
      MMIN1 = L - 1
      DO200 J=1,MMIN1
      K1 = J
      PFACT1 = PFACT1 * K1
 200        CONTINUE
      XNUM(I) = XNUM1/PFACT1
 100        CONTINUE
      DO300 I=2,M
      N = I
      XNUM2 = (XKP**N) * (( 1.-((N*B)/V))**N)
      PFACT2 = 1
      DO400 J=1,N
      K2 = J
      PFACT2 = PFACT2 * K2
 400        CONTINUE
      XDEN(I) = XNUM2/PFACT2
 300        CONTINUE
      DO600 I=1,M
      XNUSUM = XNUSUM + XNUM(I)
      XDESUM = XDESUM + XDEN(I)
 600        CONTINUE
      C(II) = XNUSUM / XDESUM
      DO900 I=1,20
      XNUM(I) = 0.0
      XDEN(I) = 0.0
 900        CONTINUE
 500        CONTINUE
C
C     OUTPUT TO DATA FILE:
C
      DO1000 I=1,40
      C(I)= C(I) * 11.2111
 1000       CONTINUE
      DO700 I=1,40
      WRITE (7,800) XP(I),C(I)
 700        CONTINUE
```

```
800       FORMAT (1X,F7.1,3X,F9.3)
      TYPE*, 'RENAME NEW DATA FILE'
      STOP
      END

************************************************************************
C         RUBI24.FOR
C     PREDICTION OF BINARY DATA AT 297.15 K
C
C     OWNER: G.W. MILLER
C     DATE:  2 APR 84
C     FILENAME: RUBI24.FOR
C
C
      IMPLICIT REAL * 8 (A-H,O-Z)
      DIMENSION XPO2(30),XPN2(30),XPT(30),CO2(30),CN2(30)
      OPEN(UNIT=7,NAME='RBIN24.DAT',TYPE='NEW',DISPOSE='SAVE')
      OPEN(UNIT=9,NAME='RBIO24.DAT',TYPE='NEW',DISPOSE='SAVE')
C
C     NOMENCLATURE:
C
C     CO2 = AMT OXYGEN ADSORBED (MOLECULES/CAVITY)
C     CN2 = AMT NITROGEN ADSORBED (MOLECULES/CAVITY)
C     XKO2 = HENRY CONSTANT FOR OXYGEN (MOLECULES/CAV*TORR)
C     XKN2 = HENRY CONSTANT FOR NITROGEN (MOLECULES/CAV*TORR)
C     BO2 = OXYGEN EFFECTIVE MOLECULAR VOLUME (A**3)
C     BN2 = NITROGEN EFFECTIVE MOLECULAR VOLUME (A**3)
C     V = CAVITY VOLUME (A**3)
C     MO2 = NUMBER OF OXYGEN MOLECULES PER CAVITY AT SATURATION
C     MN2 =    "   "  NITROGEN    "     "     "    "     "
C     XPO2 = OXYGEN PARTIAL PRESSURE (TORR)
C     XPN2 = NITROGEN PARTIAL PRESSURE (TORR)
C     NDATA = NUMBER OF DATA POINTS
C
C     INPUT:
C
      XKO2 = 0.0004234D00
      XKN2 = 0.001902D00
      BO2 = 38.8D00
      BN2 = 97.D00
      MO2 = 20
      MN2 = 8
      V = 776.D00
      NDATA = 14
C
      XPO2(1) = 65.1D00
      XPO2(2) = 75.2D00
      XPO2(3) = 135.8D00
      XPO2(4) = 207.7D00
```

```
      XPO2(5) = 299.D00
      XPO2(6) = 403.2D00
      XPO2(7) = 415.5D00
      XPO2(8) = 578.3D00
      XPO2(9) = 619.1D00
      XPO2(10) = 728.9D00
      XPO2(11) = 755.6D00
      XPO2(12) = 829.9D00
      XPO2(13) = 847.D00
      XPO2(14) = 887.D00
C
      XPN2(1) = 100.9D00
      XPN2(2) = 115.3D00
      XPN2(3) = 229.9D00
      XPN2(4) = 367.9D00
      XPN2(5) = 569.8D00
      XPN2(6) = 747.2D00
      XPN2(7) = 817.2D00
      XPN2(8) = 1230.9D00
      XPN2(9) = 1261.2D00
      XPN2(10) = 1642.9D00
      XPN2(11) = 1676.7D00
      XPN2(12) = 1935.7D00
      XPN2(13) = 1944.1D00
      XPN2(14) = 2124.2D00
C
C     CALCULATIONS:
C
      DO6 M=1,NDATA
      XPT(M) = XPO2(M) + XPN2(M)
  6   CONTINUE
      BA = BO2
      BB = BN2
      INUMJ = MN2 + 1
      IDENJ = INUMJ
      INUMI = MO2 + 1
      IDENI = INUMI
      DO100 III=1,NDATA
      ICHECK = 0
      XKAPA = XKO2 * XPO2(III)
      XKBPB = XKN2 * XPN2(III)
 2222        XDEN = 0.0
      XNUM = 0.0
C
C     CALCULATION OF DOUBLE SUMMATION IN NUMERATOR:
C
      DO200 J=1,INUMJ
      JN = J - 1
      XJN = JN
```

```
   PFACJN = 1.
   IF(JN) 9999,903,904
904        DO300 K=1,JN
   KA = K
   PFACJN = PFACJN * KA
300        CONTINUE
903        DO400 I=1,INUMI
   IN = I - 1
   XIN = IN
   CHKERN = (XIN * BA) + (XJN * BB)
   IF(CHKERN.GT.V) GO TO 400
   MN = JN + IN
       C2 = (XKAPA**IN) * (XKBPB**JN)
   XMAJ1= C2 * ((1.D00-((XIN*BA)/V)-((XJN*BB)/V))**MN)
   PFACIN = 1.
   IF(IN) 9999,919,911
911        DO912 K=1,IN
   KB = K
   PFACIN = PFACIN * KB
912        CONTINUE
919        IF(ICHECK) 9999,913,914
913        MGAS = IN
   GO TO 915
914        MGAS = JN
915    CN = ((MGAS * XMAJ1) / PFACIN) * (1.D00 / PFACJN)
   XNUM = XNUM + CN
400        CONTINUE
200        CONTINUE
C
C  CALCULATION OF DOUBLE SUMMATION IN DENOMINATOR:
C
   DO500 J=1,IDENJ
   JD = J - 1
   XJD = JD
   PFACJD = 1.
   IF(JD) 9999,916,917
917        DO600 K=1,JD
   KC = K
   PFACJD = PFACJD * KC
600        CONTINUE
916        DO700 I=1,IDENI
       ID = I - 1
   XID = ID
   CHKERD = (XID * BA) + (XJD * BB)
   IF(CHKERD.GT.V) GO TO 700
   PFACID = 1.
   IF(ID) 9999,918,933
933        DO800 K=1,ID
   KD = K
```

```
   PFACID = PFACID * KD
 800        CONTINUE
 918        MD = JD + ID
        C4 = (XKAPA**ID) * (XKBPB**JD)
   XMAJ2= C4 * ((1.D00-((XID*BA)/V)-((XJD*BB)/V))**MD)
   CD = (XMAJ2 / PFACID) * (1.D00 / PFACJD)
        XDEN = XDEN + CD
 700        CONTINUE
 500        CONTINUE
   IF(ICHECK) 9999,920,921
C
C  CALCULATION OF ADSORBED CONCENTRATIONS:
C
 920        CO2(III) = XNUM / XDEN
   ICHECK = ICHECK + 1
   GO TO 2222
 921        CN2(III) = XNUM / XDEN
 100        CONTINUE
   DO333 LL=1,NDATA
   CO2(LL) = CO2(LL) * 11.2111D00
   CN2(LL) = CN2(LL) * 11.2111D00
 333        CONTINUE
C
C  OUTPUT:
C
 922        DO1100 N=1,NDATA
   WRITE(9,14) XPO2(N),CO2(N)
 1100       CONTINUE
 14 FORMAT(1X,F7.1,3X,F9.4)
   DO1200 N=1,NDATA
   WRITE(7,15) XPN2(N),CN2(N)
 1200       CONTINUE
 15 FORMAT(1X,F7.1,3X,F9.4)
 9999       STOP
   END


*****************************************************************************
C       IAST24.FOR
C  THIS PROGRAM CALCULATES xO2,qT,qO2, and qN2
C  AT 297.15 K USING THE IAST THEORY OF MYERS AND
C  PRAUSNITZ.
C
   IMPLICIT REAL * 8 (A-H,O-Z)
   DIMENSION XPO2(30),XPN2(30),PT(30),YO2(30),YN2(30)
   DIMENSION XO2(30),XN2(30),PO2PU(30),PN2PU(30),XNO2PU(30)
   DIMENSION XNN2PU(30),XNT(30),XNO2(30),XNN2(30)
   OPEN(UNIT=7,NAME='IASO24.DAT',TYPE='NEW',DISPOSE='SAVE')
   OPEN(UNIT=8,NAME='IASN24.DAT',TYPE='NEW',DISPOSE='SAVE')
```

```
      OPEN(UNIT=9,NAME='IAST24.RES',TYPE='NEW',DISPOSE='SAVE')
C
C     INPUT:
C
      XPO2(1) =  65.1D00
      XPO2(2) =  75.2D00
      XPO2(3) =  135.8D00
      XPO2(4) =  207.7D00
      XPO2(5) =  299.D00
      XPO2(6) =  403.2D00
      XPO2(7) =  415.5D00
      XPO2(8) =  578.3D00
      XPO2(9) =  619.1D00
      XPO2(10) = 728.9D00
      XPO2(11) = 755.6D00
      XPO2(12) = 829.9D00
      XPO2(13) = 847.D00
      XPO2(14) = 887.D00
C
      XPN2(1) =  100.9D00
      XPN2(2) =  115.3D00
      XPN2(3) =  229.9D00
      XPN2(4) =  367.9D00
      XPN2(5) =  569.8D00
      XPN2(6) =  747.2D00
      XPN2(7) =  817.2D00
      XPN2(8) =  1230.9D00
      XPN2(9) =  1261.2D00
      XPN2(10) =  1642.9D00
      XPN2(11) =  1676.7D00
      XPN2(12) =  1935.7D00
      XPN2(13) =  1944.1D00
      XPN2(14) =  2124.2D00
C
      NDATA = 14
C
C     PARAMETERS FOR CALC. OF THE SPREADING PRESS. OF O2.
      SOP1 = .0045521D00
      SOP2 = 2.2479D-05
      SOP3 = 1.00323D00
C
C     PARAMETERS FOR CALC. OF THE SPREADING PRESS. OF N2.
      SNP1 = .054163D00
      SNP2 = 2.2830D-04
      SNP3 = 0.83329D00
C
C     PARAMETERS FOR CALC. OF THE N2 ISOTHERM.
      QOP1 = 0.00466905D00
      QOP2 = .0000462853
```

```
C
C    PARAMETERS FOR CALC. OF THE O2 ISOTHERM.
     QNP1 = 0.0475481
     QNP2 = 5.16372D-04
     QNP3 = .8263D00
C
C    CALCULATIONS:
C
     DO100 I=1,NDATA
     PT(I) = XPO2(I) + XPN2(I)
 100         CONTINUE
     DO200 I=1,NDATA
     YO2(I) = XPO2(I) / PT(I)
     YN2(I) = XPN2(I) / PT(I)
 200         CONTINUE
     DO888 I=1,NDATA
     ICHECK = 0
     XXPN2 = XPN2(I) + 1.D00
 500         T1 = ((XPO2(I) * XXPN2) / (XXPN2 - XPN2(I)))**SOP3
     T2 = (T1 * SOP1) / (1.D00 + (SOP2 * T1 ))
     T3 = XXPN2**SNP3
     T4 = (T3 * SNP1) / (1.D00 + (SNP2 * T3))
     T5 = T4 -T2
     GO TO(600,601,602) ICHECK
 600         IF(T5) 501,555,502
 501         XXPN2 = XXPN2 + 1.D00
     GO TO 500
 502         XXPN2 = XXPN2 - 1.D00
     ICHECK = ICHECK + 1
     GO TO 500
 601         IF(T5) 650,555,651
 650         XXPN2 = XXPN2 + .1D00
     GO TO 500
 651         XXPN2 = XXPN2 - .1D00
     ICHECK = ICHECK + 1
     GO TO 500
 602         IF(T5) 660,555,555
 660         XXPN2 = XXPN2 + .01D00
     GO TO 500
 555         PN2PU(I) = XXPN2
 888         CONTINUE
C
     DO700 I=1,NDATA
     C1 = PN2PU(I) - XPN2(I)
     PO2PU(I) = (XPO2(I) * PN2PU(I)) / C1
 700         CONTINUE
     DO800 I=1,NDATA
     XO2(I) = XPO2(I) / PO2PU(I)
     XN2(I) = 1.D00 - XO2(I)
```

```
800         CONTINUE
    DO900 I=1,NDATA
    C2 = 1.D00 + (QOP2 * PO2PU(I))
    XNO2PU(I) = (QOP1 * PO2PU(I)) / C2
    C3 = PN2PU(I)**QNP3
    C4 = 1.D00 + (QNP2 * C3)
    XNN2PU(I) = (QNP1 * C3) / C4
900         CONTINUE
    DO1000 I=1,NDATA
    RNT = (XO2(I) / XNO2PU(I)) + (XN2(I) / XNN2PU(I))
    XNT(I) = 1.D00 / RNT
    XNO2(I) = XNT(I) * XO2(I)
    XNN2(I) = XNT(I) * XN2(I)
1000        CONTINUE
    DO1100 I=1,NDATA
      II = I
    WRITE(9,930) II
    WRITE(9,901) XPO2(I),XPN2(I),PT(I),PO2PU(I),PN2PU(I)
    WRITE(9,902) YO2(I),YN2(I),XO2(I),XN2(I)
    WRITE(9,903) XNO2(I),XNN2(I),XNO2PU(I),XNN2PU(I),XNT(I)
1100        CONTINUE
930         FORMAT(//,1X,'POINT NO.:',I3)
901         FORMAT(1X,'PO2=',F8.2,' PN2=',F8.2,' P=',F8.2,'    PO2*=',F8.
    12,' PN2*=',F8.2)
902         FORMAT(1X,'YO2=',1X,F6.4,1X,' YN2=',1X,F6.4,'  XO2=',2X,F6.4,
    1'  XN2=',1X,F6.4)
903         FORMAT(1X,'QO2=',F8.3,' QN2=',F8.3,' QO2*=',F8.3,' QN2*=',F8.
    13,' QT=',F8.3)
    DO1200 I=1,NDATA
    WRITE(7,904) XPO2(I),XNO2(I)
    WRITE(8,904) XPN2(I),XNN2(I)
1200        CONTINUE
904         FORMAT(1X,F8.2,3X,F8.3)
    STOP
    END
```

REFERENCES

(1) Lee,H. and D.E. Stahl,AIChE Symposium Series,No.134,Vol.69, 1,(1973).

(2) Davis,J.C.,Chemical Engineering,Oct,(1972).

(3) Stewart,H.A., and J.L. Heck,Chemical Engineering Progress, Vol.65,No.9,(1969).

(4) Heck,J.L.,Oil and Gas Journal,Vol.78,122,(1980).

a5) Alexis,R.W.,Chemical Engineering Progress,Vol.63,No.5,69, (1967).

(6) Keller,G.E.,and R.L.Jones,ACS Symposium Series,No.135,275, (1980).

(7) Breck,D.W.,"Zeolite Molecular Sieves",Wiley,New York,(1974).

(8) Manatt,S.A.,Aviat.Space and Environ. Med.(52)11:645-653, (1981).

(9) Hinman,P.V.,AFFDL-TM-75-178,Air Force Flight Dynamics Laboratory,Wright-Patterson AFB,OH,(1976).

(10) Miller,R.L.,K.G.Ikels,M.J.Lamb,E.J.Boscola,and R.H.Ferguson, Avait. Space Environ. Med. 51(7):665-673,(1980).

(11) Cooke,J.P.,K.G.Ikels,J.D.Adams,and R.L. Miller,Avait. Space Environ. Med.,51:537-541,(1980).

(12) Horrigan,D.J.,C.H. Wells,M.M.Guest,G.B.Hart,and Goodpasture,Avait. Space Environ.Med.,50:357-362,(1979).

(13) Milton,R.M.,"Commercial Development of Molecular Sieve Technology",in "Molecular Sieves",Soc. for Chemical Industry,London,(1968)

(14) Grandjean,F.,C.r.hebd.Seanc. Acad. Sci. Paris,Vol.149,866, (1909).

(15) Weigel,O.,and E.Z.Steinhoff,Kristallogr. Kristallgeom., Vol.61,125,(1925).

(16) Pauling,L.,Proc. Nat. Acad. Sci.,U.S.,Vol.16,453,(1930).

(17) Taylor,W.H.,Z. Krist.,Vol.74,1,(1930).

(18) Barrer,R.M.,and D.A. Trans.Faraday Soc.,Vol.40,195,(1944).

(19) ------,J. Soc.Chem.Ind.,Vol.64,130,(1945).

(20) ------,and L.Belchetz,Ibid,Vol.64,131,(1945).

(21) ------,Proc.Roy.Soc.(London),A167,392,(1938).

(22) Milton,R.M.,"Molecular Sieves",Soc.of Chem.Ind.(London), (1968).

(23) Milton,R.M.,Union Carbide Corporation,U.S.Patent 2,882,244 (1959).

(24) Breck,D.W.,and E.M.Flanigen,in "Molecular Sieves", Soc. for Chemical Industry,London,(1968).

(25) Barrer,R.M.,and J.W.Sutherland,Proc.Roy.Soc.,A237,439, (1956).

(26) Skarstrom,C.W.,Esso Research and Engineering,U.S. Patent No. 2,944,627 (1960).

(27) --------------,Annals of New York Academy of Science, Vol.72,751,(1959).

(28) --------------,C.W.,British Patent 850,443.

(29) Smith,J.V.,Mineralogical Soceity of America,Special Paper No.1,(1963).

(30) Oscik,J.,"Adsorption",John Wiley and Sons,New York,(1982).

(31) Ruthven,D.M.,Separation and Purification Methods,5(2), 189-246,(1976).

(32) Young,D.M.,and A.D.Crowell,"Physical Adsorption of Gases", Butterworth and Co.,London,(1962).

(33) Smith,J.V.,J.Chem.Soc.,p.3754,(1964).

(34) Derrah,R.I.,and D.M.Ruthven,Canad.J.Chem.,Vol.53,996,(1975).

(35) Shendalman,L.H.,and J.E.Mitchell,Chemical Engineering Science,Vol.27,1449-1458,(1972).

(36) Mitchell,J.E.,and L.H.Shendalman,AIChE Symposium Series, Vol.69,No.134,25,(1973).

(37) Weaver,K.,and C.E.Hamrin,Chem.Eng.Sci.,Vol.29,1873,(1974).

(38) Whitley,M.D.,and C.E.Hamrin,Jr.,ACS Symp.Ser.,No.135, (1980).

(39) Collins,H.W.,and K.C.Chao,AIChE Symposium Series,No.134, Vol.69,

(40) Stuart,F.X.,and D.T.Camp,AIChE Symposium Series,No.134, Vol.69,

(41) Sargent,W.H.,and C.J.Whitford,Adv.Chem.Series,Vol.102,144, (1971).

(42) Breck,D.M.,Journal of Chemical Education,Vol.48,678,(1964).

(43) Barrer,R.M.,and J.A.Davies,Proc.Roy.Soc.,A320,289,(1970).

(44) Dorfman,L.R.,and R.P.Danner,AIChE Symposium Series,No.71, 152,(1975).

(45) Ruthven,D.M.,K.F.Loughlin,and K.A.Holborrow,Chem.Eng.Sci., Vol.28,701,(1973).

(46) Ruthven,D.M.,AIChE Journal,Vol.22,No.4,753,(1976).

(47) Barrer,R.M.,and J.A.Lee,Surface Science,Vol.12,354,(1968).

(48) Schirmer W.,G.Fiedrich,A.Grossman,and H.Stach,First Conference on Molecular Sieve Zeolites,London,(1967); proceedings Soc.Chem.Ind.,276,(1968).

(49) Sips,R.,J.Chem.Phys.,Vol.16,490,(1948).

(50) Hill,T.L.,"Introduction to Statistical Thermodynamics", Addison-Wesley,Reading,Mass.,(1960).

(51) Barrer,R.M., F.W. Bultitude,and J.W.Sutherland,Trans. Faraday Soc.,Vol.53,1111,(1957).

(52) Ruthven,D.M.,Nature Phys. Sci.,Vol.232,70,(1971).

(53) Barrer,R.M.,and J.W.Sutherland,Proc.Roy.Soc.(London), A237,439-463,(1956).

(54) Rabinowitsch,E.and W.C. Wood,Trans.Faraday Soc.,Vol.32, 947-956,(1936).

(55) Breck,D.M.,and R.W.Grose,Adv.in Chem.,Vol.121,319,(1973).

(56) Dubinin,M.M.,Chem.Revs.,Vol.60,235,(1960).

(57) ------------,O. Kadlec,and A. Zukal,Coll.Czech.Chem. Commun.,Vol.31,406,(1966).

(58) Ruthven,D.M.,and K.F.Loughlin,J.Chem.Soc.Faraday Trans. I,Vol.68,696,(1972).

(59) Glessner,A.J.,and A.L.Myers,C.E.P. Symposium Series,Vol.65, 73,(1969).

(60) Myers,A.L.,and I.M.Prausnitz,AIChE Journal,Vol.11,121, (1965).

(61) M.Polanyi,Ver handt. Deut.Phys.,Geo.,Vol.16,1012,(1914).

(62) Ruthven,D.M.,and R.I.Derrah,J.Chem.Soc.Faraday Trans I, Vol.71,2031,(1975).

(63) Kondis,E.S.,and J.S.Dranoff,"Molecular Sieve Zeolites", Adv.Chem.Sec.102, Am.Chem.Soc., Washington,D.C.,p171, (1971).

(64) Garg,D.R.,and D.M.Ruthven,Chem.Eng.Sci.,Vol.29,571,(1974).

(65) Weast,R.C.,ed.,"Handbook of Chemistry and Physics",56th, Ed.,CRC Press,(1975).

(66) Maslan,F.D.,and T.M.Littman,Ind.Eng.Chem.,Vol.45,1566, (1953).

(67) Domine,D.,and L.Hay,"Molecular Sieves",204,Soc.of Chem.Ind., London,(1968).

(68) Peterson,D.,in "Adsorption and Ion Exchange with Synthetic Zeolites",W.H.Flank,ed.,(1980).

(69) Data of Union Carbide Corporation presented here by permission.

(70) Schweitzer,"Handbook of Separation Techniques",Mcgraw-Hill Book Co.,(1979).

(71) Sorial,G.A.,W.H.Granville,and W.O.Daly,Chemical Engineering Science,Vol.38,No.9,1517,(1983).

(72) Van Ness,H.C.,Ind. and Eng. Chem. Fund.,Vol.8,No.3,(1969).

(73) Sircar,S.,and R.Gupta,AIChE Journal,Vol.27,No.5,806,(1981).

(74) Hirschfelder,J.O.,Curtiss,C.F.,and Bird,R.B.,"Molecular THeory of Gases and Liquids",Wiley,New York,(1954).

(75) Derrah,R.I.,K.F.Loughlin,and D.M.Ruthven,J.Chem.Soc., Faraday Trans I,Vol.68,1947,(1972).

(76) Eberly,P.E.,IE Chem. Prod. Res. Dev.,Vol.8,140,(1969).

(77) Kondis,E.S.,and J.S.Dranoff,Ind.Eng.Chem.Proc.Design Dev., Vol.10,108,(1971).

(78) Mckee,D.W.,and Hamlen R.P.,Union Carbide Corporation,unpublished results.

(79) Pigford,R.L.,Baker B.,and Blum D.E.,Ind.Eng.Chem.Fund.,Vol.8, 144,(1969).

(80) Chan,Y.I.,F.B.Hill,and Y.W.Wong,Chem.Eng.Sci.,Vol.36,243-251,(1981).

(81) Brunauer,S.,"The Adsorption of Gases and Vapours",Princeton University Press, Princeton, (1945).

(82) Knaebel,K.S.,and F.B.Hill,Chem.Eng.Sci.,(submitted 1983).